Immunotherapeutic approaches in the treatment of melanoma

Oliver George Donnelly

Submitted in accordance with the requirements for the degree of
Doctor of Philosophy

The University of Leeds
School of Medicine

November 2012

The candidate confirms that the work is his own, except where work which has formed part of jointly-authored publications has been included. The contributions of the candidate and the other authors to the work has been explicitly indicated overleaf. The candidate confirms that appropriate credit has been given within the thesis where reference has been made to the work of others.

1 Preface

1.1 Acknowledgements

This research has been carried out by a team which has included Professor Alan Melcher, Professor Peter Selby, Dr Fiona Errington-Mais, Dr Lynette Steele, Dr Elizabeth Ilett, Miss Karen Scott, Dr Victoria Jennings, Dr Jacquelyn Bond, Dr Roger Philips, Mr Howard Peach, Professor Richard Vile, Mr Timothy Kottke, Mrs Jill Thompson, Dr Rosa Diaz, Dr Diana Rommelfanger-Konkol, Dr Jose Pulido, Dr Aaron Johnson, Dr Fang Jin, Mr Brett Carlson, Dr Keith Furutani, Ms Kelly Classic, Mr Raymond Phelps. Further collaboration is acknowledged from Mrs Daisy Stockbridge and Mr Harry Donnelly.

Professor Alan Melcher, Dr Fiona Errington-Mais and Professor Peter Selby supervised all elements of the thesis, contributing to analysis, interpretation and design of all the work described. Dr Lynette Steele contributed to the design and implementation of several elements of chapter 4. Miss Karen Scott and Dr Victoria Jennings helped with several experiments described in chapter 4. Dr Roger Philips helped design the multi-layer experiments described in chapter 4 and Dr Jacquelyn Bond helped perform the subsequent confocal microscopy. Mr Howard Peach supplied the explanted melanoma tissue used in chapter 4. Professor Richard Vile, Dr Elizabeth Ilett and Dr Jose Pulido contributed to the analysis, interpretation and design of elements of the work described in chapters 5 and 6. Mr Timothy Kottke supplied some of the virus used in chapters 5 & 6 and completed elements of two of the experiments described in chapter 5. Dr Rosa Diaz and Dr Diana Rommelfanger-Konkol helped with some of the experiments described in chapter 5. Mrs Jill Thompson trained the candidate in basic mouse handling procedures and performed, in accordance with institutional regulations, all animal injections. Dr Aaron Johnson, Dr Fang Jin and Mr Brett Carlson gave advice for several elements of chapter 6. Dr Keith Furutani and Ms Kelly Classic helped design the brachytherapy experiments described in chapter 5, Dr Keith Furutani produced the brachytherapy dosimetry illustrated in chapter 5. Mr Raymond Phelps helped design the brachytherapy plaques used in chapter 5 and produced some of the tools subsequently used in the production

and loading of plaques. Mrs Daisy Stockbridge gave editorial advice for the Max Perutz award submissions. Mr Harry Donnelly co-designed the poster shown in appendix 9.2.

My own contributions, fully and explicitly indicated in the thesis, have been the conception, design, performance, analysis and documentation of all experiments and resultant data except where clearly stated.

The candidate was funded throughout the period of study by a fellowship from the Medical Research Council UK.
For the period of the thesis that resulted in the data shown in chapters 5 and 6 the candidate received additional funding from the Royal Society of Medicine, London, in the form of the Ellison-Cliffe travelling fellowship.

Without the help of everyone in Alan Melcher's lab, even Liz Ilett, I would have floundered even more than I did. Karen Scott helped with chromium assays whilst others were shirking the radiation. Discussions with Dr Vicki Jennings were always terrifically revealing. Anita Storrar was always hugely helpful with navigating the inner workings of the University's sometimes-arcane processes, but was particularly helpful in organising the move to the US. Many of those from the neighbouring labs were generous with their blood and support, and pub quiz expertise. Professor Selby seemed incapable of offering anything other than excellent advice during our monthly supervisions.

Dr Lynette Steel was the first person in the lab to teach me any of the techniques, and did so in such a patient and entertaining fashion that I was persuaded to persist, despite my overwhelming incompetence. She also bakes a good cake.

Dr Errington-Mais was my principal supervisor over the course of the 3 years, even when she abandoned her post citing maternity. Given her advancing years its perhaps no surprise that she constantly talks about her imminent retirement, but I hope for everyone's sake that she can hold on for a couple of years yet. She is a great teacher and critic (in the best possible sense), who had the patience to

read through all the drafts of thesis - apart from this bit, which she would have shredded immediately.

Professor Richard Vile very kindly agreed to take me on for a year, and managed to resist the temptation to exert the power he had to have me deported. He also gave me two of the best pieces of advice I have ever had; I intend to stick to them religiously, but it would be inappropriate to repeat them here.

Professor Alan Melcher was and is an outstanding supervisor and mentor, and will hopefully remain both for a good while yet. I could not discern any good reason for him to take me on, and invest as much time in me as he has, but I'm profoundly grateful that, in this case at least, his judgment was so awry...

My parents, Brian and Jane Donnelly, gave a lot to put me in the position such that I could pursue this type of work and I hope they think it might have been worthwhile. My family, Humphrey, Wilfred and Jade, tolerated a frequently absent father/husband and made the decision to move abroad easier than I could have hoped. We've moved home ten times in the last five years, purely so that I could pursue an academic career, and I'm immeasurably grateful for their collective patience and support. Moreover, without them, it would all be pointless anyway…

T.S.L.R.

1.2 Abstract

Immunotherapeutic approaches to treat cancers have been pursued for many years with very little success. However recent success in the treatment of melanoma, have confirmed the potential utility of the approach.
Oncolytic viruses are emerging therapies that work in part by directly killing cells they infect, but also by stimulating anti-tumour immune responses. Radiotherapy is generally considered an immune-suppressive treatment but recent preclinical evidence suggests that it can render cancer cells susceptible to immune-mediated attack and generate anti-tumour immunity when combined with additional therapies.

In the work described measles virus, a potential oncolytic virus, kills human melanoma cells, both immortalised cell lines and freshly resected primary cells, and generates an inflammatory pattern of cytokines, chemokines and danger signals as it does so. The virus, and virus-treated cancer cells enhance innate effector cells and mature dendritic cells. Virally treated melanoma cells stimulate adaptive T-cell anti-melanoma responses.

External beam radiotherapy in the palliative dose range was combined with combinations of adoptive cell therapy and vesicular stomatitis virus and did not enhance therapy. Sealed-source brachytherapy was also combined with adoptive cell therapy and virotherapy, but without synergy.

In order to study the effects of existing and proposed immunotherapeutic approaches against melanoma that has metastasised to the brain, a model of intracranial melanoma was established and in initial therapy experiments survival was improved following treatment with intravenous oncolytic virotherapy.

Immunotherapeutic approaches hold promise for the treatment of melanoma. Clinical testing of measles virus in trials with patients suffering from metastatic melanoma should be considered.

1.3 Plain language summary

For a long time the immune system has been considered irrelevant in the treatment of cancer. Most patients who develop cancer have perfectly normal immune systems during the period that the cancer developed. Thus the argument goes if the immune system could play a role it would have done so already. Moreover conventional therapies, namely chemotherapy and radiotherapy, famously suppress the immune system; people having chemotherapy are at much higher risk of catching infections, for example. These are the views held by most doctors, including the specialists who treat cancer. Increasingly all of these views can be challenged. Cancers do develop despite apparently normal immune systems, but it's not a smooth ride for them. Many cancer therapies do have side effects that dampen the immune system, but they can also have some positive effects.

Cancers have to evade the immune system during their development and emerge from the process having acquired several tricks that make them invisible to the body's defences. This raises the prospect of subverting that subversion; by developing therapies that can overcome the immune evasion that most cancers set up, it will be possible to recruit a person's own immune system to attack their cancer.

Some viruses are better at infecting cancer cells than normal human cells. These oncolytic viruses are being developed across the world in labs and also in clinical trials. A strain of measles, commonly used in vaccinations, is one such oncolytic virus that I have used in laboratory models of melanoma to show two things. Firstly the measles virus kills melanoma cells. Secondly the measles virus is able to trigger an immune response against the melanoma. Based on these data I'm developing a trial that will test the measles virus for patients with melanoma.

Amongst its many effects, medical students are taught that radiotherapy is immunosuppressive. In many senses this is true but it is a complicated picture. Giving radiotherapy to the whole body will eliminate many of the cells required to produce an immune response, but we don't often give radiotherapy to the whole body. Modern radiotherapy tends to focus on ever more precisely directed areas for treatment; the tumour and as small an area around it as possible. Immune cells in that area are likely to be damaged by the radiation, but other

cells outside the treatment region may even benefit from the therapy. Tumour cells treated by radiotherapy seem to become more visible to the immune system and release signals that are capable of activating immune cells. Several groups worldwide have found ways to make radiotherapy combine with the immune system in mouse models of cancer. However in my models I found that there was little positive effect; this contradicts the results of other scientists, but suggests that if radiotherapy can be used in concert with the immune system then doses and timing will need to be carefully worked out before we can get the best results for patients.

One of the areas that melanoma will commonly spread to is the brain, in fact melanoma spreads to the brain more commonly than almost any other cancer. This is horribly debilitating for patients and always carries a bleak prognosis when it happens. One of the challenges for any cancer therapy is to reach the brain, as it is carefully protected behind a unique obstacle called the blood-brain barrier. This blood-brain barrier keeps the brain safe from infections but actually obstructs many therapies reaching their targets. In order to find ways to allow immunotherapies to reach the brain I established a model in mice that will be used to test how well existing and new therapies reach cancers hiding behind the blood-brain barrier.

1.4 Table of contents

1 Preface ... 3

1.1 Acknowledgements ... 3

1.2 Abstract ... 6

1.3 Plain language summary ... 7

1.4 Table of contents ... 9

1.5 Table of figures ... 13

1.6 Abbreviations ... 16

2 Introduction ... 20

2.1 Melanoma ... 22

2.2 Immunology of Cancer ... 29

2.2.1 Tumour-associated antigens ... 33

2.2.2 Immunology of melanoma ... 34

2.3 Adoptive cell therapy ... 35

2.4 The immune effects of conventional therapies ... 39

2.5 Oncolytic viruses ... 42

2.5.1 Measles virus ... 48

2.6 Radiotherapy ... 55

2.7 Summary ... 60

3 Materials and methods ... 61

3.1 Reagents and media ... 61

3.2 Prepared media ... 64

3.3 Buffers ... 66

3.4 Cell lines ... 67

3.5 Tissue culture ... 68

3.6 Viral bulking and titration ... 69

3.6.1 Measles virus ... 69

3.6.2 Vesicular Stomatitis Virus ... 70

3.7 Flow cytometry ... 70

3.8 Flow cytometry antibodies ... 71

3.9 Enzyme linked Immunosorbent assays (ELISA) ... 71

3.10 ELISA antibody dilutions and recombinant standards ... 73

3.11 Human in vitro experiments ... 74

3.11.1 Viability assays 74
3.11.1.1 Live/Dead® assay 74
3.11.1.2 Methylthiazolyldiphenyl-tetrazolium bromide, MTT 74
3.11.2 Western blots 74
3.11.3 Multilayer models 75
3.11.4 Confocal Microscopy 75
3.11.5 Isolation of human peripheral blood mononuclear cells and magnetically-activated cell sorting (MACS) 76
3.11.6 Preparation of human dendritic cells 76
3.11.7 HLA-A2 phenotyping of blood cells 77
3.11.8 DC cultured with filtered tumour conditioned media (TCM) 77
3.11.9 Preparation of DC-Mel888 cocultures 77
3.11.10 Preparation of priming cultures 78
3.11.11 CD107 assay 78
3.11.12 Intracellular IFNγ 78
3.11.13 Chromium release assay 79
3.12 Mouse in vitro experiments 80
3.12.1 Preparation of murine cells 80
3.12.2 MACS selections 80
3.12.3 T-cell activation 80
3.12.4 Discrimination of host lymphocytes from adoptively transferred cells 80
3.12.5 Intracellular IFN in response to antigen stimulation 81
3.13 Mouse In vivo experiments 81
3.13.1 Basic procedures 82
3.13.2 Therapeutic administrations 82
3.13.3 Radiotherapy 83
3.13.4 Brachytherapy 83
3.13.5 Intracerebral tumour implantation. 84
4 Measles virus versus melanoma 86
4.1 Introduction 86
4.2 Results 87
4.2.1 CD46 expression on melanoma cell lines 87
4.2.2 Morphological changes following MV treatment. 90
4.2.3 Viability assays following MV treatment 99
4.2.4 Viral replication 104
4.2.5 Characteristics of MV-induced melanoma cell death 106

4.2.6 Human melanoma primary cells 114
4.2.7 3-dimensional culture models 118
4.2.8 Actions of MV on elements of the innate immune system 122
4.2.9 Actions of MV on Dendritic cells 126
4.2.10 Actions of MV upon the Adaptive anti-tumour immune response 132
4.2.10.1 CD107 assays 133
4.2.10.2 Intracellular IFNγ 133
4.2.10.3 Chromium release assay 138
4.2.10.4 Pentamer staining 139
4.3 Discussion 141

5 Enhancing the combination of adoptive cell therapies and virotherapies with the addition of local radiotherapy 146
5.1 Introduction 146
5.2 Results 148
5.2.1 Combinations of systemic oncolytic virus, ACT and RT 148
5.2.2 Optimal timings of combination therapy 153
5.2.3 The persistence of adoptively transferred T-cells 158
5.2.4 Total body irradiation 162
5.2.5 Pmel + VSV-gp100 168
5.2.6 Brachytherapy 174
5.3 Discussion 180

6 Developing a model of intracranial melanoma 183
6.1 Introduction 183
6.1.1 The Blood-brain barrier (BBB) 183
6.1.2 Existing models of intracranial disease 185
6.1.3 Adaptation of a previously described method 187
6.2 Results 190
6.2.1 Characteristics of the model 190
6.2.2 Tolerability 192
6.2.3 Monitoring tumour burden 192
6.2.4 Immunohistochemistry 194
6.2.5 Magnetic resonance imaging 194
6.2.6 Therapy studies 197
6.3 Discussion 200

7 Summary and conclusions 203

8 References.....208

9 Appendices.....233

9.1 Max Perutz submissions.....233

9.2 SET for Britain poster 2012.....239

9.3 Publications.....241

1.5 Table of figures

Figure 1. Melanoma cases (1975-2010) 21
Figure 2. Preponderance of melanoma in younger people 24
Figure 3. Inhibition of the immunological synapses 28
Figure 4. Immune editing of tumours 30
Figure 5. The evolution of T-cell receptors in adoptive cell therapy 38
Figure 6. OV-treatment of tumours leads to adaptive anti-tumour immune responses 46
Figure 7. The measles virion 51
Figure 8. Immunologically relevant extra-nuclear effects of radiotherapy 58
Figure 9. CD46 expression on melanoma cell lines 89
Figure 10. Cytopathic effect of MV upon Mel888 91
Figure 11. GFP expression in Mel888 treated with MV-GFP 92
Figure 12. Cytopathic effect of MV upon Mel624 93
Figure 13. GFP expression in Mel624 treated with MV-GFP 94
Figure 14. Cytopathic effect of MV upon MeWO 95
Figure 15. GFP expression in MeWO treated with MV-GFP 96
Figure 16. Cytopathic effect of MV upon SkMel28 97
Figure 17. GFP expression in SkMel28 treated with MV-GFP 98
Figure 18. Oncolytic activity of MV against melanoma cell lines (Live/Dead) 100
Figure 19. Oncolytic activity of MV against melanoma cell lines (MTT) 103
Figure 20. Viral replication 105
Figure 21. Cytokine release by melanoma after treatment with MV 109
Figure 22. IFN release by melanoma after treatment with MV 110
Figure 23. Detection of HMGB1 by Western blot 112
Figure 24. HMGB1 release from cells following treatment with MV 113
Figure 25. Human melanoma primary cells 116
Figure 26. The effects of MV upon human melanoma primary cells 117
Figure 27. Multilayer model of melanoma 119
Figure 28. MV efficacy in a multilayer model of melanoma 121
Figure 29. Stimulation of innate effectors by MV 124
Figure 30. Stimulation of NK cells by MV 125
Figure 31. Susceptibility of DC to treatment with MV 127

Figure 32. Effects of MV-treated melanoma supernatant on DC....130
Figure 33. Effects of MV-treated melanoma cells on DC....131
Figure 34. Schematic representation of priming assays....135
Figure 35. Priming assays: Surface expression of CD107 following treatment with MV....136
Figure 36. Priming assays: IFNγ response following treatment with MV....137
Figure 37. Priming assays: Lysis of melanoma by CTL in response to MV treatment....140
Figure 38. Proposed trial design....145
Figure 39. Combination of 8 Gy, ACT and virotherapy....149
Figure 40. Survival following combinations of 8 Gy, ACT and virotherapy....150
Figure 41. Combination of 4 Gy, ACT and virotherapy....151
Figure 42. Survival following combinations of 4 Gy, ACT and virotherapy....152
Figure 43. Optimising the timings of therapy....154
Figure 44. Optimising the timings of therapy (survival)....155
Figure 45. Optimising the timings of therapy....156
Figure 46. Optimising the timings of therapy (survival)....157
Figure 47. Persistence of adoptively transferred cells....160
Figure 48. IFN production from TDLN CD8+ T-cells....161
Figure 49. Whole body versus local irradiation....164
Figure 50. Survival following whole body versus local irradiation....165
Figure 51. Combinations of whole body and local irradiation....166
Figure 52. Survival following combinations of whole body & local irradiation....167
Figure 53. Local or whole body RT plus Pmel and VSV-gp100....170
Figure 54. Survival following local or whole body RT plus Pmel & VSV-gp100....171
Figure 55. Local or whole body RT plus naïve Pmel & iv VSV-gp100....172
Figure 56. Local or whole body RT plus activated Pmel and iv VSV-gp100....173
Figure 57. Development of brachytherapy....177
Figure 58. The effect of brachytherapy on B16-Ova tumours....178
Figure 59. Brachytherapy in combination with virotherapy & adoptive cell therapy....179
Figure 60. Stereotactic injection of tumour cells....189
Figure 61. Characteristics of the intracranial melanoma model....191

Figure 62. High frequency ultrasound of intracranially injected B16 melanoma 193
Figure 63. MRI images following intracranial injection of B16-Ova 196
Figure 64. Pilot studies of therapeutic strategies in the intracranial model of metastatic melanoma 199

1.6 Abbreviations

AACR	American Association of Cancer Research
ACT	Adoptive cell therapy
APC	Antigen presenting cells
ARRIVE	Animal research: reporting in vivo experiments guidelines
ATCC	American type culture collection
BBB	Blood-brain barrier
BHK	Baby hamster kidney
CART	Chimeric antigen receptor T-cells
CCL21	Chemokine (C-C motif) ligand 21
CD	Cluster of differentiation
CEA	Carcinoembryonic antigen
CLL	Chronic lymphocytic leukaemia
CNS	Central nervous system
CPE	Cytopathic effects
CPM	Counts per minute
CRUK	Cancer Research UK
CT	Computed tomography
CTL	Cytotoxic T lymphocytes
CTLA4	Cytotoxic T lymphocyte-associated antigen 4
DC	Dendritic cell
DICOM	Digital imaging and communications in medicine
DMEM	Dulbecco's modified Eagle's media
DMSO	Dimethylsulfoxide
DNA	Deoxyribonucleic acid
EBRT	External beam radiotherapy
EGFR	Epidermal growth factor receptor
ELISA	Enzyme linked immunosorbent assay
ESMO	European society of medical oncology
ESO	European society of oncology
F	MV fusion protein
FACS	Fluorescence activated cell sorting

FCS	Foetal calf serum
FITC	Fluorescein isothiocyanate
FoxP3	Forkhead box P3
GFP	Green fluorescent protein
GM-CSF	Granulocyte macrophage colony-stimulating factor
gp100	Glycoprotein 100
H	MV haemagglutinin protein
H&E	Haematoxylin and eosin
HBSS	Hank's balanced saline solution
HLA	Human leukocyte antigen
HMGB1	High mobility group box 1
HPV	Human papilloma virus
HSV	Herpes simplex virus
i.c.	Intracranial
ICA	Intra-carotid arterial injection
ICP34.5	Infected cell protein 34.5
IDO	Indoleamine 2,3 dioxygenase
IFN	Interferon
IHC	Immunohistochemistry
IL	Interleukin
IMDM	Iscove's modified Dulbecco's medium
ip	Intraperitoneal
iv	Intravenous
L	MV large protein
LPS	Lipopolysaccharide
M	MV matrix protein
MACS	Magnetic activated cell sorting
MART1	Melanoma antigen recognised by T-cells
MDSC	Myeloid derived suppressor cells
MFI	Median fluorescence intensity
MHC	Major histocompatibility complex
MOI	Multiplicity of infection
MRI	Magnetic resonance imaging

MTT	Methylthiazolyldiphenyl tetrazolium bromide
MV	Measles virus (Edmonston strain)
MW	Molecular weight
N	MV nucleocapsid protein
NAP	Neutrophil activating protein
NARA	Neutralising anti-reovirus antibodies
NCI	National cancer institute
NIS	Sodium-Iodide symporter
NK	Natural Killer
NMR	Nuclear magnetic resonance
OV	Oncolytic viruses
Ova	Ovalbumin
P	MV phosphoprotein
PBMC	Peripheral blood mononuclear cells
PBS	Phosphate buffered saline
PCR	Polymerase chain reaction
PD1	Programmed cell death 1
PDL1	Programmed cell death 1 ligand 1
PE	Phycoerythrin
PET	Positron emission tomography
PFA	Paraformaldehyde
RAG	Recombination activating gene
RANTES	Regulated and normal T-cell expressed and secreted
RECIST	Radiological
RNA	Ribonucleic acid
RNP	Ribonucleoprotein
RPMI	Roswell Park Memorial Institute medium
RT	Radiotherapy
s.c.	Subcutaneous
SBRT	Stereotactic body radiotherapy
scFv	Single-chain variable region antibody fragments
SCID	Severe combined immunodeficiency
SEM	Standard error of the mean

SLAM	Signalling lymphocyte-activation molecule
SMO	Smoothened
SPECT	Single photon emission computed tomography
T-cell	Thymic derived lymphocyte
T-regs	Regulatory T-cells
TAA	Tumour associated antigen
TBI	Total body irradiation
TCID50	Tissue culture infectious dose 50%
TCM	Tumour-conditioned media
TCR	T-cell receptor
TDLN	Tumour-draining lymph nodes
Th1	T-helper 1
TIL	Tumour-infiltrating lymphocytes
TLR	Toll-like receptor
TNF	Tumour necrosis factor
TW	Transwells
UV	Ultraviolet
VRS	Virchow-Robin space
VSV	Vesicular stomatitis virus
wtMV	Wildtype measles virus (Pathogenic strain)

2 Introduction

Efforts to generate anti-tumour immune responses in cancer patients have been studied for over a hundred years, but many scientists and clinicians were (or are) profoundly sceptical that such efforts could ever be fruitful. Janeway and pre-Janeway models of the immune system suggested that the immune system would not and could not act against tumours derived from host cells. The broadly equal incidence of tumours amongst immunosuppressed versus immune-competent patients supported such pessimism. Several developments have challenged that view, but most compellingly the recent emergence of Ipilimumab as an effective melanoma treatment has confirmed that the immune system can be compelled to act against tumours and produce real benefits for patients with cancer.

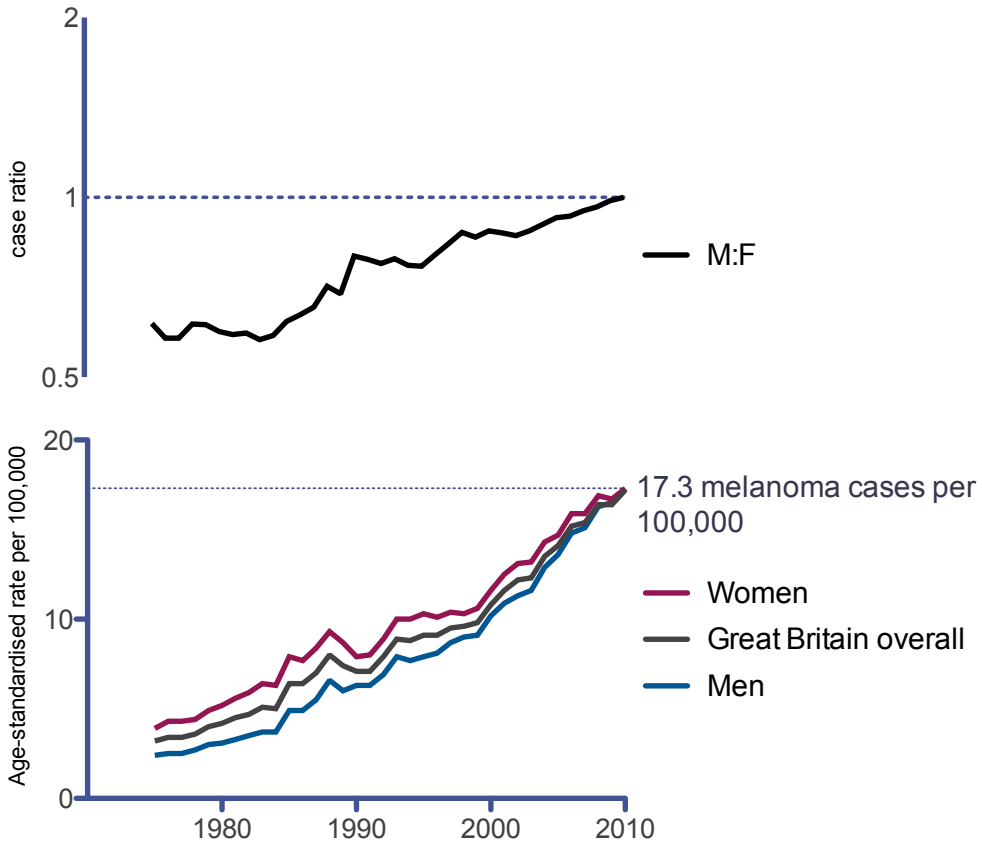

Figure 1. Melanoma cases (1975-2010). A. Cases of melanoma in men have caught up with those occurring in women. B. Age-standardised rates show consistent increases, in both men and women, over at least 35 years. Data obtained from CRUK CancerStats website, originally derived from the Office of National statistics, the Welsh Cancer Intelligence and Surveillance Unit and the Information Services Division Scotland.

2.1 Melanoma

Melanoma is a malignancy derived from melanocytic cells. Though melanomas most commonly develop in the skin, melanocytes have their embryological origin in the neural crest, and therefore non-cutaneous melanomas may also arise in the eye, alimentary tract and meninges. Unlike the other skin cancers, melanoma has a strong proclivity toward metastasis, even from small primary tumours. Macroscopically, cutaneous melanomas tend to be heavily pigmented, though amelanotic lesions are not uncommon. Melanomas are recognised clinically as asymmetric lesions with irregular borders and variegated pigmentation, as well as the size and evolution over time of the lesion, and to no small degree, a clinician's experience. There are numerous subtypes of melanoma, associated with differing behaviours and prognoses, which are based on specialist histological examination (Garbe et al., 2012). An important element of the histological assessment is to measure the depth of invasion, which is critical in determining the stage (Balch et al., 2009).

12,818 people were diagnosed with melanoma in the UK in 2010 (CRUK website, accessed 2012-09-23). The age-standardised rate has risen over the last 35 years, with a dramatic rise in the last decade (Figure 1). Historically melanoma more commonly affected women than men, but the gender imbalance has recently resolved and melanoma is now the 6th most common cancer diagnosis for each, and the fifth overall. The incidence has increased more rapidly than any of the other common cancers, particularly during the last decade, and not simply due to increasing public awareness or early presentation (Lee and Weinstock, 2009; Linos et al., 2009).

As with most cancers the age-specific rate of melanoma increases decade-by-decade (Figure 2). However the increase begins earlier in life than the other common cancers; as a fraction of the age-specific rate for all cancers, melanoma peaks in the third decade for women and the fourth to fifth decades for men (Figure 2B). Because of this early emergence, melanoma is the second commonest cancer of women between 15 and 49 years, after breast cancer, and

second only to testicular amongst men of the same ages (CRUK website). Of course in absolute numbers most cases still occur in older people (Figure 2C).

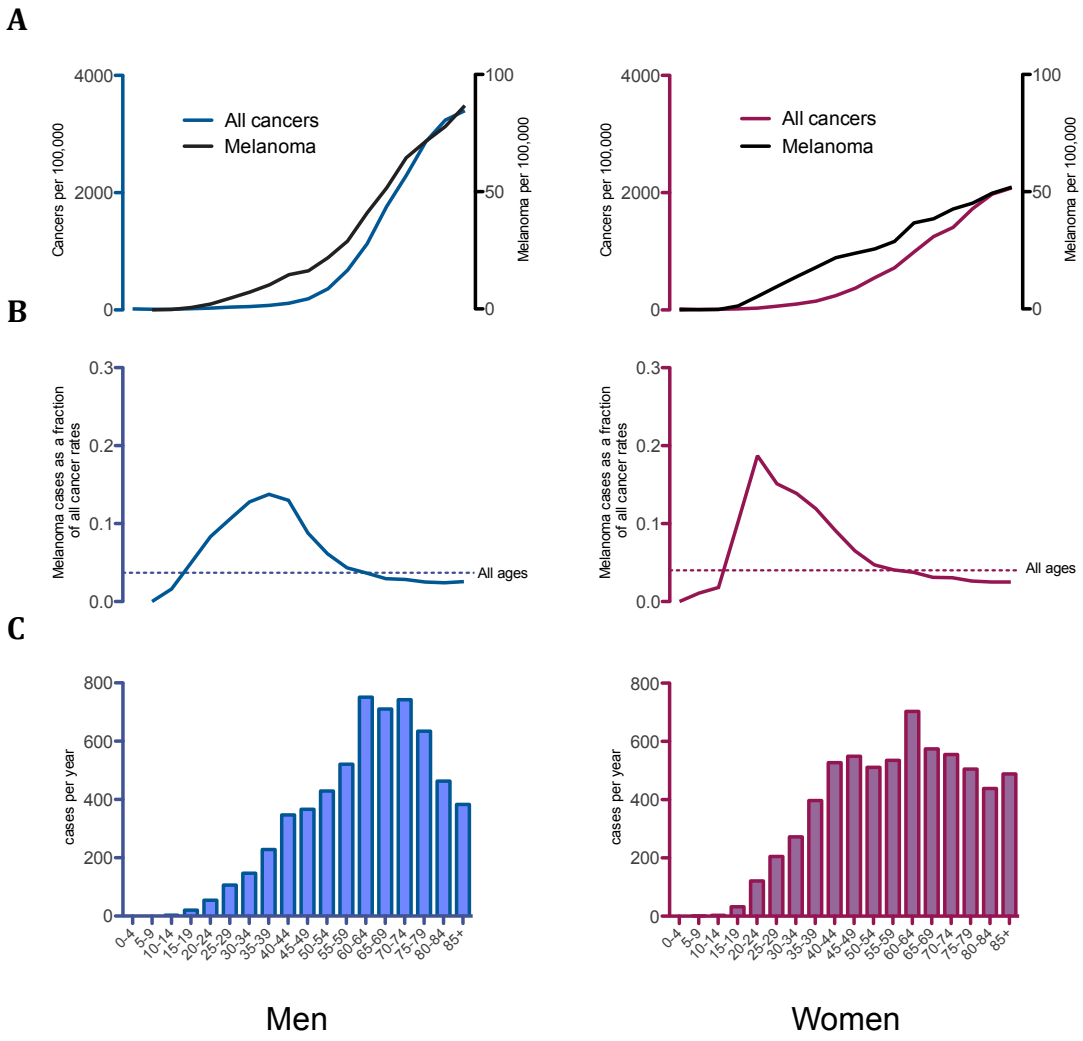

Figure 2. Preponderance of melanoma in younger people. A. Melanoma rates increase with age, in common with other cancers, however there is a relative preponderance of the cancer in younger age groups, in contrast to other cancers (note the differing scales of each axis). B. The age-specific rate of melanoma is expressed as a fraction of the age-specific rate of all cancers and illustrates the early emergence of melanoma compared to other cancers. C. The absolute number of melanoma cases per year in each age group. Data obtained from the CRUK CancerStats website, originally derived from the Office of National statistics, the Welsh Cancer Intelligence and Surveillance Unit and the Information Services Division Scotland.

The aetiology of melanoma is multifactorial though exposure to UV radiation is a likely (Menzies, 2008), albeit controversial (Shuster, 2008), risk factor. Sunbed-use is widely implicated as potentially causative (Boniol et al., 2012), despite some evidence to the contrary (Elliott et al., 2012). Certainly melanoma is more common wherever there is confluence of fair-skinned Caucasians with high-levels of sunlight (Garbe et al., 2012).

A family history of melanoma increases an individual's risk, but such cases may only contribute to less than 10% of the burden of disease (Olsen et al., 2010). Familial atypical multiple mole-melanoma syndrome is the most common familial syndrome, though others such as xeroderma pigmentosum and albinism also lead to melanomas (Bonadies and Bale, 2011).

Although early-stage melanomas are commonly cured by surgical excision, locally advanced or metastatic melanoma has a dismal prognosis. The survival of patients with melanoma varies from 97% at five years for patients with small, easily resected tumours, through to 33% at one year for patients with the most advanced metastatic disease (Balch et al., 2009). One UK cancer registry has reported that 20% of patients aged 65 or over were found to be stage III or IV at the time of diagnosis, though the rate was 7% amongst younger patients (Eastern Cancer Registration and Information service, cited on the CRUK website).
Surgery or radiotherapy are commonly used to control limited volumes of metastatic disease in order to allay symptoms, and in some situations to improve survival, but systemic treatments are the mainstay of treatment for metastatic melanoma (Garbe et al., 2012).

Chemotherapy for melanoma continues to be used, commonly dacarbazine or temozolomide, despite a limited response rate (13-20%) and no improvement in survival (Eggermont and Kirkwood, 2004). Treatments with immunomodulatory agents such as recombinant interferon alpha 2b (IFNα2b) or interleukin-2 (IL2) have been attempted. Both are associated with significant toxicity and minimal survival benefits in the adjuvant setting (Tsao et al., 2004). Metastatic melanoma

has been treated with intravenous IL2, with one trial achieving a response rate of 16%; moreover some patients benefited from enduring complete responses (Atkins et al., 1999). Unfortunately treatment with IL2 is profoundly toxic and given the low rates of significant clinical benefit, and cost, its use has not become routine.

Ipilimumab is a human monoclonal antibody directed against CTLA-4 (cytotoxic T lymphocyte-associated antigen-4). In the process of CD8+ T-cell stimulation, dendritic cells (DC) present antigen to the T-cell receptor in the context of MHC class I, along with co-stimulatory signals (including B7.1/CD80 and B7.2/CD86). The co-stimulatory, or 'second', signals are recognised by CD28 on the T-cell, triggering activation as shown in Figure 3A. The activated T-cell will then begin to upregulate surface expression of an inhibitory molecule – CTLA-4. CTLA-4 competes with CD28 for the B7 markers and in so doing terminates T-cell activation, acting to regulate cytotoxic T-cell responses. Inhibition of CTLA-4 by Ipilimumab maintains T-cell activation and resulted in objective responses in around 15% of patients with metastatic melanoma, and prolonged survival by two to three months (Figure 3B) (Hodi et al., 2010; O'Day et al., 2010; Ribas, 2012). The action of Ipilimumab is not specific to anti-melanoma lymphocytes and therefore its major limitation is the generation of significant autoimmune toxicities, which can be life-threatening (Attia et al., 2005; Berthod et al., 2012). Several autoimmune manifestations are already well recognised and include hepatitis, vitiligo and dermatitis, and enterocolitis.

Melanoma frequently metastasises to the brain; isolated metastases may be resected, and limited numbers of small metastases may be treated by stereotactic radiosurgery (personal communication, Dr P. Hatfield, 2012). Melanoma brain metastases are associated with very poor outcomes, and as such are often an exclusion criteria in clinical trials, however there has been a report of a small study showing some efficacy of ipilimumab in this setting (Margolin et al., 2012). Further work to identify therapies that continue to be effective for intracranial disease is clearly needed.

For several decades researchers and clinicians have trialled several immunotherapeutic approaches in the treatment of melanoma, but without ever

reliably improving on the existing standard of care. Ipilimumab was the first therapy shown in randomised clinical trials to prolong survival in patients with metastatic melanoma. It is a toxic therapy for many patients, and the response rate is relatively low, but its efficacy further asserts that the immune system can be coerced into yielding significant benefits for patients with melanoma.

The first ever report of an effective therapy in the treatment of metastatic melanoma was followed within months by another (Donnelly et al., 2012b). Vemurafenib is an inhibitor of mutated forms of BRAF, present in around half of metastatic melanomas. Half the patients treated with vemurafenib benefited from objective responses, and early analysis suggests a 3-month improvement in progression-free survival (Chapman et al., 2011).

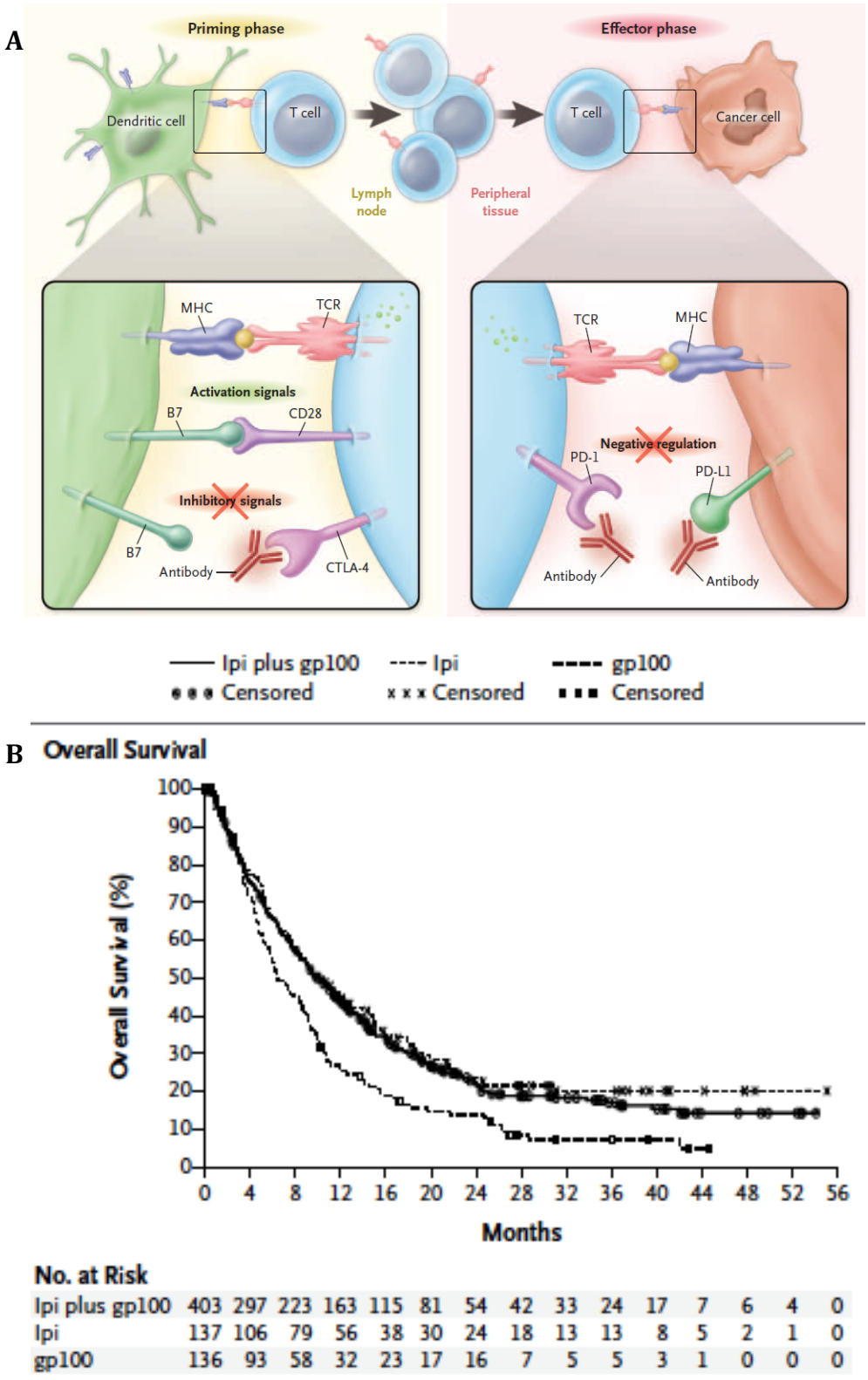

Figure 3. Inhibition of the immunological synapses. A. Schematic illustrating the synapse between DC and lymphocytes, and lymphocytes with their targets. Both CTLA-4 and PD1/PDL1 serve to regulate T-cell responses; accordingly inhibitory antibodies can enhance anti-tumour immune responses. B. Phase III clinical testing of Ipilimumab, an anti-CTLA4 monoclonal antibody, improved survival in patients with metastatic melanoma.
Figures reproduced with permission from; [Ribas, Antoni. "Tumor Immunotherapy Directed at PD-1." *New England Journal of Medicine* 366, no. 26 (June 28, 2012): 2517–2519.] and [Hodi, F. et al. "Improved Survival with Ipilimumab in Patients with Metastatic Melanoma." *N Engl J Med* 363, no.8 (June 14, 2010) 711-723.], both copyright Massachusetts Medical Society.

2.2 Immunology of Cancer

Most cancers arise in patients possessed of perfectly normal immune systems, and most cancers arise from previously normal, autologous cells. Unsurprisingly then, the existence or absence of a role for the immune system in cancer development and elimination was controversial for a long time (Dunn et al., 2002). However the theories of immunoediting and immunosurveillance are increasingly accepted, and the recent re-drafting by Hanahan and Weinberg of their seminal hallmarks of cancer seems to have cemented the importance of the immune system(Hanahan and Weinberg, 2011; Finn, 2012). Emerging autochthonous cancers are recognised by innate immune effector cells. Innate cells such as NK-cells will destroy cancers cells, releasing cellular debris for processing by antigen presenting cells, which in turn can activate an adaptive immune response, specific for tumour-associated antigens (Kim et al., 2007; Finn, 2012). The immune system has the upper hand against these small emerging tumours and may successfully eliminate the tumour at this point; if so then it is intriguing to speculate on the number of initiated cancers that never successfully emerge as detectable tumours (Dunn et al., 2002). However if the immune system fails to eliminate the cancer then tumours and the immune system likely exist in a state of equilibrium; the immune system unable to eradicate the tumour completely and the tumour unable to outgrow without re-activating innate and adaptive responses (Dunn et al., 2002). In the process all outgrowing tumour clones that are sufficiently immunogenic are eliminated, and only immunologically-muted outgrowths will succeed; thus tumours that do eventually escape control in immune-competent hosts have effectively evolved to evade immune responses, so-called immune editing (Prestwich et al., 2008a). The preclinical model which most elegantly supports this theory used immune competent and immune incompetent mice (Shankaran et al., 2001). Tumours were elicited in mice following subcutaneous injection of the mutagen methylcholanthrene, and arose more commonly and more quickly in mice deficient for lymphocytes or interferon pathways, or both, when compared to wild type mice of the same strain. Tumours arising in the knockout mice without fully functioning immune systems, when transplanted to syngeneic mice with normal immune systems, failed to grow (Figure 4).

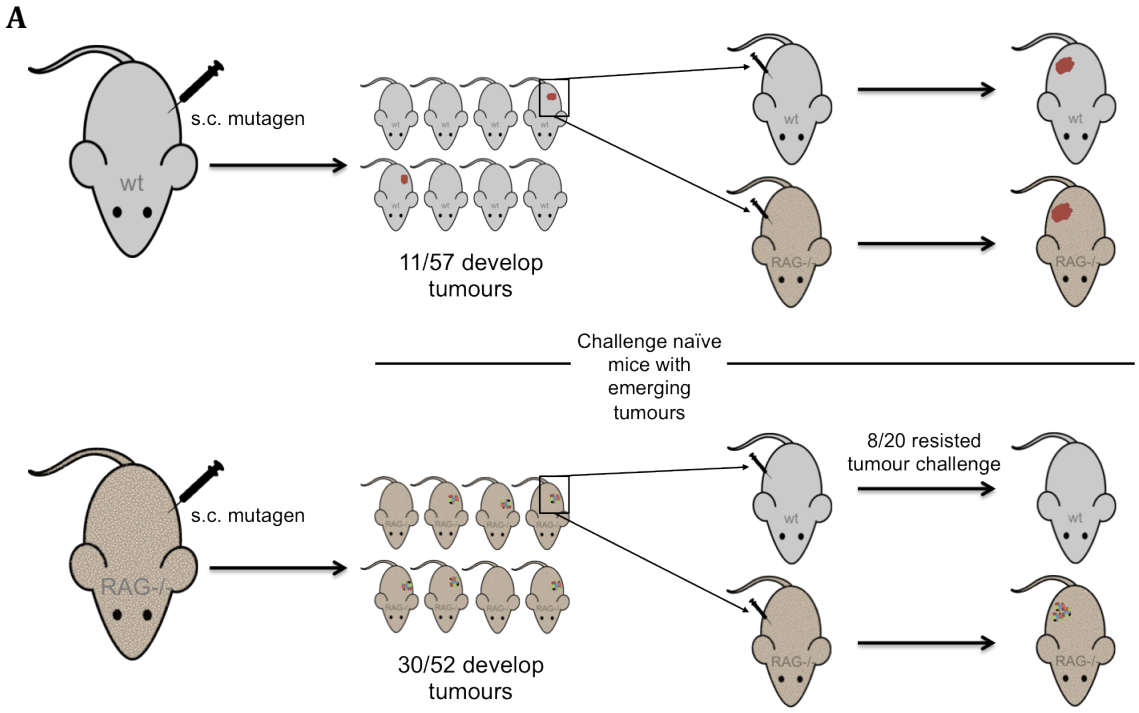

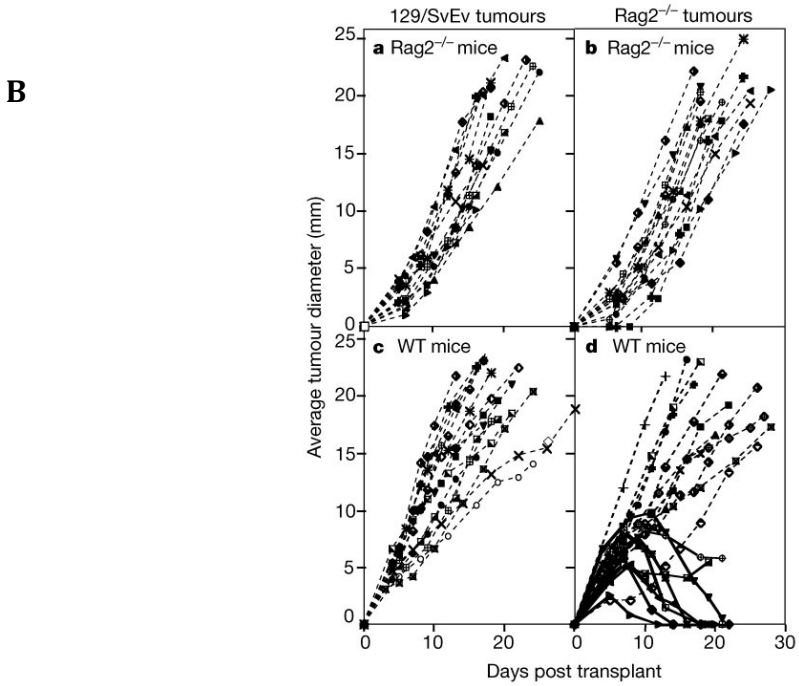

Figure 4. Immune editing of tumours. A. Shankaran et al. injected mice with subcutaneous mutagen and monitored the animals for the development of sarcomatous tumours. Tumours developed in wildtype mice, but they were slower to emerge, and less frequent, than in syngeneic mice lacking functional lymphocytes (RAG-/- knockout mice). When the tumours were harvested and reinjected into naïve mice, of each strain, wildtype mice were found to be resistant to tumours from RAG-/- mice. These data suggest that tumours developing in immunodeficient mice retain their immunogenicity, whereas those that are able to emerge in an immunocompetent host have been 'edited' by the immune system resulting in immunologically silent tumours. B. Figure taken from the original paper described above, showing the kinetics of the emerging tumours. Solid lines indicate tumours that completely regressed.
Figure 4B reprinted by permission from MacMillan Publishers Ltd. Shankaran, et al. "IFNγ and Lymphocytes Prevent Primary Tumour Development and Shape Tumour Immunogenicity." *Nature* 410, no. 6832 (April 26, 2001): 1107–1111.

Tumours that do successfully evade competent immune systems do so in a number of ways. Tumours commonly obscure their antigens from immune examination by downregulating MHC class I expression and interrupting antigen processing and MHC loading pathways (Meissner et al., 2005; Zitvogel et al., 2006; Campoli and Ferrone, 2008). Low expression of class I molecules can leave cells vulnerable to innate attack, but tumour cells can resist at least one of the established cell killing mechanisms that lymphocytes employ by expressing inhibitors of granzyme B, and are also able to release the ligands that Natural Killer cells (NK) principally use to recognise their targets (Bladergroen et al., 2002; Groh et al., 2002). Furthermore the function of incoming lymphocytes is attacked by tumour cells, which express Fas ligand (CD95L) on their surface, and simultaneously downregulate their own expression of the Fas receptor (Real et al., 2001; Whiteside, 2002). Moreover by reducing expression of adhesion molecules present on the intimal surface of tumour vasculature the ability of immune cells to enter tumours is diminished (Castermans and Griffioen, 2007; Wu, 2007; Schmidt et al., 2012).

Tumours also release cytokines and other soluble mediators that either deter immune cells, or impede their function, including indoleamine 2,3 dioxygenase (IDO) (Uyttenhove et al., 2003). IDO is an enzyme that degrades tryptophan, leading to local depletion of the essential amino acid which in turn inhibits T-cell proliferation (Curti et al., 2009). It is worth noting that examining the role of these factors in isolation can lead to mixed results, and cytokines may have starkly contrasting effects systemically or locally (Teng et al., 2011). A study in 2002 found colorectal tumour cells transfected to overexpress interleukin-10 (IL10) inhibited systemic immunity (Kawamura et al., 2002). Contrastingly a more recent study found that IL10 contributes to successful immunosurveillance of tumours by upregulating MHC class I, and pegylated IL10 caused regression of established tumours in vivo, recruiting CD8+ T-cells to the tumours (Mumm et al., 2011).

Architectural or organisational changes can also modify the effects of a competent immune system. CCL21-expressing melanoma tumours in mice, despite recruiting more leukocytes and APC grew to be much larger than the same tumour cell line expressing lower levels of CCL21 (Shields et al., 2010). The

authors found that CCL21 drove tumours to adopt a phenotype that mimics the stroma of lymph nodes, recruiting suppressive immune cells, which in turn promoted tolerogenic responses.

The role of host immune cells subverted to suppress other immune cells is well recognised. The CD25+ subset of CD4+ T-cells makes up around 10% of circulating CD4+ cells and plays a key role in diminishing anti-tumour immunity. Mice deficient for CD4+CD25+ cells develop a broad spectrum of autoimmune disorders indicating that these regulatory T-cells (T-regs), manage the homeostasis of immune responses (Dranoff, 2005). Levels of circulating CD4+CD25+ T-regs were considerably higher in patients with metastatic melanoma when compared to healthy volunteers, or patients with early stage melanomas, though the relative importance of circulating and tumoural T-regs remains unclear (McCarter et al., 2007). A further marker, FoxP3 is clearly important in identifying these suppressive lymphocytes, and has been associated with a poorer prognosis in patients with ovarian cancer, though FoxP3 is a less clear cut marker of suppressive cells in humans than it is in mice (Curiel et al., 2004; Vries et al., 2011). The mechanisms by which T-regs exert their effects are varied, but include secretion of inhibitory cytokines and direct effects on DC, such as inducing their expression of IDO and inhibiting expression of the costimulatory receptors (Sakaguchi et al., 2009).

A further species of cell that tumours recruit to protect themselves from immune responses are the myeloid-derived suppressor cells (MDSC) (Gabrilovich and Nagaraj, 2009). MDSC suppress by a range of actions, predominantly contact-dependent, and including stimulating the generation of T-regs (Lechner et al., 2010). Myeloid-derived cells have also been shown to contribute to tumour recovery in mice, after therapeutic radiotherapy (Kozin et al., 2010). Although MDSC have certainly been demonstrated to be present in increased numbers in cancer patients, some evidence suggests that their importance in humans in vivo is somewhat less than that observed in mice; given the challenges of identifying the various subsets of MDSC, across both species, further correlative studies will be needed to confirm that assertion (Gros et al., 2012).

2.2.1 Tumour-associated antigens

The notion that the immune system serves only to distinguish between native antigen (self) and alien antigen (non-self), was rebuffed by Matzinger's refinement of the immunological model, which sought to explain the prevalence of autoimmune diseases (Matzinger, 1994). Matzinger's danger hypothesis asserted that the immune system processes antigen, in part at least, according to the environment in which it is encountered (Matzinger, 2002). Accordingly, although all non-virally initiated cancers would be expected to express only native antigens, those antigens can yield immune responses if they are processed in an immunologically 'dangerous' context (Offringa, 2009).

Tumour-associated antigens (TAA) have been categorised as follows (Buonaguro et al., 2011; Restifo et al., 2012):

- **Unique TAA** (formerly tumour-specific antigens) are the product of gene mutations confined to transformed cells and therefore expressed only by cancer cells (Rommelfanger et al., 2012). Several antigens once thought to be tumour-specific have subsequently been identified from other, non-transformed sources, hence the altered nomenclature.
- **Differentiation antigens** are persisting markers of the cancer's tissue of origin. In melanoma these antigens are often considered acceptable targets, however for most other tumour sites targeting these antigens could result in unacceptable toxicity.
- **Cancer-testis antigens** are expressed on normal cells during embryological development but are subsequently lost until cancer mutations revive their expression. They may continue to be expressed in germ cells but immunological privilege (absent expression of MHC) allows for targeting of these antigens with minimal risk of toxicity (Restifo et al., 2012).
- **Widely-occurring overexpressed antigens** are expressed on several normal cell types but are aberrantly overexpressed on cancer cells, allowing some distinction of tumour from healthy tissues. p53, Her2 and Survivin are examples (Buonaguro et al., 2011).
- **Viral antigens** may be expressed in tumours resulting from oncogenic viruses such as Epstein-Barr or HPV.

It must be remembered that successfully generating a response against any of these antigens carries the risk of causing coincident autoimmune toxicities, if the antigen is expressed elsewhere in the host.

2.2.2 Immunology of melanoma

Melanoma is widely considered to be a particularly immunogenic tumour, even though some suggest that perception was borne more of necessity than rigorous analysis (Houghton et al., 2001). Nevertheless human and murine melanomas are commonly used in preclinical models, both in vitro and in vivo, of tumour immunology and immunotherapies, probably for practical reasons as much as immunological. The relative accessibility of many metastatic melanoma lesions, and the paucity of treatment options hitherto available mean that human tissue has often been widely available for study, and topical mutagens allowed the development of murine melanoma cell lines. Accordingly numerous reagents have been developed and are commercially available for the study of melanoma immunology, perhaps more so than most other tumour sites. Moreover the lack of effective therapies and the significant numbers of young patients probably enhance recruitment to trials for metastatic melanoma relative to some other tumour sites (Houghton et al., 2001; Maio, 2012).
Practical considerations aside there is certainly evidence that melanoma is a paragon tumour with which to study potential immunotherapies:

- Spontaneous and complete tumour regressions have been reported in melanoma primaries, and some degree of regression is quite commonly evident on histological examination of resected melanoma primary lesions (Menzies and McCarthy, 1997; Martires KJ, 2012).
- Despite cost, low response rates and toxicity precluding widespread use, clinicians making use of interleukin-2 (IL2), interferon-α (IFNα) and adoptive cell therapy (ACT) have convincingly adduced that immune manipulations can impact on established metastatic melanoma (Atkins et al., 1999; Dudley and Rosenberg, 2003; Mocellin et al., 2010; Maio, 2012).

- Tumour-infiltrating lymphocytes (TIL) in melanoma lesions are associated with a better prognosis (Clemente et al., 1996; Mihm Jr et al., 1996).
- Numerous TAA have been, and continue to be, identified in melanoma (Houghton et al., 2001).

2.3 Adoptive cell therapy

Despite the numerous impediments to their function, lymphocytes capable of recognising a wide range of TAA are commonly present in tumours – TIL. Adoptive cell therapy (ACT) involves surgically excising a metastatic lesion (predominantly melanoma) then extracting the TIL and expanding them in culture with IL2 (Dudley and Rosenberg, 2003). The lymphocytes that are successfully expanded are examined for evidence of reactivity to TAA, prior to reinfusion into patients (Dudley et al., 2003). Current iterations of the approach include preconditioning patients before the lymphocyte infusion with combinations of chemotherapy and total body irradiation (up to 12 Gy) to deplete circulating lymphocytes that would otherwise compete for cytokines (Restifo et al., 2012). Lymphodepletion also allows homeostatic expansion of the infused lymphocytes.

Predominantly used for patients with metastatic melanoma, the therapy has impressive results. Over the course of three trials, enrolling 93 patients, Rosenberg reports complete responses in 20 patients, 19 of whom remained apparently free of disease at least 57 months later (Rosenberg et al., 2011; Restifo et al., 2012). Results outside the context of a randomised clinical trial must always be interpreted with caution, and by the authors' own admission these are carefully selected patients, but a 20% complete response rate in the context of heavily pretreated melanoma remains an astounding result.

There are significant limitations to the approach:

- Patients must have surgically accessible disease, and be fit enough to tolerate the surgical procedure required to obtain enough tissue.
- Ex vivo preparation of TIL is technically challenging, and around 50% of patients never receive treatment because the culture fails to yield enough lymphocytes for re-infusion (Dudley et al., 2003; Johnson et al., 2009).

- The conditioning regimens are extremely toxic, limiting the number of patients who are suitable for treatment. Rosenberg reports at least 1 treatment related death amongst 93 treated patients (Rosenberg et al., 2011).

Most concerning is the fact that despite longstanding experience at the National Cancer Institute in Bethesda, no other centre routinely performs ACT, suggesting that despite apparent efficacy for a subset of patients the therapy in its current form is simply impracticable for widespread use.

Rosenberg and others have attempted to refine ACT by developing T-cells engineered to express a defined T-cell receptor (TCR). The group cloned a TCR to the MART1 antigen (melanoma antigen recognised by T-cells, also known as Melan-A (Coulie et al., 1994; Kawakami et al., 1994)), from a patient who had experienced a good response after reinfusion of expanded TIL (Dudley et al., 2002; Hughes et al., 2005). Peripheral CD8+ lymphocytes collected from 31 patients were transfected with a retroviral vector expressing the anti-MART1 TCR (Morgan et al., 2006). Responses were seen in only 4 of the treated patients. A subsequent trial, using TCR with higher affinity for either MART1 or gp100, achieved responses in 9 of 36 treated patients, but at the cost of off-target toxicities (Johnson et al., 2009).

Despite the apparently reduced efficacy of this approach compared to TIL-based ACT (patients receiving engineered lymphocytes did not have the complete lymphodepleting regimen which improves the effectiveness of TIL-ACT), there are considerable potential advantages. Preparation of lymphocytes collected from peripheral blood is technically easier, and considerably more tolerable for patients than a surgical procedure to access tissue. The process is also quicker, as more lymphocytes can be collected, and less time is needed for ex vivo expansion. The therapy is based around the retroviral vector, which makes it considerably easier to implement in other centres, when compared to the particular expertise needed in the generation of activated tumour-antigen-specific TIL.

A limitation of the approach is that the vector used, and therefore the lymphocytes produced, are HLA-restricted, so either a panel of vectors must be

produced, or a significant proportion of patients will not be suitable for the therapy.

In order to circumvent that critical limitation other groups have developed the use of chimeric antigen receptors. These are receptors expressed on the surface of T-cells that recognise antigen using a single chain antibody fragment rather than TCR, in an HLA-independent manner. The first generation of chimeric antigen receptor T cells (CART) had the extracellular antibody fragment tethered to an intracellular CD3-ζ domain in order to stimulate T-cell functions (Brenner and Heslop, 2010). These first generation CART cells were limited by a lack of proliferation and survival in vivo, so subsequent vectors have encoded additional costimulatory signalling domains (Figure 5). In a recent report that has garnered much attention third generation CART cells, targeted against CD19, were given to patients with refractory CLL, resulting in improved blood counts and, in one patient, apparent tumour lysis syndrome (Kalos et al., 2011; Porter et al., 2011).

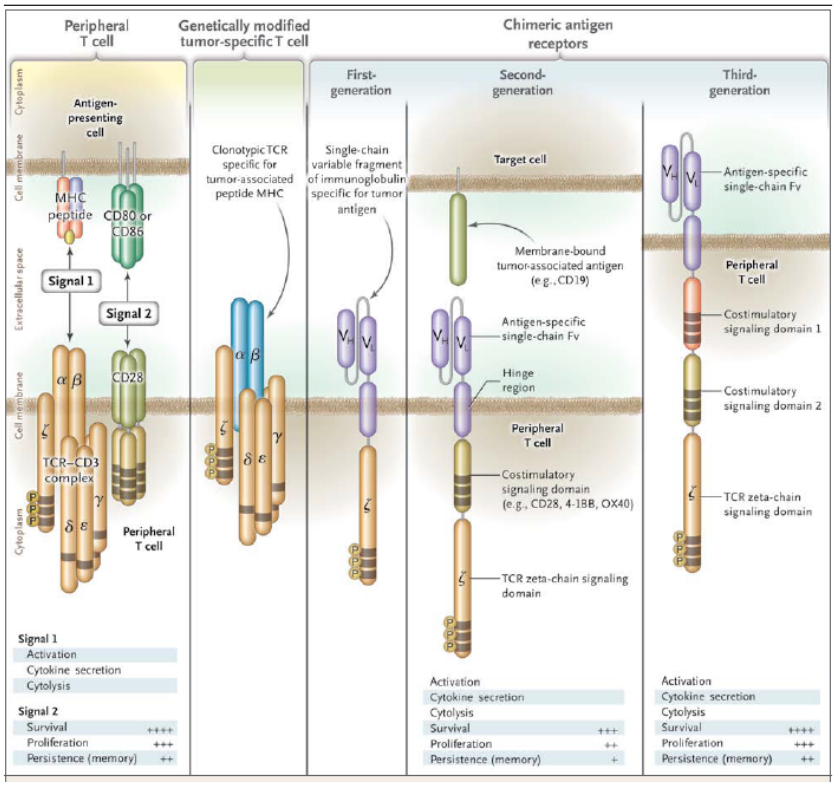

Figure 5. The evolution of T-cell receptors in adoptive cell therapy. Antigen recognition, whether presented by MHC molecules to the αβ chains of a native TCR, or recognised by the variable region of a single-chain antibody fragment doesn't stimulate T-cell proliferation unless accompanied by additional signals. Chimeric antigen receptors have developed to include additional intracellular signalling domains.

Reproduced with permission from Urba, WJ, and Longo, DL. "Redirecting T Cells." *The New England Journal of Medicine* 365, no. 8 (August 25, 2011): 754–757. copyright Massachusetts Medical Society.

2.4 The immune effects of conventional therapies

The concept of immunogenic cell death is emerging as an important mode of action for several existing cancer treatments (Golden et al., 2012). Cell death that releases tumour-associated antigens along with damage-associated molecular patterns or danger signals may mature DC or other APC to recruit anti-tumour immune responses. A significant amount of preclinical evidence now suggests that conventional therapies such as chemotherapy and radiotherapy, in addition to their canonical mechanisms, can cause inflammatory cell death that recruits immune responses (Zitvogel et al., 2008). Indeed in a number of models the efficacy of chemotherapy and radiotherapy are diminished in mice lacking elements of the immune response (Ma et al., 2010).

Much of the work in this areas has come from the groups of Guido Kroemer and Laurence Zitvogel, beginning with their finding, published in 2005, that chemotherapy-induced cell death could yield anti-tumour immune responses (Casares et al., 2005). The seminal publication from the group demonstrated that several chemotherapy agents, and local radiotherapy, killed cancer cells and in so doing stimulated the dying cells to release High Mobility Group Box 1 (HMGB1) (Apetoh et al., 2007b). HMGB1 is a potent danger signal that is recognised by the Toll-like receptor 4 (TLR4) within DC. DC are in turn activated to process and cross-present released TAA to T-cells. The paper went on to demonstrate that the generation of antitumour immunity as a result of immunogenic cell death was in fact a requisite of therapy, rather than just an incidental effect – mice deficient for TLR4 obtained considerably less benefit from chemotherapy or radiotherapy than the wildtype mice.

A previous paper from the same group found that a critical determinant of whether cell killing was immunogenic or not was the exposure, or not, of calreticulin on the surface of dying tumour cells (Obeid et al., 2007b). Exposed calreticulin on the external surface of cells acts as an ‘eat-me’ signal to phagocytic cells. Insult to the endoplasmic reticulum appeared to be the critical effect of therapies that yield immunogenic cell death and was independent of the efficiency of cell killing (Panaretakis et al., 2009).

One criticism of these findings has been that a relatively small number of groups have been able to demonstrate these effects. Ciampricotti et al. recently published a direct retort to the work of Zitvogel and Kroemer. Ciampricotti et al. reported that the effect of the immune system did not contribute to the efficacy of platinum-based chemotherapy in models of spontaneously-developing mammary tumours (Ciampricotti et al., 2012). No difference in the response to chemotherapy was seen in RAG knockout mice compared to RAG heterozygotes. The authors contend that their model is a far better mimic of the way that human tumours emerge, i.e. in the presence of a functioning immune system, and that the findings of Zitvogel and Kroemer are in part due to the artifice of using mutagens or implanting large numbers of immortalised tumour cells. Zitvogel and Kroemer were afforded an immediate right-to-reply, and in the same journal issue argued that the effects they had previously reported are likely to be extremely dependent on the therapy used, the tumour treated and host-related factors (Zitvogel and Kroemer, 2012). It is also worth noting that their 2006 paper included a retrospective analysis of 280 breast cancer patients, stratified according to TLR4 polymorphisms, which found worse progression-free survival after anthracycline-based chemotherapy for women with an aberrant TLR allele (Apetoh et al., 2007b).
A separate group reported that even Imatinib, the doyen of rationally designed molecular therapies, generates and relies upon immune responses; treatment with imatinib reduced tumour cell production of IDO in mice with gastrointestinal stroma tumours, and successful therapy was diminished when CD8+ T-cells were depleted (Balachandran et al., 2011).

Taken together these data suggest that careful selection of anticancer therapy could be combined with other strategies to yield more robust anti-tumour immunity than either alone. Moreover combining novel immune-based approaches with proven therapies is likely to be a more appealing strategy to patients and clinicians than simply testing new immunotherapies alone.
Some of the established methods by which a cancer will endeavour to evade and overcome host immune responses are described above, though of course more are known, and yet more are not – some of the mechanisms specifically

identified in murine melanoma, as opposed to other tumour types, are listed in Overwijk's review (Overwijk, 2005). What seems clear is that simply generating an adaptive response against a tumour antigen is unlikely to be sufficient; successful immunotherapy will presumably need to overcome tumour-mediated immune suppression, sometimes referred to as 'breaking tolerance' (Mapara and Sykes, 2004). Most of the mechanisms employed by a tumour are corruptions of normal systems in place to protect against inadvertent and inappropriate autoimmune responses, and therefore overcoming them has remained challenging. Notably the immunotherapies that have demonstrated efficacy, discussed above, have only produced benefits for a small proportion of the patients treated, but often profound benefits for that minority – most of the patients who completely respond to ACT for metastatic melanoma have remained free of disease throughout their follow-up (Rosenberg, 2012). It is possible, though speculative, that the cancers of that minority mount only minimal barriers to immunotherapy, which can be overcome simply by force of numbers when bombarded by ACT (Overwijk, 2005). Approaches which are able to reverse the immunosuppressive environment created by tumours may therefore improve the response rates of existing immunotherapeutic approaches.

2.5 Oncolytic viruses

Oncolytic viruses (OV) are naturally occurring or genetically engineered viruses, which specifically replicate in and kill malignant cells, whilst sparing non-transformed cells (Kirn et al., 2001). Their study and development emerged as a result of the long history of sporadic cancer remissions associated with viral illnesses (Kelly and Russell, 2007). Although efforts to use viruses have been pursued since the 1940s and 50s, in the last two decades advances in virology and molecular biology have accelerated progress in the field. At present around 20 such OV are being studied for oncolytic potential preclinically, and half a dozen have been administered in clinical trials (Donnelly et al., 2012a).

The unmodified OV in use are suitably benign in most humans: Newcastle disease virus is a pathogen for poultry but not associated with illness in people (Donnelly et al., 2012a). Vesicular stomatitis virus (VSV) doesn't cause serious or widespread illness in humans but is of particular concern in cattle as its clinical pattern mimics foot and mouth disease (Pringle, 2001). Its use, preclinical or therapeutic, is currently prohibited in the UK (personal communication Prof A. Melcher 2012) but is used in several laboratories in North America, and a clinical trial is underway in the USA (personal communication Prof R. Vile 2012). Reovirus is thought to cause one of the legion of unnamed and trivial viral illnesses of childhood, but not serious illness in adulthood (Forsyth et al., 2008). Measles virus (MV), as discussed further below, is a serious pathogen but the strains in use as OV are based on attenuated vaccine products (Donnelly et al., 2013).

Other viruses, with genuine pathogenic potential, are also in use, but have been attenuated by genetic modification. Adenovirus generally has the E1 gene deleted, herpes simplex virus (HSV) commonly has its neurovirulence gene (ICP34.5) deleted, and thymidine kinase is removed from vaccinia strains before use (Kelly and Russell, 2007; Merrick et al., 2009; Donnelly et al., 2012a).

The selectivity of OV can be mediated by viral tropism for receptors overexpressed, or uniquely expressed, on cancer cells relative to normal cells (Anderson et al., 2004). Alternatively, or additionally, aberrant cellular pathways within cancer cells, such as deficient IFN responsiveness, make them more conducive hosts for OV, compared to normal cells (Stojdl et al., 2000; Critchley-

Thorne et al., 2009). Engineered viruses can also be rendered dependent on tissue-specific promoters for successful viral replication, or in the case of vaccinia lacking thymidine kinase, cycling cells for the production of nucleotides (Merrick et al., 2009; Donnelly et al., 2012a).

The clinical experience with OV has predominantly focussed on addressing concerns about safety, both to patient and their attendants. Thus far there have been no significant safety concerns and for most viruses the doses reached in phase I trials have been limited by manufacturing issues, rather than dose limiting toxicities (Donnelly et al., 2012a; Russell et al., 2012). Clear evidence of efficacy is somewhat lacking so far. H101, a modified adenovirus was tested in a randomised phase III trial, performed in China, in which patients with head and neck cancers received intratumoural injections of the virus in combination with systemic chemotherapy. The results were analysed in a per protocol fashion, and an improvement in response rate from 40% to 79% was reported (Xia et al., 2004). Survival data were incompletely gathered, apparently due to the challenges associated with follow up in rural areas of the world's most populous country. More recently a phase III trial of OncoVex, a type I HSV engineered to express GM-CSF (granulocyte macrophage colony-stimulating factor), and with deletions of the genes encoding ICP34.5 and ICP47, has completed accrual and data are expected in early 2013. In the preceding phase II trial 50 patients with metastatic melanoma, were treated with intratumoural injections of the virus into accessible lesions. 10 patients had complete responses, and there were objective responses in some uninjected visceral metastases (Senzer et al., 2009). The clinical experience of OV so far has asserted their safety but more needs to be done to demonstrate or enhance efficacy (Bell, 2010).

The concept of OV was originally based on the premise that a successful therapy would be mediated by the direct oncolytic activity of a virus, however there is burgeoning recognition amongst the field that a significant element of therapy is in fact the development of antitumour immune responses as a result of treatment with OV (Russell et al., 2012). There is abundant evidence from pre-clinical studies that therapy with OV can stimulate both innate and adaptive anti-tumour immune responses (Errington et al., 2008a, 2008b; Prestwich et al.,

2008b, 2008c, 2009a; Worschech et al., 2009). The Melcher group has published extensively on the immune consequences of treatment with OV, principally reovirus. Having demonstrated the oncolytic activity of reovirus in several human melanoma cell lines in vitro they also identified an inflammatory pattern of cytokines released in the course of oncolysis that contrasted with killing by conventional modalities (Errington et al., 2008b). This cytokine release activated dendritic cells, as did direct treatment with reovirus, which in turn were able to enhance innate tumour cell killing (Errington et al., 2008a). Subsequent work demonstrated that DC cultured with reovirus-treated melanoma cells were able to cross-present melanoma antigens and prime melanoma-specific T-cell responses from autologous lymphocytes, in both in vitro and in vivo models (Prestwich et al., 2008b). Similar results have also been reported in models of mesothelioma and ovarian cancer using measles and reovirus respectively (Gauvrit et al., 2008 and personal communication Dr V Jennings 2011). An in vivo study of mice bearing either colorectal or melanoma tumours, treated intratumourally with HSV found increases in tumour antigen-specific T-cells (Toda et al., 1999).

Moreover there is evidence from pre-clinical models that, in some tumour-OV dyads at least, therapy is in fact dependant on the immune enhancing effects of OV, rather than direct oncolysis per se (Diaz et al., 2007; Wongthida et al., 2010; Prestwich et al., 2009b). Diaz et al demonstrated that therapy with VSV reduced the metastatic burden in melanoma-bearing immune-competent C57BL/6 mice, but not in lymphocyte depleted mice (Diaz et al., 2007). Prestwich et al reported similar discrepancies between C57BL/6 and SCID mice (Prestwich et al., 2009b). Additionally, tumour cell lines that are resistant to OV in vitro, have responded in vivo, suggesting the need for elements of the immune system to mediate therapy (Apostolidis et al., 2007; Prestwich et al., 2009b).

Several clinical trials of OV have taken the opportunity to explore translational endpoints, including the immunological effects of therapy, albeit within early phase, non-randomised trials. As mentioned above, trials of OncoVEX in melanoma patients have demonstrated tumour responses, including uninjected lesions (Senzer et al., 2009). A companion report identified evidence of MART1 specific anti-tumour immune responses, when tissue samples from trial patients

were compared with untreated non-trial melanoma patients, with decreased numbers of suppressive Tregs and MDSC observed within treated tumours (Kaufman et al., 2010).

In one of his innumerable and exemplary expostulations of the traditional view of OV efficacy, Prestwich details the proposed mechanisms by which OV are thought to overcome tumour-generated immunosuppression and raise adaptive immune responses (Prestwich et al., 2008c and Figure 6).

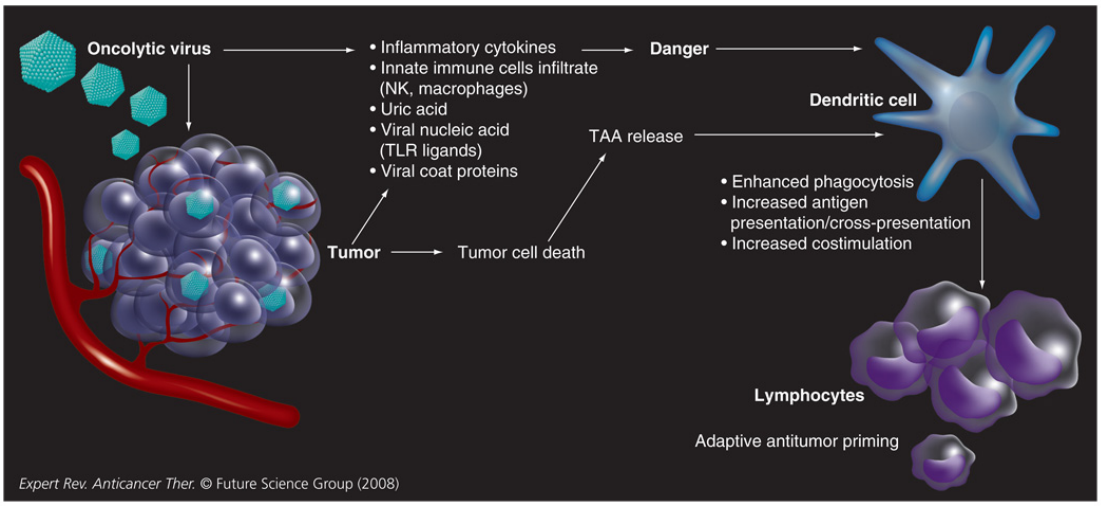

Figure 6. OV-treatment of tumours leads to adaptive anti-tumour immune responses. In addition to direct oncolysis, OV will stimulate infected tumour cells to release numerous inflammatory cytokines and danger signals that recruit and activate DC. These DC in turn will take up and present TAA, priming anti-tumour immune responses.
Reproduced from Prestwich et al. "Oncolytic Viruses: a Novel Form of Immunotherapy." *Expert Review of Anticancer Therapy* 8, no. 10 (October 2008): 1581–1588 with permission of Expert Reviews Ltd.

The best route of delivery for OV remains contentious (Donnelly et al., 2012c). A concern about the practicability of OV was that systemic delivery would result in significant anti-viral immune responses, which could clear the virus, and abrogate therapy (Donnelly et al., 2012c). Systemically administered viruses will adhere to erythrocytes and other blood cells, be bound up within the spleen and liver, and face neutralisation by neutralising antibodies and complement. Circulating antibodies will be present for commonly encountered viruses, and will be produced whenever repeated doses of OV are used (Iankov et al., 2007; White et al., 2008). Clinical testing of OncoVEX was performed with intra-tumoural injections in an effort to circumvent such concerns (Senzer et al., 2009).

Two recently reported studies have shown that OV can reach tumours, even in the face of neutralising antibodies, though the mechanisms involved are the subject of ongoing investigations (Breitbach et al., 2011; Adair et al., 2012). Breitbach et al. administered intravenous JX594 to patients with a variety of tumours (Breitbach et al., 2011). JX594 is a vaccinia virus derived from the Wyeth strain, modified to remove viral thymidine kinase, armed with GM-CSF and labelled with β-galactosidase (Merrick et al., 2009). Patients with a number of different tumour types receiving the higher doses of virus had evidence (immunohistochemistry for viral proteins or β-galactosidase, or polymerase chain reaction for viral sequences) of viral gene or protein expression, including one patient who had pre-existing anti-vaccinia antibodies.

Another study involved delivery of intravenous reovirus daily for up to five days 1-4 weeks before surgical resection of hepatic metastases (Adair et al., 2012). In contrast to the Breitbach study, all ten patients had existing neutralising anti-reovirus antibodies (NARA), which increased over the course of repeated doses of reovirus. Reovirus was identified in resected tumours by IHC, but crucially replicating virus was recovered by plaque assay. This finding provides compelling evidence that intravenously delivered virus can reach tumour. A further notable result from this study was the identification of replicating virus, by plaque assay, in the peripheral blood mononuclear cells (PBMC), granulocytes and platelets. Reovirus was detected in plasma by PCR, but not plaque assay, suggesting that the virus was functionally neutralised by NARA, but carried

safely by elements of the cell fraction. It has previously been reported that oncolytic viruses can be loaded onto or into several cell species ex vivo, then readministered to enhance delivery to tumours, in a mechanism commonly referred to as hitchhiking (Ilett et al., 2009, 2011; Peng et al., 2009). The results of Adair's clinical study suggest that hitchhiking is a phenomenon that can occur entirely in vivo, without the need for an ex vivo loading step; if so this newly identified process could be augmented in order to enhance the efficacy of OV therapy.

2.5.1 Measles virus

Measles virus (MV) was one of the first viruses tested as a potential oncolytic virus (OV). Indeed some of the earliest reports of cancer regressions associated with viral infections, which in turn prompted the genesis of the field, were following the measles illness (Bluming and Ziegler, 1971; Kelly and Russell, 2007).

The pathogenic or wild type strain of MV (hereafter wtMV) remains a significant cause of morbidity and mortality worldwide; the WHO website estimates that there continue to be 139,000 deaths per year as a result of wtMV infections. This is despite the existence of an efficacious and safe vaccine strain for over half a century. Enders and Peeble were the first to isolate MV from throat swabs taken from a young boy called David Edmonston in 1954 (Katz, 2009). After repeated passages in several cell lines the resulting strain, known as the Edmonston strain, has fathered the generation of most MV vaccines ever since. After a long history of application as a replication competent but attenuated vaccine the Edmonston strain of MV (hereafter simply MV) has been demonstrated to be safe and well tolerated (Blechacz and Russell, 2008).

Measles is a single-stranded negative-sense RNA enveloped morbillivirus of the paramyxoviridae family. The viral genome is 16 kb in length and encodes 8 proteins within 6 genes (Griffin and Oldstone, 2009) (Figure 7).

MV binds its cell surface receptors using the fusion (F) and haemagglutinin (H) viral envelope glycoproteins. A trimer is formed between one F-protein and a dimer of H-proteins that forms a spike exposed on the surface of the viral

membrane. When the H-protein binds its receptor conformational changes are induced in the F-protein, triggering the fusion process (Navaratnarajah et al., 2009). CD46 has been demonstrated to be the preferred receptor for the Edmonston strain (Dörig et al., 1993). CD46, also known as the membrane cofactor receptor, is expressed on all nucleated human cells. It binds the complement components C3b and C4b and serves as a cofactor for their proteolytic inactivation, protecting host cells from complement-mediated lysis by the membrane attack complex (Kemper and Atkinson, 2009). CD46 is internalized on cells infected with EdMV, which could perhaps render the cell more vulnerable to complement-mediated lysis (Gerlier et al., 1995). wtMV strains require an alternative receptor, CD150, also known as signalling lymphocyte-activation molecule (SLAM); the Edmonston strain is also able to use this receptor (Tatsuo et al., 2000). SLAM is expressed predominantly on immune cells and the dependence of wtMV on this cell-surface protein probably explains the predilection of wtMV for lymphoid cells and immunosuppressive clinical manifestations (Dhiman et al., 2004). Two groups have recently reported that Nectin4, a protein overexpressed on several tumour types, is an additional receptor for both the wtMv and Edmonston strains (Mühlebach et al., 2011; Noyce et al., 2011).

Once a virion has fused with a target cell and successfully transcribed viral mRNAs, viral spread can be propagated by two mechanisms; in addition to generating and shedding new viral particles, cells may directly fuse with uninfected neighbours by virtue of viral F and H expression. This leads, in vivo and in vitro, to the characteristic cytopathic effect (CPE) of giant multinuclear cells or syncytia, large fused cells that may contain hundreds of nuclei. Warthin and Finkeldey independently recognised such appearances in the lymph nodes of children suffering measles infection (Paik et al., 2002).

The nucleocapsid (N) protein, phosphoprotein (P) and large (L) protein, together with the 16k negative-sense single strand RNA, form the ribonucleoprotein (RNP), with P and L also forming the RNA-dependent RNA polymerase (RdRp). Matrix protein (M) underlies the viral membrane and is thought to interact with the transmembrane domains of F and H. Regions within the P gene encode the remaining proteins, C and V; whilst neither is involved in viral structure, nor

requisite for viral replication, they may play roles within host cells moderating IFN signalling pathways (Fields et al., 2007).

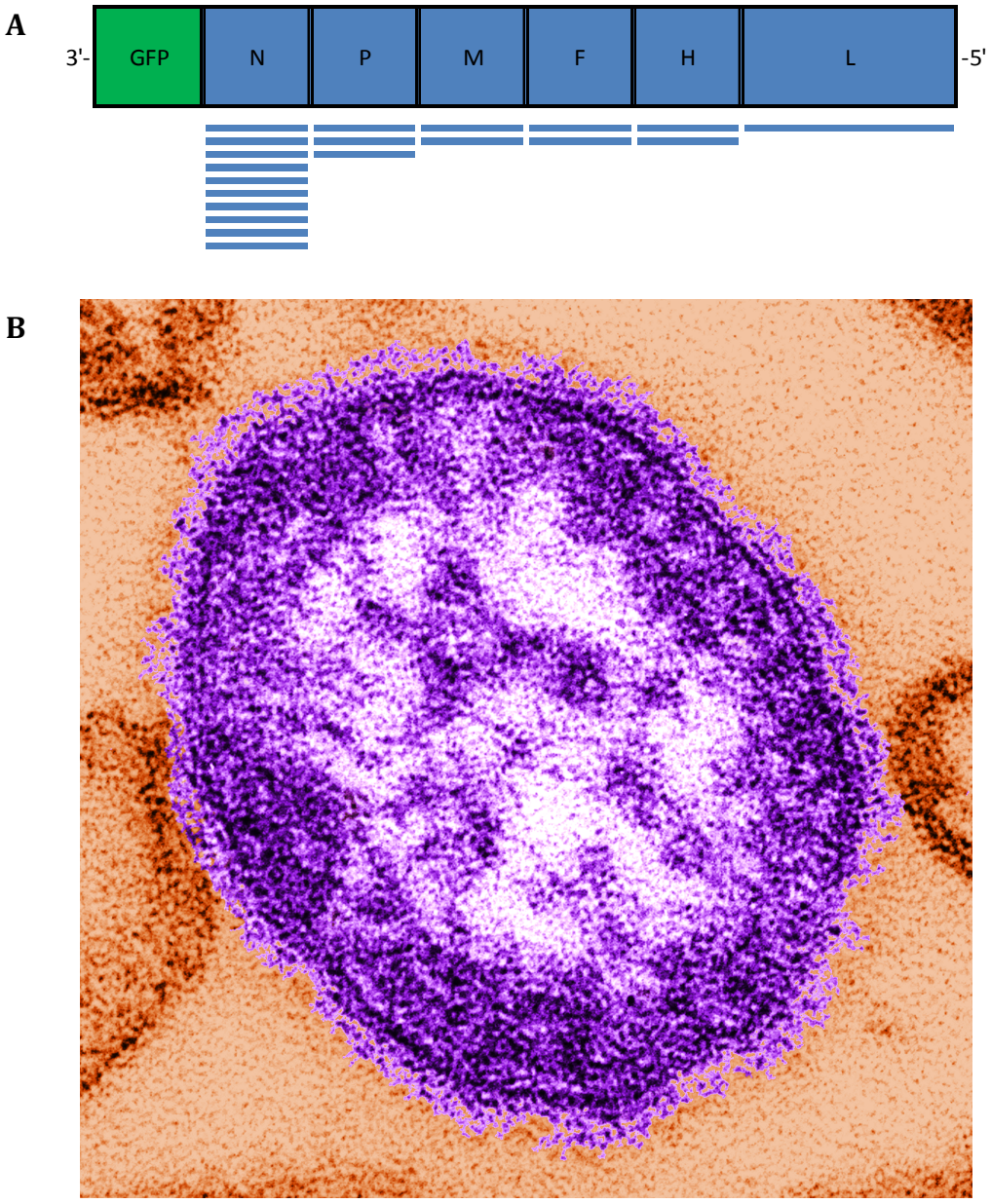

Figure 7. The measles virion A. Schematic representation of the MV genome and depiction of the relative transcription levels of each gene (N nucleocapsid; P phosphoprotein, M matrix, F fusion, H haemagluttinin, L polymerase. C and V proteins are encoded within the P gene.). This figure illustrates a MV expressing GFP. Most published MV variants express inserted genes at the 3' end. B. Coloured transmission electron microscopy of a measles virion.
Figure 7A adapted from Duprex,and Rima. "Using Green Fluorescent Protein to Monitor Measles Virus Cell-to-Cell Spread by Time-Lapse Confocal Microscopy." In *Green Fluorescent Protein*, 297–307, 2002. Figure 7B courtesy of C. Goldsmith and W. Bellini, via the Public Health Image Library of the Center for Disease Control and Prevention, freely available at phil.cdc.gov.

Study of MV as a potential OV has been performed by several groups internationally, but most importantly by teams at the Mayo clinic, USA. They have demonstrated the virus' efficacy against a number of human tumours, based on in vitro techniques and xenograft models and performed preclinical toxicity assessments (Grote et al., 2001; Peng et al., 2003b; Fielding, 2005; Hasegawa et al., 2006; Myers et al., 2007, 2008; Blechacz and Russell, 2008). Other groups have also explored the virus, most notably a small study of intratumoural injections of MV for 5 patients with cutaneous T-cell lymphoma was performed in Switzerland (Heinzerling et al., 2005; Kunzi et al., 2006). The Swiss group found, in addition to tumour regressions, some evidence of increased T-cell recruitment to tumours, although patients were also treated with systemic IFNα prior to virotherapy.
The preclinical data have in turn led to early-phase clinical trials in patients with ovarian cancer, glioblastoma multiforme, multiple myeloma and mesothelioma, with the virus proving to be well tolerated when delivered systemically, intraperitoneally or intracranially (Msaouel et al., 2009). No maximum tolerated dose has yet been reported, instead manufacturing limits currently cap the dose at around 10^{10} $TCID_{50}$ (personal communication Dr Mark Federspiel 2012).

Most of the efforts of the Mayo group have focussed on the direct oncolytic potential of MV, rather than the immunological consequences of such therapy. Several variants of MV have been developed by appending recombinant proteins or single-chain variable region antibody fragments (scFv) on the MV H protein, which then target tumours more specifically. Latterly several groups have sought to improve the efficacy of MV by 'arming' the virus in a number of ways (Table 1). The development of MV has closely mirrored that of the whole OV field, in that initial concerns about safety rightly necessitated some diminution of viral efficacy; as toxicity has proved to be a rare problem with OV, so many groups are now seeking to restore, or increase, viral potency.

Targeting

Mechanism	Target	Tumour	Reference
scFv expressed in MV H protein	CEA	Multiple	(Hammond et al., 2001)
	CD20	Non-Hodgkin's lymphoma	(Bucheit et al., 2003)
	CD38	Myeloma	(Peng et al., 2003a)
	Folate receptor	Ovarian	(Hasegawa et al., 2006)
	EGFR	Gliomas	(Allen et al., 2006)
	Prostate-specific membrane antigen	Prostate	(Liu et al., 2009)
Expression of integrin binding proteins on H protein	Tumour neovasculature	Multiple	(Hallak et al., 2005) (Ong et al., 2009)
IL13 expression on H protein	IL13 receptor	Gliomas	(Allen et al., 2008)
Urokinase expression	Urokinase receptor	Multiple	(Jing et al., 2009)

Arming

Armament		Reference
GM-CSF	Enhanced neutrophil recruitment and activation	(Grote et al., 2003)
Prodrug convertase	Local activation of prodrug enhances therapeutic index and kills bystander cells	(Ungerechts et al., 2007b) - (Ungerechts et al., 2007a)
Wildtype P protein	Restores viral ability to suppress IFN release & response, enhancing intratumoural spread	(Haralambieva et al., 2007)
* Wildtype N, P, L	Overcomes host IFN responses	(Meng et al., 2010)*
IFNβ	Immune recruitment and activation	(Li et al., 2010)
Neutrophil Activating Protein (NAP)	Expression of an H.Pylori-derived protein enhances the generation of antitumour immunity	(Iankov et al., 2012)
CEA	CEA is an inert and measurable marker that allows tracking of viral replication in vivo	(Peng et al., 2002)
Sodium-Iodide symporter (NIS)	Imaging of viral spread with ^{123}I, or therapy with ablative ^{131}I	(Dingli et al., 2004)

Table 1. Refinements of MV. Initially concentrating on better targeting of virus, developments have more recently moved to efforts to enhance the efficacy of virotherapy with MV. Asterisk indicates a non-Mayo Clinic publication.

A key publication by Gauvrit et al. showed that the Schwarz strain of MV, has oncolytic activity against human mesothelioma, causing apoptosis and syncytia formation (Gauvrit et al., 2008). Moreover the group observed phagocytosis of MV-infected mesothelioma cells by dendritic cells, which in turn were matured, and able to cause the proliferation of T-cells specific for mesothelioma-associated antigen. Measles is commonly perceived to be an immunosuppressive virus because of the potent immunosuppression associated with the wildtype virus. Gauvrit demonstrated that by contrast a vaccine strain of MV, as might be expected given its longstanding use in prophylaxis, is not immunosuppressive in an in vitro model. Specifically DC, which are thought to be particularly vulnerable to the effects of wtMV were not found to be susceptible to the Schwarz MV. Though little of the work with MV undertaken by the Russell group has explored the immunogenicity of therapy with MV, and was predominantly done in immunodeficient mice bearing xenografts, the group has previously reported the role of neutrophils in MV-therapy. Comparing MV modified to express GM-CSF, with unmodified MV, Grote et al. identified neutrophils as enhancing virotherapy (Grote et al., 2003). A recent follow-up by one of the original authors suggests that this stimulation of neutrophils is achieved only by MV, and not wtMV, and argues that this differential effect on neutrophils is key to the success of MV as an oncolytic agent (Zhang et al., 2012). The Mayo group have recently sought to exploit this phenomenon by generating MV which expresses a neutrophil activating protein (NAP) (Iankov et al., 2012). The NAP used is derived from H.pylori and significantly enhanced therapeutic efficacy in a number of tumour models.

As discussed above several groups have sought to evade neutralising host anti-viral immunity, which might deplete systemically administered virus. The groups based at the Mayo clinic have described the use of T-cells and mesenchymal stem cells for viral hitchhiking (Ong et al., 2006a; Mader et al., 2009).

Notably, prior to the research outlined in this thesis there were no published reports describing the use of MV in melanoma, either as a directly oncolytic agent, or as an activator of the innate or adaptive immune systems (Donnelly et al., 2013).

2.6 Radiotherapy

Radiotherapy (RT) was used to treat cancers almost as soon as the existence of X-rays was identified. In external beam RT high-energy photons generated by a linear accelerator are directed toward the tumour and a minimal margin of surrounding tissue. Brachytherapy is the use of internal radiation sources, generally sealed sources such as the titanium coated pellets of Iodine-125 that are used in prostate brachytherapy and plaque-based brachytherapy for ocular melanoma. In either format of RT, high energy photons interact with the tissue they traverse, depositing energy and triggering ionising events. These events in turn lead to the generation of reactive oxygen species that can damage components of the cell, critically DNA. When DNA in the cell is damaged beyond the ability of the cell to repair it, that cell becomes replication-incompetent and will either undergo apoptosis or mitotic catastrophe when it does try to replicate. Classical radiobiological experiments, including the use of microbeam irradiators to selectively target organelles, isolated the nucleus as the critical organelle of the cell that mediates vulnerability to radiation; most other forms of damage are generally thought to be repaired or ignored (Joiner and Van der Kogel, 2009; Hall and Giaccia, 2011). The therapeutic index of RT is based on the deficient damage sensing and repair pathways of most cancer cells, relative to adjacent normal tissue. In practice the dose delivered to tumour is generally limited by the dose that adjacent normal structures can safely tolerate.

The sensitivity of different tumours to the effects of radiotherapy varies according to histology, and generally melanoma has been considered to be one of the most radioresistant tumours. Though RT is certainly used in the palliative setting for melanoma, there has been little enthusiasm to expand its use otherwise (Stevens and McKay, 2006). Despite this, a recent clinical trial has demonstrated a small advantage in local control when RT is used as an adjuvant treatment after high-risk lymph node dissections (Burmeister et al., 2012). Irradiating lymph node basins is invariably associated with morbidity, and the treatment did not result in an overall survival benefit. These results are unlikely to yield major changes in clinical practice, however they do confirm that RT can have activity against melanoma.

The potential immune enhancing effect of radiotherapy has been much neglected, partly because early researchers chose to focus on human tumour and cell lines, reasoning that the resulting estimates of radiosensitivity and fractionation

sensitivity would be more clinically applicable. Of course this meant that much of the early radiobiology was studied in immune deficient mouse models, or human in vitro cell cultures, such that the immune element of therapy would inevitably be overlooked.

RT is known to have numerous effects on tumour cells that could enhance their immunogenicity (Figure 8). Proteins damaged by ionising events are marked for degradation, increasing the pool of peptides within the cytoplasm and in turn enhancing MHC class I expression on the cell surface; a key paper by Reits et al. found irradiated cells express novel antigens and were more vulnerable to the effects of ACT in mouse models (Reits et al., 2006). Whereas tumour cells often depress expression of Fas receptor in order to evade cytotoxic T cells, irradiated cancer cells upregulate the Fas receptor (Chakraborty et al., 2004). Obeid et al. demonstrated that RT results in exposure of calreticulin on the surface of cells irradiated in vivo, an established eat-me signal as discussed above (Obeid et al., 2007a, 2007b). A further group found evidence that blocking the translocation of calreticulin to the surface of cells impeded their phagocytosis by DC (Perez et al., 2009). A study of the effects of ultraviolet radiation, and some chemotherapy agents, found that the exposure of calreticulin is not dependent on damage to DNA but instead mediated by effects upon the endoplasmic reticulum (Panaretakis et al., 2009). Irradiated cancer cells release danger signals, including HMGB1 and adenosine triphosphate and in mouse models, wherein RT successfully controls established tumours, depletion of the TLR4 pathway that responds to HMGB1 led to diminished therapy (Apetoh et al., 2007b; Ohshima et al., 2010). Further work has supported the concept that the efficacy of RT in immune competent mouse models is at least in part mediated by, and therefore partly dependent upon, elements of the immune system. The growth of B16 melanoma tumours established on C57BL/6 mice was slowed by 25 Gy external beam RT, but when the mice were pretreated with a CD8-depleting antibody any benefit from RT was lost (Lee et al., 2009).

Although the role of the immune system in radiotherapy is far from recognised or accepted in the clinical environment several groups have explored combination therapies in the preclinical setting that seek to harness this relatively newly posited effect. The growth factor Flt-3, expands numbers of DC. Chakravarty et al.

established Lewis lung tumours on the footpads of mice, which rapidly metastasise to the lung (Chakravarty et al., 1999). The combination of local RT, limited to the footpad tumours, with a systemic agent that expands numbers of DC, Flt-3, resulted in cures in 50% of treated mice.

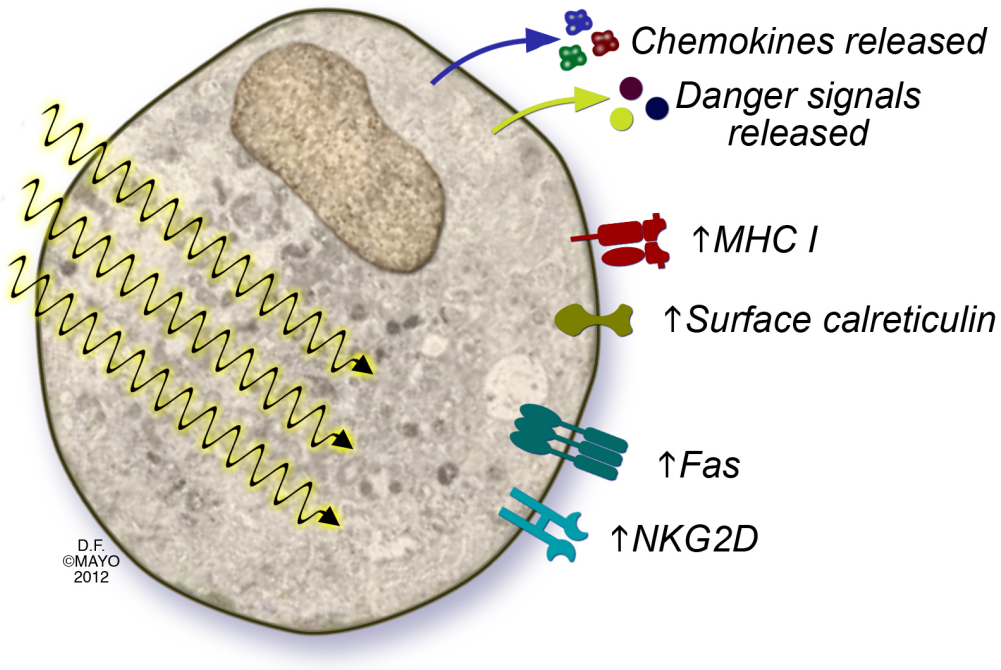

Figure 8. Immunologically relevant extra-nuclear effects of radiotherapy. Irradiated tumour cells release inflammatory cytokines and chemokines and danger signals including HMGB1 and ATP. RT has also been shown to cause upregulation of antigen presentation, including novel RT-induced antigens, and increased expression of MHC class I. RT upregulates receptors and ligands on tumour cells that enable the actions of cytotoxic T-cells and innate effector cells, such as the Fas receptor and NK ligands.
Figure prepared with David Factor, Mayo Clinic Illustrations Department, for a manuscript pending submission.

Demaria et al. confirmed this effect in a bilateral flank tumour model of breast cancer, in which unilateral RT combined with Flt-3 yielded responses in the unirradiated tumour, in a tumour-specific fashion (Demaria et al., 2004); the effect could not be repeated in nude mice, by either group. Responses in tumours outside the treatment field have been noted sporadically over many years of radiation oncology, and R.H. Mole coined the expression 'abscopal' (*ab* – away from, *scopal* - target) in his presentation in 1952 (Mole, 1953). The mechanism by which abscopal responses occur remains uncertain, though the groups of Demaria and Formenti who are at the forefront of this field assert that their preclinical data strongly suggest that it is an immune phenomenon. Further supporting that notion, combination of CTLA-4 blockade with local radiotherapy in mice resulted in abscopal tumour responses (Demaria et al., 2005). Demonstrating some of the challenges that remain to this potential synergy, it was observed that successful combination of local RT with systemic anti-CTLA-4 was very dependant on the RT fraction sizes used (Dewan et al., 2009).

Several observational studies have found supporting evidence that the immune effects of RT are relevant in clinical treatments, and not just in mice; at least three papers have described the effects of pelvic RT on enhancing numbers of effector T-cells, both circulating and within subsequently resected lymph nodes (Schaue et al., 2008; Battaglia et al., 2010; Tabi et al., 2010). Some small scale studies have combined RT and immune manipulations in patients with modest success (Gulley et al., 2005; Formenti and Demaria, 2009; Hasumi et al., 2011). RT for melanoma is being re-explored, not least given the emergence of modern hypofractionated radiotherapy techniques that better fit the established radiobiology of melanoma (Stevens and McKay, 2006; Jahanshahi et al., 2012). Therefore one of the most appealing combinations, given the recent success of ipilimumab, would be to combine the blockade of CTLA-4 with stereotactic body radiotherapy (SBRT). Such trials are reportedly underway (clinicaltrials.gov and personal communication Dr Bar-Ad 2012) and a case has recently been reported of abscopal responses in a solitary patient treated with ipilimumab and SBRT (Postow et al., 2012).

2.7 Summary

Therapy for melanoma has changed considerably over the course of the period of post-graduate study described within this thesis. The emergence of ipilimumab, and vemurafenib, have finally begun to change the outlook for patients with metastatic melanoma. Despite this progress the numbers of patients experiencing significantly improved survival with therapy is low. Longer established immune approaches such as ACT have yet to demonstrate that they can be widely applied, though developments in CAR-T cells hold promise. Given the evidence that immune-mediated therapies can result in clinical benefits it is therefore appropriate to explore additional therapies that can generate immune responses, or enhance immunotherapies.

OV are emerging as viable clinical therapies that can stimulate anti-tumour immune responses. MV has not previously been tested in melanoma, despite reaching clinical testing in a number of other tumour sites.

RT is a longstanding and readily clinically deliverable therapy that is being reconsidered in melanoma, just as its immune effects are being identified.

Therefore the aims of the studies described within the following chapters were as follows;

1. Determine the oncolytic activity of measles virus in human melanoma cells.
2. Determine the effects of measles, and measles-induced melanoma cell death upon cells of the innate and adaptive immune systems.
3. Explore combinations of external beam radiotherapy with adoptive cell therapy and virotherapy.
4. Explore combinations of brachytherapy with adoptive cell therapy and virotherapy.
5. Develop an intracranial model of melanoma, with which to test therapeutic strategies in the context of a commonly encountered pattern of melanoma metastasis.

3 Materials and methods

For the sake of clarity and brevity reagents, media, buffers and cell lines are initially listed, along with details of sources and suppliers. Further details, where appropriate, follow in the subsequent text describing the techniques used. Human and mouse experiments were performed on different sites, therefore important distinctions in the reagents used are provided. When identical products were used on both sites, but from different intermediary suppliers, only the UK supplier or UK branch is detailed.

3.1 Reagents and media

Reagent	Supplier	Location
Amphotericin	Sigma	Poole, UK
BSA (Bovine serum albumin as lyophilised powder)	Sigma	Poole, UK
Chromium-51	Perkin Elmer	Risley, UK
DMEM – Human use (Dulbecco's modified Eagles media)	Gibco, Invitrogen	Paisley, UK
DMEM – Murine use (Dulbecco's modified Eagles media)	HyClone, Thermo Scientific	Barrington, IL, USA
DMSO (Dimethylsulfoxide)	Sigma	Poole, UK
EDTA	Sigma	Poole, UK
FCS - Human use (foetal calf serum) heat inactivated at 56°C for 30 minutes prior to storage	BioSera	East Sussex, UK
FCS - Murine use supplied heat inactivated by the manufacturer	Gibco, Invitrogen	Paisley, UK
Gentamicin	Sigma	Poole, UK
HBSS (Hank's balanced saline solution)	Sigma	Poole, UK
HEPES buffer	Sigma	Poole, UK
IMDM (Iscove's modified Dulbecco's medium)	Gibco, Invitrogen	Paisley, UK
Insulin, transferrin, selenium	Gibco,	Paisley, UK

Reagent	Supplier	Location
	Invitrogen	
Interleukin 2 (IL-2)	R&D systems	Abingdon, UK
Interleukin 4 (IL-4)	R&D systems	Abingdon, UK
Interleukin 7 (IL-7)	R&D systems	Abingdon, UK
Ketamine	Mayo pharmacy supplies	
L-glutamine	Gibco, Invitrogen	Paisley, UK
Live/Dead ® assay	Invitrogen	Paisley, UK
MTT (Thiazolyl Blue Tetrazolium Bromide)	Sigma	Poole, UK
Neomycin (G418 sulfate)	CellGro	Manassas, Va
Non-essential amino acids	Sigma	Poole, UK
Opti-MEM	Invitrogen	Paisley, UK
PBS – Human use (Dulbecco's phosphate buffered saline)	Oxoid	Basingstoke, UK
PBS – Murine use	Thermo Scientific	Barrington, IL, USA
Penicillin	Sigma	Poole, UK
PenStrep (Penicillin/streptomycin)	CellGro	Manassas, Va
Recombinant human gp100	Mayo Peptide synthesis facility	
RPMI (Roswell Park Memorial Institute medium)	Gibco, Invitrogen	Paisley, UK
Saponin	Sigma	Poole, UK
SIINFEKL Octomeric amino acid sequence from ovalbumin	Mayo Peptide synthesis facility	
Sodium Azide	Sigma	Poole, UK
Streptomycin	Sigma	Poole, UK
Triton X-100	Sigma	Poole, UK
Trp2	Mayo Peptide synthesis facility	

Reagent	Supplier	Location
Trypan Blue	CellGro	Manassas, Va
Trypsin-EDTA	Sigma	Poole, UK
VSV surface antigen	Mayo Peptide synthesis facility	
Xylazine	Mayo pharmacy supplies	

3.2 Prepared media

Prepared media	Constituents
Complete medium – human in vitro use	DMEM 10% v/v FCS 1% v/v L-glutamine
Complete medium – murine in vitro use	DMEM 10% v/v FCS 4mM L-glutamine (added by manufacturer)
Complete medium (Vero cells)	DMEM 5% v/v FCS 1% v/v L-glutamine
Complete medium (B16-Ova cells)	DMEM 10% v/v FCS 1% v/v L-glutamine 5 mg/mL neomycin Sterile filtered after preparation
Complete tissue media (Human melanoma explants)	RPMI 10% v/v FCS 1% v/v L-glutamine 25 mg/L gentamicin 1 U/L penicillin 1 µg/L streptomycin 0.1 mg/L amphotericin 1% v/v non-essential amino acids 1% v/v insulin, transferrin and selenium 25 mM HEPES buffer
Cytotoxic T-lymphocyte media (CTL media)	RPMI 7.5% v/v human serum 2 mM L-glutamine 1% v/v 0.45 mM sodium pyruvate 1% v/v 25 mM HEPES 1% v/v non-essential amino acids 20 µM 2β-mercaptoethanol

Prepared media	Constituents
Monocyte media (for preparation of dendritic cells)	RPMI 10% v/v FCS 2 mM L-glutamine 5000 U/mL IL-4 800 U/mL GM-CSF
OT1 T-cell media	IMDM 5% v/v FCS 1% penicillin/streptomycin 0.1% v/v 2β-mercaptoethanol 50 U/mL IL-2 1 µg/mL SIINFEKL
All prepared media were stored at 4° C and warmed to 37° C prior to use, unless otherwise indicated	

3.3 Buffers

Compound reagent	Constituents
FACS (fluorescence-activated cell sorting) buffer (mouse)	PBS 0.1% w/v BSA 0.1% w/v sodium azide
FACS buffer (human)	PBS 1% v/v FCS 0.1% w/v sodium azide
MACS buffer (mouse)	PBS 0.5% w/v BSA 2mM EDTA
MACS buffer (human)	PBS 1% v/v FCS 2mM EDTA
Red cell lysis buffer (mouse)	Distilled water 0.15 M Ammonium chloride (Sigma) 10 mM Potassium bicarbonate (Sigma) 0.1 mM EDTA pH adjusted to 7.2-7.4 then sterile filtered
Laemmli buffer	Distilled water 0.0625M Tris buffer 10% v/v glycerol 2% v/v SDS 5% v/v β-mercaptoethanol, 0.025% v/v bromophenolblue

3.4 Cell lines

Origin	Cell line	Medium	Supplier/source	
Human	Mel888 Mel624 MeWO SkMel28	Complete medium	CRUK (Cancer research UK)	
African green monkey	Vero (green monkey kidney)	Complete medium (5% FCS v/v)	ATCC (American type culture collection)	Virginia USA
Hamster	BHK (baby hamster kidney)	Complete medium		
Murine (C3H/An)	L929	Complete medium		
Murine (C57BL/6)	B16-Ova; stably transfected to express Ovalbumin and a neomycin resistance gene	Complete medium + neomycin	Longstanding kind gift from Edith Lord	Department of microbiology and immunology, University of Rochester medical center, Rochester, NY, USA
Low passage, master bank cell line stocks were stored in liquid nitrogen between uses. Cell lines were routinely tested for mycoplasma contamination and found to be free of infection.				

3.5 Tissue culture

All cell handling was performed in a dedicated tissue culture facility using Nuaire Class II biological safety cabinets (human cell work) or Sterigard class II safety hoods (mouse cell work), and standard aseptic precautions. A dedicated Class II biological safety cabinet was available for all work using MV or MV-GFP. All cells were grown in dedicated Sanyo MCO-20A1C CO_2 incubators (human cell work, supplied by Sanyo, Loughborough, UK) or Forma series Scientific water-jacketed CO_2 incubators (mouse work, supplied by Thermo Scientific) at 37°C, humidified and supplemented with 5% CO_2 unless otherwise stated. Cells were routinely grown in vented plastic tissue culture flasks with adherent surface areas of 25, 75, 150 or 175 cm^2 and passaged before reaching confluency. Plasticware for human in vitro experiments were supplied by Corning Costar, High Wycombe, UK. Flasks and other plasticware for mouse work were supplied by BD Falcon San Jose, Ca, USA. For passage and harvest of cells media was aspirated and discarded, then trypsin-EDTA added (0.2 mL for T25 cm^2 flasks, 0.5 mL for T75 cm^2 flasks and 1.5 mL to T150 cm^2 or T175 cm^2 flasks). After harvest, cells were washed with media in order to neutralise residual trypsin-EDTA.

All cell washing was performed by centrifugation at 1500 rpm for 5 minutes at room temperature with an Eppendorf 5810R centrifuge (Fisher scientific, Loughborough, UK) unless otherwise stated and using BD Falcon tubes, either 15mL or 50mL.

Cells for freezing were resuspended in freezing media comprising 10% DMSO in FCS and cooled to -80°C (at -1°C per minute) then kept at -80°C if used within 1-2 weeks, or in liquid nitrogen if stored for longer periods. Cells were recovered from frozen by brisk thawing in a 37°C water bath then washed in media to remove residual DMSO.

Routine microscopy was performed using a CKX41 indirect microscope (Olympus, Southend-on-sea, UK). Photographs were taken using a C-7070 camera mounted on a CKX41 indirect microscope (all Olympus). Routine cell counts were performed with 0.2% trypan blue exclusion using a haemocytometer (Fisher Scientific).

Fresh melanoma explants were collected under the auspices of a pre-existing ethical approval, and anonymised and logged upon receipt, in accordance with guidance from the Human Tissue Authority. After rinsing with HBSS, tumours were coarsely dissected by scalpel, passed through a cell strainer (Sigma) and treated

with either collagenase I or III or both (Worthington, Lakewood, USA) at 37°C in complete tissue media for 1 hour. Resulting cell suspensions were placed in flasks in complete tissue media to allow adherence of melanoma cells.

3.6 Viral bulking and titration

3.6.1 Measles virus

Two strains of MV were kindly supplied by S. Russell, Mayo Clinic, Minnesota, USA, at second passage. The Edmonston MV strain was derived from a cDNA as described previously (Radecke et al., 1995). A GFP-expressing MV, based on the same clone but with GFP encoded upstream of the viral N protein was also kindly furnished (Peng et al., 2002). Both viruses were titrated against VERO cells to estimate the $TCID_{50}$ (Tissue culture 50% infectious dose) using a 96 well plate format and the Reed-Muench method of calculation (Reed and Muench, 1938; Fields et al., 2007). Briefly VERO cells were seeded at 7000 cells in 50 µL media per well into 96 well plates. Viral preparations were then added in serial 10-fold dilutions to each column. The viral titre was calculated, based on the number of wells with evidence of the characteristic MV cytopathic effect (CPE) 6 days later, thus;

$$\log_{10}\left(\frac{TCID_{50}}{ml}\right) = L + d(s - 0.5) + \log_{10}(v^{-1})$$

$$Where\ L = negative\ \log_{10}(greatest\ dilution\ where\ all\ wells\ positive)$$

$$d = \log_{10} dilution\ factor$$

$$p_{dilution\ column} = proportion\ of\ positive\ wells\ in\ one\ column$$

$$s = \sum p_{dilution\ column}\ , where\ p_{dilution\ column} \neq 1$$

$$v = volume\ of\ inoculum$$

MV stocks were bulked as required from P2 or P3 virus as follows (personal communication from Elizabeth Hadac, 2009): T75 flasks were each seeded with $1.5x10^6$ subconfluent VERO cells and allowed to adhere overnight. The following day supernatant media was discarded and P2 or P3 virus was added at a multiplicity of infection (MOI) of 0.02 (i.e. $3x10^4$ $TCID_{50}$) in 2mL of Opti-MEM reduced serum media (Invitrogen) per flask. Cells were replaced in an incubator and gently agitated every 30minutes to ensure widespread and evenly distributed infection. After 2 hours 10mL of complete DMEM was added to each flask. Between 24 and 48 hours later, when microscopy revealed 50% syncytial coverage, flasks

were moved to 32°C for 8-12 hours (generally overnight) and then restored to 37°C. When cells reached 80% syncytial coverage supernatant was discarded and cells harvested with a cell scraper using minimal volumes of Opti-MEM. Cells were then subjected to 3 freeze/thaw cycles by immersion in a methanol and dry ice mixture to release cell-associated virions. Virus was aliquoted and stored at -80°C.

3.6.2 Vesicular Stomatitis Virus

VSV-Ova amplification was performed by infecting subconfluent BHK in 15 cm diameter culture dishes with stock VSV-Ova at an MOI of 0.01 in serum free media. After 1 hour the media was aspirated and replaced with complete media. After 24-36 hours the completion of cytopathic effect was confirmed and the supernatant first clarified by centrifugation at 1500rpm for ten minutes, then filtered using 0.45 μm pore size vacuum driven Nunc Nalgene filtration units (Thermo scientific). The resulting filtrates were further purified by cushion centrifugation through 10% w/v sucrose in PBS at 27000 rpm for 1 hour at 4°C using an Optima L-90k Ultracentrifuge with SW32 swinging bucket rotor (Beckman Coulter, Pasadena Ca, USA). The resulting pellets were resuspended in PBS and further centrifuged through 10% sucrose prior to final resuspension in 1mL PBS and division into aliquots.

VSV-Ova from amplification was titrated using plaque assay. Cultures of L929 were prepared in 6 well plates, seeding $7.5x10^5$ cells per well overnight. The following day viral dilutions were prepared by serial ten-fold dilutions with serum-free DMEM. Media was aspirated from each well, the cells washed with PBS and then 1mL of each viral dilution applied to each well. After one hour the viral media was discarded and cells overlaid with 2mL of an equal mixture of 1% noble agar and double strength DMEM with 20% v/v FCS, both having been equilibrated to 42°C prior to use. Plaques were visible and counted within 48 hours. VSV-GFP and VSV-gp100 were kind gifts from Mr Tim Kottke, Mayo Clinic.

3.7 Flow cytometry

Cells were washed and stained in FACS buffer after addition to FACS tubes (BD biosciences, Cowley, UK) unless otherwise indicated. After washing, cells were stained with the appropriate volume of antibody for 20 minutes at 4°C. Cells were subsequently washed again and fixed in 200-300 μL 1% paraformaldehyde (PFA) and stored at 4°C, shielded from light, prior to acquisition.

Intracellular staining was performed after fixation by washing cells with 2mL FACS buffer, resuspending the pellet in 0.5mL 0.3% w/v saponin (Sigma) in FACS buffer for 15 minutes at room temperature. Cells were then centrifuged at 4°C and resuspended in 0.1% w/v saponin in FACS buffer with antibody to the relevant intracellular antigen and incubated at 4°C for 30 minutes. Where secondary antibodies were required the cells were washed with 0.1% w/v saponin prior to incubation with an appropriately conjugated secondary antibody. Cells were then washed with 0.1% w/v saponin and resuspended in 200-300 µL FACS buffer prior to immediate acquisition.

Flow cytometry of human cells was performed using a 2-laser, 4-colour BD Biosciences FACSCalibur and arising data analysed using the manufacturer's CellQuest Pro software. Cytometry of murine cells was performed by the Mayo clinic flow cytometry core facility. The resulting data was analysed by the candidate using FlowJo software.

3.8 Flow cytometry antibodies

Target molecule	Fluorochrome	Volume added$_{(to \approx 5x10^4 cells)}$	Manufacturer
CD107a/b	FITC	1 µL	BD Pharmingen
CD150	PE	2 µL	BD Pharmingen
CD40	PE	2 µL	Invitrogen
CD46	FITC	2 µL	BD Pharmingen
CD56	PE	2 µL	Serotec
CD8	FITC	1 µL	ProImmune
CD80	PE	2 µL	BD Pharmingen
CD86	PE	2 µL	BD Pharmingen
Goat anti-mouse Ig	FITC	2 µL	BD Pharmingen
gp100 (clone HMB45)	N/A	5 µL	NeoMarkers
HLA-A*201	N/A	5 µL	CRUK services
IFNγ	FITC	2 µL	BD Pharmingen
Isotype control	Triple (MultiMix)	2 µL	Dako
Melan-A	N/A	5 µL	Santa Cruz

3.9 Enzyme linked Immunosorbent assays (ELISA)

NUNC 96 well MAXISORP flat-bottomed plates (Thermo Scientific) were used unless otherwise stated. 100µL capture antibody was added to each well, diluted

as detailed in section 3.10, in 0.1M $NaHCO_3$, and the plate left overnight at 4°C. Plates were then washed three times with 0.05% v/v Tween (Sigma) diluted in PBS (PBS/Tween), using a Skan Washer 300B (Molecular devices, Sunnyvale, USA). Non-specific antibody binding was blocked by adding 200µL of 10% v/v FCS in PBS to each well for at least 2 hours at room temperature. After a further three washes, as above, known concentrations of recombinant proteins were added in triplicate to standard wells. 'Blank' wells were prepared by adding appropriate media alone. Samples were added in triplicate with or without dilution in relevant media to obtain values within the dynamic range of the standard curves. Plates were subsequently wrapped and stored at 4°C overnight. Plates were washed six times and 100µL detection antibody added to each well, after appropriate dilution (section 3.10) in 10% v/v FCS in PBS and subsequently incubated for 2 hours at room temperature. After a further 6 washes 100µL of ExtrAvidin Alkaline Phosphatase (Sigma), diluted 5000-fold in PBS/Tween, was added to each well. After 1 hour at room temperature and 3 washes with PBS/Tween followed by three washes with water, 100µL of the substrate p-Nitrophenyl phosphate (SigmaFast™ Sigma) was added to each well. Plates were then kept shielded from light until developed and then analysed using a multiwell scanning spectrophotometer (MultiskanEX Microplate Photometer, Thermo Scientific) reading absorbance at 405nm.

For some assays commercially available kits were used and the instructions within adhered to. DuoSet® ELISA from R&D systems were used to assay RANTES and IL-28A according to the manufacturer's instructions up until conjugation of the detection antibody, at which point local protocol and reagents were used for simplicity and reproducibility. The Verikine™ Human Interferon Beta ELISA kit (PBL interferon source) was provided with precoated multiwell plates and used in complete accordance with the manufacturer's instructions and supplied reagents.

3.10 ELISA antibody dilutions and recombinant standards

Cytokine	Capture/Detection	Dilution	Top Standard	Supplier
IL 6	Capture	1/500	2000pg/mL	BD
	Detection	1/500		
IL 8	Capture	1/500	500pg/mL	BD
	Detection	1/500		
IL 10	Capture	1/500	2000pg/mL	BD
	Detection	1/1000		
IL 28A	Capture	1/180	8000pg/mL	R&D
	Detection	1/180		
IFNβ	Capture	Varied according to batch and accompanying instructions	4000pg/mL	PBL Interferon source
	Detection			
CCL5/RANTES	Capture	1/360	1000pg/mL	R&D
	Detection	1/360		

3.11 Human in vitro experiments

3.11.1 Viability assays

3.11.1.1 Live/Dead® assay

The Red Live/Dead® fixable dead cell stain kit (Invitrogen) was used as it permits fixation of samples with PFA prior to analysis. The reagent is a fluorescent reactive dye that reacts with cellular amines. The reagent crosses the compromised cell membranes of dead cells and binds intracellular amines as well as cell surface amines, resulting in higher signal from dead cells compared to live. 7.5 x 10^4 cells were seeded into 24 well plates and after 24 hours treated with virus at various doses. Cells were harvested, after the required duration of infection, with PBS and trypsin and washed in PBS. Cell pellets were then resuspended in 1 ml PBS with 1 µL of Live/Dead dye reconstituted according to the manufacturer's instructions. Cells were then incubated for 15 minutes at room temperature prior to a further wash with PBS followed by a wash with 1% v/v FCS in PBS. Cells were then fixed in 1% PFA and stored at 4°C prior to flow cytometry.

3.11.1.2 Methylthiazolyldiphenyl-tetrazolium bromide, MTT

8000 cells were seeded in triplicate into 96 well plates and after 24 hours treated with virus at various doses. After the required duration of infection 20 µL of 5mg/mL MTT diluted in PBS, was added to each well. After 4 hours all media was carefully aspirated from plates, without disrupting the adherent monolayer, and replaced with 150 µL reagent grade DMSO (Fisher sciences). After 5 minutes at 37°C, to allow solubilisation, plates were sealed and analysed using a multiwell scanning spectrophotometer (MultiskanEX Microplate Photometer, Thermo Scientific, Rochester, USA) reading absorbance at 550 nm and viability calculated by normalisation to 100% against untreated control wells.

3.11.2 Western blots

Cell pellets and cell-free supernatants were prepared by plating 3x10^6 melanoma cells in T75 flasks and the following day adding virus at an MOI of 0, 0.1 or 2.5. After 24, 48 and 72 hours cells and supernatant were harvested. Cell-free supernatant was kept at -80°C until analysis. Stacking and running gels were prepared using constituents as prescribed previously (Sambrook, 1989) and poured into prefabricated cassettes (Invitrogen Life technologies). 20µL cell free supernatants made up 1:1 with Laemmli buffer were loaded into sample lanes and

2 µl of protein molecular weight markers added to control lanes (Odyssey® from LI-COR Biosystems, Lincoln, USA). Gels were run using the XCell SureLock™ Mini Cell system (Invitrogen) and a Bio-Rad laboratories PowerPac™ HC. Gels were run at 160-180V for around 60 minutes. Protein transfer was performed at 25V for 120 minutes, using Hybond™-C super membrane (Amersham Biosciences, Little Chalfont, UK). Membranes were blocked in Odyssey blocking buffer (LI-COR Biosciences) and washed with three changes of PBS/0.1% v/v Tween between stains. Staining for HMGB1 was performed using a monoclonal mouse anti-human HMGB1 antibody (R&D systems, Abingdon UK) used at 1-2µg/mL in a 1:1 mix of blocking buffer and PBS/0.1% Tween. Goat anti-mouse conjugated with AlexaFluor 680 (Molecular probes, Invitrogen) was used as a secondary antibody at 0.2µg/mL . The LI-COR Odyssey® Infra-red imaging system was used for analysis. Actin staining was performed the following day for cell lysates using murine anti-β actin (AbCam) at 0.3µg/mL, counterstained with IRDye800 conjugated affinity purified polyclonal Rabbit anti-Mouse IgG (Rockland, Gilbertsville, USA) used at 0.1µg/mL.

3.11.3 Multilayer models

The method was adapted from methodology used to mimic small molecule passage through vascular endothelium (personal communication from Dr Roger Phillips, University of Bradford). $2x10^5$ cells were seeded into ThinCert™ tissue culture inserts for multiwell plates, TW (Greiner Bio-One, Stroudwater, UK). After initial optimizing experiments 8.0µm pore size TW were used with Mel624 cells. TW were handled using sterilised forceps to prevent contamination. For 5-6 days media was replaced daily in both the TW and the underlying well, taking care not to disrupt cells. The change of media colour was noted as a possible indicator of cell proliferation; indirect microscopy was of limited effectiveness in visualising cells. Integrity of the multilayer was inferred from the absence of obvious holes on microscopy and the ability of the TW to maintain a column of media above the fluid level in the underlying well. Virus was added to the underlying well to try and maintain the three dimensional architecture in the face of the disruption caused by viral infection.

3.11.4 Confocal Microscopy

TW were prepared for imaging by immersion in 1% PFA overnight. The following morning TW were rinsed in PBS by gentle immersion in sequential containers of

sterile PBS after cautious aspiration of residual PFA. The TW were immersed in 1% FCS in PBS and blocked for two hours. TW were then aspirated and immersed for 5 minutes in 300nM DAPI (Invitrogen) diluted in PBS, and thoroughly rinsed in serial changes of PBS as above.

TW were imaged on glass-bottomed culture dishes using an Eclipse TE2000-E microscope and the data analysed using EZ-C1 FreeViewer software v3.5 (both from Nikon Instruments Europe, Kingston, UK).

3.11.5 Isolation of human peripheral blood mononuclear cells and magnetically-activated cell sorting (MACS)

Human buffy coats and cones were supplied by the National Blood Service (NBS). Fresh blood was obtained from healthy donors according to existing protocols and ethical approval. After dilution 1:1 with HBSS, blood was layered onto LymphoPrep (Axis-Shield, Kimbolton, UK) in 50mL Falcon tubes and spun at 800g for 25 minutes without brakes. The buffy layer was then collected using wide tipped pastettes and cells were washed in HBSS and pelleted by centrifugation at 400g for ten minutes. A final wash in MACS buffer (1% FCS and 2 mM EDTA diluted in PBS), or HBSS was performed, dependent upon the intended use, and the cells pelleted as above.

If required PBMC were resuspended in 25 mL freezing media and frozen in 1 mL aliquots for subsequent use.

3.11.6 Preparation of human dendritic cells

PBMC were prepared as above, the final wash being performed in MACS buffer. The cell pellet was resuspended in 80 µL MACS buffer per 10^7 cells and incubated with 5-10 µL per 10^7 cells (dependent on the number of cells required) CD14 MicroBeads (Miltenyi Biotec, Bisley, UK) for 15 minutes at 4°C then washed in MACS buffer. After resuspending cells in 500µL MACS buffer per 10^8 cells the suspension was applied to LS columns (Miltenyi) in a magnetic field. After three rinses columns were removed from the magnetic field and CD14+ cells harvested by forced expulsion of 5mL MACS buffer through the columns, into 15mL Falcon tubes. CD14+ cells were counted and resuspended at $2x10^6$/mL in monocyte media and grown in T25 flasks for 5 days prior to use.

3.11.7 HLA-A2 phenotyping of blood cells

The HLA-A2 phenotype was tested, where necessary, after separation as described above.

10^5 separated cells were added to each of two FACS tubes then washed in FACS buffer. 2 µL of BB7.2 antibody (CRUK) was added to one tube and both then incubated at 4°C for 30 minutes. Cells were then washed with FACS buffer and 2 µL of a goat anti-mouse FITC-conjugated antibody added to each tube. Cells were incubated at 4°C for 30 minutes and finally washed with FACS buffer, then fixed in 1% PFA and stored at 4°C prior to flow cytometry.

3.11.8 DC cultured with filtered tumour conditioned media (TCM)

DC prepared from Buffy coats or cones as described above and after 5 days of culture in DC media were cocultured with TCM. TCM was prepared by plating $4x10^6$ Mel888 in T75 flasks and infecting with MV at an MOI of 0, 0.1 or 2.5 the following day. 48 hours after infection the media was harvested and centrifuged to pellet any floating cells. The resulting supernatant was then filtered through 0.2µm cell strainers and again through Viresolve filters (Millipore, Watford, UK) to remove all virions prior to subsequent experiments. DC were harvested after 5 days and resuspended in fresh DC media at a cell density of $1x10^6$/mL and 2 mL put into each of 5 wells in 6 well plates. 2 mL of TCM was then added to appropriate wells. 2 mL DMEM or 2 mL DMEM with lipopolysaccharide (LPS) at 250 ng/mL were used as controls. The following day DC and media were harvested and centrifuged, the supernatant aliquoted and stored at -80°C. DC were washed with FACS buffer then stained with CD80 PE, CD83 PE CD86 PE, CD40 PE, Class I FITC or class II FITC for flow cytometry.

3.11.9 Preparation of DC-Mel888 cocultures

DC prepared from Buffy coats or cones as described above and after 5 days of culture in DC media were cocultured with Mel888 for priming experiments. $4x10^6$ Mel888 cells were seeded in T75 and the following day infected with MV in 2mLs Optimem, at an MOI of 0.1 or 1, 2.5 or Optimem alone for control. After 2 hours cells were rinsed with PBS and fresh DMEM replaced. The following day Mel888 cells were harvested, washed with RPMI and counted. Day 5 DC were harvested and washed with RPMI, then cocultured at a ratio of 3 Mel888 : 1 DC in fresh DC media. Cocultures were then incubated overnight in T25 or T75 flasks, laid flat in a

37°C incubator to allow Mel888 to adhere. For phenotypic studies the DC prepared as above were washed with FACS buffer then stained with CD80 PE, CD83 PE CD86 PE, CD40 PE, Class I FITC or class II FITC for flow cytometry.

3.11.10 Preparation of priming cultures

PBMC were isolated as described above and cocultures of DC with Mel888/MV-Mel888 established as above. After 24 hours of DC-Mel888 coculture, non-adherent DC were harvested and cocultured with freshly thawed autologous PBMC. Cocultures were established in CTL media at a ratio of around 1 DC:20 PBMC dependent upon the number of cells obtained and maintained at a cell density of 2-4x10^6/mL. IL-7 was added to cocultures at 5 ng/mL of media. For the duration of cocultures flasks were regularly inspected and fresh media and cytokines added as required. IL-2 was added at 30 U/mL on day 4 only. After one week PBMC-DC cocultures were re-stimulated with DC from further DC-Mel888/MV-Mel888 cocultures. A schematic of the assay is shown in Figure 34, page 135.

3.11.11 CD107 assay

CD107a and CD107b are markers normally present on cytotoxic granules but transiently exposed on the surface of cells following degranulation. Based on the method of Betts et al. it is possible to identify cells that degranulate in response to stimulation by culture with anti-CD107a and anti-CD107b (both BD biosciences) (Betts et al., 2003). Brefeldin A is included in the culture to prevent recycling of exposed CD107. The cells of interest were co-cultured with their proposed targets at a 1:1 ratio in either CTL media or, for innate experiments, RPMI with 10% v/v FCS, in the presence of FITC-labelled anti-CD107 antibodies. After one hour incubation at 37° brefeldin A was added to a final concentration of 10 µg/mL and the culture continued for a further four hours. Samples were then washed with FACS buffer prior to further staining with either anti-CD8 for lymphocyte assays or CD56 for innate studies. Samples were then fixed in 1% PFA before flow cytometry.

3.11.12 Intracellular IFNγ

At the same time as preparing cocultures for CD107 assay 1:1 cocultures of effector and target cells were prepared in suitable media and incubated at 37°. After one hour brefeldin A was added to a final concentration of 10 µg/mL then the cells

incubated for a further four hours. Samples were washed with FACS buffer prior to staining with either anti-CD8 for lymphocyte assays or CD56 for innate studies. After fixation with 1% PFA cells were then permeabilised with 1mL of 0.3% w/v saponin (Sigma) for 15 minutes at room temperature. Cells were washed with FACS buffer then incubated with anti-IFNγ diluted in 0.1% w/v saponin

3.11.13 Chromium release assay

The chromium release assay uses target cells loaded with ^{51}Cr; when lysed by effector cells the target cells release ^{51}Cr into the supernatant, which can in turn be detected and quantified by a scintillation counter.

A million target cells were harvested, washed and centrifuged to form a cell pellet in a falcon tube. The supernatant was discarded and around 100 μCi of ^{51}Cr added to the tube, then the cells incubated for one hour at 37°C. Cells were then washed three times with HBSS to remove ^{51}Cr that had not been taken up then resuspended in CTL media. Effector cells were added to wells of a round-bottomed 96 well plate (Nunc) in serial halving dilutions. The ^{51}Cr-labelled target cells were then added to wells containing effector cells, resulting in a range of effector:target ratios from 100:1 downwards. Triplicate wells were prepared for each ratio. In experiments examining adaptive T-cell responses 5000 unlabelled K562 cells, which are particularly susceptible to innate effectors, were added to every well to competitively exclude innate killing of loaded targets. For each cell line used, and for each experiment performed a further control plate was prepared to quantify maximum and minimum target lysis; Labelled targets were added to wells containing CTL media alone, or 1% triton X-100 the latter a detergent which causes profound disruption of cell membranes. Effector cells were not added to any such wells, but K562 were included when used in sample wells. The coculture sample plate and control plate were incubated at 37°C for four hours before the cells were pelleted by centrifugation. 50 μL of supernatant was then transferred, without dislodging the pellet, to scintillation plates (Lumaplate, Packard Biosciences). Once the scintillation plates had dried (at least overnight) the quantity of released ^{51}Cr was determined using a 1450 Microbeta Jet Liquid Scintillation and Luminescence counter (Wallac). The counts per minute (CPM) were converted to percentage specific lysis using the formula;

$$Percentage\ specific\ killing = 100 \times \left(CPM_{sample} - CPM_{spontaneous\ release}\right) \div \left(CPM_{maximum} - CPM_{spontaneous}\right)$$

3.12 Mouse in vitro experiments

3.12.1 Preparation of murine cells

Tissues harvested from mice were prepared by macerating through 100 μm cell strainers (BD Falcon) in cold PBS followed by washing with cold PBS. Where necessary erythrocytes were removed by resuspension for 2 minutes in 5-10 mL red cell lysis buffer, followed immediately by 2 washes in cold PBS.

3.12.2 MACS selections

T-cells were isolated from splenocytes with a negative MACS selection method, using a pan T-cell isolation kits and equipment according to the manufacturer's instructions (Pan T-cell Isoloation Kit II, Miltenyi Biotech). Single cell suspensions were prepared from spleens and lymph nodes then resuspended in MACS buffer and incubated with a cocktail of biotinylated antibodies with a broad range of specificities, other than CD8. After a ten minute incubation at 4°C anti-biotin magnetically labelled antibodies where then added with additional MACS buffer and the cells incubated for a further 15 minutes at 4°C. The cells were then washed, resuspended in MACS buffer and the suspension passed through a magnetic column. The eluate containing T-cells was collected, the cells were washed twice with PBS before resuspension in PBS at 10^7 cells per mL for intravenous administration to mice.

3.12.3 T-cell activation

Activated T-cells were prepared by preparing single cell suspensions from spleens and lymph nodes then treating the cells with red cell lysis buffer. After two washes cells were resuspended in T-cell media at 10^6 cells per mL, supplemented with IL-2 and relevant antigen (SIINFEKL or hgp100). 2 mL of the cell suspension was placed into each well of 24 well plates and the cells incubated for up to 7 days. Cells were monitored daily and media refreshed as needed, with fresh IL-2. Activated cells proliferated such that the cells needed to be split ¼ after 2 days. Cells were washed with cold PBS prior to administration to mice on the fifth or sixth day after initial preparation.

3.12.4 Discrimination of host lymphocytes from adoptively transferred cells

In most experiments Thy1.2+ C57BL/6 mice were used, but in order to assess the ability of adoptively transferred lymphocytes to reach tumours and tumour-draining lymph nodes (TDLN) a further experiment was prepared in which Thy1.1

C57BL/6 were inoculated with B16-Ova tumours and then treated with lymphocytes from Thy1.2 OT1 mice. At the time of euthanasia tumours, TDLN and spleens were harvested from the recipient mice and single-cell suspensions prepared as before. Cells were treated with red cell lysis buffer as required, then washed with FACS buffer. 0.5 µL each of anti-Thy1.1-FITC, anti-Thy1.2-PE and anti-CD8a-PECy7 were added to the cells for 20 minutes at 4°C. After two washes with FACS buffer, cells were fixed in 4% PFA prior to flow cytometry.

3.12.5 Intracellular IFN in response to antigen stimulation

Single cell suspensions prepared from tumours, tumour-draining lymph nodes and spleens were resuspended in OT1 medium at an approximate concentration of 2 x 10^6 cells per mL. 200 µL was added to wells in V-bottomed 96 well plates. Each well was supplemented with 0.4 µL of recombinant peptide(human gp100, trp2, SIINFEKL, VSV), along with 2 µL of golgi plug. Cells were then incubated for 4 hours at 37°C. After the incubation cells were washed with FACS buffer then incubated with 0.5 µL of anti-Thy1.1-FITC, anti-Thy1.2-PE and anti-CD8a-PECy7 for 20 minutes at 4°C, prior to further washing with FACS buffer. Cells were then permeabilised with the BD Cytofix/Cytoperm kit, used in keeping with the manufacturer's instructions. Briefly, washed cells were resuspended in the kit Cytofix/Cytoperm reagent for 20 minutes at 4C, then washed twice with PERM wash buffer. Cells were then resuspended in PERM wash buffer and stained with anti-IFNγ for 30 minutes at 4°C. After two final washes cells were resuspended in 4% PFA prior to flow cytometry. Isotype controls for each fluorophore were prepared; as were positive controls in order to establish suitable compensation levels.

3.13 Mouse In vivo experiments

All mouse protocols were reviewed and approved by the Mayo Foundation Institutional Animal Care and Use Committee (IACUC). All mice were housed in the Mayo animal care facility. Mice obtained from other facilities were housed in an on-site quarantine facility prior to use.

C57Bl/6 were obtained from the Jackson laboratories (Bar Harbor, ME, USA) and used at ages from 6-8 weeks in all protocols. Female Thy1.2 mice were used in most experiments, but female Thy1.1 were used when discrimination between host and adoptively transferred T-cells was needed (see Figure 47, page 160). OT1

and pmel transgenic mice were obtained from the Vile laboratory's own breeding programme. All animal procedures were performed after requisite in-house training and either directly by, or under the supervision of, Mrs Jill Thompson, veterinary technician to Professor Vile. In order to maintain consistency and objectivity, as advised by the ARRIVE guidelines, Mrs Thompson performed the majority of tumour measurements (Kilkenny and Altman, 2010).

3.13.1 Basic procedures

Tumours were established in the right flanks of animals by subcutaneous injection of $5x10^5$ cells resuspended in 100 µL PBS. Cells were prepared by initial harvest with trypsin followed by three washes in 4°C PBS prior to resuspension at $5x10^6$ cells per mL.

Tumours were measured thrice weekly by caliper and their antero-posterior and lateral dimensions recorded. Mice were euthanized if the tumours exceeded 1 cm in any dimension, if there was evidence of ulceration or impending ulceration, or if the animal showed any signs of distress. Euthanisation was performed by CO_2 inhalation in all cases.

3.13.2 Therapeutic administrations

Therapy was applied intravenously, intratumourally or by the intraperitoneal route. All administrations were performed by Mrs Thompson, or under her direct supervision. After briefly pre-warming mice using a heat lamp to elicit venodilation, intravenous access was obtained by placing unsedated mice into a custom jig that exposes the tail. Venous access was obtained with Kendall monoject 28 gauge tuberculin syringes (Tyco healthcare).

Naïve T-cells, both OT1 and pmel, were administered intravenously with a standard dose of 10^6 cells in 100 µL cold PBS.

Activated cells, both OT1 and pmel, were administered intravenously with a standard dose of 10^7 cells in 100 µL cold PBS. A higher dose was used for activated cells because of their lesser potential for expansion in vivo.

SIINFEKL was administered intravenously with a standard dose of 0.1 mg per mouse in 100 µL PBS. Intravenous virus (VSV-Ova or VSV-GFP) was administered at a standard dose of 5×10^8 pfu

Intratumoural and intraperitoneal injections, which were performed using Kendall monoject tuberculin syringes, were limited to 50 µL and 100 µL respectively.

Anaesthesia was achieved using inhalational isofluorane delivered via an oxygen-driven clinical-grade vapouriser to an induction chamber or nose cone, titrated to effect, with the exception of intracranial injections, which were performed using intraperitoneal anaesthesia detailed below.

3.13.3 Radiotherapy

Mice were secured for external beam radiotherapy in a mouse jig with single flank shield (Precision Xray Inc., North Branford, CT, USA) that restrains the animals without the need for anaesthesia and was well tolerated (Travis et al., 1982). The 7 mm thick lead shield, with a semi-lunar cutout over the right flank, was placed over the jig to restrict dose to the tumour and adjacent tissue. 300 kV photons were delivered from a Maxitron 300 kilovoltage irradiator (General Electric, no longer manufactured) at a source-to-surface distance of 0.7 m and a dose rate of 1.2 Gy/min. Treatment setup was calibrated by physicists from the Mayo clinic radiation oncology department prior to starting experiments.

For some experiments a ^{137}Cs source was used in a Mark I model 25 irradiator (J.L. Shepherd and associates San Fernando Ca, USA). For locally boosted treatments mice were placed in the same jig as described above. For whole body treatments mice were housed in 1 L beakers on a rotating platform within the irradiator housing to deliver evenly distributed dose. Experiments using the ^{137}Cs irradiator were performed by, or under direct supervision of, Mr Tim Kottke, as US federal regulations restrict access to high activity sources.

3.13.4 Brachytherapy

Sealed sources containing Iodine-125 were obtained from the Mayo departments of radiation safety and radiation oncology after use in patients for prostate cancer brachytherapy or ocular melanoma. No patient-related information was kept after the sources were returned to radiation safety. The location and use of each source was recorded and details kept by the radiation safety department. The seeds available were determined by clinical necessity and so different activities had to used within the experiments described. An equal distribution of seed activities was maintained amongst experimental groups unless otherwise indicated.

Silastic plaques were prepared from sheets of 2 mm tissue-grade silastica obtained from the Mayo engineering department. 8 mm diameter discs were cut using a custom-made aluminium punch. ^{125}I seeds were inserted into the discs by creating

a pilot hole with 20 gauge hypodermic needles. For some experiments the plaques were overlain with a centrally placed 6mm diameter disc of 1 mm thick lead sheet, secured and covered with adhesive silastic (Dow Corning adhesives, Midland, MI). This made the overall thickness of the plaque 3.5 mm but the addition of lead shielding reduced the emergent activity by 90%, with resultant benefits to personnel exposure, and allowing the use of higher activity seeds. After preparation the plaques were autoclaved prior to surgical insertion.

For insertion of plaques mice were anaesthetized with inhalational isofluorane. After cleaning with betadine a 2 cm craniocaudal incision was made medial to the palpable tumour. A pouch was prepared overlying the tumour using blunt dissection and the plaque inserted. The pouch was closed using surgical clips and the mouse observed until seen to have recovered from the effects of anaesthesia. After insertion of plaques mice were housed in a dedicated radiation facility within the animal house, until the plaques were removed. Removal was performed using inhalational isofluorane anaesthesia. Plaques were readily extracted with minimal dissection and the incision reclosed with surgical clips. Clips were removed after 9 days, once the wound was well healed.

Computed tomography images were captured using a high-resolution micro-SPECT/CT system (X-SPECT, Gamma Medica Ideas, Inc., Northridge, CA). Micro-CT images were acquired, without SPECT acquisition, in 3 minutes (600 ms, 360 images) at 0.5 mA and 60 kV. Mice were anaesthetised with inhalational isofluorane throughout. The data were transferred according to DICOM (digital imaging and communications in medicine) protocols to the radiation oncology physics department for dosimetry estimation. An initial approximation of dose to tumours from one seed was given by the point source TG-43 formula, wherein;

$$Dose\left(\frac{cGy}{hour}\right) = Air\ Kerma\ Strength \times Dose\ Rate\ Constant \times Radial\ Dose\ Fraction \div r^2$$

The dose rate constant for ^{125}I is 0.965 cGy/hour/unit and radial dose fraction approximates to unity.

3.13.5 Intracerebral tumour implantation.

Mice were anaesthetized with a combination of ketamine (100 mg/kg) and Xylazine (10 mg/kg) (both supplied by Mayo pharmacy) mixed and given intraperitoneally. Once adequate anaesthesia was confirmed the head was cleaned

with betadine and the eyes covered with an artificial tear preparation. A small midline incision was made behind the eyes to the level of the ears. Skin was bluntly pushed to the right side to allow access to the site for the burr hole, 2 mm anterolateral to the bregma. A Dremel multi-tool (ACE Hardware, Rochester, MN, USA) fitted with a 2 mm cutting bit was used to make the burr hole under direct vision. Mice were then transferred to a stereotactic jig and secured by tooth hoop. A Hamilton syringe with a fixed 26 gauge fine bore needle was then guided to the burr hole, until the needle tip was seen to rest on the meningeal or cerebral surface. The syringe was then driven down between 2-3 mm, dependent on the size of the mouse, and infusion of cell suspension performed at 1 μL per minute with an additional minute after completion of the infusion. The needle was then withdrawn and in some experiments the burr hole occluded with bone wax before suturing the incision with 4-0 vicryl on a rb-1 curved needle.

Mice were monitored and warmed by heat lamp until seen to have fully recovered from the effects of anaesthesia. Once tumour cells had been implanted mice were checked daily for any evidence of tumour burden. Specifically impaired gait, persistent hunching or emaciation were taken as evidence of unacceptable tumour burden and mice displaying such symptoms were immediately euthanized.

Tissue was extracted for histology at the time of euthanasia and immediately immersed in prefilled pots containing 30 mL 10% neutral buffered formalin (Fisher Scientific) then sent to the Mayo animal studies histology department for further analysis.

4 Measles virus versus melanoma

4.1 Introduction

The Edmonston strain of MV has been studied as a potential OV across a wide range of preclinical tumour models (Donnelly et al., 2013). Its oncotropism is predominantly due to overexpression of one of the key MV receptors, CD46, on the surface of most tumour cells. Pre-clinical promise has led to clinical trials in myeloma, ovarian cancer, glioma, mesothelioma and lymphoma, but the virus had not previously been studied, clinically or pre-clinically, in melanoma (Donnelly et al., 2012a).

In addition to direct oncolysis several OV have been demonstrated to cause inflammatory cell death, capable of enhancing innate anti-tumour immunity and priming adaptive anti-tumour immune responses (Prestwich et al., 2008c). Indeed in some pre-clinical models the therapeutic efficacy of OV is in fact predominantly mediated by immune sequelae, rather than oncolysis per se (Prestwich et al., 2009b). MV stimulates immune responses in models of mesothelioma, but its immune effects have been otherwise little explored (Gauvrit et al., 2008).

The experiments described below first sought to test the oncolytic activity of MV against in vitro models of human melanoma, and then to assess the immunological effects of MV treatment, exploring its potential as a therapeutic agent for patients with melanoma.

4.2 Results

4.2.1 CD46 expression on melanoma cell lines

wtMV has a tropism for immune cells and DC, thought in part to contribute to the immunosuppression associated with the measles illness (Grosjean et al., 1997; Permar et al., 2006; Schneider-Schaulies and Schneider-Schaulies, 2009). Nectin-4 has recently been identified as a receptor for the wild type virus and is likely to be relevant for oncolytic strains too, however it is thought to be more important for exiting the cell (Mühlebach et al., 2011). The principle receptor to which wtMV is able to bind is CD150, also known as the signalling lymphocyte activation marker (SLAM), commonly expressed on DC and lymphocytes (Erlenhofer et al., 2002; Dhiman et al., 2004). By contrast the Edmonston strain has acquired additional tropism for CD46, ubiquitously expressed on nucleated human cells. CD46 is the membrane cofactor receptor which serves to bind and neutralise components of the complement pathway, specifically C3b and C4b, acting as cofactor for their proteolytic degradation. Its function therefore is to regulate complement-mediated lysis, preventing inappropriate attack by complement proteins. CD46 is upregulated on several human malignancies, presumably as a defence against complement mediated lysis, and it is reported that this is one of the mechanisms of MV oncotropism (Anderson et al., 2004; Ong et al., 2006b).

CD46 binds to the F (fusion) and H (haemagglutinin) structural proteins of MV, and the resulting trimer undergoes conformational changes that lead to viral entry (Navaratnarajah et al., 2008, 2009). Subsequent viral transmission between cells is also mediated by CD46; an infected cell will produce F and H proteins that are in turn expressed on its surface. These surface F and H proteins bind CD46 on adjacent uninfected cells, which leads to cell-to-cell fusion, resulting in giant multinucleated syncytia (Duprex et al., 1999; Duprex and Rima, 2002).

Experiments with cell lines transfected to express varying amounts of CD46 have shown that the efficiency of viral entry is directly related to levels of CD46 expression (Ong et al., 2006b). In contrast the phenomenon of cell-to-cell fusion requires a threshold level of CD46 expression, but increasing levels do not significantly increase the efficiency of fusion.

Given that CD46 or CD150 expression on melanoma cells would be a requisite for successful oncolysis by MV, the human melanoma cell lines Mel888, Mel624, MeWO and SkMel28 were stained with FITC-labelled anti-CD46 or anti-CD150

mAb prior to flow cytometry to determine the levels of surface expression. As expected no cell line expressed CD150 (data not shown) but, as shown in Figure 9, all four cell lines express surface CD46, suggesting possible susceptibility to MV.

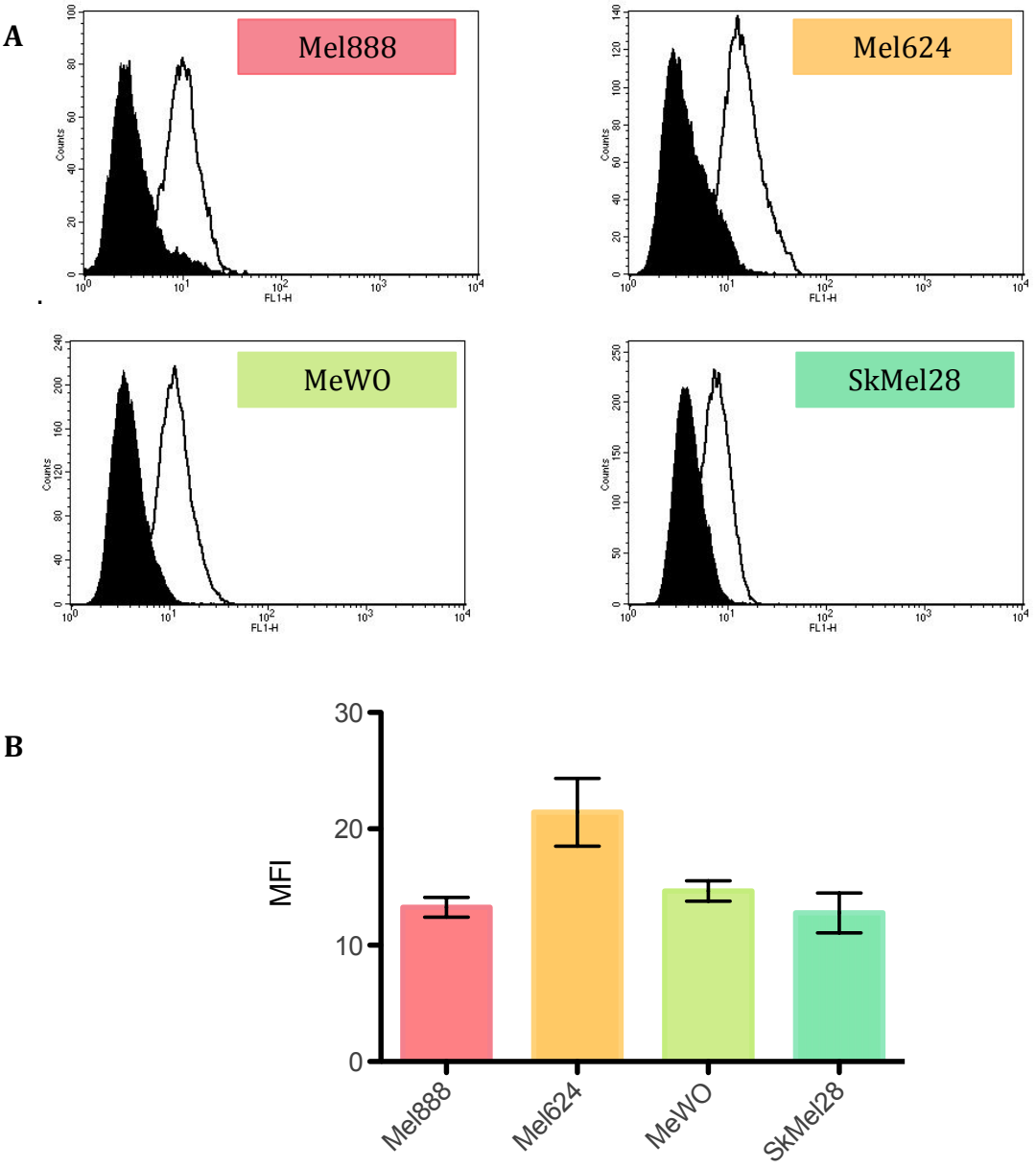

Figure 9. CD46 expression on melanoma cell lines. Melanoma cell lines (Mel888, Mel624, MeWO and SkMel28) were examined for surface expression of CD46, a MV receptor, by flow cytometry after staining with a FITC-conjugated monoclonal anti-CD46 antibody. A. Representative histograms indicate cells stained with an isotype control antibody (filled histograms), and cells stained with anti-CD46 (open histograms). B. Median fluorescence intensity (MFI) was recorded from three separate experiments. Error bars indicate the standard error of the mean values (SEM).

4.2.2 Morphological changes following MV treatment.

The characteristic cytopathic effect (CPE) of MV is to produce giant multinucleated cells or syncytia. Infected cells express the fusogenic viral proteins F and H on their surface and cell-to-cell fusion ensues; the resulting syncytia may contain many hundreds of nuclei. These appearances were first described, independently, by Warthin and Finkeldy after examination of enlarged lymph nodes from children suffering wtMV infection; those authors now share an eponym as a result (Paik et al., 2002).

Cells of each of the four melanoma lines used above were treated with MV expressing GFP in serum-free viral infection media at a range of multiplicities of infection (MOI). 48 hours later the flasks were examined for evidence of CPE. As shown in Figure 10 there were clearly visible syncytia amongst Mel888 treated with MV-GFP, indeed the plaques were visible without microscopy, but are more readily seen with fluorescent microscopy as demonstrated in Figure 11. Figure 12 throughFigure 17 illustrate similar findings amongst the other cell lines, though it is clear that the speed and degree of infection varies between cell lines.

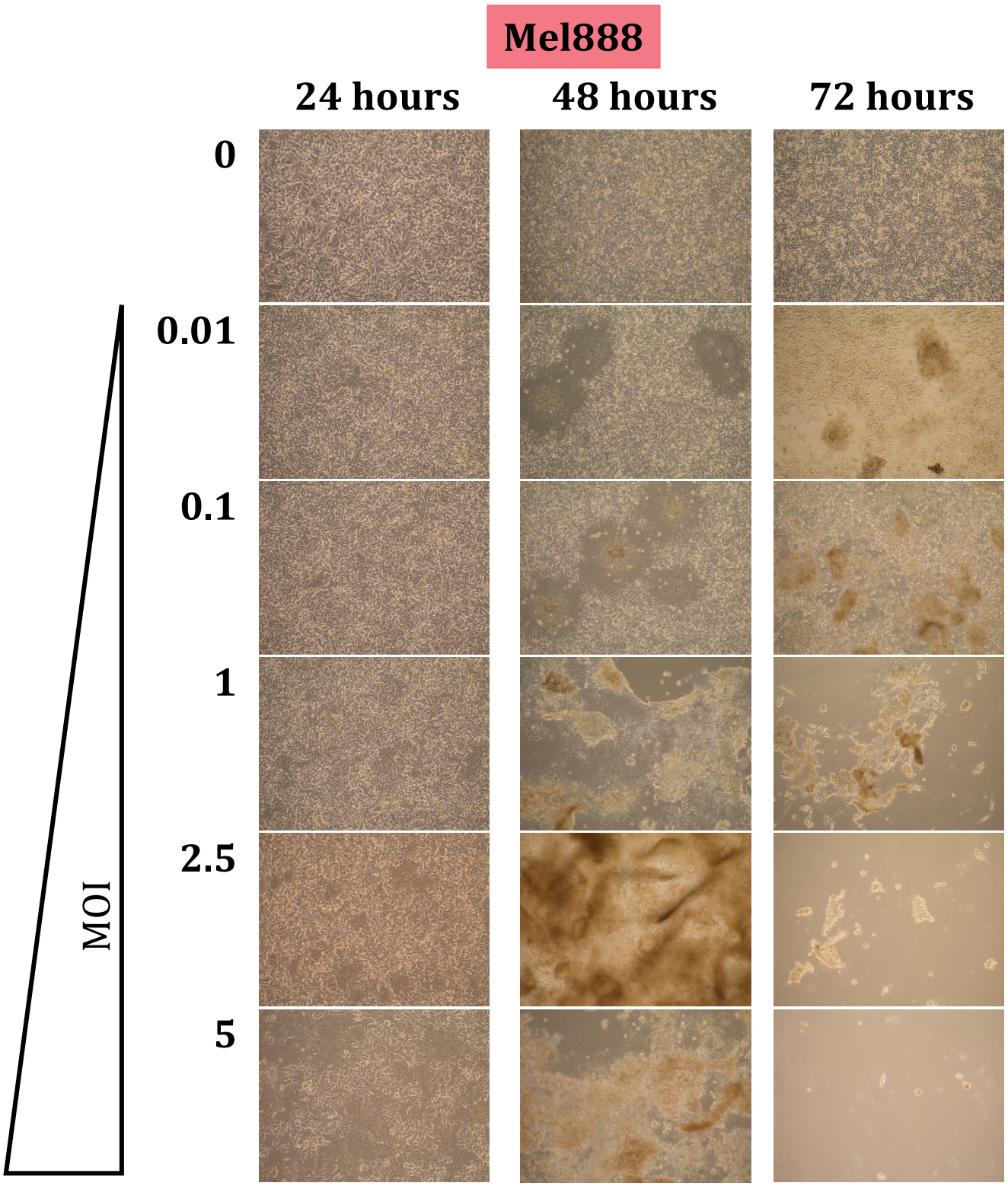

Figure 10. Cytopathic effect of MV upon Mel888. Mel888 cells were treated with MV-GFP at the MOI indicated and photographs taken using phase contrast microscopy, after 24, 48 and 72 hours.

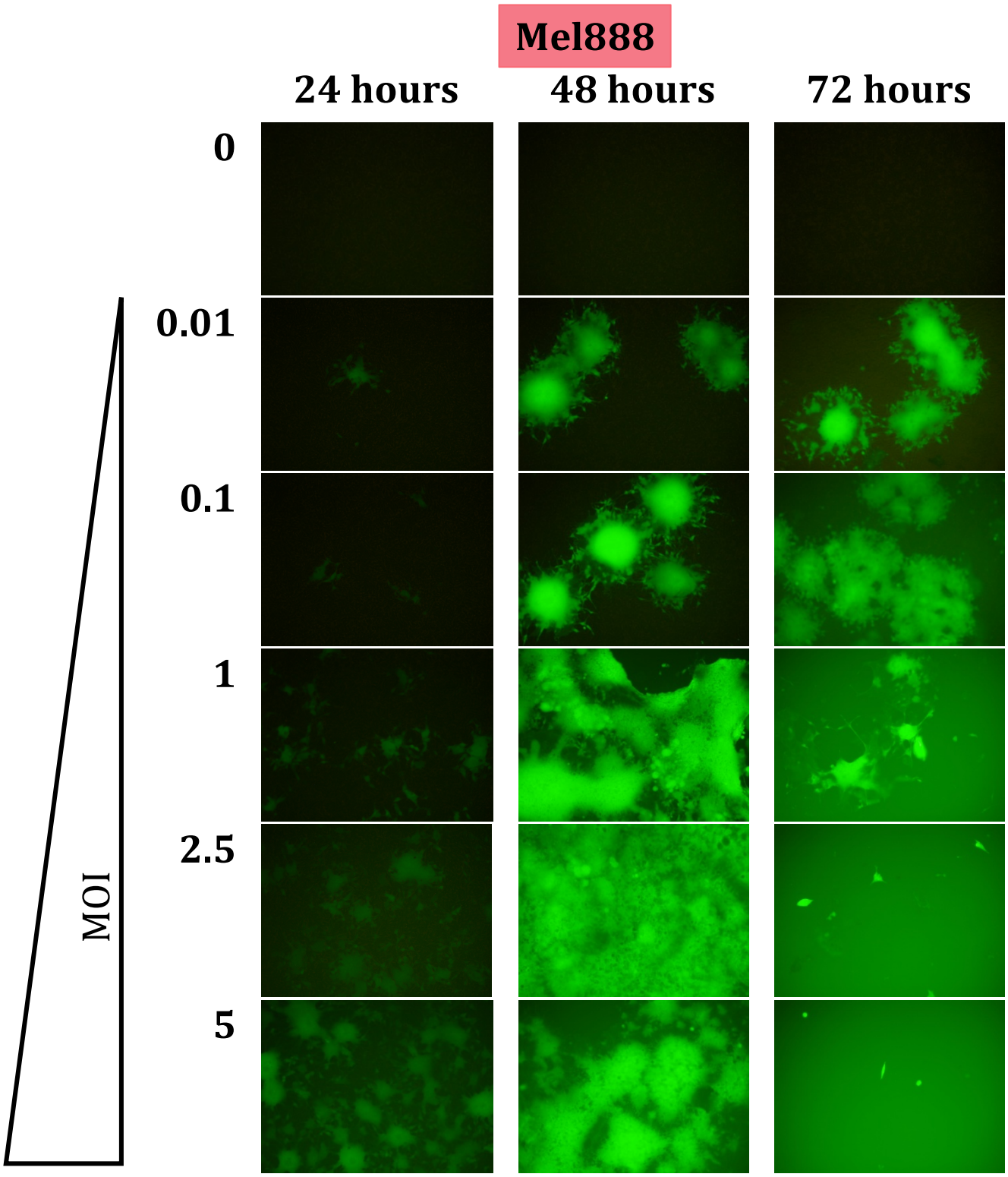

Figure 11. GFP expression in Mel888 treated with MV-GFP. Fluorescence microscopy of the same fields shown in Figure 10.

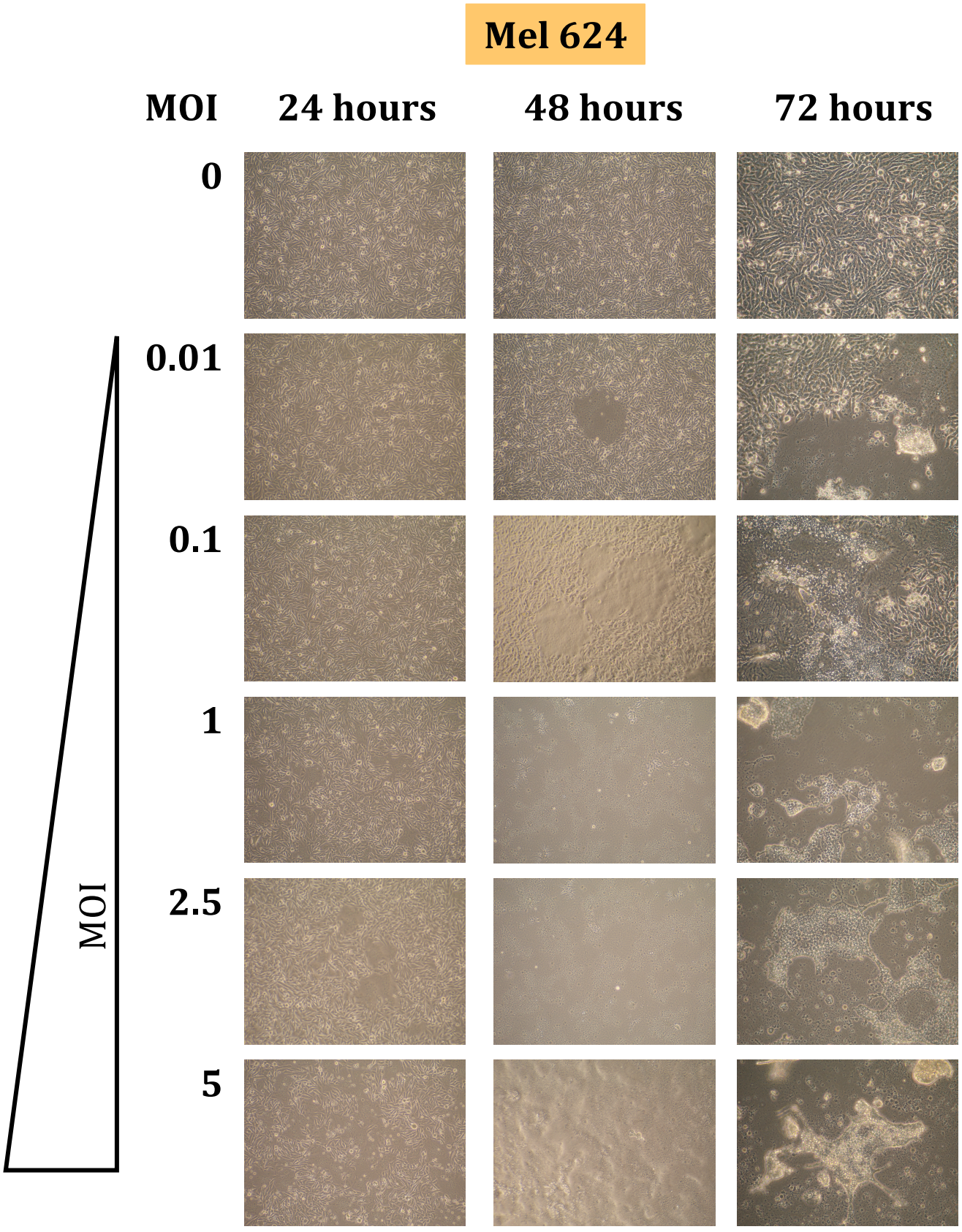

Figure 12. Cytopathic effect of MV upon Mel624. Mel624 cells were treated with MV-GFP at the MOI indicated and photographs taken using phase contrast microscopy, at 24, 48 and 72 hours.

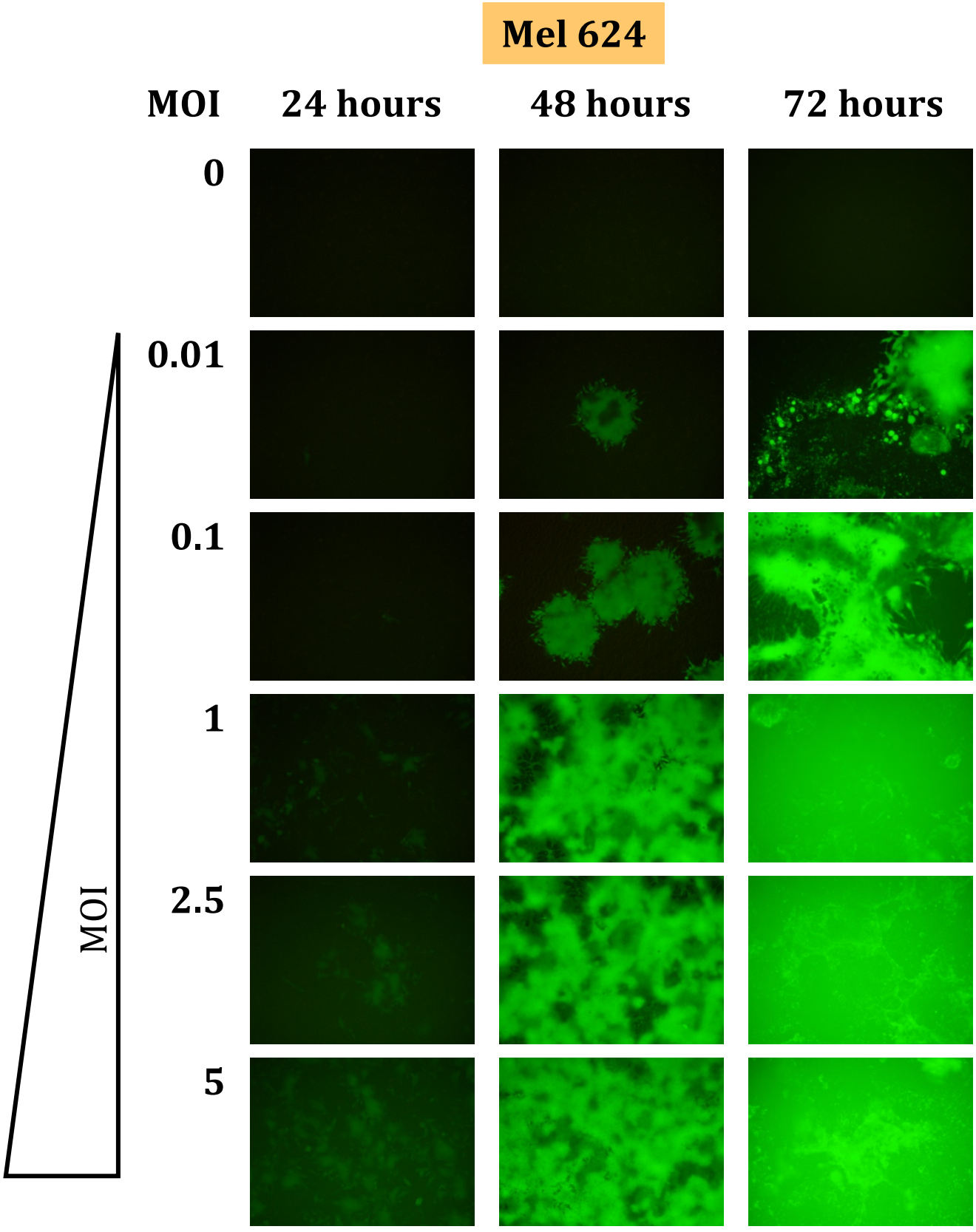

Figure 13. GFP expression in Mel624 treated with MV-GFP. Fluorescence microscopy of the same fields shown in Figure 12.

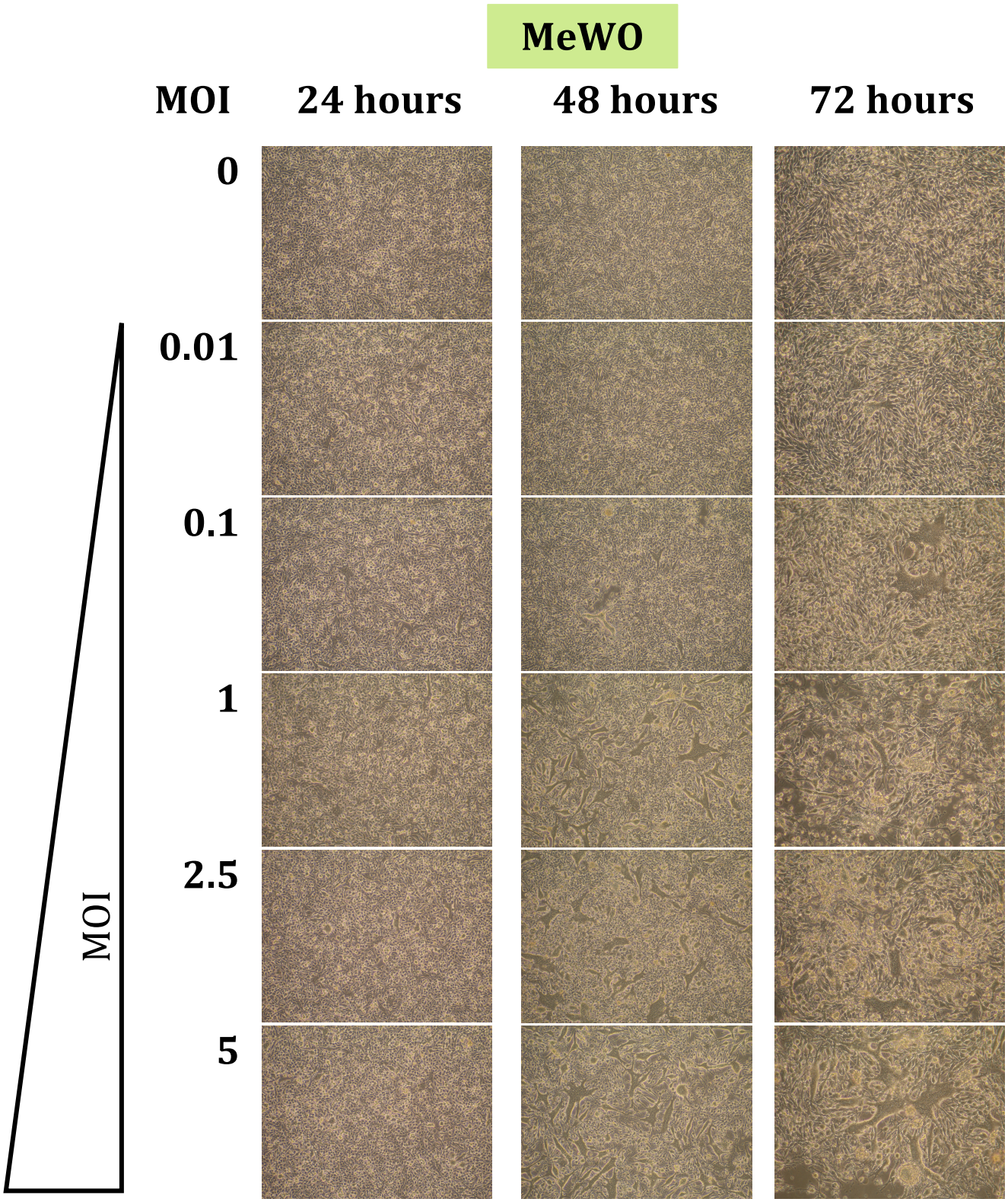

Figure 14. Cytopathic effect of MV upon MeWO. MeWO cells were treated with MV-GFP at the MOI indicated and photographs taken using phase contrast microscopy, at 24, 48 and 72 hours.

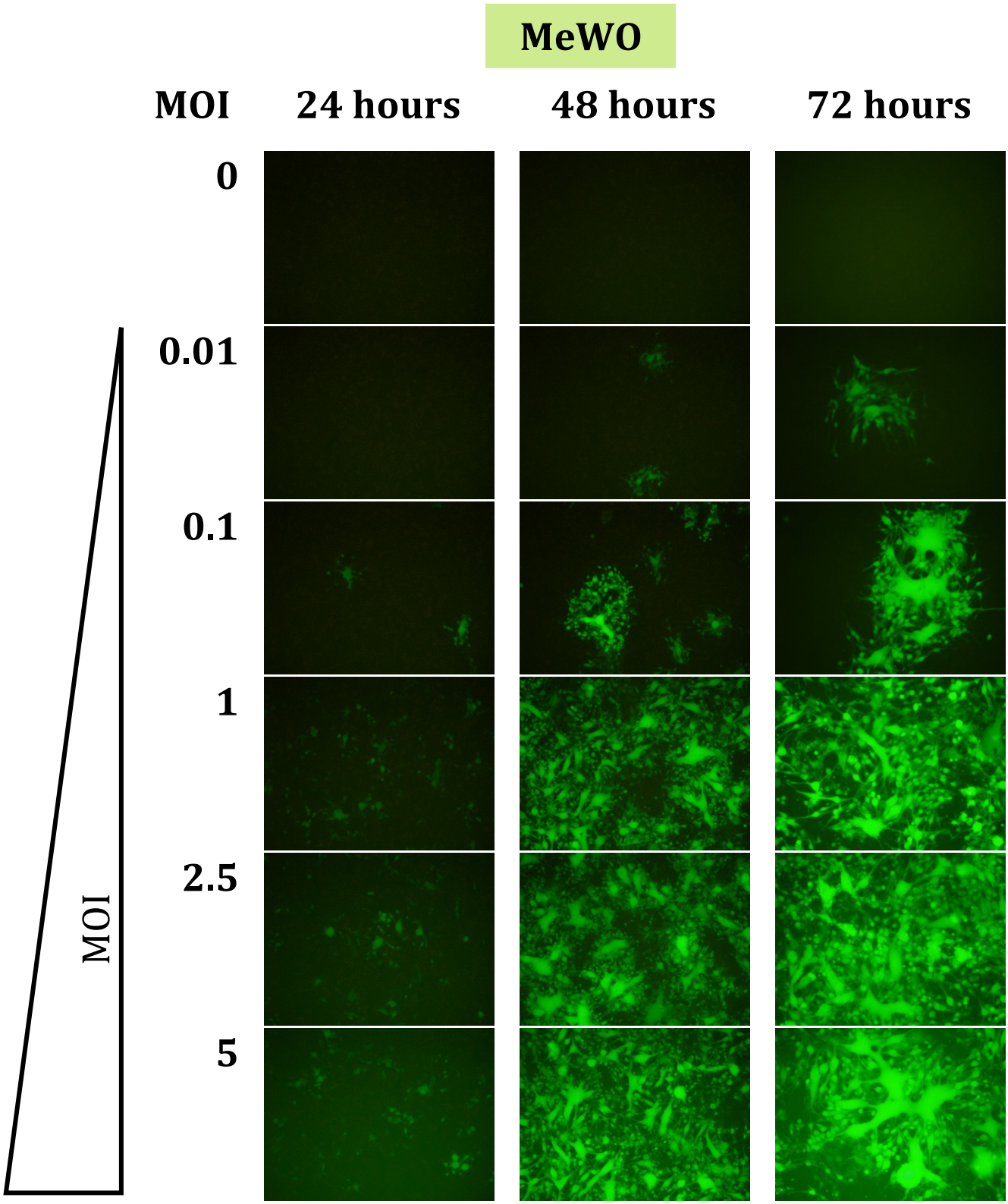

Figure 15. GFP expression in MeWO treated with MV-GFP. Fluorescence microscopy of the same fields shown in Figure 14.

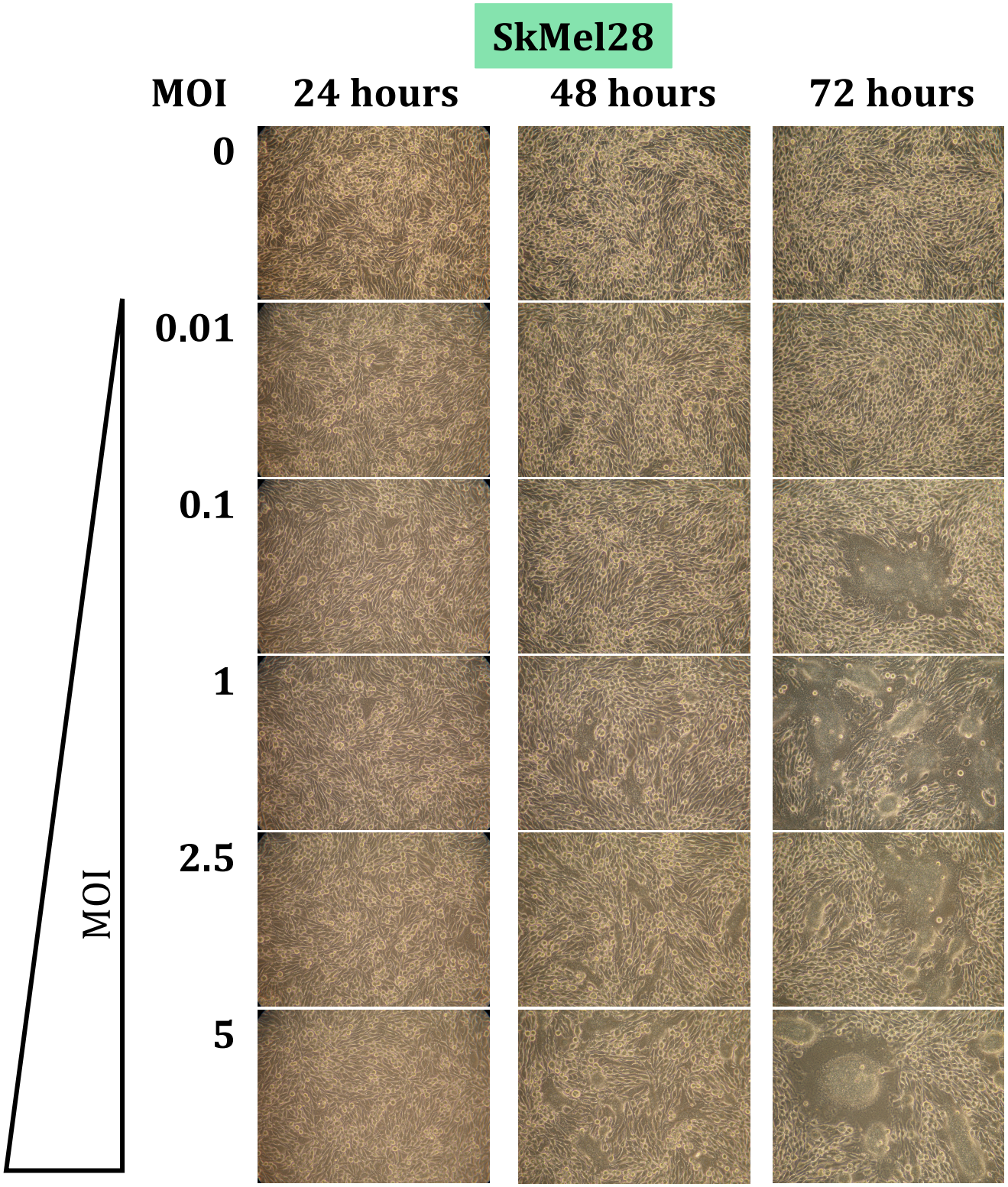

Figure 16. Cytopathic effect of MV upon SkMel28. SkMel28 cells were treated with MV-GFP at the MOI indicated and photographs taken using phase contrast microscopy, at 24, 48 and 72 hours.

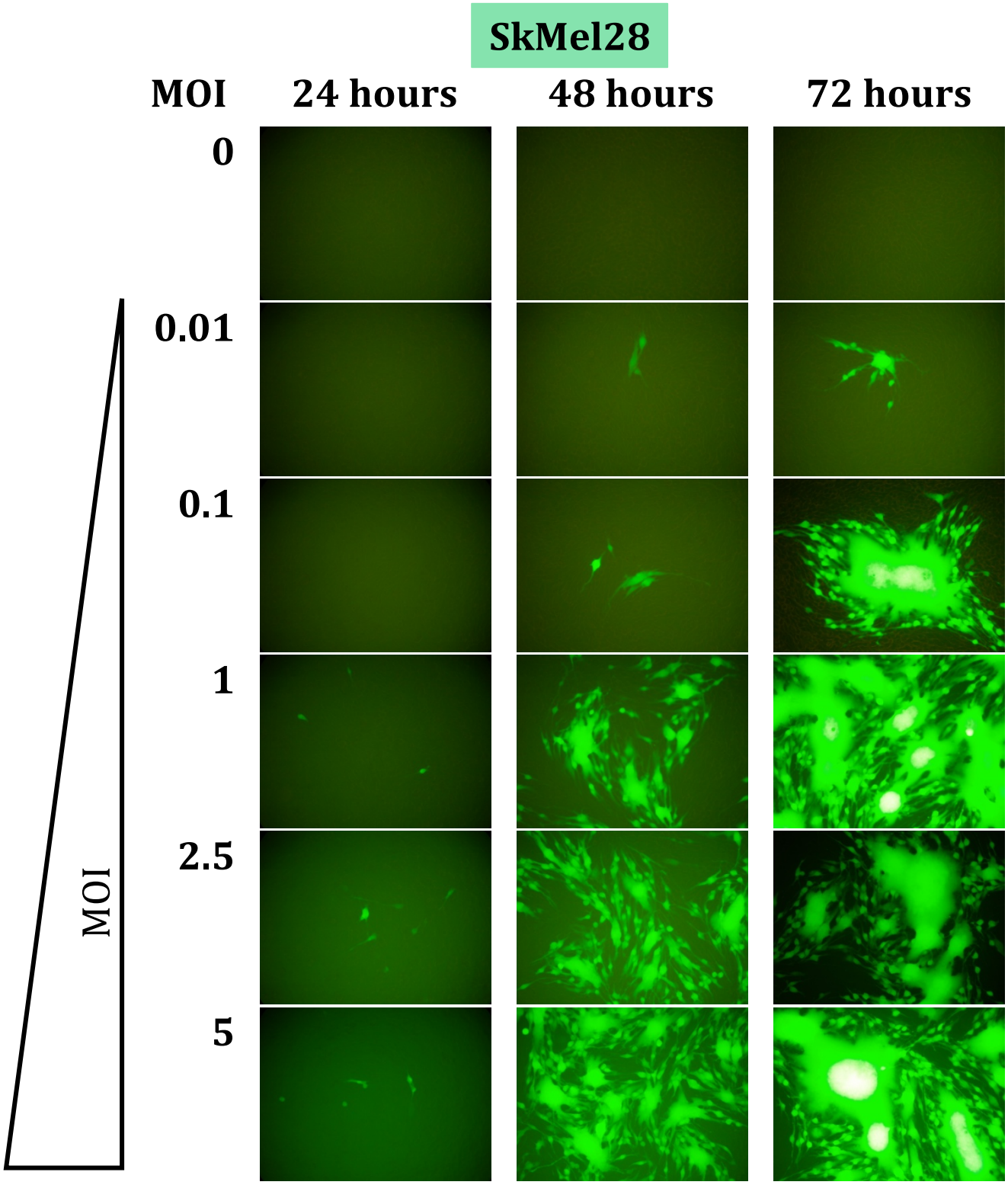

Figure 17. GFP expression in SkMel28 treated with MV-GFP. Fluorescence microscopy of the same fields shown in Figure 16.

4.2.3 Viability assays following MV treatment

To obtain objective measures of MV-mediated oncolysis of melanoma cells Live/Dead flow cytometry assays were performed. The Live/Dead reagent is a commercially available product that is based on similar principles to the more familiar propidium iodide stains; it is a non-specific amine-binding dye that readily binds, but does not cross, cell membranes. Live cells with intact external membranes will therefore have a considerably lower fluorescence when compared to dead or dying cells with disrupted membranes. MV was added in Optimem without serum at a MOI in the range indicated, to cells grown overnight in 24-well plates, and after one hour was replaced with DMEM. At 24, 48 and 72 hour intervals cells were harvested, washed and stained with the Live/Dead reagent in accordance with the manufacturer's instructions, and then fixed in 1% PFA prior to analysis by flow cytometry. After gating around the morphologically intact population to exclude non-specific binding of the dye by cellular fragments and doublets, cells were separated into positive or negative staining by comparison with untreated controls and the percentage of dead cells determined. As shown in Figure 18, very little cell death was seen at 24 hours, irrespective of MOI. However within 48 hours an increase in cells stained with the Live/Dead reagent was seen, indicating that all four melanoma cell lines were susceptible to MV-mediated oncolysis in a dose-dependent fashion. There appeared to be a threshold between 0.01 and 0.1 MOI, below which no increase in killing compared to controls was seen. Though susceptibility was similar between cell lines, Mel624 appeared slightly more resistant to the oncolytic effects of MV than the other lines, despite the microscopic and macroscopic appearances (Figure 12).

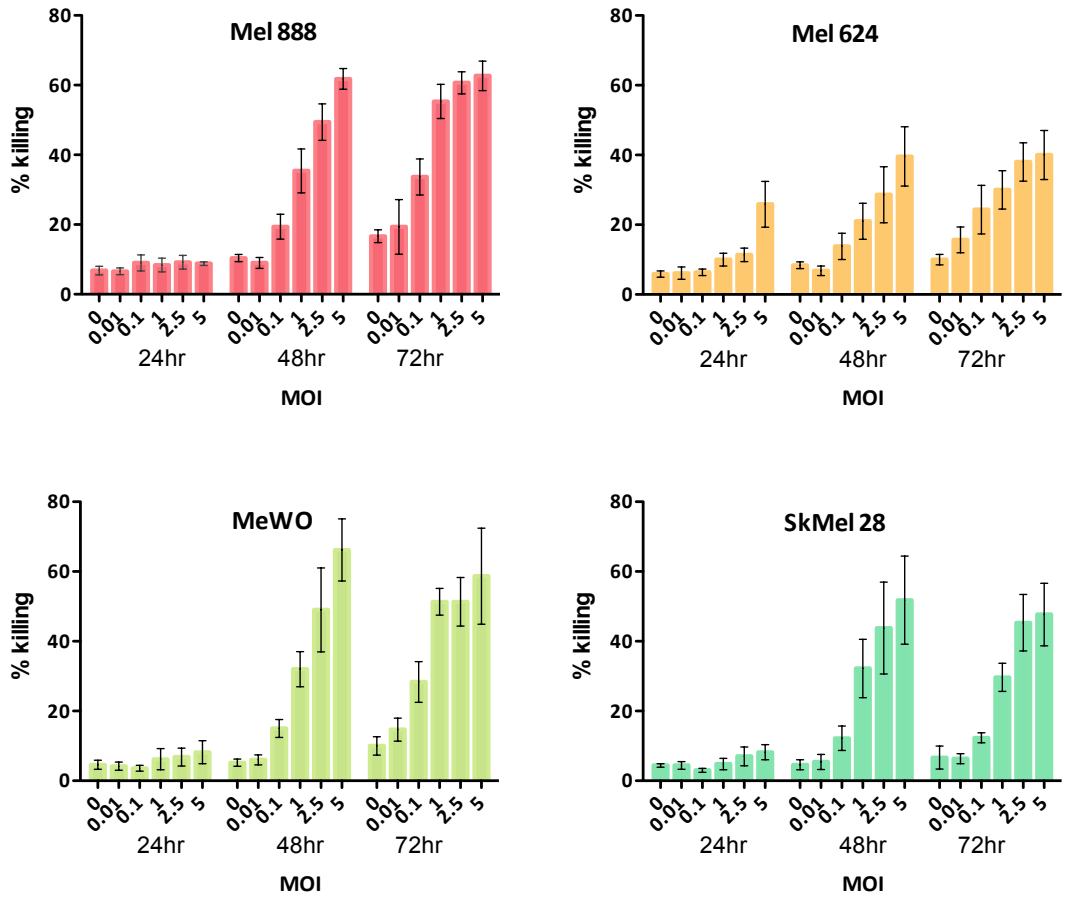

Figure 18. Oncolytic activity of MV against melanoma cell lines (Live/Dead). Tumour cells were seeded in 24 well plates and the following day treated with MV at the MOI indicated. Oncolytic activity was assessed after 24, 48 and 72 hours using the Live/Dead discriminator assay and the proportion of dead cells quantified by flow cytometry. Results shown are the mean of 5 independent experiments and error bars indicate the SEM.

It has been reported that MV-infected cells forming large syncytia may remain viable for extended periods whilst cultured with adequate numbers of intact cells (Herschke et al., 2007). This suggests that some MV-infected giant cells, fated to die, may maintain their cell membrane integrity during the period of this assay. The yellow tetrazolium salt 3-[4,5-dimethylthiazol-2-yl]-2,5-diphenyltetrazolium bromide (MTT) freely permeates cell membranes and is subsequently reduced by mitochondrial dehydrogenases, present in metabolically functional cells, to a purple-coloured formazan. The production of formazan is a colourimetrically detectable and quantifiable change which indicates the number of metabolically intact cells and is used as a measure of cell killing - the MTT assay (Liu and Dalgleish, 2009). The MTT assay was performed to corroborate the results of the Live/Dead assay as well as the appearances of cytopathic effect following MV-treatment, which suggest oncolytic efficacy of the virus.

Melanoma cell lines were grown in 96 well plates. The following day MV was added as before and MTT assay performed at 24, 48 and 72 hours after MV treatment. Results were obtained by measuring absorption at 550 nm. The percentage of cells alive in treated wells was calculated based on relative absorption; untreated wells served as controls and were assumed to be 100% alive. Results of the MTT assays are shown in Figure 19. In keeping with the results from Live/Dead assays no loss of survival was seen at 24 hours at any MOI in any cell line. By 48 hours after infection there was evidence of loss of viability of Mel624 and Mel888; MeWO and SkMel28 only began to display susceptibility by 72 hours, in keeping with the morphological changes described above.

It was noted that levels of viability were higher at low MOI, and this prompted concern that sub-therapeutic MOI appeared to stimulate proliferation of melanoma. In further experiments cell counts confirmed that there was no proliferation in cells treated at any MOI compared to untreated controls (data not shown).

The MTT reagent readily permeates intact membranes therefore it is likely that the increased absorption seen at low MOI actually reflects transiently increased metabolic activity within surviving MV-infected, multinucleated giant cells (Liu and Dalgleish, 2009).

Notably there was some discordance between the degree of susceptibility determined by Live/Dead assay when compared to MTT; i.e. by Live/Dead, Mel624

appears to be the most resistant cell line, whereas by MTT Mel624 is the most susceptible. This presumably reflects the fact that each assay measures different and surrogate markers of cell killing, and the discrepancy due to inherent variations between the cell lines. Despite the limitations of each assay it is important to note that collectively the data from Live/Dead assays, MTT assays, and the morphological changes seen, all serve to assert the susceptibility of melanoma cell lines to oncolysis by MV. Reassuringly the degree and timing of killing observed are in keeping with reports of oncolytic efficacy of MV in several other non-melanoma cancer models (Haralambieva et al., 2007; Myers et al., 2008; Dingli et al., 2009; Liu et al., 2009; Msaouel et al., 2009; Iankov et al., 2010; Li et al., 2010). Previous experience of reovirus, an alternative OV, used in models of human melanoma suggests that MV replication in, and killing of, human melanoma cell lines is slower and less effective than reovirus, though with the caveat that comparisons outwith formal head-to-head testing are unreliable (Errington et al., 2008b).

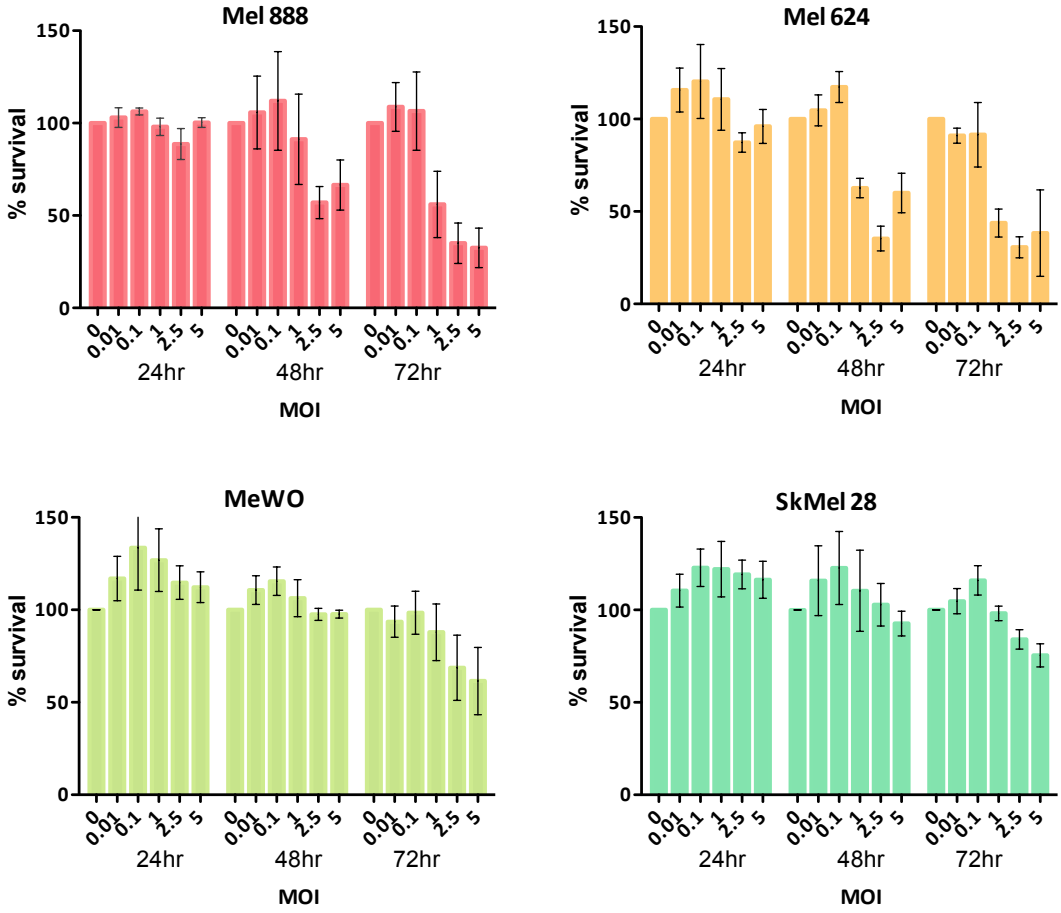

Figure 19. Oncolytic activity of MV against melanoma cell lines (MTT). Tumour cells were seed in 96 well plates and the following day treated with MV at the MOI indicated. Cell viability was assessed after 24, 48 and 72 hours using MTT assay and the proportion of metabolically active cells quantified by optical density, with viability determined in relation to untreated controls. Results shown are the mean of 4 separate experiments and error bars indicate the SEM.

4.2.4 Viral replication

One of the tenets of the OV approach is that successful viruses will reach tumours and after cell entry commandeer cellular machinery to initiate viral replication. This in-target replication has been suggested to be vital to therapy, although others have argued that much of the efficacy of OV is in fact due to effects upon the immune system (Prestwich et al., 2009a).

Melanoma cells were plated in triplicate in six well plates and after 24 hours infected at an MOI of 0.1. Cells were scraped from each well and non-adherent cells recovered from the supernatant media by centrifugation. The cells were then subjected to three cycles of freezing and thawing to release virions from intact cells or syncytia, and the viral suspension was titrated by serial ten-fold dilutions on Vero cells to quantify the TCID50 (Tissue culture 50% infectious dose) according to the method of Reed and Muench (Reed and Muench, 1938). As illustrated in Figure 20, melanoma cells treated with MV at an MOI of 0.1 yielded logarithmic increases of replicating virus by 48 hours after infection. The results shown are representative of two separate experiments.

The data presented so far assert the conventional oncolytic potential of MV in melanoma; namely that the virus successfully infects, replicates within and kills melanoma cell lines. Notably however this is likely only to be one component of OV efficacy in the clinical setting, and others have demonstrated that generation of an anti-tumour immune response is requisite for therapy in some in vivo models of OV (Prestwich et al., 2009b). Therefore the inflammatory potential of MV, in the setting of melanoma, was examined.

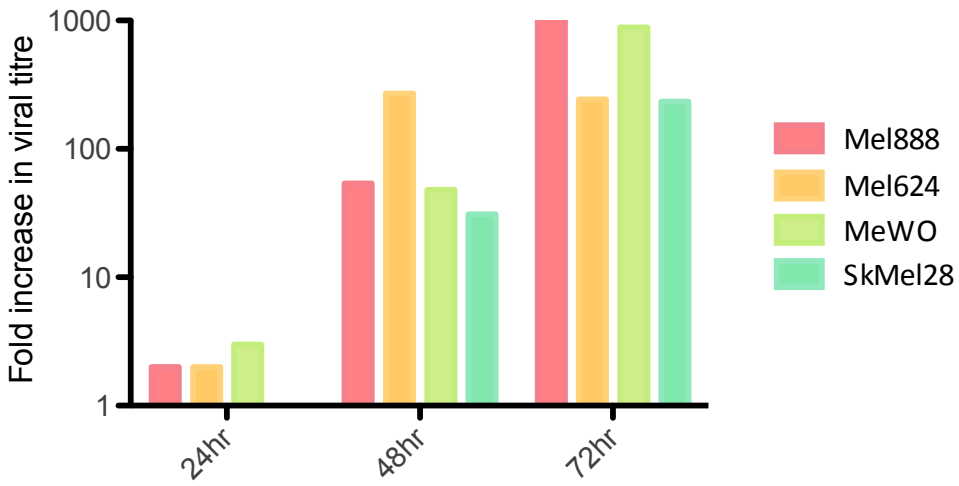

Figure 20. Viral replication. Cells from each melanoma line were plated in 24 well plates and the following day treated with MV in serum-free media to an MOI of 0.1. At the time points indicated adherent and non-adherent cells were harvested then subjected to three cycles of freezing and thawing then added, after serial ten-fold dilutions, to Vero cells in order to establish the viral titre, and the fold-increase calculated. Results shown are representative of two separate experiments.

4.2.5 Characteristics of MV-induced melanoma cell death

As would be expected, the use of MV as a paediatric vaccine MV stimulates a Th1-skewed inflammatory cytokine response (Ovsyannikova et al., 2003); clearly a very different setting from oncolytic virotherapy, but this at least suggests that treatment with MV may generate the inflammatory milieu capable of enhancing anti-tumour immunity. It has previously been shown in melanoma cell lines that cytokine and chemokine release following OV-mediated cancer cell death contributes to the generation of innate and adaptive immune responses and bystander killing (Errington et al., 2008a, 2008b).

In parallel with the cytotoxicity assays described above, supernatant media was collected from cells 24, 48 and 72 hours after treatment with MV at a range of MOI. This tumour-conditioned media was clarified by centrifugation and stored at -80°C before analysis for a range of cytokines by ELISA, the results of which are shown in Figure 21 and Figure 22.

The release of chemokines and cytokines varied amongst the different cell lines but some patterns were evident. A dose-dependent increase in levels of IL6 was seen from Mel888, Mel624 but to low absolute levels, and to a somewhat higher level with MeWO cells (Figure 21). IL6 is often described as a pleiotropic cytokine, thought to be involved in tumour initiation and known to be pro-inflammatory, but its precise actions in the context of melanoma are not yet clear (Culig and Puhr, 2012; Hoejberg et al., 2012, F.Errington-Mais, A. Melcher and J. Newton-Bishop, personal communications 2012).

IL8, another inflammatory cytokine that has been implicated in the recruitment of macrophages and neutrophils to the tumour microenvironment, was elicited in a dose dependent fashion from all four cell lines tested (Waugh and Wilson, 2008). IL8 is also released by neutrophils in response to infection with MV (Zhang et al., 2012).

RANTES (Regulated upon Activation, Normal T-cell Expressed, and Secreted, also known as CCL5) is a chemokine involved in recruiting several species of immune cells including cytotoxic T-cells and has been shown to enhance the ability of CD4+ T-cells to stimulate anti-tumour responses (Lapteva and Huang, 2010; González-Martín et al., 2012). Mel888, Mel624 and SkMel28 all released RANTES in a dose dependent fashion following treatment with MV (Figure 21).

IFN are the prototypical anti-viral cytokines and non-malignant human epithelial cells, treated with an alternative strain of MV, produced IFN in response to cell-to-cell fusion (Herschke et al., 2007). One of the oncotropic mechanisms of OV often cited is the deficient IFN response present in many tumour cells (Critchley-Thorne et al., 2009). This is often conflated with deficient production of IFN despite previous reports to the contrary; primary cells from ovarian cancer patients, and myeloma patients produce type I interferons in response to the Edmonston strain of MV, though at considerably lower levels than shown in Figure 22 (Haralambieva et al., 2007). Production of IFNα, IFNβ and IFNλ/IL28 has previously been reported in a lung adenocarcinoma cell line, following treatment with wtMV, and was apparently mediated by TLR3 recognition of double stranded RNA (Berghäll et al., 2006). Single stranded viral RNA is recognised by TLR 7 and 8, but neither are thought to be present in epithelial or endothelial cells (Tissari et al., 2005). MV may also stimulate IFN production by other mechanisms as it has been shown that the act of virus fusing with a cell membrane (specifically a virus-like peptide based on HSV-type 1) can elicit an IFN response, independently of subsequent intracellular viral recognition (Holm et al., 2012).

Accordingly all four melanoma cell lines released significant quantities of at least one species of either type I (α/β) or III (λ) IFN (Figure 22). The production of type I IFN by tumour cells in response to MV has previously been considered to be potentially deleterious to OV therapy as cells normally respond to IFN by down regulating cellular machinery required for viral synthesis (Haralambieva et al., 2007). However malignant cells commonly have defects in their IFN-response pathways such that they, more than adjacent normal tissue, are unlikely to benefit from IFN-mediated protection, theoretically enhancing the therapeutic index (Critchley-Thorne et al., 2009). Moreover type I IFN have direct antiproliferative and cytotoxic activity against melanoma, and are in clinical use in some treatment centres (Johns et al., 1992; Kubo et al., 2008; Mocellin et al., 2010). Type I IFN have been used clinically to treat melanoma, and have been demonstrated preclinically to be critical in the generation of innate and adaptive responses (Johns et al., 1992; Haralambieva et al., 2007).

Though they act through different receptor pathways the type III IFN, such as IL28, seem to have many downstream properties in common with the type I IFN, including antiviral and antiproliferative actions (Uzé and Monneron, 2007). IL28

has antitumour activity against murine melanoma, and causes upregulation of MHC class I molecules (Lasfar et al., 2006). In a mouse model of melanoma, in which it was previously demonstrated that successful virotherapy is dependent upon host innate and adaptive immune responses, IL28 was produced by innate effector cells in response to virotherapy with VSV and blockade of IL28 abrogated such therapy (Diaz et al., 2007; Wongthida et al., 2010). These data suggest that melanoma cells, normally muted in their communication with the immune system, respond to treatment with MV by producing a range of cytokines and chemokines, including interferons which would be expected to have autocrine or bystander antitumour effects.

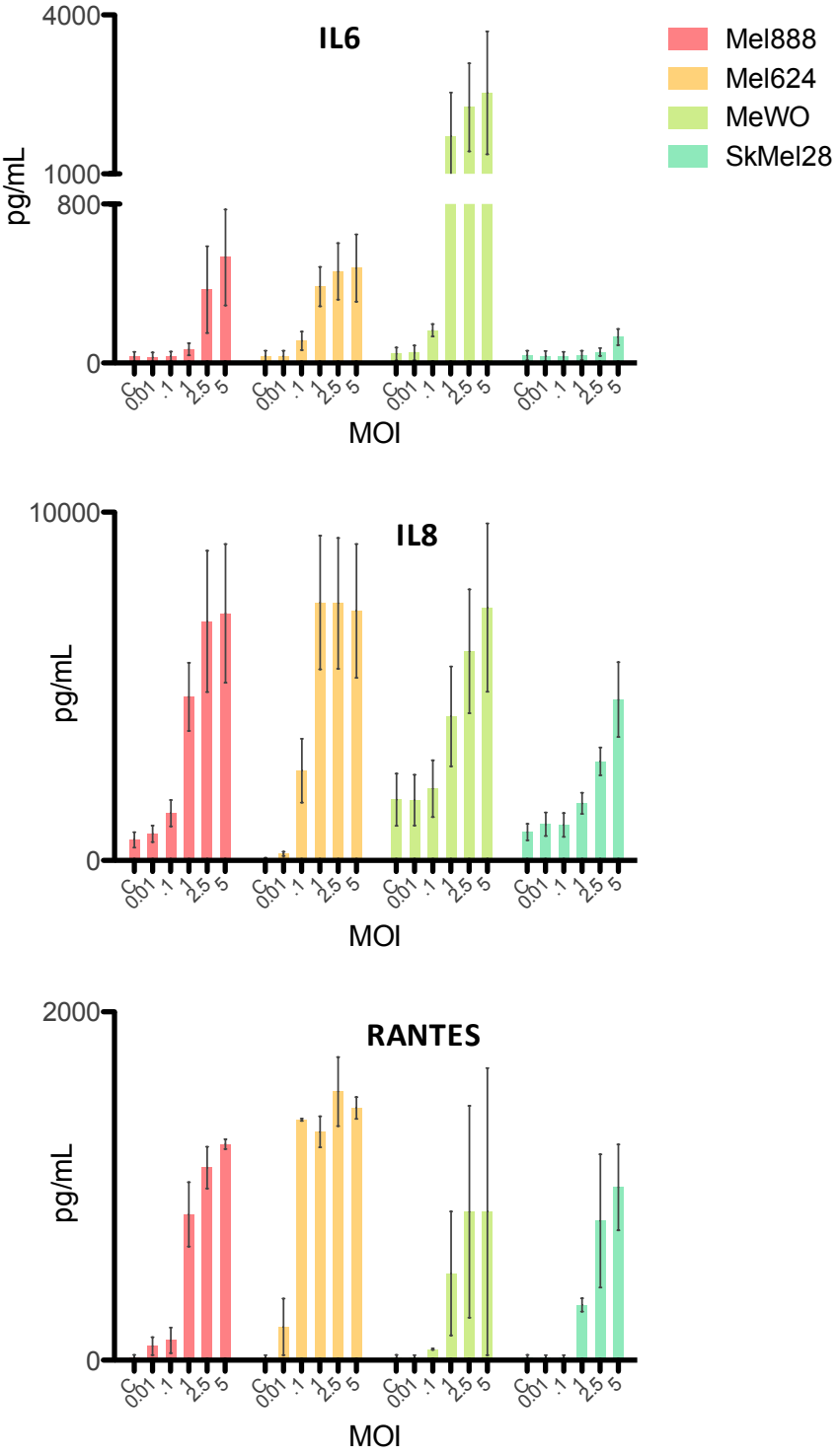

Figure 21. Cytokine release by melanoma after treatment with MV. Melanoma cell lines were plated in 24 well plates and treated at the range of MOI indicated. After 48 hours supernatant media was collected and centrifuged to remove non-adherent cells, then analysed for presence of the cytokines IL6, IL8 and RANTES by ELISA. Results shown are the mean of two (RANTES) or three (IL6 & IL8) separate experiments and error bars indicate the SEM

.

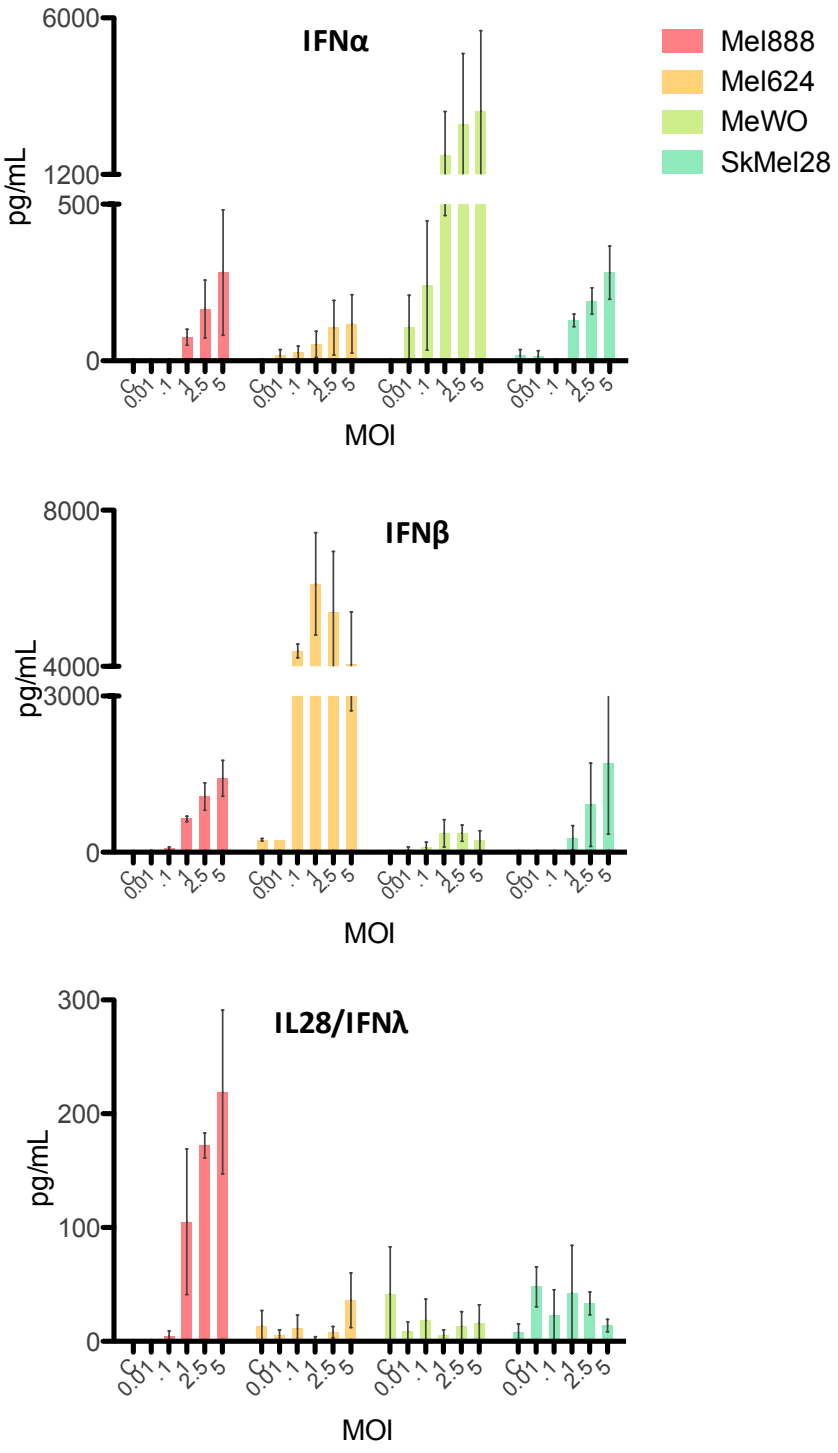

Figure 22. IFN release by melanoma after treatment with MV.Melanoma cell lines were plated in 24 well plates and treated at the range of MOI indicated. After 48 hours supernatant media was collected and centrifuged to remove non-adherent cells, then analysed for presence of the cytokines IFNα, IFNβ and IFNλ by ELISA. Results shown are the mean of two separate experiments and error bars indicate the SEM.

HMGB1 is a recently recognised and potent danger signal, capable of activating DC via TLR4 and MyD88 and contributing to cancer cell susceptibility to conventional therapies (Scaffidi et al., 2002; Lotze and Tracey, 2005; Apetoh et al., 2007a; Bianchi and Manfredi, 2007; Klune et al., 2008; Tang et al., 2010; Huang et al., 2011a). At the time of these experiments there was no widely available assay with which to perform ELISA, so cell free supernatants were analysed by western blot instead. The assay was developed to exclude the possibility that simian HMGB1 was contaminating supernatant media from tumour cell cultures after treatment with MV (prepared as it was from lysates of the African green monkey kidney cell line; Vero). Virus was added to cells after dilution in serum-free media and after one hour the cells were rinsed with PBS and then fresh virus-free FCS-supplemented media restored. As shown in Figure 23 there was no detectable HMGB1 in the supernatant media immediately after the wash steps described above. Moreover, although HMGB1 was readily detectable in the viral stock, the dilutions used in experiments reduced the concentration of HMGB1 below the detection limit of the assay described. Subsequent experiments involving treatment with MV were performed by adding virus for one hour, and then rinsing and replacing with fresh virus-free media. Cell-free supernatants were prepared for western blotting by diluting 1:1 with Laemmli buffer and stained blots analysed by infrared fluorescence.

Figure 24 demonstrates that at 48 hours after treatment with MV there was detectable HMGB1 in the supernatant of Mel888, Mel624 and MeWO, and traces present from SkMel28. By contrast, uric acid, another established danger signal, was not detected in the supernatant of any of the cells at any MOI using a commercially available ELISA kit (data not shown).

The release of cytokines, chemokines, IFN and danger signals suggests that melanoma lesions infected by MV will generate an inflammatory milieu, capable of modifying the immune balance.

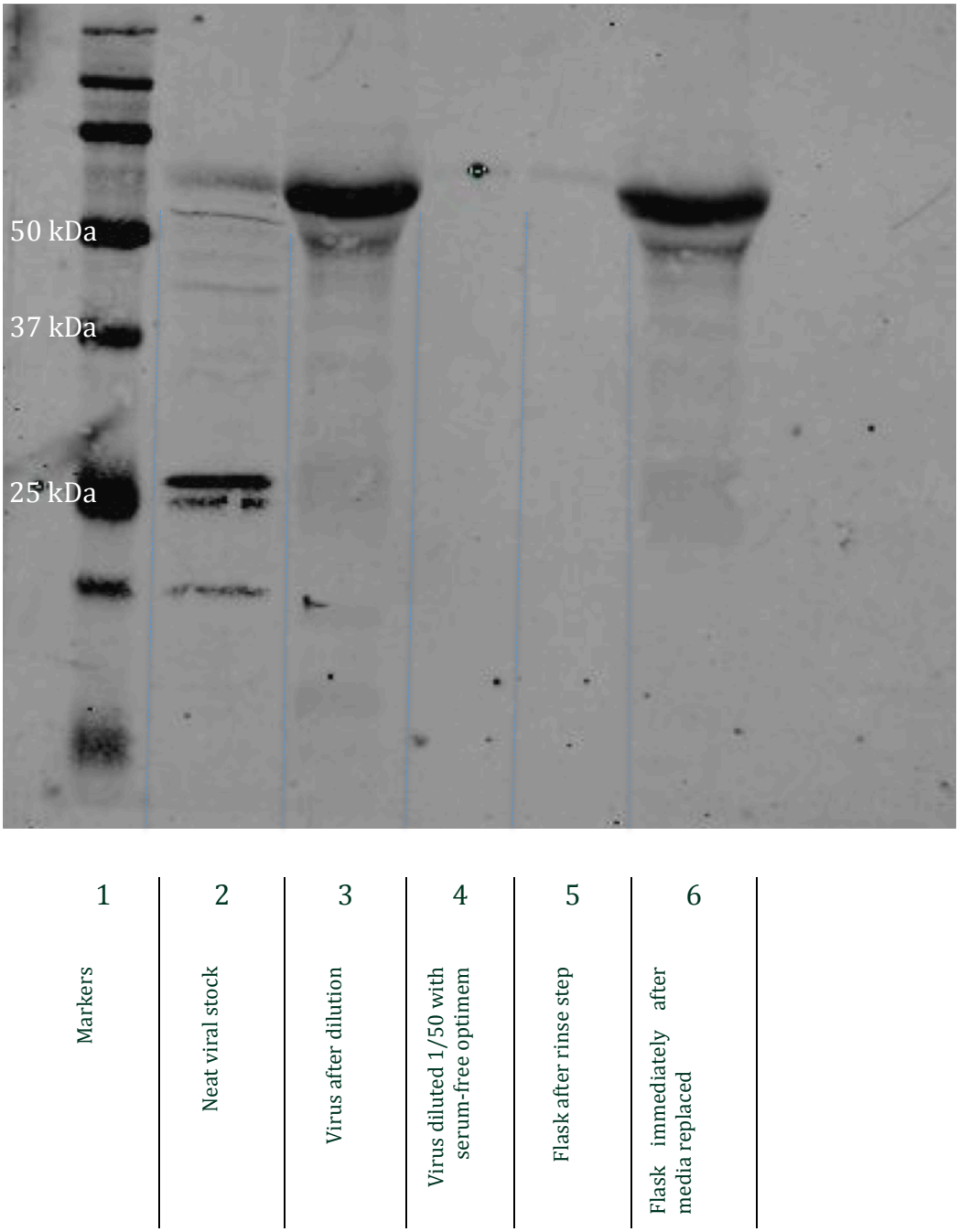

Figure 23. Detection of HMGB1 by Western blot. Optimisation of HMGB1 detection assays was necessary to exclude inadvertent detection of HMGB1 present in the viral stock as a result of preparation using simian cell lines. Lane 2, adjacent to the marker bands demonstrates that simian HMGB1 is present (with an effective molecular weight of 25-30 kDa) and cross-reacts with the anti-human HMGB1 antibody used for subsequent experiments. However after dilution in either plain or complete media (lanes 3 and 4 respectively) the levels of simian HMGB1 fall below the detectable threshold, and a rinsing step (lane 5) was also used in all MV treatments. The prominent bands in lanes 3 and 6 are albumin (MW 67 kDa).

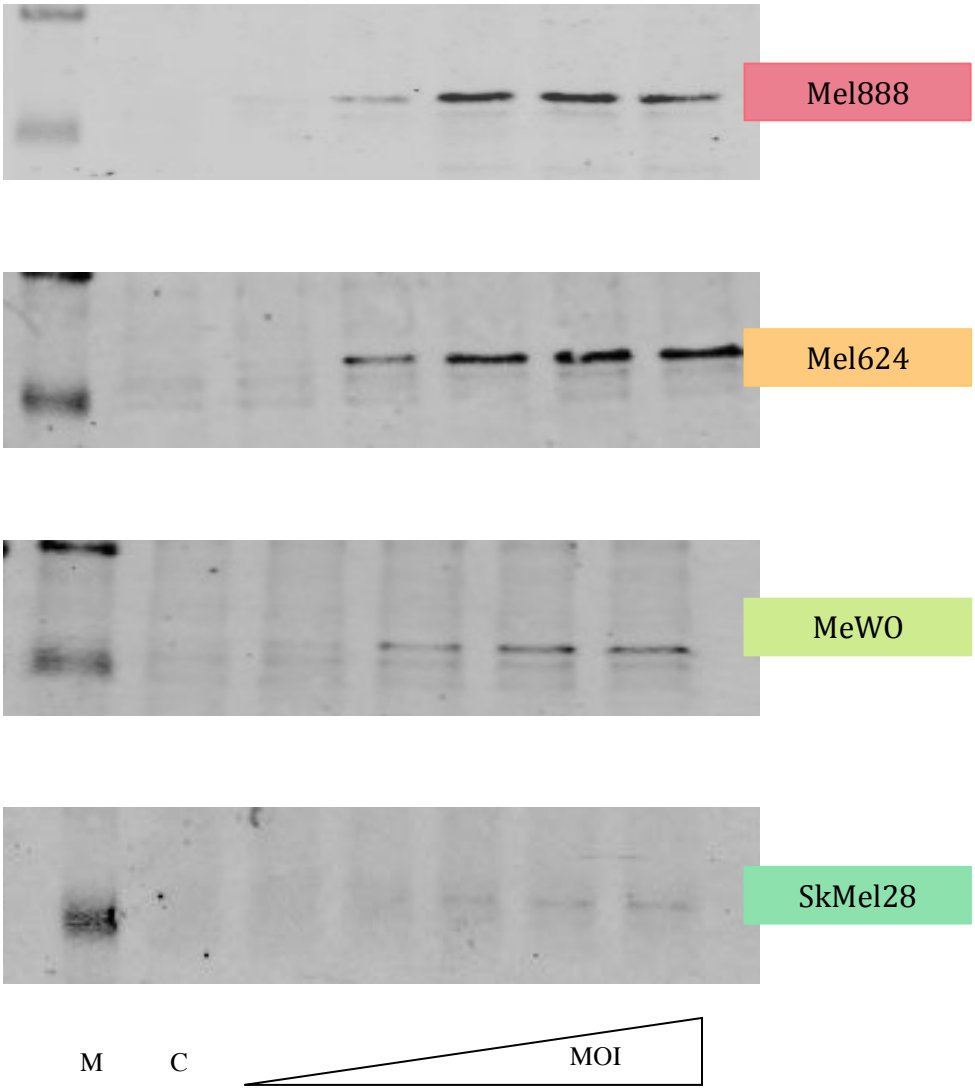

Figure 24. HMGB1 release from cells following treatment with MV. Cell-free supernatant was collected from melanoma cells 48 hours after treatment with MV at MOI between 0.01 and 5 in serum-free media. The supernatant was prepared for western blot by mixing 1:1 with Laemmli buffer prior to loading onto SDS-PAGE gel, along with marker proteins (M) and supernatant from untreated cells (C). After running and transfer, membranes were air-dried for 30 minutes, soaked in blocking buffer for 45 minutes, then incubated with mouse anti-human HMGB1 monoclonal antibody overnight at 4°C. The following day blots were washed three times then incubated with a secondary goat anti-mouse antibody conjugated to AlexaFluor 680 prior to imaging using the LI-COR odyssey infrared imaging system. Results shown are illustrative of two separate experiments.

4.2.6 Human melanoma primary cells

High risk melanoma of the arm commonly recurs in the axillary lymph nodes (Burmeister et al., 2012). These recurrences carry a grave prognosis but are often resected to aid palliation. Tissues from such procedures performed in Leeds were obtained shortly after surgery and used to prepare single cell suspensions in order to generate human melanoma primary cells. Given the widely understood limitations of relying entirely on immortalised cell lines, these primary cells were used to further examine the oncolytic activity of MV (Abbott, 2003).
Contemporaneously resected lesions were histologically confirmed as melanoma, and cells used were found to express intracellular gp100 and melan-A by flow cytometry (or previously by immunohistochemistry; (Errington et al., 2008b)) and have morphology in keeping with melanoma (Figure 25).
As shown in Figure 26 the primary cells were permissive to MV infection, displaying GFP after treatment with MV-GFP. Although syncytia were visible they were less obvious than seen in the established cell lines, and CPE took considerably longer to evolve. This presumably reflects the much longer cell doubling time of primary cells; passage times for the primary cells was in the order of weeks, cf. circa 2 days for Mel888. Live/Dead assays were performed as before, albeit at later time points, and confirmed the susceptibility of melanoma to the oncolytic activity of MV. Cell free supernatants from MV-treated primary cells were also used for ELISA; the limited number of cells available precluded the wide panel of cytokines examined in figures Figure 21 through Figure 23, however MV-treated cells from two of three donors tested produced RANTES, in keeping with the results seen using cell lines. Primary cells from one donor produced considerable amounts of IL6 in response to MV treatment. IL8 was produced by cells from all three donors at levels little affected by MV.
Thus human melanoma primary cells, isolated and grown in tissue culture are susceptible to killing by MV, consistent with the results seen using immortalised human melanoma cell lines. Despite the challenges involved in working with human primary cells, compared to established cell lines, these data suggest that the effect of MV are not attributable to the artifice associated with cell lines, affirming the apparent susceptibility of human melanoma to MV.
The variability of killing seen amongst cell lines, and between donors suggests that there are tumour-associated factors that determine MV-vulnerability; for that

reason Zimmerman et al have reported a method using precision cut tumour slices for ex vivo testing of MV efficacy as a way of improving patient and virus selection (Zimmermann et al., 2009).

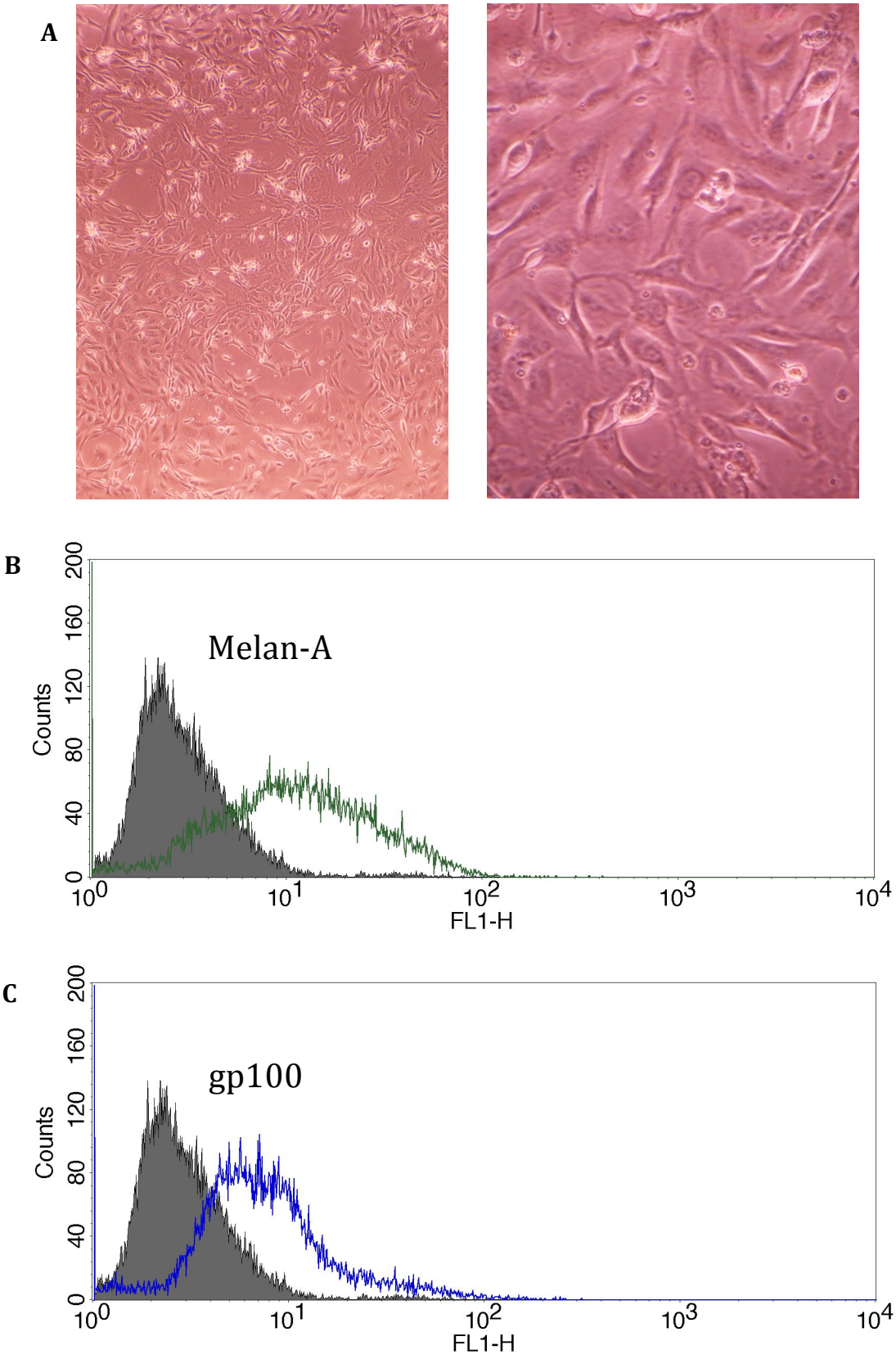

Figure 25. Human melanoma primary cells. Freshly resected nodal metastases were used to prepare single cell suspensions then plated in order to establish human melanoma cell primaries. A. Whilst at low passage (third or fourth) these cells were observed to have morphology in keeping with cells of the melanoma cell lines. Cells from three of four primary cell lines were permeabilised with 0.1% saponin then stained with (B) anti-gp100, or (C) anti-melan-A and analysed by flow cytometry. Grey histograms show isotype controls. Representative results from one of three donors are shown

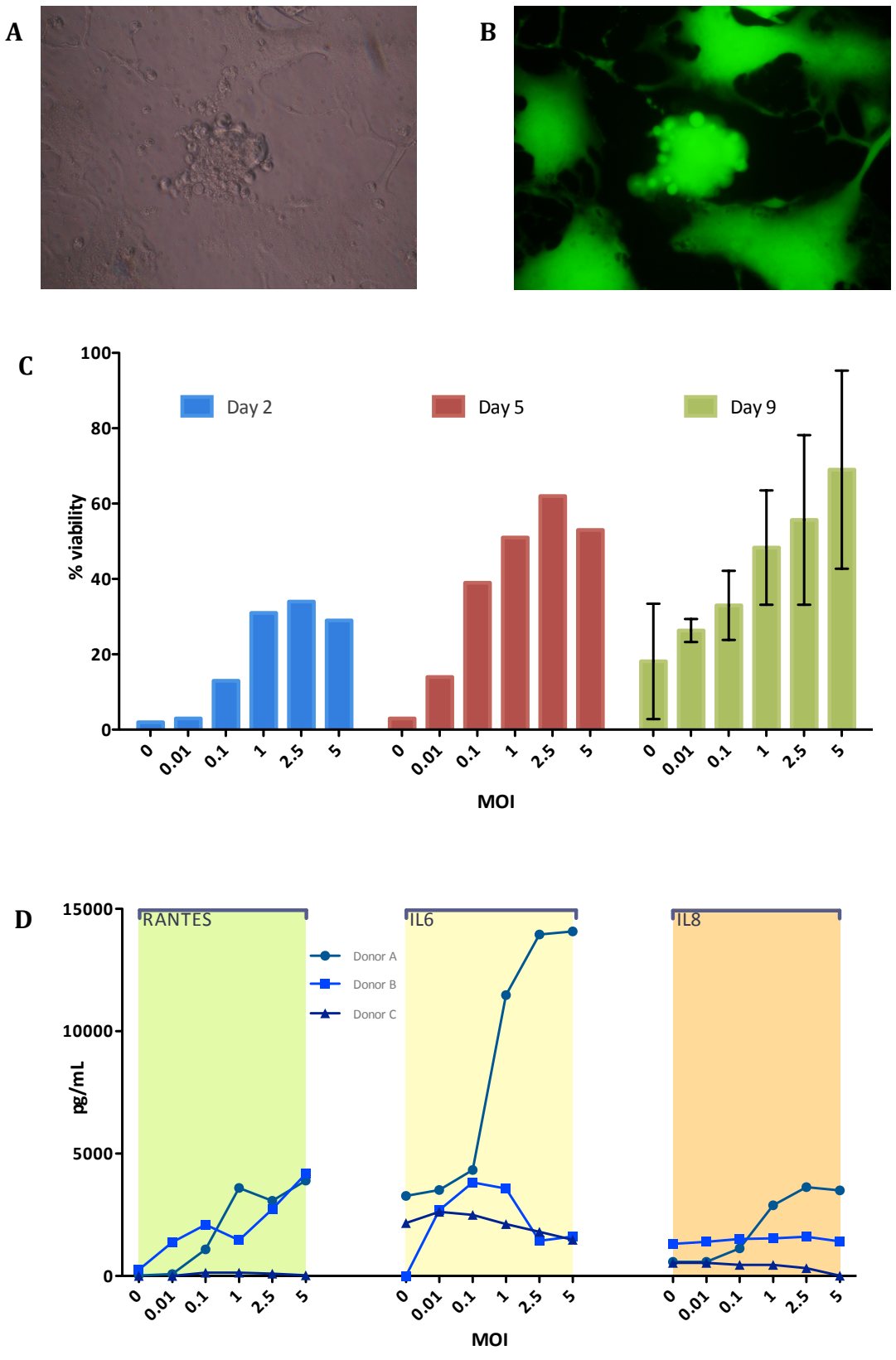

Figure 26. The effects of MV upon human melanoma primary cells. Primary cells were treated with MV or MV-GFP at a range of MOI. A. Cytopathic effects were seen after treatment with MV-GFP by bright field microscopy. B. Illumination with UV illustrates both the central syncytia with blebbed membranes, but also GFP-expressing syncytia at the periphery of the image, that are not immediately obvious in the bright-field micrograph. C. Live/Dead assays, performed as described in Figure 18, but at prolonged time points, confirmed a dose-dependent loss of cell viability after treatment with MV (day 9 results are the mean values from three donors and error bars indicate the SEM). D. Supernatants were collected and analysed by ELISA for the presence of the cytokines shown. Results from each of the three donors are shown.

4.2.7 3-dimensional culture models

Assays using cells in monolayer culture are readily performed and reproduced, but are well recognised to bear significant caveats (Lee et al., 2007). In vivo tumours exist, on the whole, in three-dimensional structures and have cell-to-cell interactions throughout their membrane. These interactions may obscure viral receptors or impede viral transmission. Initially freshly resected melanoma tissues were used to prepare fine slices that can be maintained in culture; this was based on the previous report of the use of hepatic tumour slices, however melanoma tumour have different physical characteristics and the technique proved, after several efforts at optimisation, unhelpful (Zimmermann et al., 2009).

Spheroids or multilayer models are increasingly being described in preclinical therapy studies, including oncolytic viruses. Adenoviral infection of ovarian cancer cell lines was four-fold more productive in a monolayer model when compared to a spheroid model (Lam et al., 2007). Studies of ovarian cancer cells prepared from ascites, normally susceptible to oncolysis by a myxoma virus, showed that the same cells formed into spheroids became resistant to the virus (Correa et al., 2012). Moreover studies of the melanoma cell line NA8 show that basal gene expression varies considerably when the cells are grown in monolayer compared to spheroids (Ghosh et al., 2005) . Levels of IL8 and CXCL1 expression were particularly upregulated in cells in the spheroid configuration.

Methodology in use to test the penetration of candidate molecules through vascular endothelium was adapted to perform qualitative assessments of the ability of MV to infect cells cultured in a three-dimensional system (Evans et al., 2009). A schematic illustration of the model is shown in Figure 27.

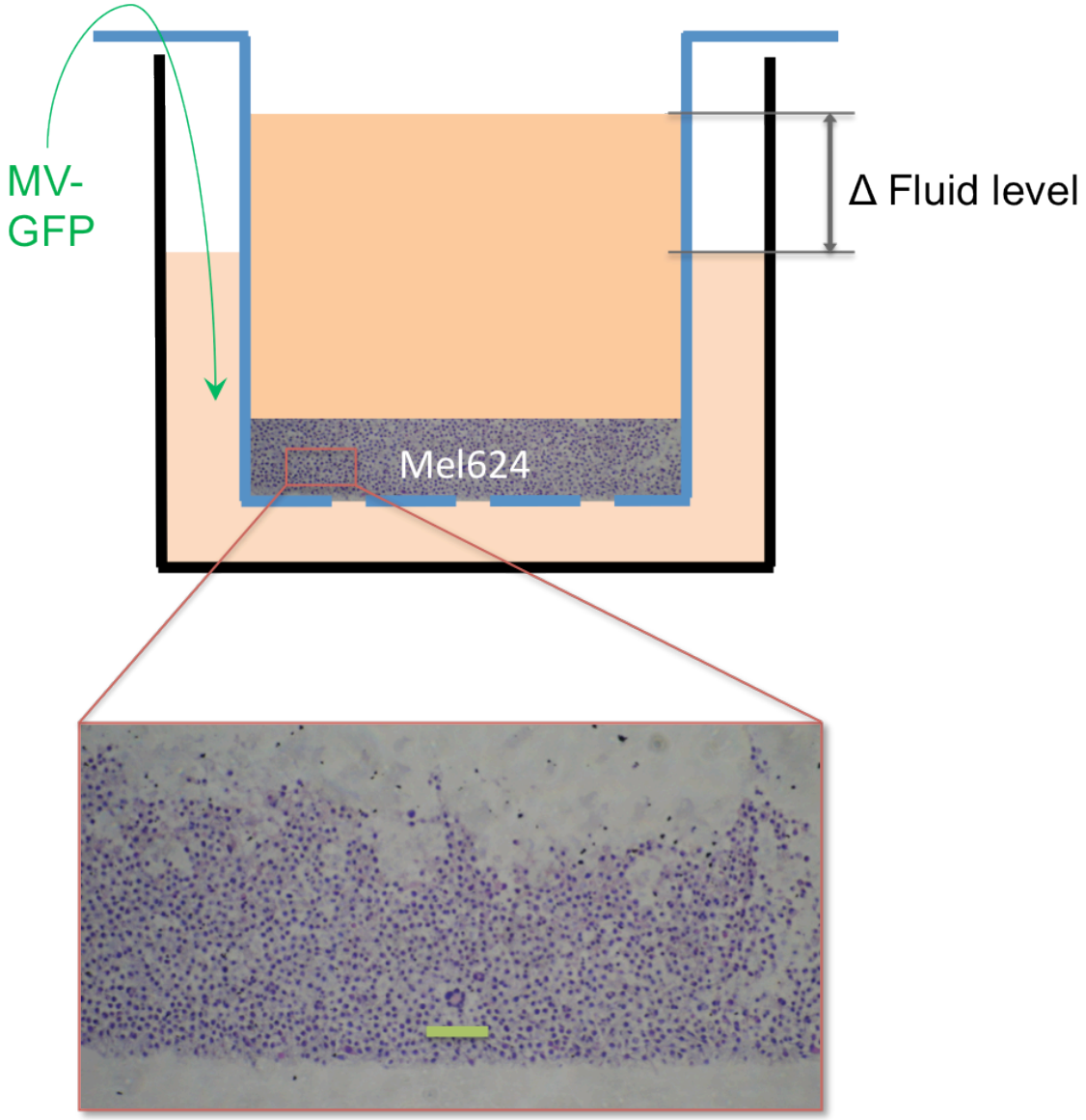

Figure 27. Multilayer model of melanoma. Mel624 cells were added to transwells immersed in media. After three to five days the cells impaired fluid exchange across the transwell membrane such that additional media applied to the transwell did not equilibrate with the underlying well (Δ Fluid level), and this was coincident with changes in the colour of media; at which point the multilayer models were deemed ready for treatment with MV. After early experiments MV was added to the lower chamber to avoid cytopathic effect threatening the integrity of the multilayer. (Inset) H&E stained transverse slice through the multilayer. The base of the multilayer, which rested on the transwell membrane, is more densely ordered than the rather friable appearance of the upper aspect. This multilayer had been treated with MV-GFP and a syncytium is visible in the very centre of the image above the green line.

Given the thickness of cells in a multilayer model conventional microscopy is of no use in examining cells. It was possible to extract the multilayer by cutting the membrane from the transwell and then mounting in wax. This allowed for transverse microtome sectioning of the multilayer (Figure 27) but the procedure was extremely delicate and several multilayers were lost or damaged using this process. Instead confocal microscopy allowed for the intact transwell to be placed on a microscopy stage, without the need for extraction or manipulation of the multilayer within. The greater penetrative ability of laser light used in confocal microscopy overcomes the limitations faced by conventional microscopy in terms of light path.

Transwells containing Mel624 were prepared and MV-GFP added to the underlying wells. 48 hours after infection the transwells were immersed overnight in 1% PFA then stained with DAPI one hour prior to confocal imaging. Representative images in Figure 28 illustrate that multi-layered Mel624 cells remained permissive to MV infection. Syncytia were formed that extend vertically throughout the thickness of the multilayer and adopt complex pedunculated structures not otherwise seen in conventional two-dimensional models. These large syncytia contained several dozen DAPI-stained nuclei, hinting at the number of cells subsumed within. These admittedly qualitative data further assert the oncolytic activity of MV in melanoma. The ability of MV to infect in a direct cell-to-cell manner may circumvent any impediment to virion movement caused by cell to cell junctions (Sattentau, 2008).

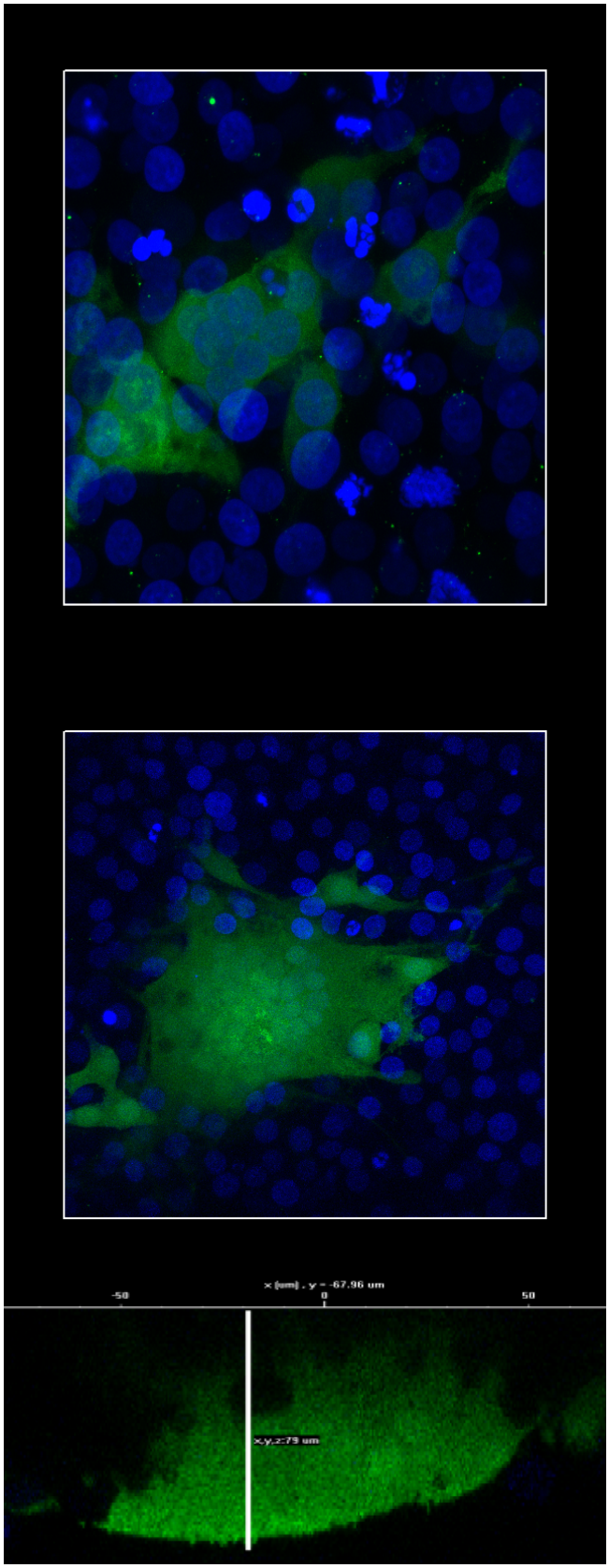

Figure 28. MV efficacy in a multilayer model of melanoma. Confocal microscopy of Mel624 plated in transwells 48 hours after treatment with MV-GFP and having been counterstained with DAPI reveals complex multinucleated syncytia, the largest of which (middle image) contain several dozen nuclei. Lateral renderings, produced as a composite of a z-stack of horizontal images, reveal that the syncytia extend for the full thickness of the multilayer.

4.2.8 Actions of MV on elements of the innate immune system

Reovirus has previously been shown to enhance innate tumour killing by NK cells and whole populations of PBMC (Errington et al., 2008a; Adair et al., 2012). Studies of oncolytic VSV and reovirus have demonstrated the critical necessity of innate stimulation to mediate therapeutic efficacy (Prestwich et al., 2009a). In order to investigate similar phenomena following treatment with MV, PBMC from healthy donors were prepared from fresh blood and cultured overnight in the presence of MV at an MOI of 1. The following day the ability of treated versus untreated PBMC to kill radioactively labelled (^{51}Cr) Mel888 targets was assayed at a range of PBMC to target ratios. As shown in

Figure 29 MV-treated PBMC killed Mel888 far more effectively than untreated PBMC. As expected the killing was not specific to melanoma, and similar results were noted when the ovarian cancer cell line Skov-3 was used as targets. NK cells are the archetypal innate effectors, and as shown in

Figure 29 there was upregulation of CD69 expression amongst the CD3-CD56+ fraction of PBMC, following overnight treatment with MV. CD69 is associated with activation of lymphocytes, and enhancement of their cytotoxic potential. Levels of DNAM1, NKG2D and CCR7 on NK cells did not change with MV-treatment (data not shown). Having identified evidence of NK cell activation, after treatment with MV, further demonstration of their role in the enhanced innate killing of tumour targets was sought using the CD107 assay of degranulation in response to targets. CD107a and CD107b are proteins normally resident on the inner membrane of cytotoxic granules (Betts et al., 2003; Betts and Koup, 2004). At the time of degranulation these markers are transiently exposed on the surface of cells, before recycling pathways scavenge the residues. With the use of protein transport inhibitors such as brefeldin CD107a/b accumulates on the surface of degranulating cells and can be detected using fluorescently tagged antibodies. PBMC from healthy donors were treated overnight with MV and the following day co-cultured with Mel888 targets. After 1 hour of co-culture brefeldin A was added to the media, prior to a further four hours of culture. Cells were then harvested and stained for flow cytometry. As seen in Figure 30 the population of cells that expressed CD107a or b in response to melanoma targets was predominantly CD3-CD56+, consistent with NK cells, and this degranulation was enhanced amongst PBMC that had been treated with MV

overnight. Notably there was no evidence of degranulation in response to MV in the absence of targets.

It is worth noting that though these data examine an element of the innate immune system, clearly there are multiple other effectors. Neutrophils, for example, are known to respond both directly to MV and to MV-infected tumours, and in one model at least contribute significantly to the innate anti-tumour efficacy seen following MV treatment (Grote et al., 2003; Zhang et al., 2012).

In keeping with previous reports of the effects of OV upon innate effector cells these data demonstrate phenotypic and functional changes in NK cells following treatment with MV.

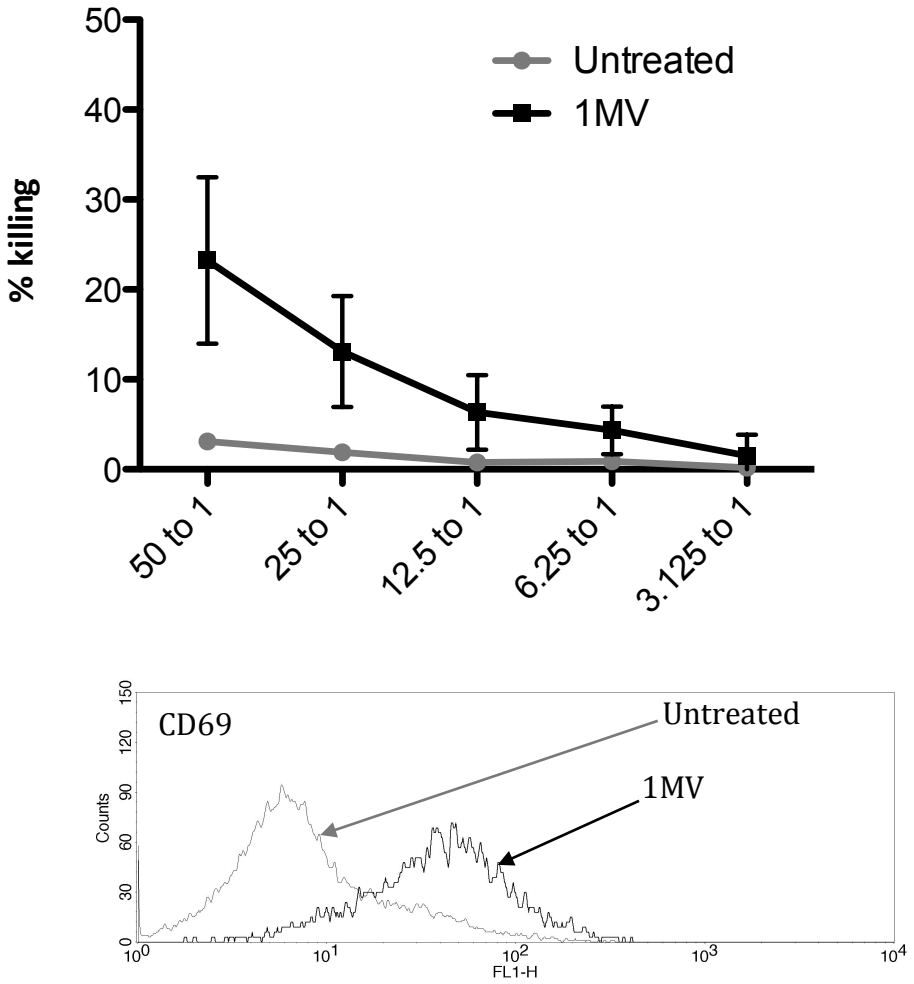

Figure 29. Stimulation of innate effectors by MV. PBMC from healthy donors were cultured overnight after treatment with MV at an MOI of 1. A. The following day the PBMC were co-cultured with ^{51}Cr-labelled Mel888 at ratios of PBMC to Mel888 as indicated. After 4 hours the cell-free serum was assayed for chromium release to assess cytolytic function. Results shown are the mean from three healthy donors, assayed in separate experiments. Error bars indicate the SEM. B. PBMC treated overnight with MV at an MOI of 1 were stained with CD56, CD3 and CD69. Levels of surface CD69 expression in CD3-CD56+ cells with or without treatment are shown from one donor representative of the four tested in separate experiments.

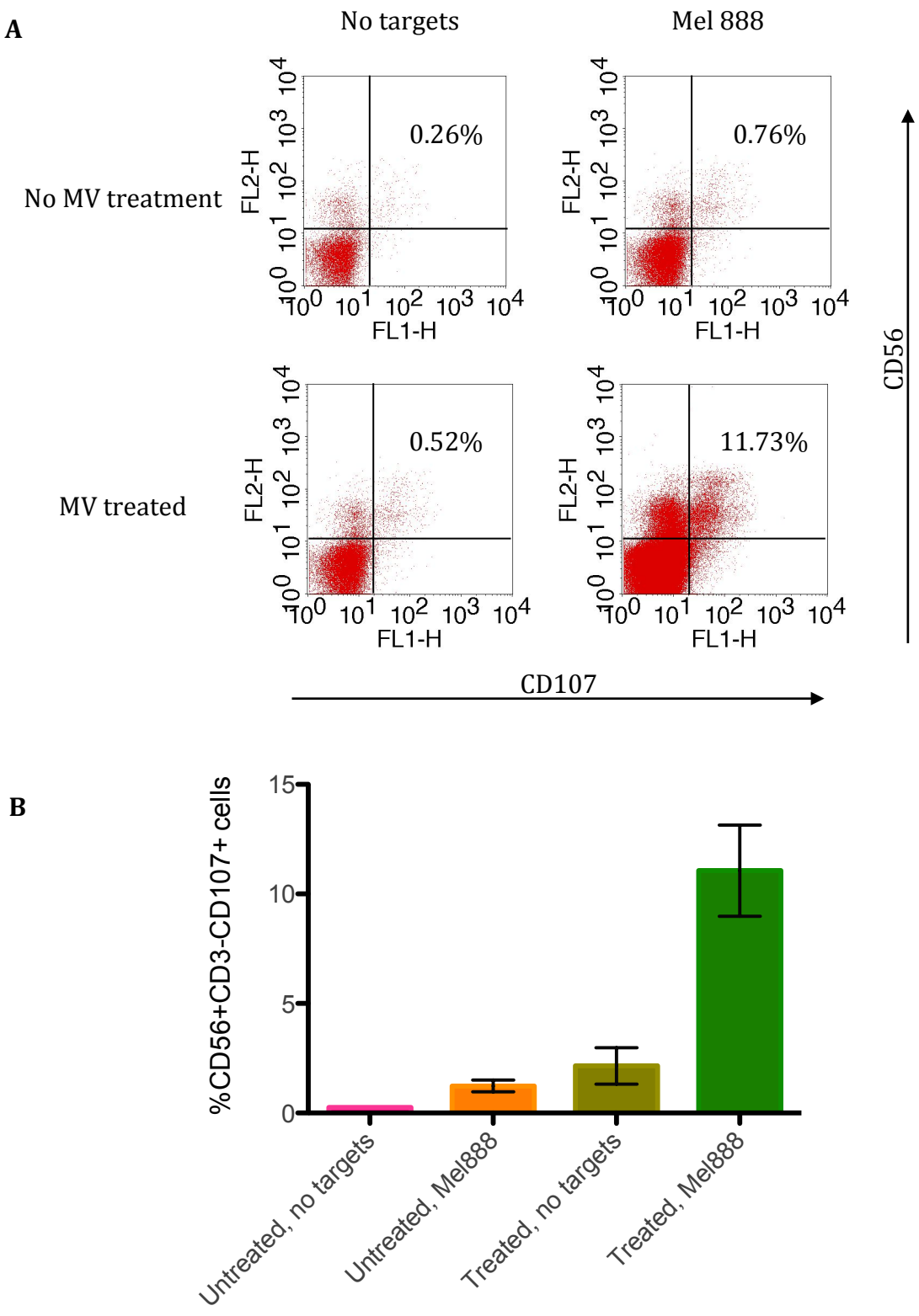

Figure 30. Stimulation of NK cells by MV. PBMC from healthy donors were cultured overnight after treatment with MV at an MOI of 1. The following day the PBMC were co-cultured with either Mel888 or no targets, in the presence of brefeldin A and anti-CD107a and b. After 4 hours the cells were stained with anti-CD56 and anti-CD3 then analysed by flow cytometry. A. Representative dot plots from one healthy donor. B. Mean values from 3 healthy donors, error bars indicate SEM.

4.2.9 Actions of MV on Dendritic cells

wtMV infection can be profoundly immunosuppressive; most of the deaths that occur due to wtMV are due to secondary, often bacterial, infections (Permar et al., 2006; Schneider-Schaulies and Schneider-Schaulies, 2009). Several explanations for the immunosuppression are espoused but the predilection of wtMV to infect immune cells is often stressed. wtMV has a solitary tropism for CD150, a marker overexpressed on DC and lymphocytes, and carriage by infected DC is a critical early step in measles infection (Griffin and Oldstone, 2009). The effects of wtMV upon DC have been argued to be critical in the development of the immunosuppression associated with the measles illness, specifically impairing IFN pathways and CD40-mediated maturation of DC (Grosjean et al., 1997; De Witte et al., 2006). By contrast MV (rather than wtMV) has been given to patients in the context of several clinical trials and immunosuppression has not been reported as an adverse event. Similarly the strain of MV in use both in these experiments, but also in OV therapy trials, is derived from the Edmonston strain and has been used extensively as a paediatric vaccine - given that context the safety profile of MV is such that toxicity to immune cells is unlikely. Moreover Gauvrit et al. using a similar strain of MV reported that DC efficiently phagocytose MV-infected tumour cells, undergoing maturation as a result (Gauvrit et al., 2008). The effects of MV and MV-treated melanoma cells upon CD14-derived DC were therefore investigated.

DC prepared from healthy donor PBMC were treated with MV at a range of MOI, and assayed after 24 and 48 hours by Live/Dead staining. As shown in Figure 31 DC were robust in the face of MV-infection, even to MOI of 2.5. In fact it was striking that maturation by a standard dose of LPS, commonly used as a DC maturation agent, possibly caused more death of DC than MV treatment.

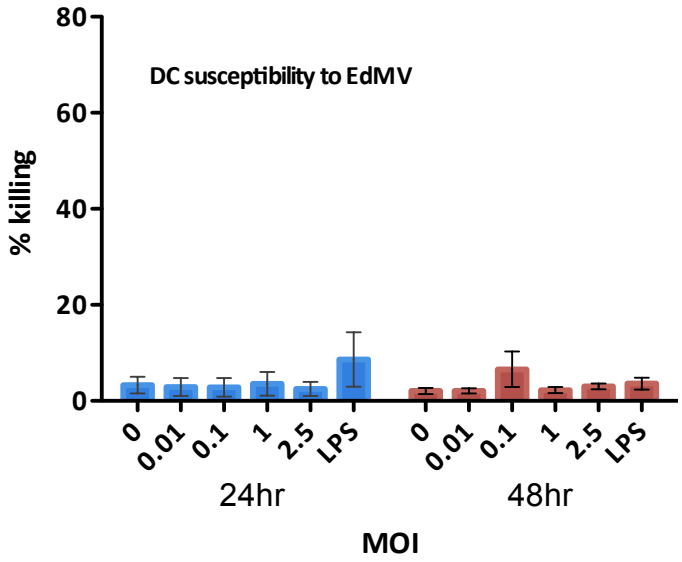

Figure 31. Susceptibility of DC to treatment with MV. DC were prepared from PBMC by CD14+ MACS selection and culture for 7 days with GM-CSF and IL4. DC were then treated with MV at the MOI indicated or LPS at 250 ng/mL. After 24 and 48 hours the DC were analysed by flow cytometry after staining with the Live/Dead reagent. Results shown are the mean of experiments using blood from three healthy donors. Error bars indicate the SEM.

DC treated with MV were additionally assessed for phenotypic evidence of maturation. In order to successfully stimulate T-cell responses, DC must present antigen in a suitable MHC context along with costimulatory molecules; in the absence of a second stimulatory signal antigen presentation will lead to anergic responses. The principle T-cell receptor for the second signal is CD28, which recognises dimers of CD80 and/or CD86 (also known as B7.1 and B7.2 respectively). This second signal is requisite for a cytotoxic T cell response, although other signals are also required (Joffre et al., 2009), thus the upregulation of CD80 and CD86 on DC is a vital element of the development of antitumour responses.

Levels of CD80 and CD86 were increased following treatment with MV, though CD40 was not affected, in experiments performed using DC prepared from 9 healthy donors (data not shown). Therefore the strain of MV in use as an oncolytic agent, in contrast to wtMV, is not toxic to DC.

In order to model the impact of MV upon DC within the tumour microenvironment, where malignant cells may be hypothesised to generate a suppressive milieu that could overcome any stimulatory capacity of MV, DC were cultured in the presence of supernatant from Mel888 cells, or MV-treated Mel888. These supernatant tumour-conditioned media, characterised in Figure 21 through Figure 24, were filtered to exclude virus and then applied to DC overnight, and the expression of phenotypic markers analysed the following day. DC were initially prepared by culture in media supplemented with IL4 and GM-CSF for up to seven days, but were then cultured without cytokines once tumour-conditioned media (TCM) was added.

As seen in Figure 32 MHC expression, both class I and II, was increased in the presence of TCM, though there was minimal difference between the effect of TCM from untreated Mel888 when compared to MV-Mel888; TCM from untreated Mel888 did not alter levels of CD80 or CD86, implying that TCM conditions DC for antigen sampling and presentation which will likely lead to anergy in the absence of a suitable second signal. However CD80 and CD86 were both consistently upregulated in response to MV-Mel888 TCM in experiments performed with DC from 4 healthy volunteers. By filtering the TCM the direct action of MV upon DC was excluded, demonstrating that Mel888 treated with MV produce a pattern of cytokines that induce phenotypic maturation of DC, including expression of

markers involved in the costimulatory signal. Although this suggests that the suppressive action of melanoma TCM is overcome by the effects of MV upon melanoma cells, it is possible that cell-to-cell inhibition could still functionally suppress DC. Therefore in order to exclude contact mediated inhibition of DC maturation, Mel888 or MV-treated Mel888 were co-cultured with DC overnight. It should be noted that in this assay the direct effects of MV upon DC cannot be excluded, though as demonstrated above (Figure 18, Figure 19 and Figure 20) there is limited viral replication or killing of Mel888 within a 24-hour period, and only limited expression of viral proteins (Figure 11). Those caveats notwithstanding, it was apparent that direct co-culture with untreated-Mel888 causes downregulation of CD86, whereas co-culture with MV-Mel888 is able to overcome the inhibitory effects of the melanoma cell, and CD86 is increased four-fold from untreated DC (Figure 33).

CD83, a further marker of DC maturation, was upregulated by coculture with MV-Mel888, but not by TCM, indicating the differential effects of soluble mediators, compared to contact-mediated effects.

The expression of CD40, involved in sustaining DC activation and function, did not change in response to TCM but was upregulated by co-culture with MV-Mel888 (Gommerman and Summers deLuca, 2011).

The precise sequence of events by which matured DC are able to stimulate T-cell responses remains the subject of intense research. The process of DC maturation, as evinced by the upregulation of surface markers that play a critical role in antigen presentation, is certainly a key step and appears to be enhanced by MV-treatment.

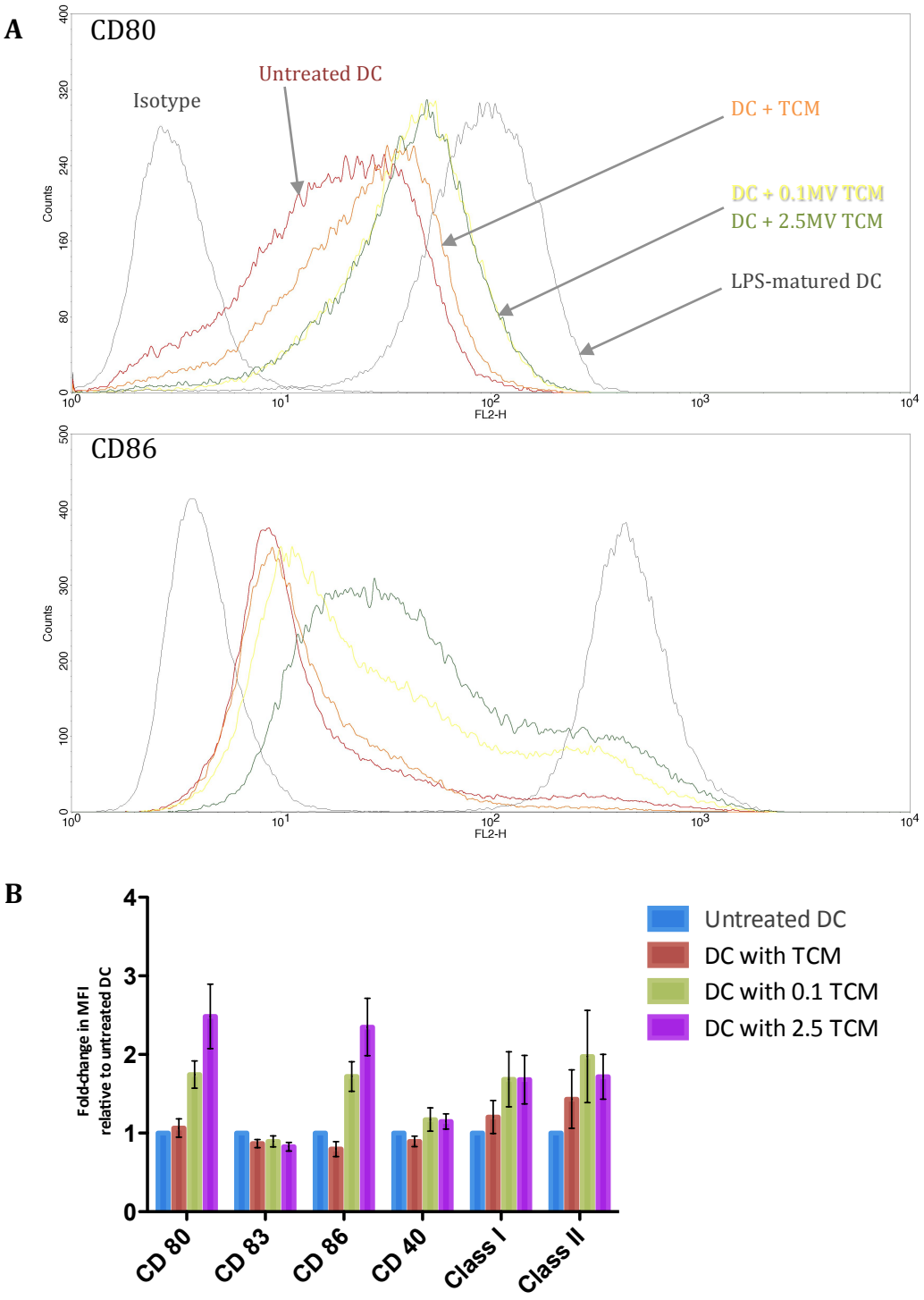

Figure 32. Effects of MV-treated melanoma supernatant on DC. Mel888 were treated with MV at the MOI indicated and after 24 hours the supernatant collected and filtered to remove non-adherent cells and virus. DC were cultured with the resulting TCM overnight and the following day levels of surface phenotype markers measured by flow cytometry. A. Representative flow cytometry plots of CD80 and CD86 expression. B. Mean fold changes in marker expression relative to DC cultured in standard melanoma cell media, from results obtained from the DC of four healthy donors. Error bars indicate the SEM.

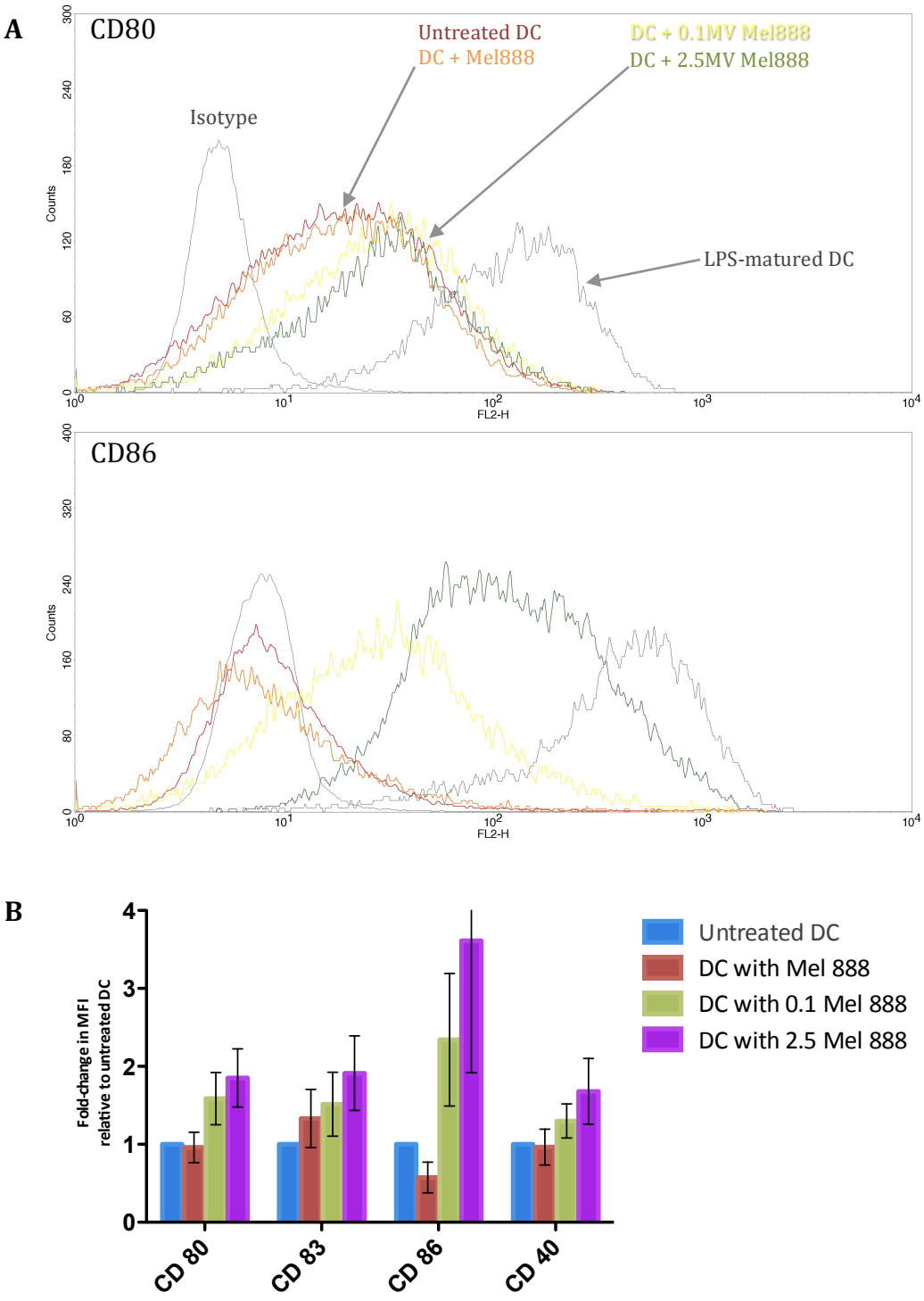

Figure 33. Effects of MV-treated melanoma cells on DC. Mel888 were treated with MV at the MOI indicated and harvested after 24 hours. DC were cultured with Mel888 or MV-treated Mel888 overnight and the following day levels of surface phenotype markers measured by flow cytometry. A. Representative flow cytometry plots of CD80 and CD86 expression. B. Mean fold changes in marker expression relative to DC cultured in standard melanoma cell media, from results obtained from the DC of four healthy donors. Error bars indicate the SEM

4.2.10 Actions of MV upon the Adaptive anti-tumour immune response

In addition to direct oncolysis, it has been posited that OV can generate therapeutic anti-tumour immunity (Prestwich et al., 2009a). Any cancer cell death may release tumour associated antigens but in the presence of suppressive cytokines, regulatory T-cells and tumour-associated macrophages, such antigen is unlikely to be usefully processed by antigen processing cells such as DC (Golden et al., 2012). By contrast OV-mediated cell death may alter the tumour microenvironment in ways that favour the generation of an immune response. As shown above MV-mediated cell death is associated with the release of chemokines and cytokines that can recruit and activate immune effector cells. HMGB1 is a danger signal that can act on DC through the TLR4/MyD88 pathway, and may prompt DC to direct their response towards activation, rather than anergy, and is induced by MV. It has previously been reported that intravenously administering reovirus to mice bearing syngeneic melanoma not only reduces tumour burden, but also primes an adaptive immune response against melanoma-associated antigen (Prestwich et al., 2008b) . The same authors also demonstrated, using human in vitro models, that reovirus-treated melanoma cells were able to activate DC, which in turn cross-primed T-cell responses against melanoma antigens. Similar results have been obtained in a model of human mesothelioma but have not otherwise been reported in melanoma (Gauvrit et al., 2008).

To test the hypothesis that MV-treated melanoma cells could activate DC and in turn prime a T-cell response against melanoma antigens long-term co-cultures were established; the procedure for these experiments is detailed below and represented schematically in Figure 34. PBMC were isolated from the buffy coats as before. Depending on cell numbers around 80% were divided amongst 20 cryovials for immediate storage at -80C. The remaining 20% were subjected to CD14+ selection and cultured in IL4 and GM-CSF for five days in order to generate DC. On the fifth day of culture the DC were split, and cultured with either Mel888, or Mel888 that had been treated with MV at an MOI of 0.1 or 1, 48 hours earlier. DC were cultured with the Mel888 or MV-Mel888 at a ratio of 1 DC to 3 melanoma cells for 24 hours. The non-adherent cells were then harvested, while the melanoma remained adherent to the flask. These DC, hereafter DC-Mel or DC-MV-Mel, were subsequently co-cultured with a proportion of their autologous PBMC. Each co-culture was established in cytotoxic T lymphocyte (CTL) media with IL2,

and IL7. The remaining PBMC were used to prepare further DC, which again were loaded with either Mel888, or MV-treated Mel888, and these DC then used to re-stimulate the PBMC/CTL in culture. After two weeks in culture, and two stimulations by autologous DC the PBMC were then subjected to various assays of T-cell function as described below.

4.2.10.1 CD107 assays

As described above, surface expression of CD107 indicates degranulation in response to targets, therefore CD107 assays were used to assess the response of PBMC, prepared as shown in Figure 34, to tumour targets. PBMC stimulated with DC-Mel888 served as controls to those stimulated with DC-MV-Mel888. Cells from each condition were co-cultured with either Mel888 or an irrelevant tumour target, Skov-3, both free from MV, or no targets at all (blanks). After one hour of co-culture brefeldin A was added, and after a further 4 hours the cells stained for CD8 and CD107a or b, and analysed by flow cytometry. The assay requires relatively few effector cells, and so was performed after one week of co-culture, immediately prior to the second stimulation with loaded DC, and a week later at completion of the experiment. As shown in Figure 35 the CD8+ cells from PBMC treated with DC-MV-Mel888 were more positive for CD107, even in the absence of targets, but there was a two-fold increase in responses against Mel888 compared to Skov-3 cells. Following the second stimulation there was an even clearer enhancement in melanoma-specific responses from the MV-treated condition than the controls. Representative data from two donors are shown in Figure 35, and are representative of results from experiments performed with 12 donors, in 9 of whom there was evidence of a specific anti-Mel888 response. Notably the degree of response varied amongst donors, as illustrated. Some donors had evidence of response after the first stimulation, whilst others remained negative until the second.

4.2.10.2 Intracellular IFNγ

IFNγ is produced by T-cells when the T-cell receptor binds its cognate antigen, and indicates T-cell activation. Accordingly after two weeks of co-culture PBMC were analysed for an IFNγ response to melanoma or irrelevant SkOV targets by intracellular staining. Cells were prepared as described above and after the four-hour co-culture were permeabilised and stained for IFNγ prior to flow cytometry.

As shown in Figure 36 there was up regulation of IFNγ response in CD8+ cells that had been exposed to DC-MV-Mel888, when compared to the control condition. Moreover this upregulation was specific to Mel888 targets, as it was not seen against SkOV cells.

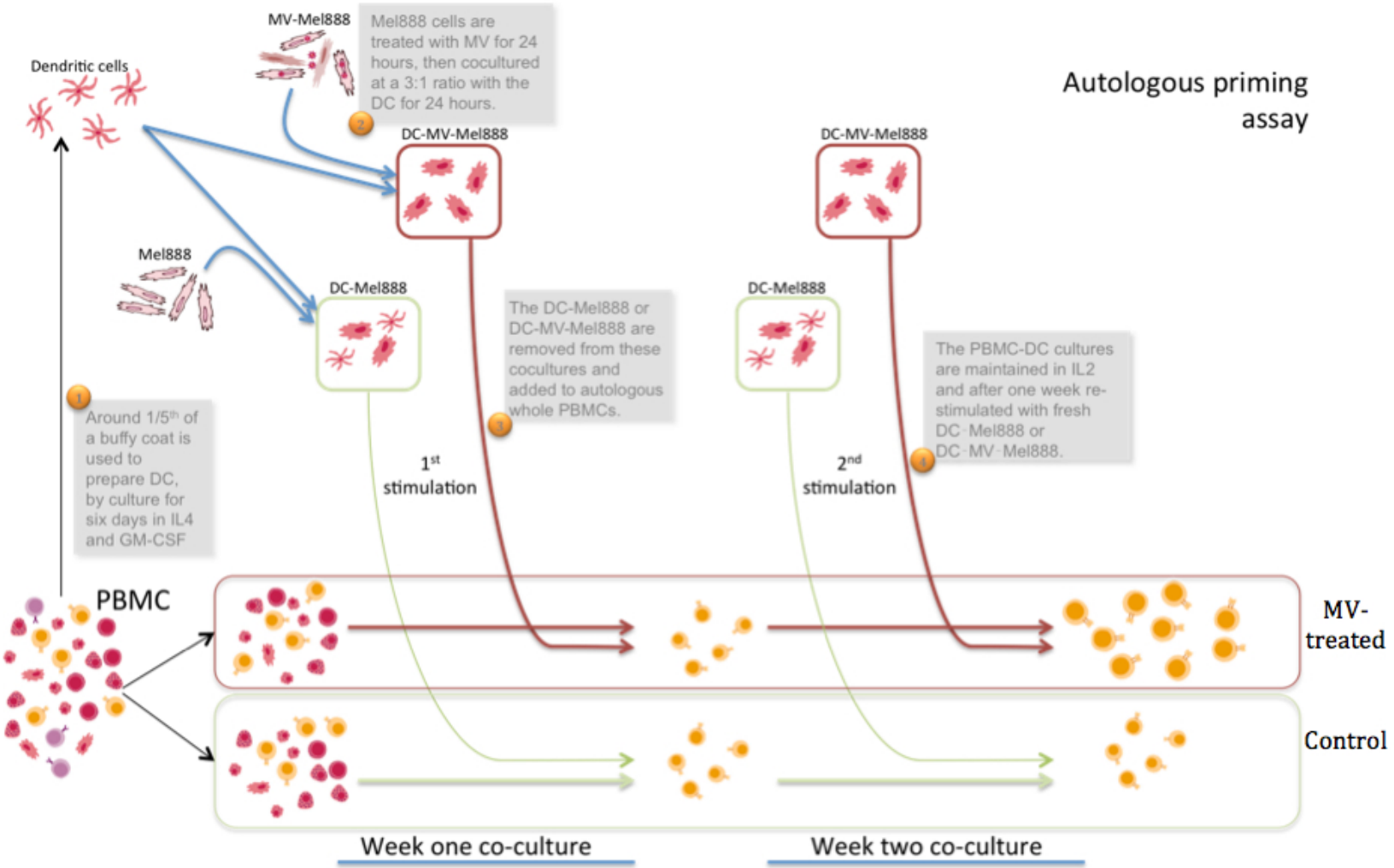

Figure 34. Schematic representation of priming assays

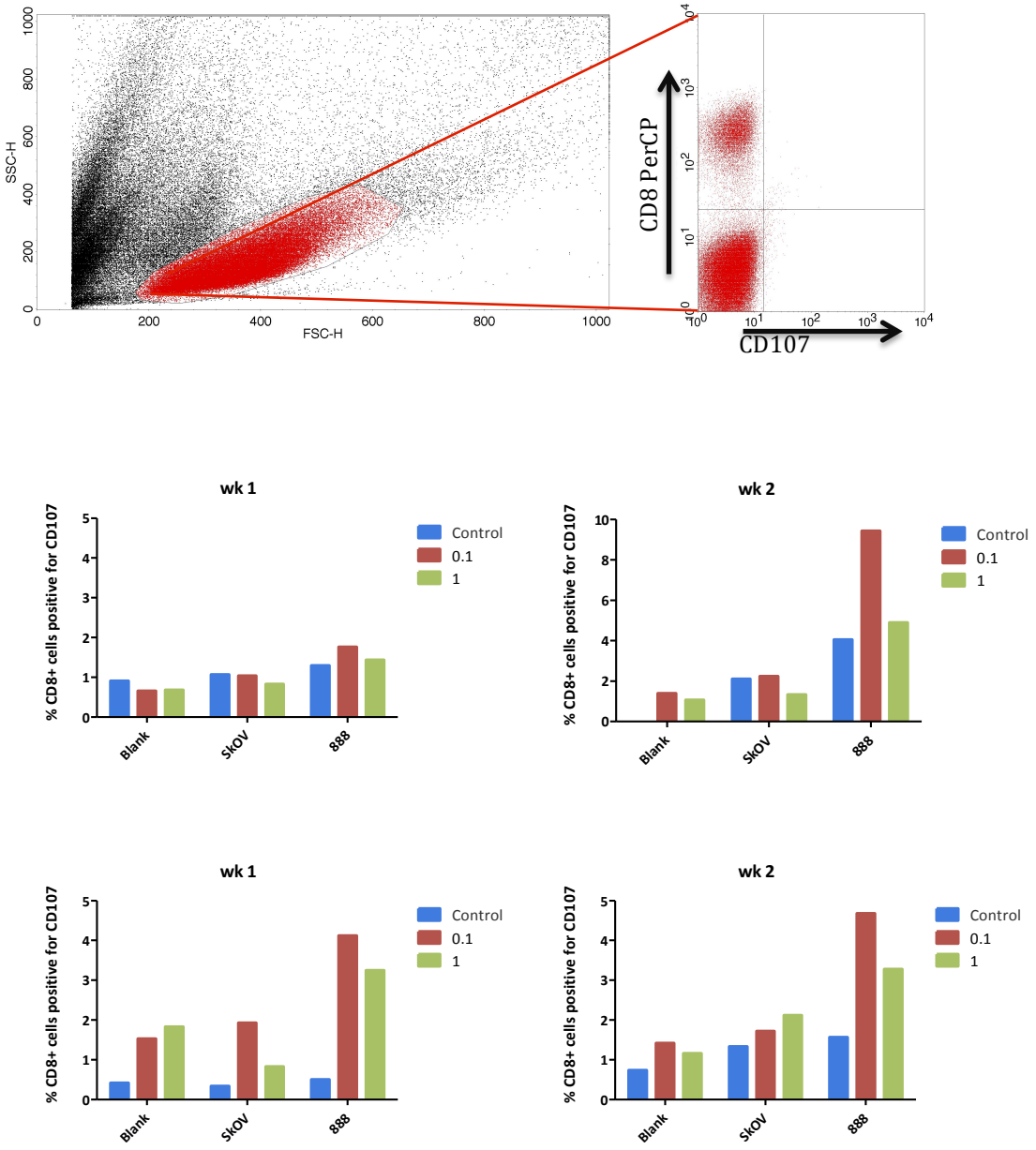

Figure 35. Priming assays: Surface expression of CD107 following treatment with MV. DC were co-cultured at a ratio of 3:1 for 24 hours with Mel888 that had or had not been treated with MV (MOI of 0, 0.1 or 1) for 48 hours. These DC were then cultured with autologous PBMC for one week and then identically prepared DC used to re-stimulate the PBMC cultures. After one and two weeks the PBMC were used in CD107 assay and analysed by flow cytometry. A. Representative FACS plot. Illustrating gating strategy. B. Results from two separate donors after one and two weeks of co-culture. Results shown are illustrative of those seen from 9 of 12 donors.

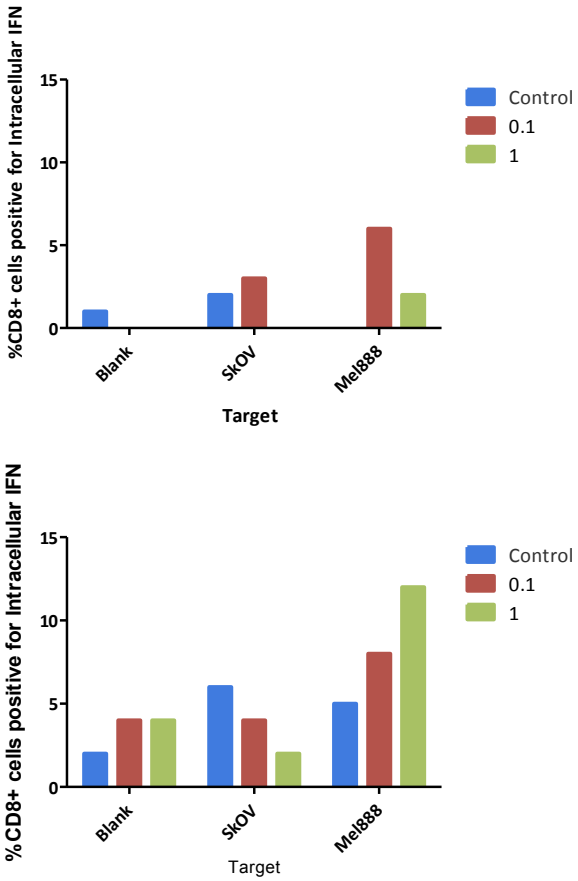

Figure 36. Priming assays: IFNγ response following treatment with MV. PBMC prepared as described in Figure 35 were used after two weeks culture to assay IFNγ production in response to tumour targets. PBMC were co-cultured with fresh Mel888 targets, or Skov-3 cells, or blank media alone, and the media supplemented with brefeldin A. After four hours the cells were fixed, then permeabilised and stained with an anti-IFNγ antibody prior to analysis by flow cytometry. The proportion of CD8+ cells that were positive for IFNγ was quantified. The results above are from two separate donors; from 12 donors a specific IFNγ response to Mel888 was identified in six assays.

4.2.10.3 Chromium release assay

In order to formally assess the cytolytic function of CD8+ T-cells prepared as described above, chromium release assays were also performed. Mel888 and irrelevant Skov-3 targets were labelled with ^{51}Cr and then co-cultured with PBMC, prepared as above. In order to extinguish the impact of non-specific cell killing by innate effector cells present within the PBMC, the co-cultures were prepared with unlabelled K562 to serve as redundant targets. The co-cultures were prepared at a range of effector to target ratios (E:T) and after 4 hours the quantity of released ^{51}Cr determined by scintography. The proportion of killing was determined by comparison with targets similarly cultured in the absence of effector cells, but with or without detergent, the former serving to indicate the level of release concordant with 100% killing. Figure 37 shows results from five donors tested in independent experiments. In one donor no enhancement of killing was seen, but in the remaining four, whilst there was little or no killing of relevant targets by PBMC that had been co-cultured with DC-Mel, by contrast co-culture with DC-MV-Mel888 enhanced killing of Mel888 to varying degrees. There was no meaningful killing of Skov-3 by any donor's PBMC, with or without MV-treatment, indicating that a melanoma-specific response was generated (data not shown).

Data from Figure 35 through Figure 37 also demonstrate that in some donors the degree of Mel888-specific enhancement was greater when the tumour cells used for priming were treated with MV at an MOI of 0.1 rather than 1. This observation was not consistent across all donors however, and in the small sample of donors in which both MOI were tested it is impossible to draw reliable conclusions on the nature of the difference. It is possible that the lower dose (which was more or as effective in three of the four positive donors) is able to generate an ideal amount of cytokines, chemokines and danger signals, as well as innate activation, without over stimulating and prematurely exhausting the generation of an adaptive T-cell response.

4.2.10.4 Pentamer staining

Tetramers and pentamers of antigenic epitopes presented in MHC molecules, labelled with fluorophore have enabled detection of defined antigen-specific T-cells, having circumvented the challenge presented by the low avidity of the T-cell receptor. One limitation is that they present antigenic epitopes on specific MHC molecules, and are therefore HLA-restricted. Most tetramers and pentamer, and indeed identified epitopes, are restricted to HLA-A2 in humans; the structure of HLA-A2 has been solved to a high resolution thus allowing empirical design of epitopes and other associated reagents.

In order to quantify the development of a T-cell response specific for a defined melanoma antigen, and presumably indicative of a broader repertoire of T-cells specific for a range of melanoma antigens, priming assays were repeated using blood from HLA-A2 +ve donors. Around 30% of local donors are HLA-A2 +ve but untested at the point of donation. Buffy coats received were therefore tested for HLA-A2 status by flow cytometry. The subset that were positive were maintained in culture with the intention of completing two stimulations by loaded DC, however at that time problems with bacterial and fungal contamination prevented successful completion of the assay.

Others have used MART-1 pentamers to demonstrate that reovirus stimulated cross priming by DC loaded with reovirus infected Mel888 (Prestwich et al., 2008b). Furthermore Gauvrit et al. performed similar assays in an in vitro model of human mesothelioma and demonstrated small increases in mesothelin pentamer positivity after CTL were primed with DC loaded with MV-treated mesothelioma cells (Gauvrit et al., 2008). Thus despite the absence of pentamer assays the data presented in Figure 35 through Figure 37, taken in the context of previous reports of priming enhanced by OV, strongly assert that MV treatment of melanoma generates an inflammatory environment that enhances DC function and generates a melanoma-specific T-cell response.

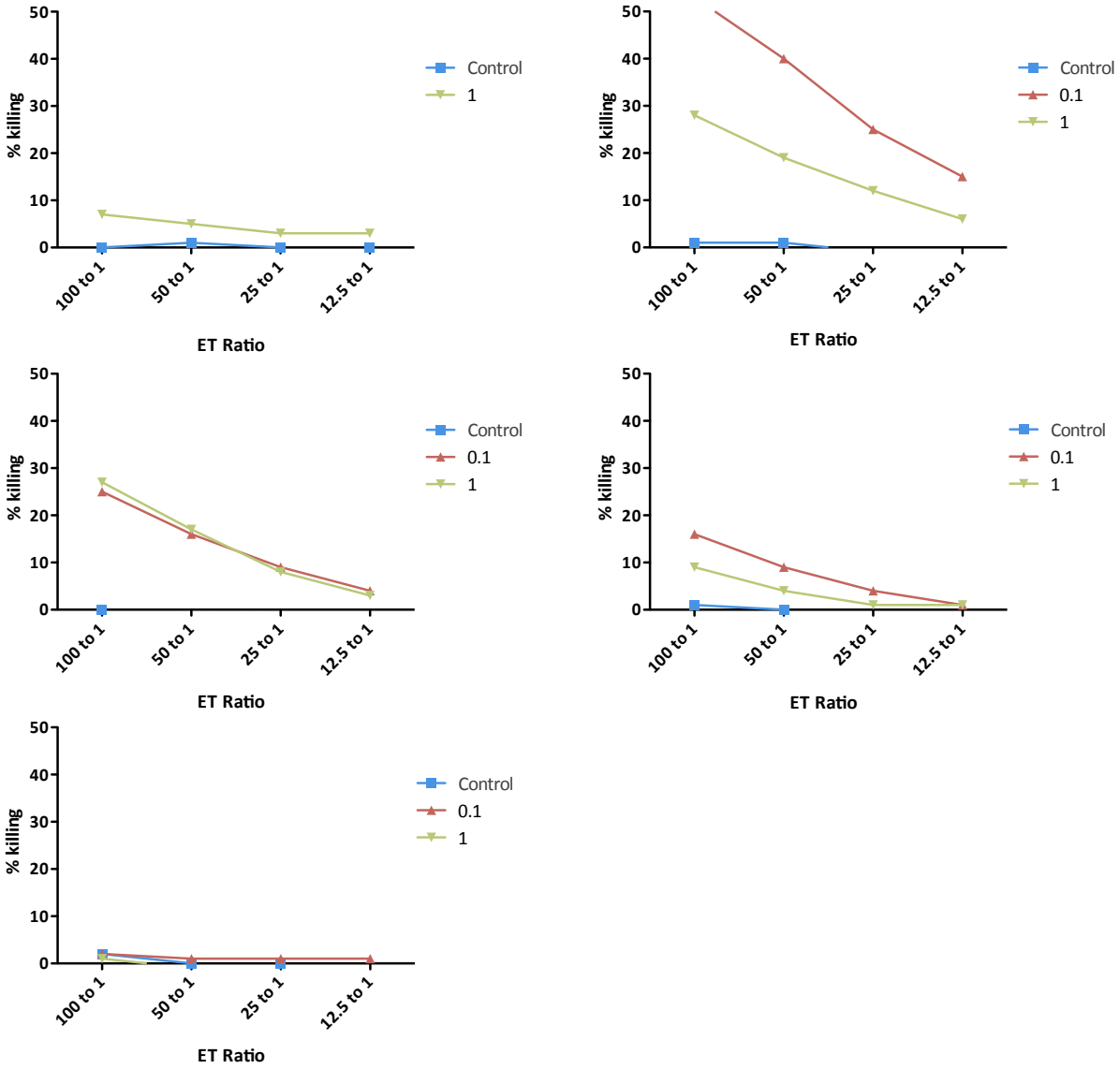

Figure 37. Priming assays: Lysis of melanoma by CTL in response to MV treatment. PBMC prepared as described above were tested for their ability to lyse tumour targets. Control refers to PBMC co-cultured with DC-Mel, 0.1 and 1 refer to PBMC co-cultured with DC-0.1MV-Mel and DC-1MV-Mel respectively. PBMC were co-cultured for four hours with ^{51}Cr-labelled Mel888 or ^{51}Cr-labelled Skov-3, in the presence of K562 to exclude the effects of innate effector cells. Results from all five donors tested are shown. Melanoma-specific killing was enhanced by MV in four out of five donors tested.

4.3 Discussion

Melanoma cell lines express CD46 at a level that is permissive both to viral entry and cell-to-cell fusion, as illustrated by the development of the classical cytopathic effect, giant multinucleated syncytia. Objective killing assays confirm the dose dependent killing of melanoma cells, both immortalised and human primary cells. In a three dimensional model of Mel624 cell-to-cell contact does not preclude viral transmission, perhaps due to the ability of MV to spread by triggering fusion of infected cells with their uninfected neighbours. The rate and degree of killing observed are consistent with that seen with MV in other tumour models, and with other oncolytic viruses used in models of melanoma.

Although the models used provide evidence of the efficacy of MV, it and other OV are unlikely to achieve meaningful clinical therapy purely on the basis of direct oncolysis; in vitro cell killing after direct application of virus at an MOI of 5 would be hard to mimic in patients. Moreover if the fraction of cells killed in such a situation is around 50%, then the cell doubling time of most tumours is likely to overcome OV as therapy. Increasingly there is recognition that the efficacy of those viruses that have succeeded is due in large part to their ability to cause an inflammatory tumour cell death and recruit anti-tumour immune responses, rather than purely being dependent on oncolysis (Prestwich et al., 2008c). In clinical testing of OncoVEX, a herpes simplex virus engineered to express GM-CSF, some patients benefitted from regression of untreated tumours, suggesting the generation of successful anti-tumour immunity (Senzer et al., 2009). Therefore the nature of MV-induced melanoma death was examined and its impact on elements of the innate and adaptive immune system explored.

The death caused by MV was inflammatory in nature, releasing a panel of cytokines, including type 1 and 3 IFN. IFN have previously been shown to activate innate and adaptive immune responses (Bonjardim, 2005). Melanoma cells appear to be unresponsive to the antiviral effects of IFN, based on their susceptibility and viral replication despite IFN production; amongst the four established cell lines tested there was no evidence of reduced viral replication or cell death in the lines that produced most IFN. In the tumours of patients it could

be postulated that adjacent non-transformed cells will presumably respond to IFN, thus enhancing the therapeutic index of MV as a treatment. Moreover IFN are known to have direct activity against melanoma (Johns et al., 1992). Three of four established cell lines released the potent danger signal HMGB1 after treatment with MV. To investigate the effects of this inflammatory death tumour-conditioned media from MV-treated melanoma was applied to DC and was observed to upregulate surface markers suggesting DC adopt an activated phenotype. Furthermore MV enhanced tumour killing by the key innate effector cells, NK cells. Finally in a model of adaptive immune priming MV-treated melanomas were able, with the assistance of DC, to prime melanoma-specific immune responses.

Though it would be appealing to extend the data presented above into animal models, better to assess the effect of a complete immune system, no useful model exists. Mice have been used extensively for research with MV though predominantly in the context of immune deficient backgrounds and bearing xenograft tumours. Moreover CD46 is not a native murine protein, limiting the applicability of mice for studying the immune consequences of MV therapy. A transgenic mouse model expressing CD46 exists, and has been used for MV study, but is on an IFN deficient background, therefore limiting its applicability to further study of the data described within this chapter (Ungerechts et al., 2007b) .

The data described have been published and have generated interest in developing clinical trials to test the ability of MV to help patients with melanoma (Skelly, 2012; Donnelly et al., 2013). The body of existing preclinical and early phase clinical toxicity data pertaining to MV, both published and pending publication, strongly indicates the safety and tolerability of MV (both MV-CEA and MV-NIS have been used clinically); therefore there is no need to repeat early phase safety testing of MV in melanoma patients (Msaouel et al., 2009; Donnelly et al., 2012a). There remain, however challenges in assessing the pharmacokinetics and pharmacodynamics of MV.

A key limitation to successful OV has been delivery of virus. Two of the viruses studied as OV are almost universally encountered during childhood in the western world; MV is a commonly used vaccine, reovirus is thought to cause no, or only minor and self-limiting, illness during most childhoods. As a consequence most prospective patients will have pre-existing antibodies to these agents. Even if a virus is chosen that is not a commonly encountered human pathogen, such as herpes or vaccinia, antibodies will be present on second and subsequent administrations (Donnelly et al., 2012c). Given these concerns many of the initial clinical trials of OV were performed using direct administration of virus, generally intratumoural injections, in an attempt to circumvent concerns about unsuccessful delivery. The phase II trial of OncoVex, an engineered type I herpes simplex virus, demonstrated promising efficacy in melanoma patients and, along with the subsequent phase III trial, demonstrated that the practical challenges involved in administering frequent injections to multiple metastatic lesions can be overcome (Senzer et al., 2009). Despite that, direct administration of OV has obvious limitations. Not all lesions can be safely accessed in all patients, particularly not on multiple occasions. Moreover surgery and radiotherapy are known to be effective local treatments; instead the challenge is to address systemic metastatic and micrometastatic disease. Two studies have demonstrated that intravenously administered virus can reach target tissues. Breitbach et al. report a phase I study of JX594 in which 23 patients with a variety of solid tumours, including four with melanoma, were found to have evidence of viral protein expression in tumour biopsies taken 8-10 days after intravenous viral administration (Breitbach et al., 2011). Adair et al. identified replicating virus within liver metastases resected a week or more after reovirus administration (Adair et al., 2012). Most importantly virus was recovered despite pre-existing anti-reovirus antibodies that were identified in all patients. Furthermore it was demonstrated that virus was carried by the white blood cells and platelets, shielding virus from neutralising antibodies. These two important studies support the principle of systemically administered OV, though further work is required to characterise the nature of systemic viral carriage as well as pursuing ancillary treatments that could enhance it.

Given the results of the preclinical experiments presented within this chapter a clinical trial was designed in order to commence testing of MV in human melanoma. Several phase I studies of MV have been performed, by a range of routes of administration, and none has shown dose-limiting toxicity (personal communication M. Federspiel and S. Russell 2012). Although other viruses, such as reovirus, have been shown to have activity against melanoma and stimulate anti-tumour immune responses, a potential advantage of MV is that its genome is readily amenable to modifications to enhance targeting of the virus, or 'arm' the virus. Initial studies made use of a MV engineered to express human carcino-embryonic antigen (CEA). CEA is an inert protein secreted by a number of tumours, mainly gastrointestinal. MV-CEA was designed to allow for pharmacokinetic studies following viral administration, by measuring serum levels of CEA using widely available routine assays. Subsequent preclinical developments directed the solitary manufacturing facility (Mayo Clinic, USA) to switch to the production of MV expressing the human sodium iodine symporter gene (NIS). NIS encodes a human protein found in the thyroid involved in iodine uptake. Preclinical studies demonstrated that MV-NIS could be tracked in vivo by administering iodine or technetium, both of which are readily taken up by cells expressing the NIS protein, and performing gamma, PET or SPECT imaging (Myers et al., 2007). MV-NIS has also been used preclinically in combination with ^{131}I, with the aim of accumulating sufficient levels of ^{131}I within virally-infected tumour cells to cause bystander killing of adjacent uninfected tumour cells (personal communication E. Galanis, 2012). Thus MV-NIS has promise both in terms of imaging viral spread and enhancing OV efficacy. The study proposed was developed at the joint ESO-ESMO-AACR clinical trials workshop in Flims 2012. In brief, the study is designed as a two-stage phase 0 protocol, as illustrated in Figure 38. An initial cohort of 5 patients who have been found to have metastatic melanoma involving the inguinal or axillary lymph node basins will be recruited shortly prior to planned surgical resection. One week prior to surgery patients will have intratumoural injections of MV-NIS, followed over the subsequent week by two ^{99}Tc SPECT scans. If any evidence of viral protein expression, i.e. NIS expression leading to focal tracer uptake, can be seen on SPECT in the first five patients undergoing intratumoural injection, then further

patients will be recruited to complete two cohorts, intravenous versus intratumoural MV-NIS. This study will aim to validate SPECT as a pharmacokinetic marker for subsequent studies. Additionally blood will be collected from patients over the course of the study and examined for evidence of anti-tumoural immune responses, which may serve as pharmacodynamic readouts in the future.

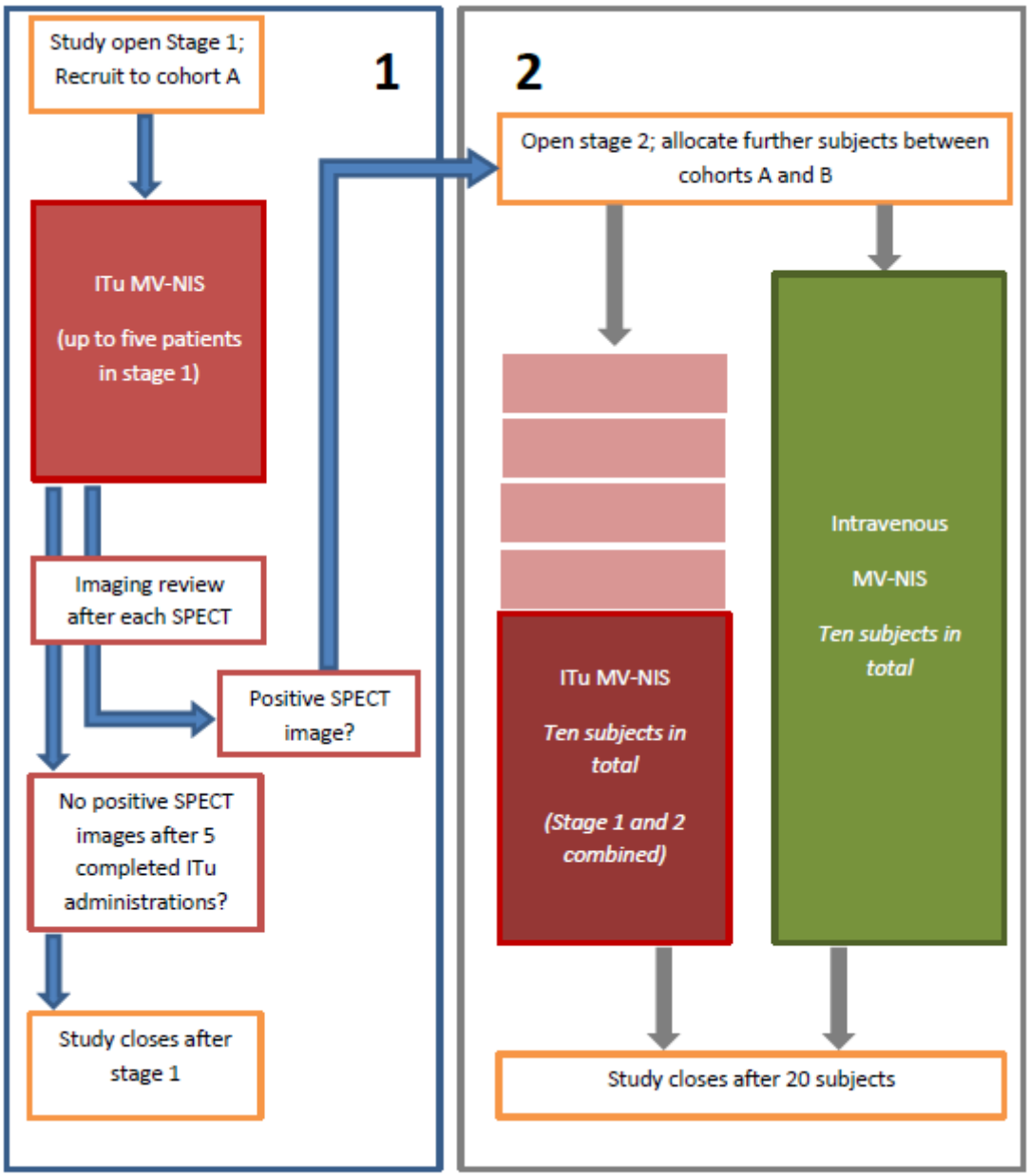

Figure 38. Proposed trial design. Schematic representation of proposed trial design examining the ability of 99Tc-enhanced SPECT to detect NIS protein expression following intratumoural or intravenous administration in melanoma patients with inguinal or axillary lymphadenopathy

5 Enhancing the combination of adoptive cell therapies and virotherapies with the addition of local radiotherapy

5.1 Introduction

Rather than simply being a cytotoxic therapy, radiotherapy (RT) has been shown, in vitro and in vivo, to enhance the immunogenicity of cancer cells(Reits et al., 2006; Bernstein and Hodge, 2012). Though its effects on immune cells are more heterogeneous, several clinical studies have shown that conventional RT protocols lead to increased numbers of circulating tumour antigen-specific T-cells (Schaue et al., 2008; Tabi et al., 2010).However, radiotherapy is little used in the treatment of melanoma, partly because there is nihilism born of traditional radiobiological assessments of the radioresistance of melanoma (Stevens and McKay, 2006; Jahanshahi et al., 2012).

Radiotherapy in the form of total body irradiation is used in the current adoptive cell therapy protocols at the NCI for metastatic melanoma(Rosenberg and Dudley, 2009). In that setting RT is thought principally to act by depleting host lymphocytes that would otherwise act as a competitive 'sink' for activating cytokines. Total body irradiation, and indeed the entire conditioning regimen in use for ACT, is extremely toxic, which limits the range of patients that can be treated in such protocols. Accordingly many groups are pursuing methods to enhance ACT without the need for prohibitively toxic pre-treatment (Cho et al., 2012). Moreover alternative immunotherapeutic approaches can be effective against melanoma in more clinically practicable formats, such as the monoclonal antibody, ipilimumab (Hodi et al., 2010).

In the following experiments the potential immune-enhancing effects of palliative-dose radiotherapy were explored. Single fraction treatments of up to 8 Gy are used in many tumour sites, including melanoma; doses of 8 Gy are associated with minimal toxicity and are readily clinically implemented. Although such doses are inadequate to control tumours, they may enhance therapy by killing tumour cells, releasing antigen and danger signals, and causing changes on and within tumour cells that render them more visible and vulnerable to cells of the immune system (Bernstein and Hodge, 2012).

It was therefore hypothesised that the addition of sub-radical doses of external beam radiotherapy to established tumours would elicit immunologically relevant changes within that tumour and its stroma, that would enhance therapy with the combination of adoptively transferred T-cells and oncolytic virus.

Although ACT routinely uses autologous tumour-infiltrating lymphocytes with a range of T-cell receptors, such therapy is difficult to model preclinically. The use of a model antigen system is a pragmatic solution that allows hypotheses to be tested using reproducible and reliable model systems. Accordingly the experiments presented below use B16 melanoma cells, derived from a C57BL/6 mouse, that have been transfected to stably express the chicken protein ovalbumin (B16-Ova). OT1 mice are transgenic animals in which lymphocytes express a T-cell receptor that recognises a peptide sequence from ovalbumin, SIINFEKL. Although a synthetic antigen system such as the B16-Ova/OT1 dyad can be criticised for being artificial it has the advantages of being well characterised and associated with a range of widely available reagents that facilitate analysis. Pmel transgenic mice, whose T-cells recognise epitopes within the gp100 melanoma-associated antigen, known to be present in human melanoma and melanocytes, as well as B16 melanoma (Rommelfanger et al., 2012). Pmel T-cells were therefore also used, in order to examine responses against a more relevant TAA. Furthermore recent efforts at enhancing ACT have included clinical testing of T-cells with specificity to a single epitope (whether by engineering the TCR or transfecting lymphocytes with a chimeric antigen receptor (Porter et al., 2011; Restifo et al., 2012)), which arguably enhances the potential applicability of these model antigen systems.

5.2 Results

5.2.1 Combinations of systemic oncolytic virus, ACT and RT

To test the potential synergies between RT, ACT and OV, B16-Ova tumours were established in C57Bl/6 mice and therapy started 7 days after tumour implantation. Mice were then treated with 8 Gy orthovoltage (150 kV) external beam radiotherapy to the tumour, with or without intravenous VSV-Ova, and with or without intravenous naïve OT1 T-cells. The OT1 T-cells used in this and all following experiments were prepared by harvesting the lymph nodes and spleens of OT1 mice and performing negative selection using a pan T-cell isolation kit to yield untouched and highly pure T-cells. Tumours were measured thrice weekly, and the mice euthanized if the tumours exceeded 1 cm in any dimension, or began to ulcerate. As shown in Figure 39, 8 Gy RT caused tumour growth delay, when compared to untreated mice, and consequently briefly prolonged survival (Figure 40). Treatment with iv VSV-Ova caused brief tumour regression, followed by rapid regrowth. The combination of RT and VSV-Ova led to some tumour regressions, but the tumours recurred. Intravenously administered naïve OT1 T-cells did not yield any tumour regressions, nor improvement in survival, and the combination of RT, OT1 and VSV-Ova did not yield and significant improvements.

Notably some mice treated with 8 Gy developed moist desquamation within the treatment field, particularly at the skin fold between the right hind limb and abdomen. Although these reactions settled spontaneously, and did not impair mobility or feeding, it was decided that for subsequent experiments the dose applied should be reduced to 4 Gy. As shown in Figure 41, a repeat of the experiment shown in Figure 39 and Figure 40, treatment with 4 Gy still resulted in delayed tumour growth, but without alteration in survival (Figure 42). No skin reactions were seen in any subsequent experiment using an applied dose of 4 Gy from the orthovoltage source. When the results of both experiments (Figure 40 and Figure 42) are considered there was no obvious enhancement of either virotherapy or ACT with the addition of RT, and the triple combination was not synergistic.

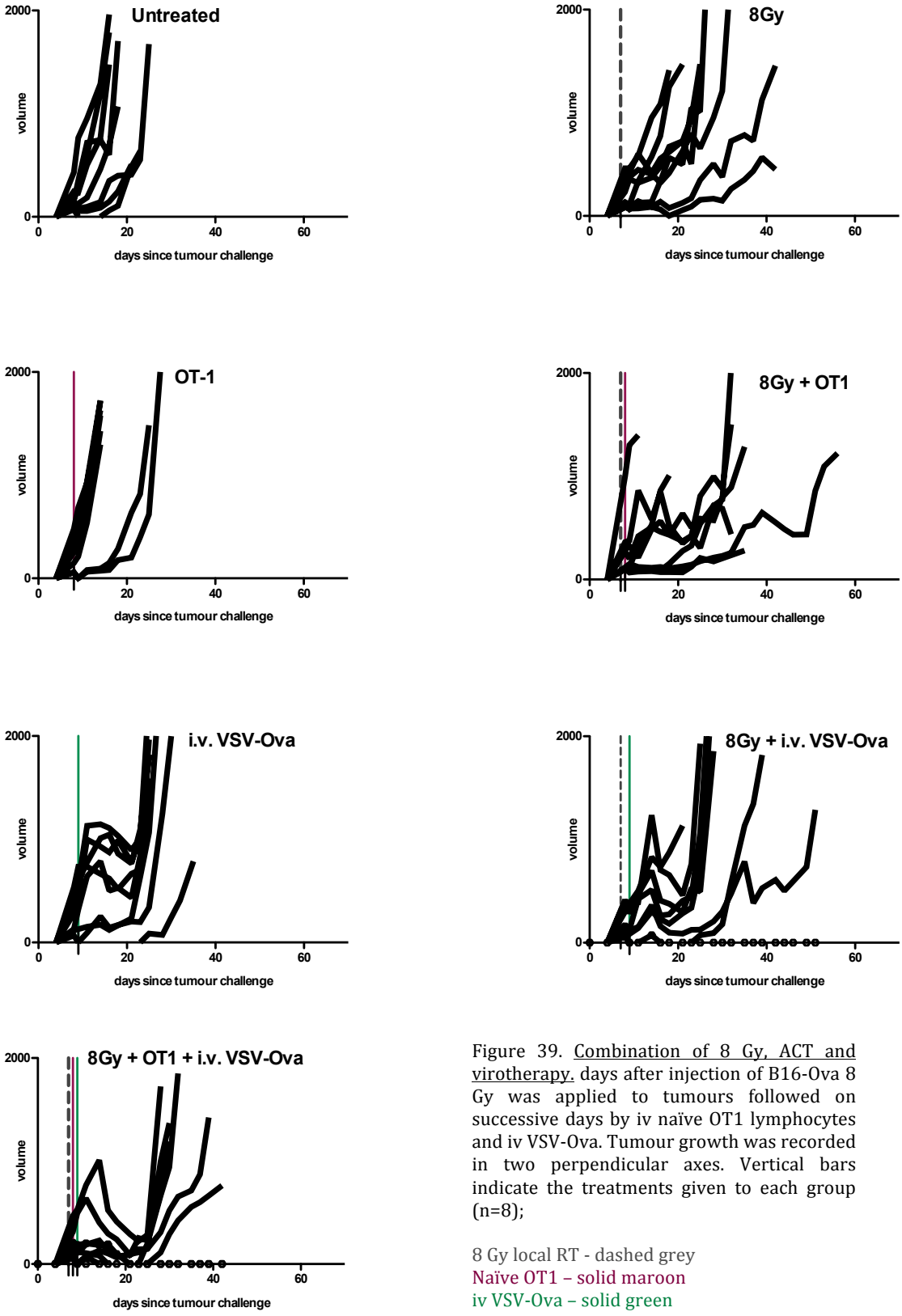

Figure 39. Combination of 8 Gy, ACT and virotherapy. days after injection of B16-Ova 8 Gy was applied to tumours followed on successive days by iv naïve OT1 lymphocytes and iv VSV-Ova. Tumour growth was recorded in two perpendicular axes. Vertical bars indicate the treatments given to each group (n=8);

8 Gy local RT - dashed grey
Naïve OT1 – solid maroon
iv VSV-Ova – solid green

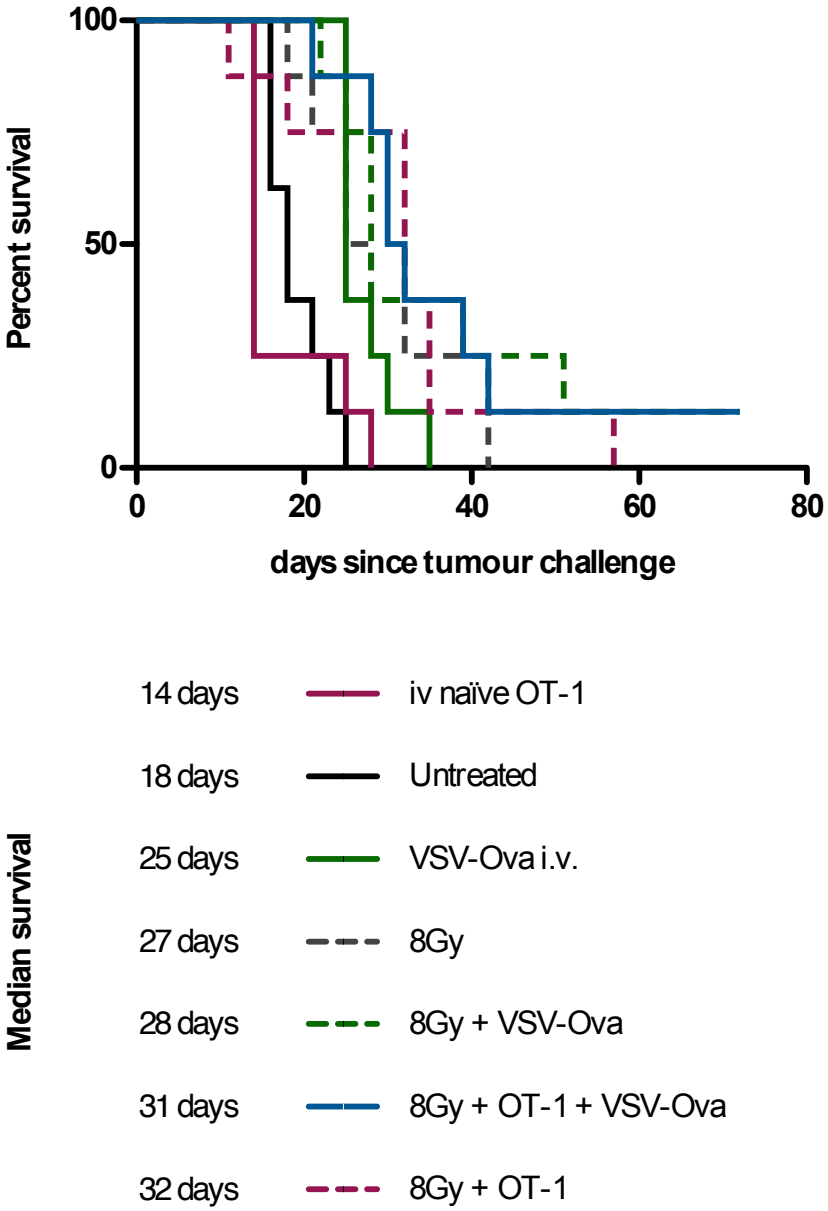

Figure 40. Survival following combinations of 8 Gy, ACT and virotherapy. Mice from the experiment illustrated in Figure 39 were euthanized when tumours reached 1 cm in any dimension. Survival and median survival for each group are indicated above.

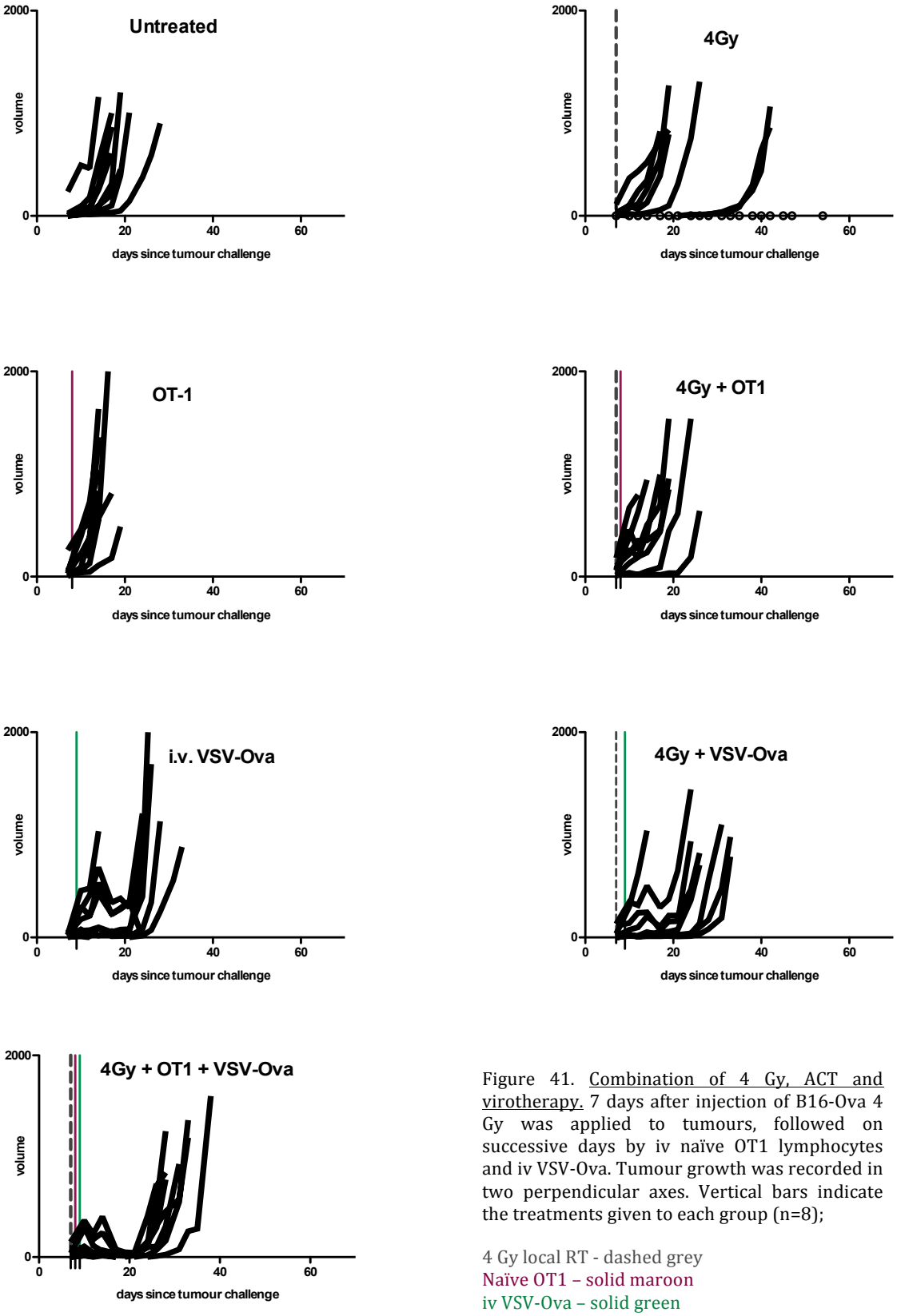

Figure 41. Combination of 4 Gy, ACT and virotherapy. 7 days after injection of B16-Ova 4 Gy was applied to tumours, followed on successive days by iv naïve OT1 lymphocytes and iv VSV-Ova. Tumour growth was recorded in two perpendicular axes. Vertical bars indicate the treatments given to each group (n=8);

4 Gy local RT - dashed grey
Naïve OT1 – solid maroon
iv VSV-Ova – solid green

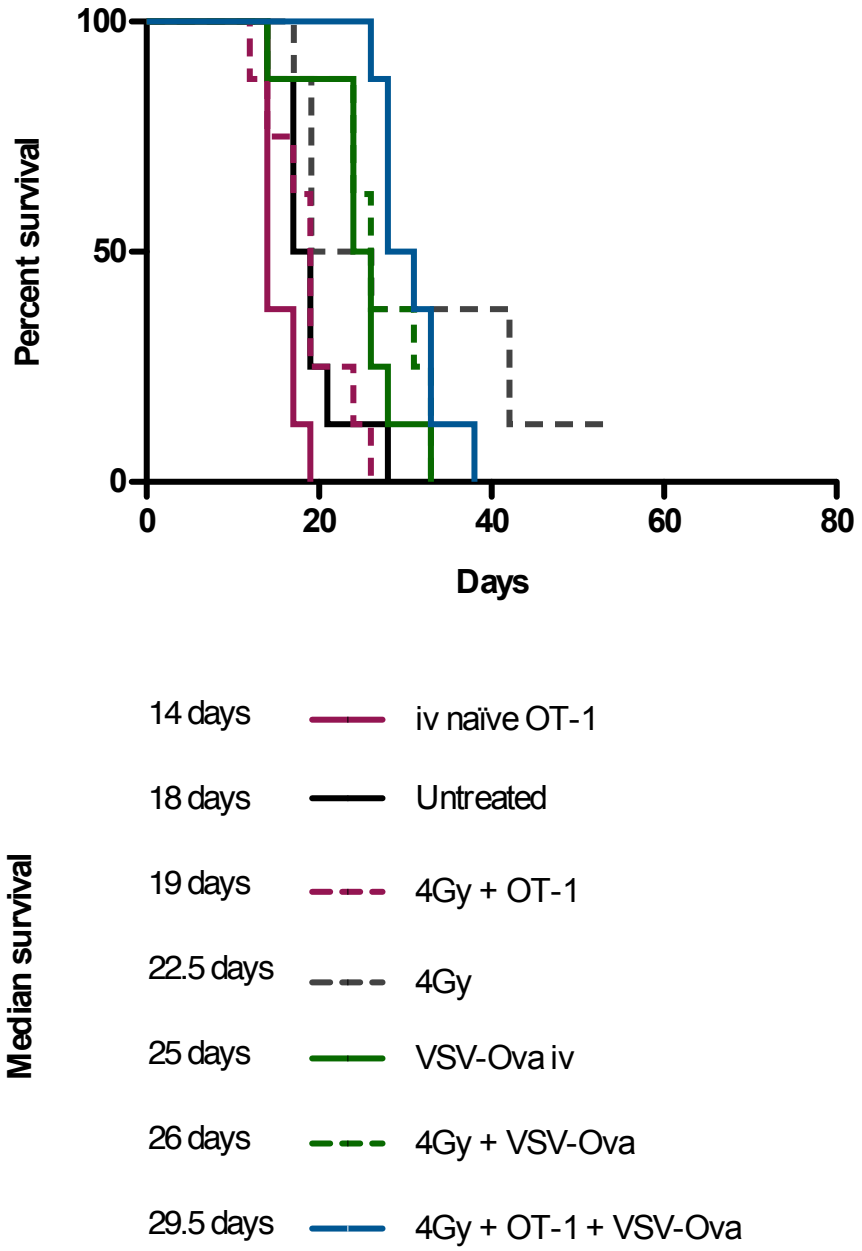

Figure 42. Survival following combinations of 4 Gy, ACT and virotherapy. Mice from the experiment illustrated in Figure 41 were euthanized when tumours reached 1 cm in any dimension. Survival and median survival for each group are indicated above.

5.2.2 Optimal timings of combination therapy

That the effects of radiotherapy take time to evolve is well established, and the time taken varies according to fraction size, dose rate and parameters within the tissue of interest. Thus it was hypothesised that immunologically relevant effects of external beam RT occur in a specific and limited time frame. The corollary of which is that the experiments described above may have failed to demonstrate synergy because a window of synergistic potential was missed in the schedule as applied. In order to test this hypothesis, mice were treated with 4 Gy on day 7 as before, and then received naïve OT1 at a range of intervals thereafter (days 8, 11, 13 and 15), followed on subsequent days by intravenous SIINFEKL with the aim of optimally activating OT1 with their cognate antigen. As shown in Figure 43 there was a delay in tumour growth and an improvement in survival (Figure 44) when the cellular therapy was delayed until day 11 or 15 (4 and 6 days after RT respectively). However no such improvements were seen with day 13 OT1, an incongruity that suggests that the apparent improvements seen in day 11 and 15 groups were in fact spurious. In a subsequent experiment, using VSV-Ova in place of SIINFEKL, no delay of tumour growth (Figure 45), nor survival (Figure 46), was seen when the interval between ACT and RT was prolonged. The rate of tumour growth prevented later time points being used, as mice would have needed to be euthanized before receiving ACT or virotherapy.

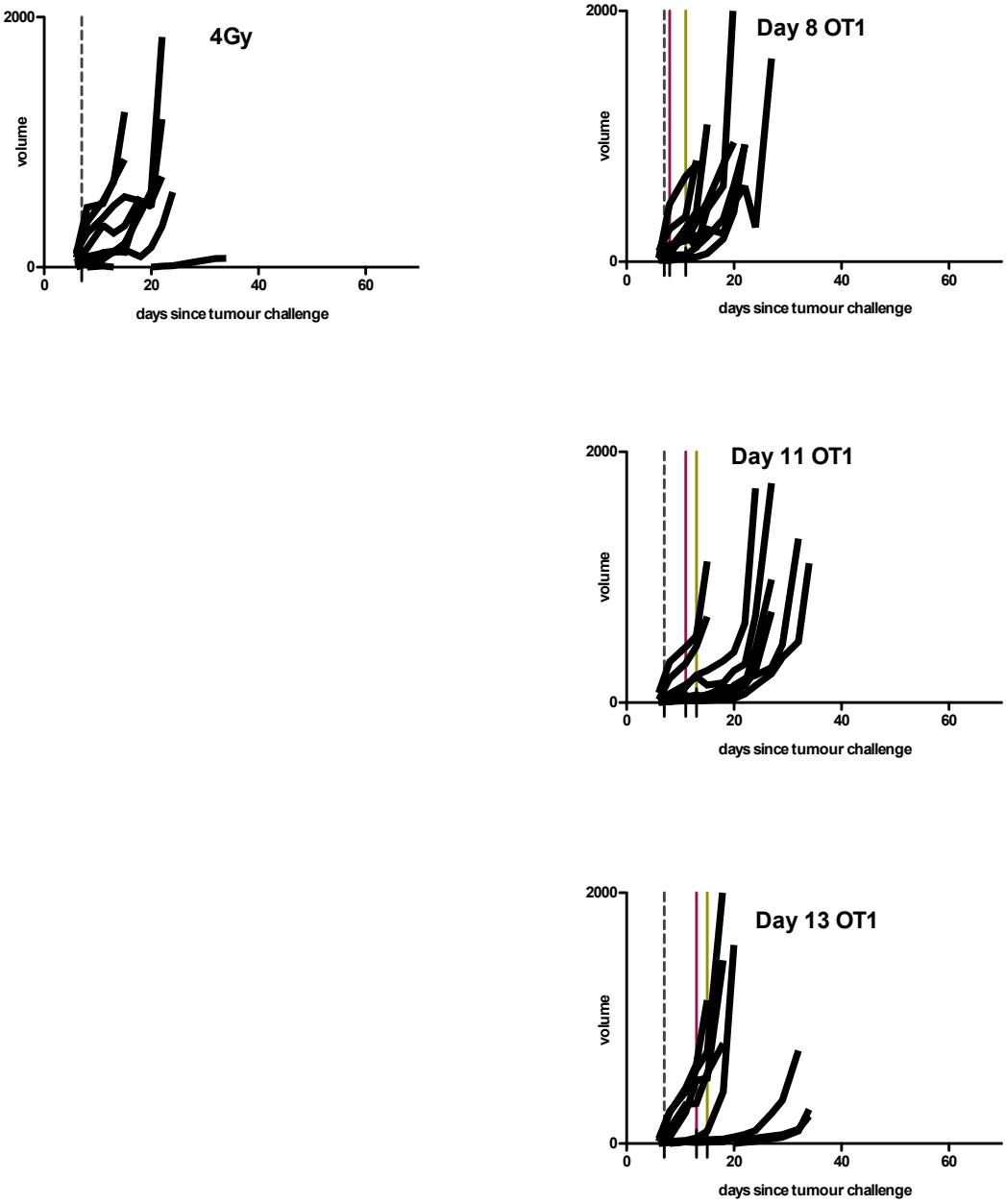

Figure 43. Optimising the timings of therapy. 7 days after injection of B16-Ova 4 Gy was applied to tumours, followed, after varying intervals, by naïve OT1 T-cells and intravenous SIINFEKL. Tumour growth was recorded in two perpendicular axes. Vertical bars indicate the timings of the treatments given to each group (n=8);

4 Gy local RT - dashed grey
Naïve OT1 – solid maroon
iv SIINFEKL – solid green

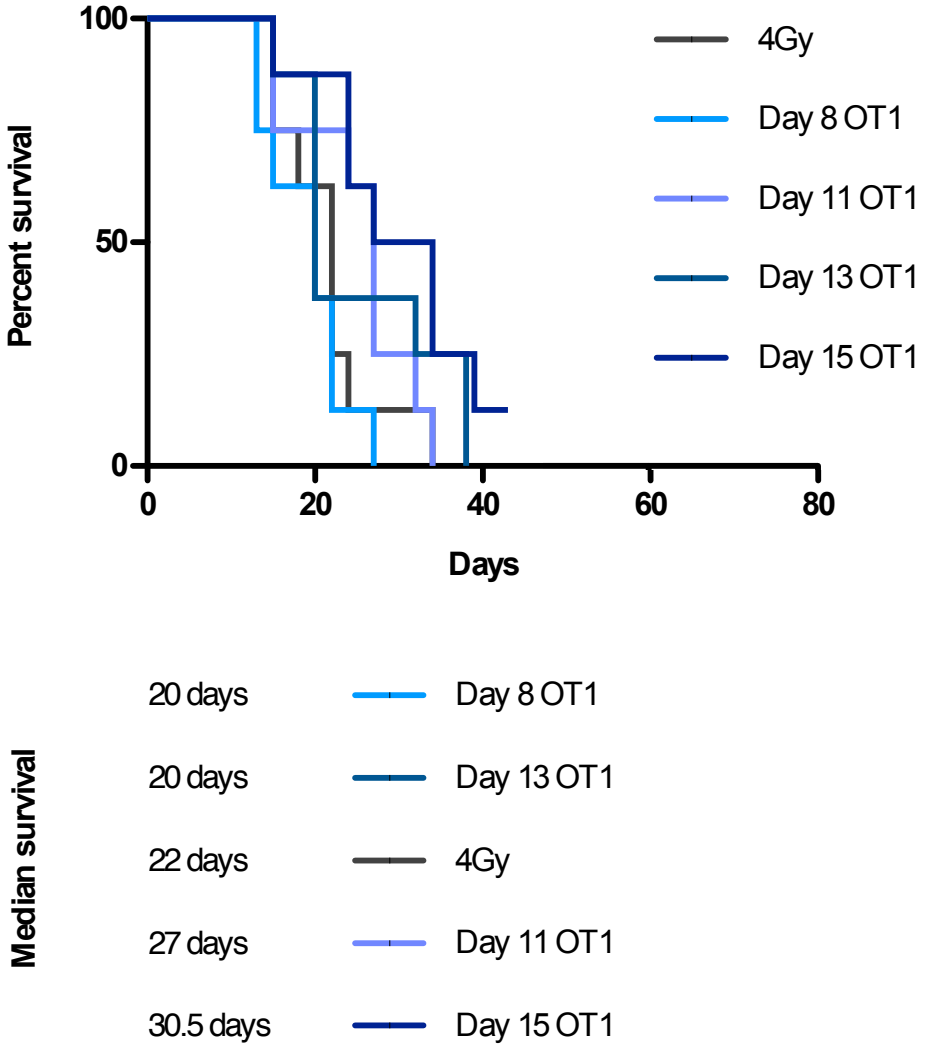

Figure 44. Optimising the timings of therapy (survival). Mice from the experiment illustrated in Figure 43 were euthanized when tumours reached 1 cm in any dimension. Survival and median survival for each group are indicated above.

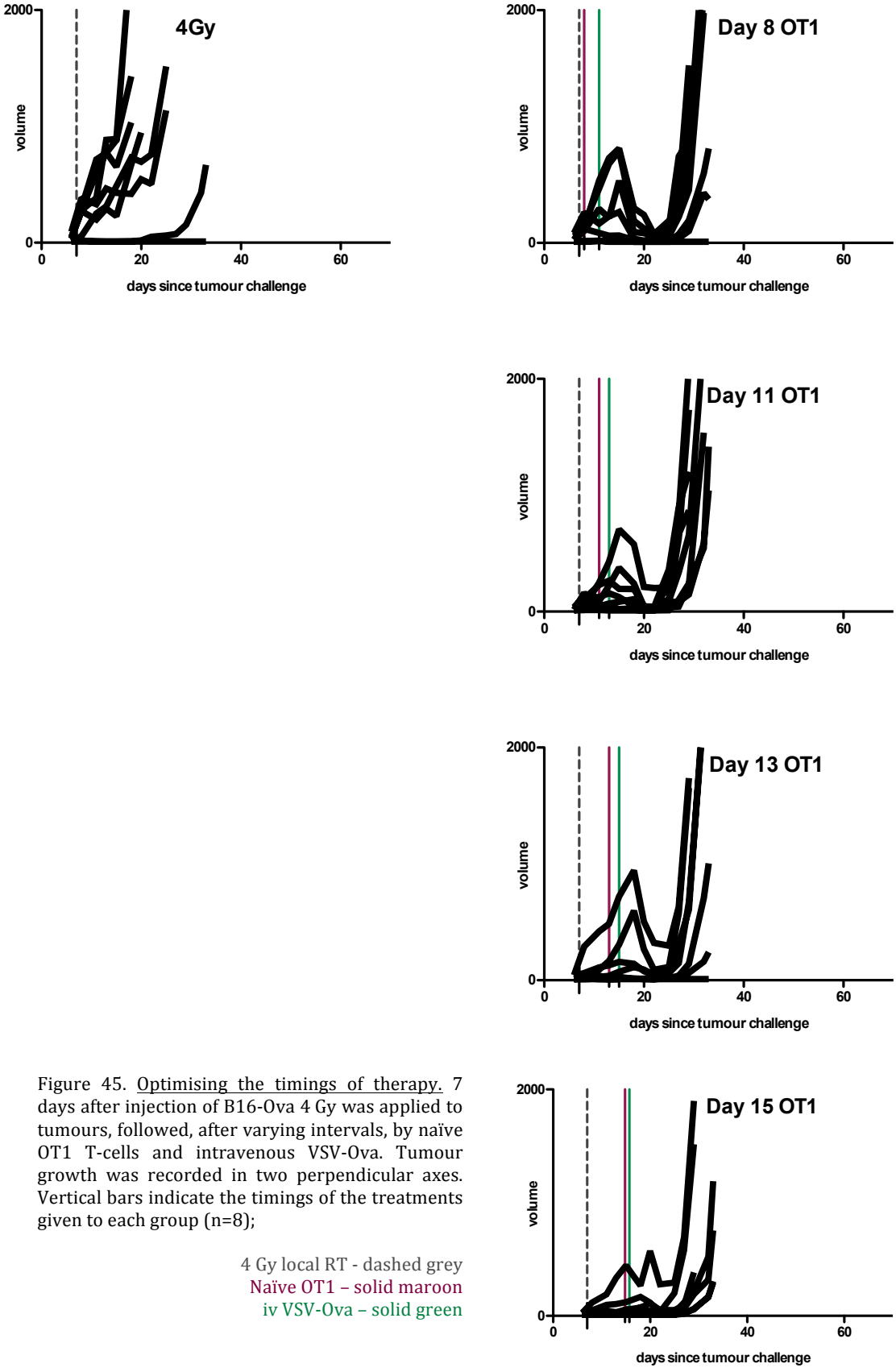

Figure 45. Optimising the timings of therapy. 7 days after injection of B16-Ova 4 Gy was applied to tumours, followed, after varying intervals, by naïve OT1 T-cells and intravenous VSV-Ova. Tumour growth was recorded in two perpendicular axes. Vertical bars indicate the timings of the treatments given to each group (n=8);

4 Gy local RT - dashed grey
Naïve OT1 – solid maroon
iv VSV-Ova – solid green

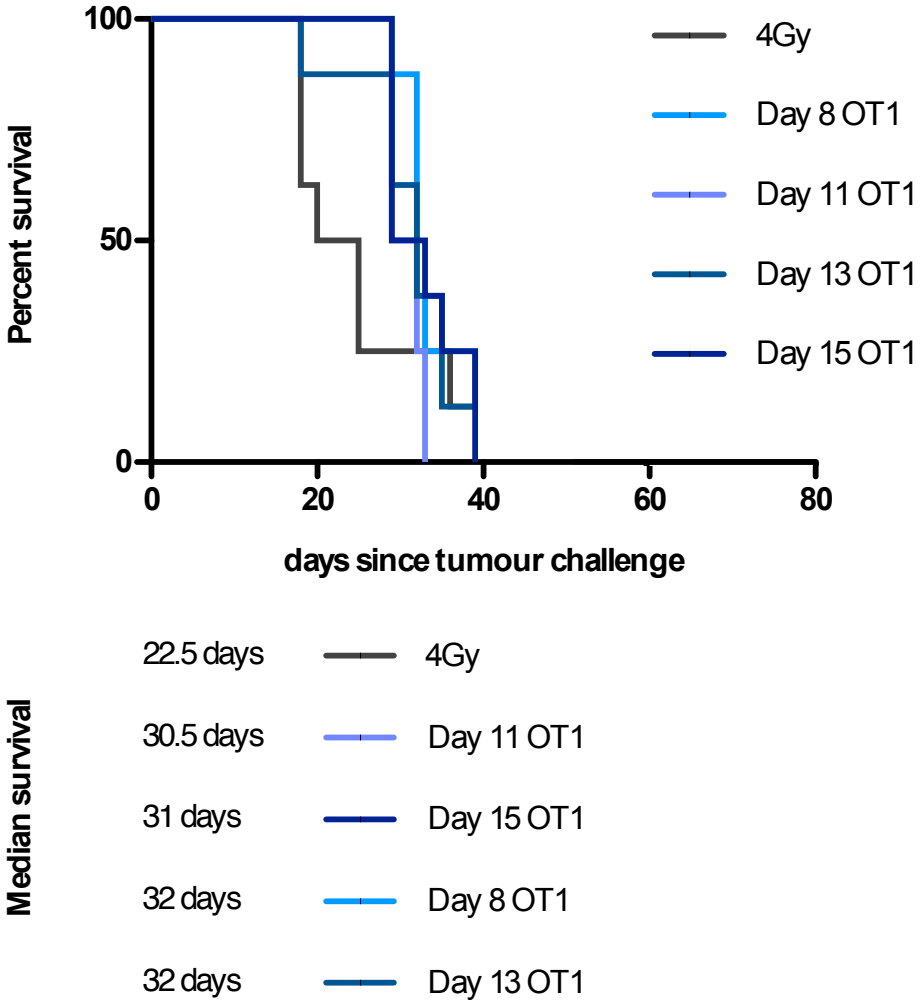

Figure 46. Optimising the timings of therapy (survival). Mice from the experiment illustrated in Figure 45 were euthanized when tumours reached 1 cm in any dimension. Survival and median survival for each group are indicated above.

5.2.3 The persistence of adoptively transferred T-cells

The effectiveness of ACT may be limited by several factors (Dudley and Rosenberg, 2003; Sanchez-Perez et al., 2007):

- Limited persistence or survival of cells
- Failure to generate memory
- Failure of cells to reach tumour or draining lymph nodes
- Failure to overcome tumour-mediated suppression
- Resistance of tumour cells to killing mechanisms.

To examine some of these parameters, mice bearing B16-Ova were treated with combinations of RT, ACT and virotherapy, and euthanized after elective intervals. Tumours, tumour-draining lymph nodes (TDLN) and spleens were then harvested and examined by flow cytometry. VSV-GFP, rather than VSV-Ova, was used to avoid conflation of anti-viral responses, as distinct from anti-tumour responses, raised against ovalbumin.

The persistence of adoptively transferred cells was examined by flow cytometry; in this experiment congenic C57BL6 mice bearing the Thy1.1 marker were used, allowing for discrimination of host lymphocytes from Thy1.2 donor OT1 cells. Adoptively transferred Thy1.2+ve cells were detected within the TDLN of all treated mice, however at low frequencies and declining over time (Figure 47). Moreover no difference in frequency or persistence was apparent when OT1 were administered with virotherapy, RT, or both. No Thy1.2 cells were detected in tumours or spleens (data not shown), suggesting that the absolute number of cells persisting to day 12, i.e. four days after administration, or trafficking to the tumour was low.

Cells prepared for use in the experiments shown in Figure 47 were also cultured ex vivo for four hours with one of a panel of antigenic epitopes, and then examined for the presence of intracellular IFNγ, indicating T-cell recognition of a cognate antigen (Figure 48). Epitopes from the TAA trp2 and gp100 were included to address the possibility of epitope spreading, wherein tumour cell killing by adoptively transferred effector cells releases TAA and danger signals that, enhanced by adaptive-to-innate cross talk, license DC to prime de novo adaptive responses. Consistent with the finding of Thy1.2+ donor cells at day 12,

an IFNγ response to SIINFEKL was detected within TDLN; no response was seen in cells from the tumour or spleen, from mice of any treatment group (data not shown). Notably there was no apparent enhancement of the response to SIINFEKL by the addition of RT or virotherapy to ACT, when examining the results from duplicate mice. At day 14 the production of intracellular IFNγ in response to SIINFEKL remained higher than untreated cells. Moreover mice that had been treated with VSV (groups C and D, indicated by triangles) appeared to have a response to the viral epitope not seen in the virus naïve groups. In addition at day 14 some mice developed a response against the TRP2 antigen, though it must be noted that the frequency of cells detected was low, as was the absolute difference in frequencies when compared to the unstimulated cells. By days 16 and 19 the frequency of cells that stained positive for intracellular IFN was too low (in keeping with the results seen in Figure 47) to be able draw meaningful conclusions.

Clearly the data presented in Figure 47 and Figure 48 do not preclude other factors limiting the efficacy of ACT, but accepting the caveats described above, it appears that a significant impediment to therapy using naïve OT1, not overcome by the addition of RT, is the limited trafficking of OT1 cells too, and persistence within, tumours and TDLN. In the context of clinical ACT for melanoma it is thought that native host lymphocytes can denigrate the efficacy of adoptively transferred cells by competing for cytokines. If local RT is able to stimulate an inflammatory response from tumours, including chemokines that could recruit immune effector cells, then host lymphocytes may also act as a chemokine sink, inhibiting recruitment. Current ACT protocols include total body irradiation in order to deplete lymphocytes and reduce the effect of the cytokine ‘sink’ – a similar approach may therefore be useful in this model.

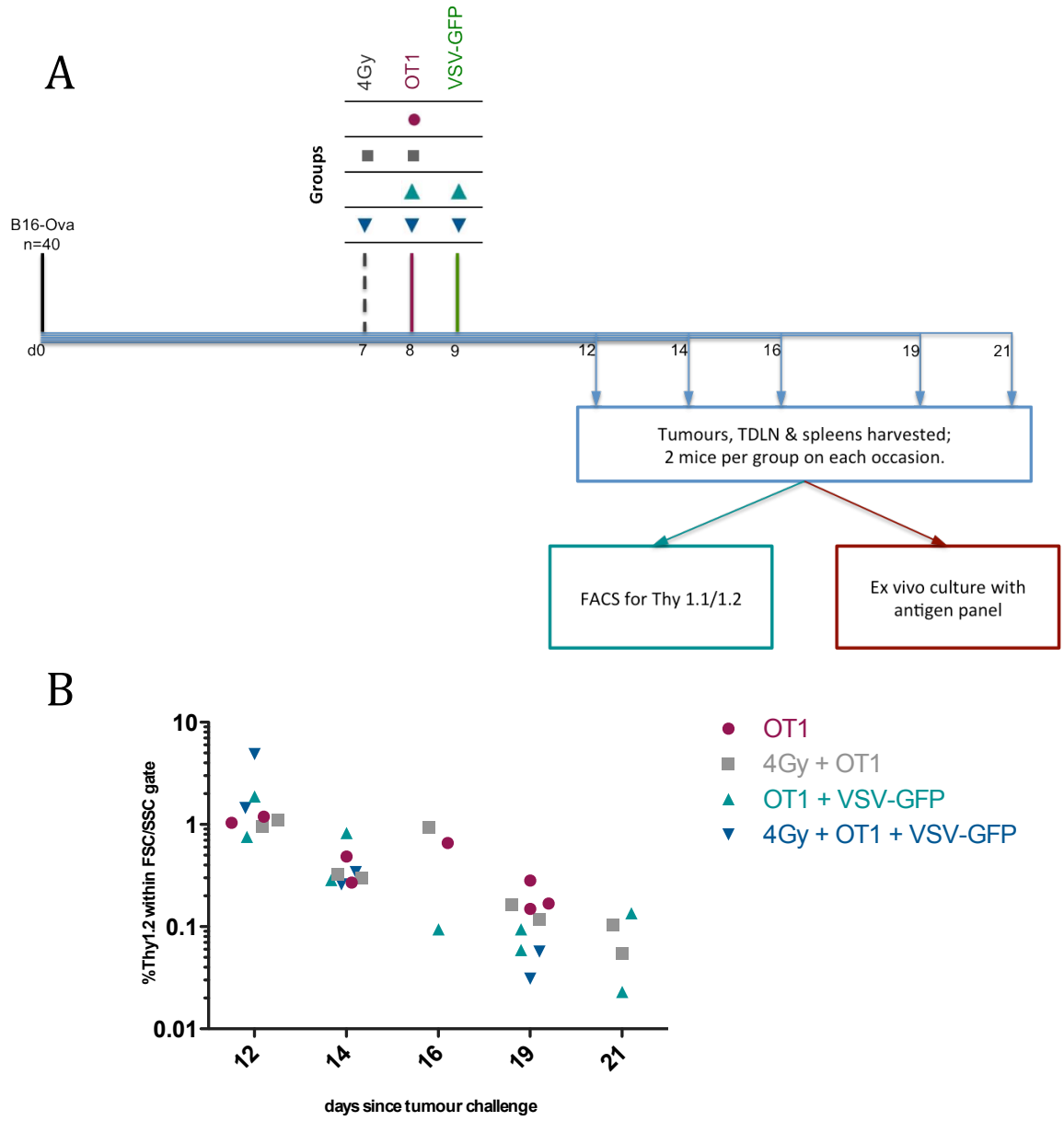

Figure 47. Persistence of adoptively transferred cells. A. Schematic illustrating that mice bearing B16-Ova tumours were treated with combinations of RT, OT1 and VSV-GFP, and two mice from each group euthanized on days 12, 14, 16, 19 and 21. If tumours reached 1 cm in any dimension mice were euthanized earlier than the pre-planned schedule. B. Tumour-draining lymph nodes were removed from mice immediately after euthanasia and analysed for the presence of adoptively transferred T-cells by flow cytometry; donor mice were Thy1.2 +ve and recipients Thy1.1, allowing for discrimination of donor T-cells from host. No Thy1.2 +ve cells were detected in the tumour or spleens of mice from any group (data not shown).

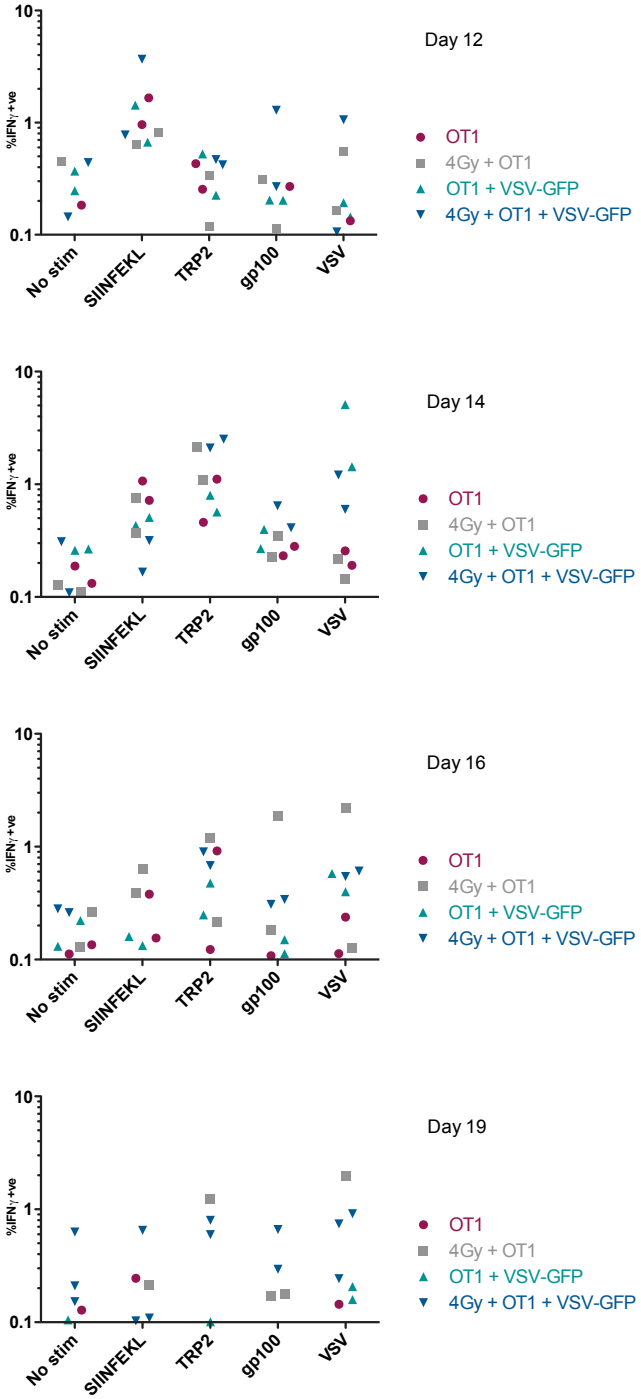

Figure 48. IFN production from TDLN CD8+ T-cells. Tumour draining lymph nodes were harvested from mice bearing B16-Ova tumours after 12, 14, 16, 19 or 21 days, and following treatment with combinations of OT1, VSV-GFP and 4Gy. Cells were cultured ex vivo for four hours in the presence of the peptides indicated and the cells then analysed for intracellular IFNγ. Results indicate the percentage of CD8+ cells that were also positive for IFNγ in each mouse. Note that the axes are logarithmic. Peptide stimulation and staining were performed on the day of harvest and FACS analysis the following day. Two mice per group were harvested on each day, according to predefined allocation; when unplanned euthanasia was required on an analysis day the additional mice were included in that day's analysis.

5.2.4 Total body irradiation

Local radiotherapy has been demonstrated to elicit changes within the tumour and its stroma that could have immunologically relevant consequences. Irradiation of the whole body (or total body irradiation, TBI) has long been known to have immunological consequences. Early experience of the bombings of Hiroshima and Nagasaki, as well as inadvertent industrial radiation exposures, revealed that doses of around 4 - 5 Gy lead to death in 50% of humans (Hall and Giaccia, 2011). In most such cases death occurs within 60 days due to the haematopoietic syndrome, in which precursor cells are sterilised by the radiation and pancytopenia ensues. Notably the lethal dose in mice, though likely to vary between strains, is estimated to be in the region of 7 Gy.

The most recently reported conditioning regimen for clinical ACT includes TBI; 12 Gy in six fractions over three days, or a single 2 Gy fraction (Rosenberg et al., 2011). In this context TBI is thought to act by depleting host lymphocytes, that would otherwise compete with adoptively transferred lymphocytes for endogenous cytokines, in turn allowing the transferred cells to proliferate. TBI may also act by depleting Tregs, and the gastrointestinal toxicity of TBI is likely to result in the release of potent danger signals such as LPS into the circulation which would serve to activate APC and lymphocytes (Somosy et al., 2002).

Whole body irradiation would be expected to enhance the efficacy of ACT and virotherapy by depleting host lymphocytes, allowing for greater proliferation of adoptively transferred naïve T-cells, by reducing competition for cytokines, and enhancing the immunogenicity and susceptibility of tumour cells. Accordingly mice bearing B16-Ova tumours were treated with OT1 cells and intravenous VSV-Ova, on sequential days after 4 Gy applied to the tumour or 4 Gy to the whole body. As shown in Figure 49 and Figure 50, there was no benefit from the addition of RT to ACT and virotherapy. Notably TBI failed to achieve better tumour control, or survival, when compared to local radiotherapy. Given that local and whole body radiotherapy would be expected to have very different patterns of immunological effects and those patterns might be complementary, in a subsequent experiment mice were treated with 4 Gy TBI, with or without an additional 4 Gy applied to the tumour alone, in combination with ACT and virotherapy (Figure 51 & Figure 52). No additive benefit was derived from the

combination RT approach when compared to OT1 and VSV-Ova alone. Notably, despite two 4 Gy fractions encompassing the tumour, separated by at most 2 hours, no mice developed skin reactions, as had previously been seen with 8 Gy. This is presumably due to some early repair during the interval between the treatments, and the skin sparing effect of the higher energy photons of the ^{137}Cs source used for TBI. Although the escalated dose was well tolerated no benefit was seen when compared to the combination of ACT and virotherapy without RT.

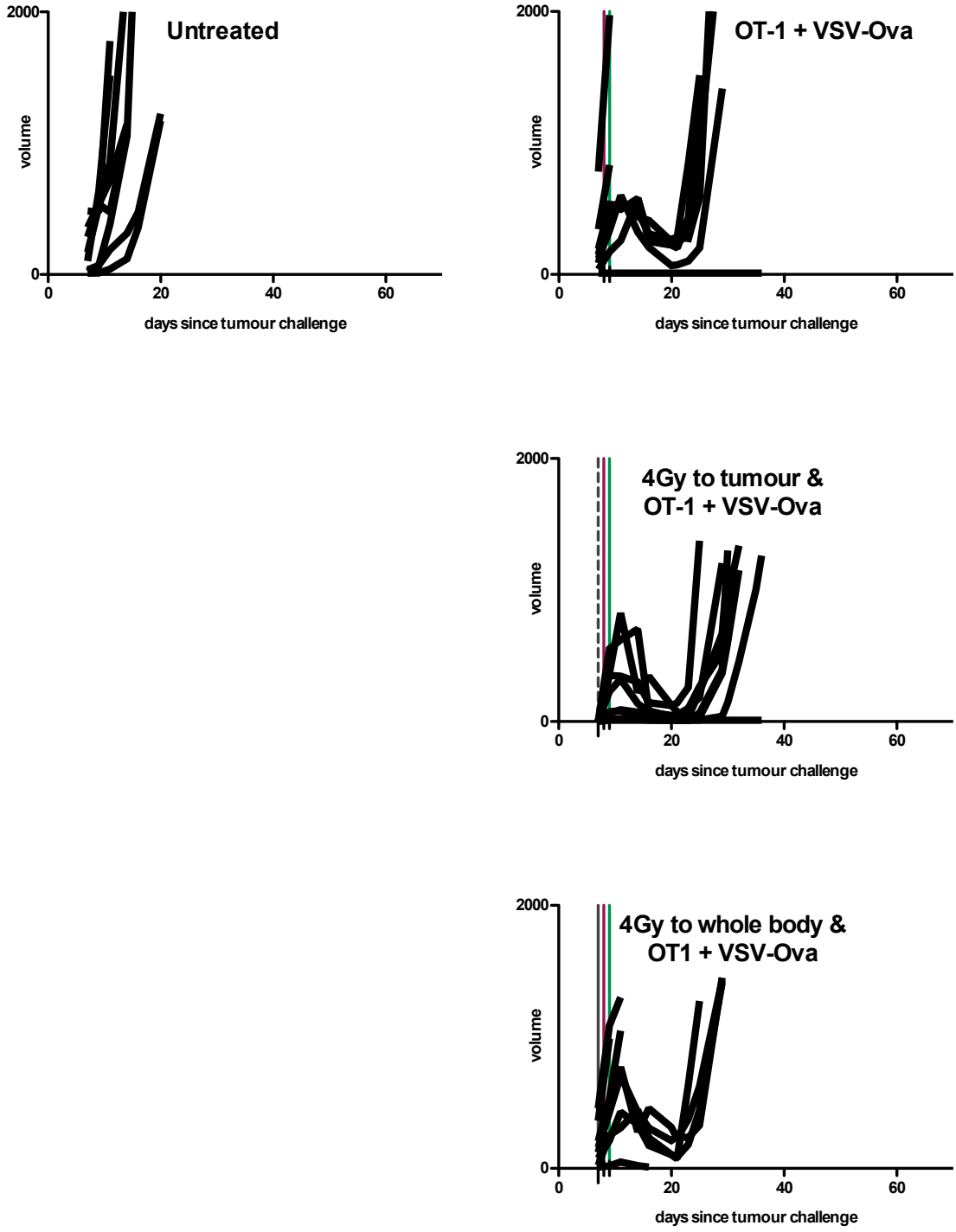

Figure 49. Whole body versus local irradiation. 7 days after injection of B16-Ova 4 Gy was applied to tumours using an orthovoltage machine, or to the whole animal using a ^{137}Cs source, followed on successive days by naïve OT1 T-cells and intravenous VSV-Ova. Tumour growth was recorded in two perpendicular axes. Vertical bars indicate the treatments given to each group (n=8);

4 Gy local RT - dashed grey
4 Gy whole body RT - solid grey
Naïve OT1 – solid maroon
iv VSV-Ova – solid green

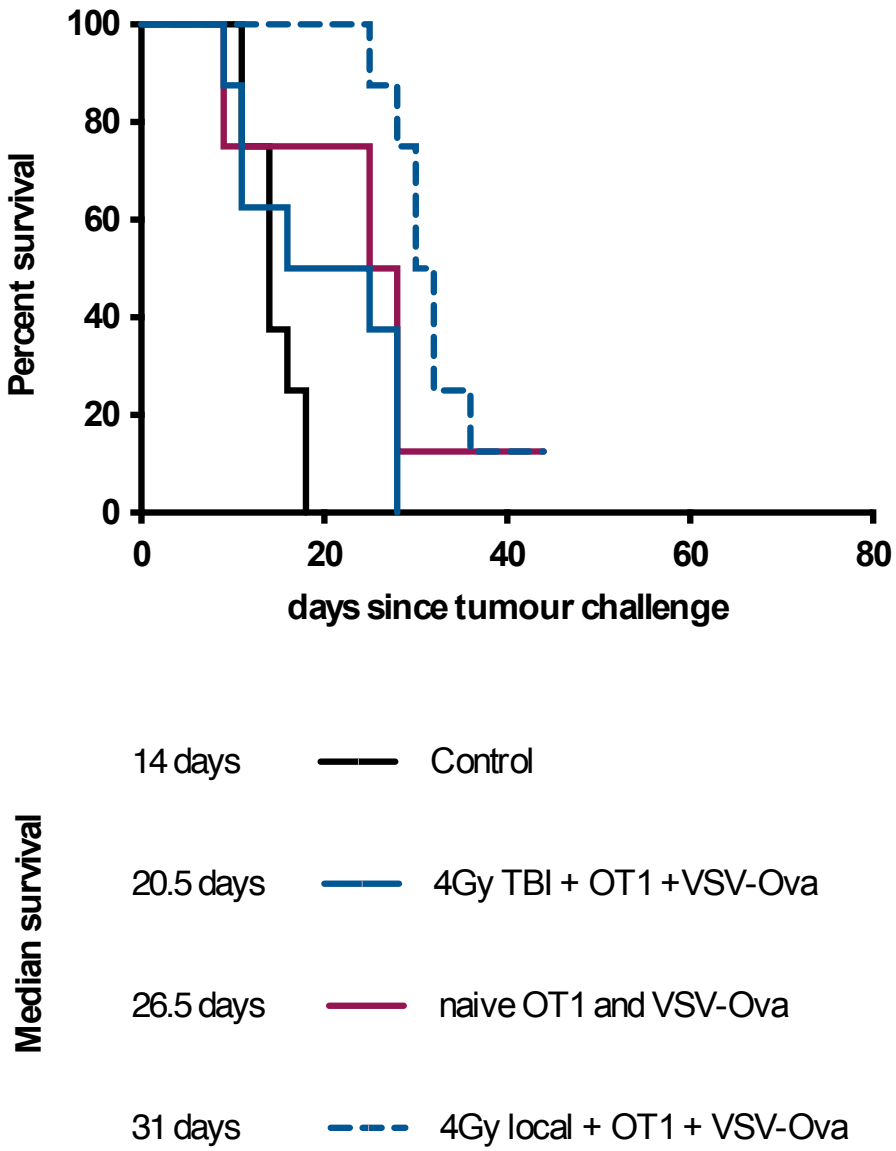

Figure 50. Survival following whole body versus local irradiation. Mice from the experiment illustrated in Figure 49 were euthanized when tumours reached 1 cm in any dimension. Survival and median survival for each group are indicated above.

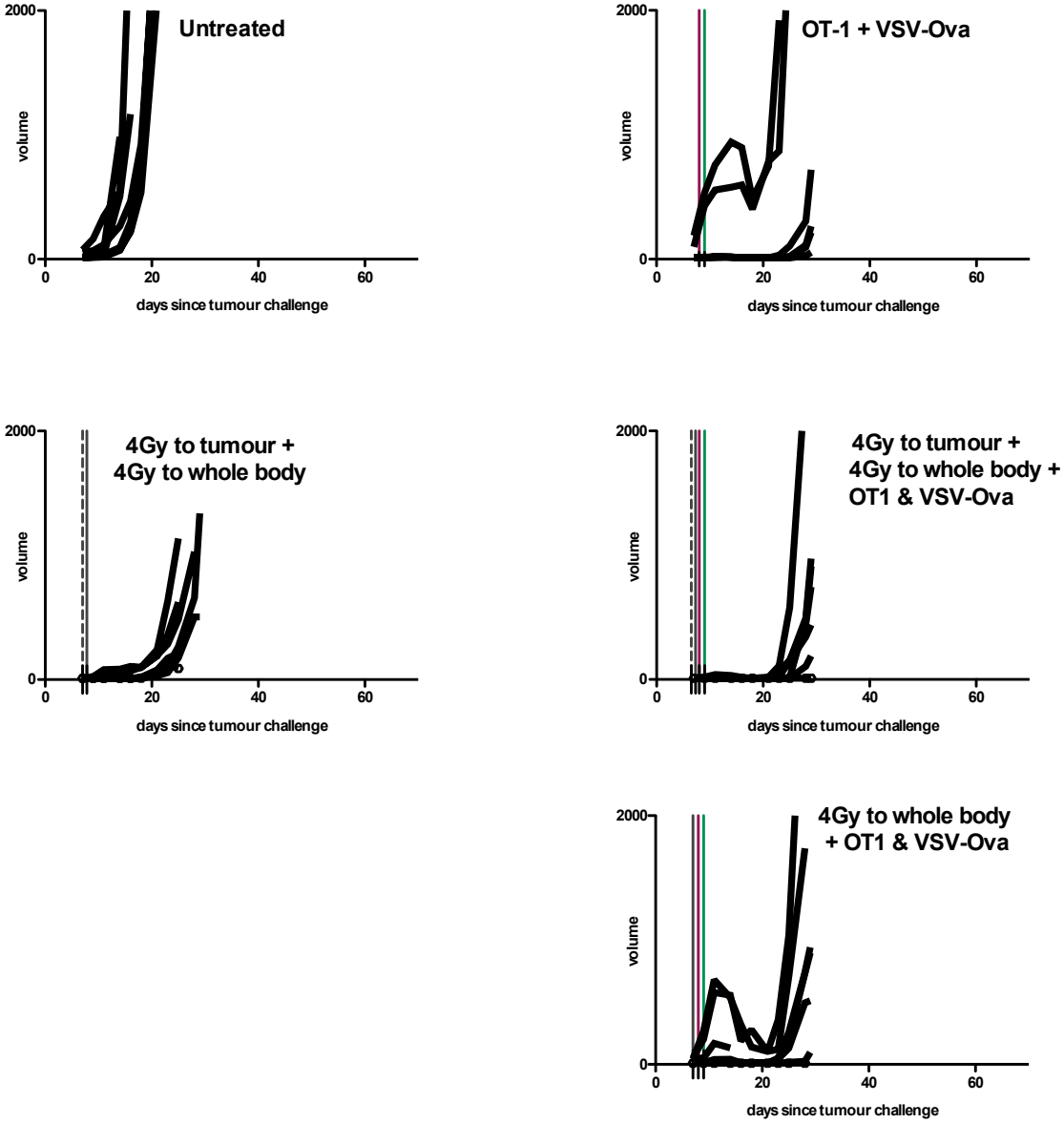

Figure 51. Combinations of whole body and local irradiation. 7 days after injection of B16-Ova mice were exposed to 4 Gy to the whole body using a ^{137}Cs source, and immediately thereafter 4 Gy to the tumour, delivered by orthovoltage source. Naïve OT1 T-cells and intravenous VSV-Ova were administered on days eight and nine respectively. Tumour growth was recorded in two perpendicular axes. Vertical bars indicate the treatment given to each group (n=8).

4 Gy local RT - dashed grey
4 Gy whole body RT - solid grey
Naïve OT1 – solid maroon
iv VSV-Ova – solid green

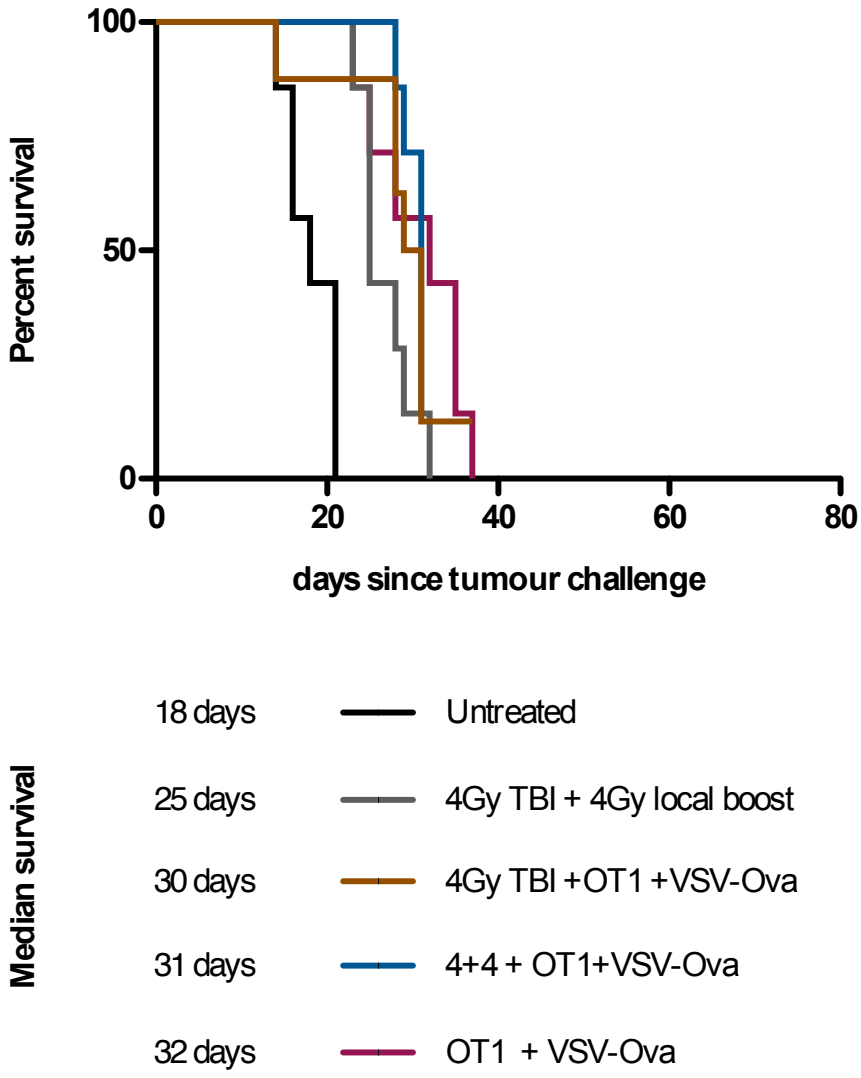

Figure 52. Survival following combinations of whole body and local irradiation. Mice from the experiment illustrated in Figure 51 were euthanized when tumours reached 1 cm in any direction. Survival and median survival for each group are indicated above.

5.2.5 Pmel + VSV-gp100

Transgenic Pmel mice express a T-cell receptor (Vα1/Vβ13) specific for an epitope within gp100 when presented on MHC class I molecules. As gp100 is a TAA, rather than tumour-specific antigen, it is found on normal melanocytes as well as melanoma. Combinations of adoptively transferred Pmel T-cells with VSV expressing gp100 have recently been reported to cure a proportion of established B16-Ova tumours, though necessitating multiple administrations (Rommelfanger et al., 2012). External beam RT was therefore combined with Pmel lymphocytes (prepared in the same way as OT1 T-cells) and VSV-gp100 to test the hypothesis that RT could enhance subtherapeutic doses, making the treatment more practicable and clinically applicable.

B16-Ova tumours were established in C57Bl/6 mice and therapy started 7 days after tumour implantation. Mice were then treated with external beam radiotherapy to the tumour, with or without intravenous naïve Pmel T-cells the following day, and intravenous VSV-gp100 a day later. Additionally the effect of local RT was compared with TBI, in concert with Pmel and VSV-gp100, with tumour growth curves shown in Figure 53 and survival in Figure 54. As shown in Figure 54 these data demonstrate that the addition of local RT to the combination of VSV-gp100 and Pmel increased median survival (from 23 to 30 days). To confirm these findings this combination was also tested in the experiment shown in Figure 55, confirming the enhanced survival seen when local RT was added to Pmel and VSV-Ova (18 to 28 days).

These survival data (local RT + Pmel + VSV-gp100) were tested for evidence of statistical significance using GraphPad Prism. The 95% confidence interval of the hazard ratios from each experiment spanned unity; (2.5 {0.8-7.6} & 2.7 {0.7-9.8}). When the survival data were combined the hazard ratio was 2.34 with a 95% confidence interval of 1.03 – 5.32. Log-rank test of the pooled survivals produced a p value of 0.04, though no adjustment was made for the multiple groups tested in each experiment.

The effect of TBI was inconsistent in the same pair of experiments; although TBI appeared to improve survival in Figure 54, no such benefit was seen in the experiment shown in Figure 55

The effect of RT on adoptively transferred activated T-cells was also studied. Naïve T-cells in combination with systemic adjuvant, such as an oncolytic virus expressing the cognate antigen, are thought to have greater potential for expansion once administered and to be less prone to exhaustion and activation-induced death than activated lymphocytes (Rommelfanger et al., 2012). Despite this, most reports of ACT have used activated lymphocytes for transfer, and therefore a comparison of RT with naïve or activated was undertaken. The data presented in Figure 55 andFigure 56 were obtained in one experiment.
Pmel lymphocytes prepared as above were activated by culture with IL2 and gp100 peptide for four days before administration to mice. The median survival of each group is shown in Figure 56. RT, local or TBI, enhanced survival by ten days when combined with activated Pmel and VSV-gp100, in keeping with the data obtained using naïve lymphocytes (Figure 54). The increased survival following the addition of RT, either local or TBI, was not a statistically significant difference (Log-rank test). There did not appear to be any benefit from activated T-cells compared to naïve.

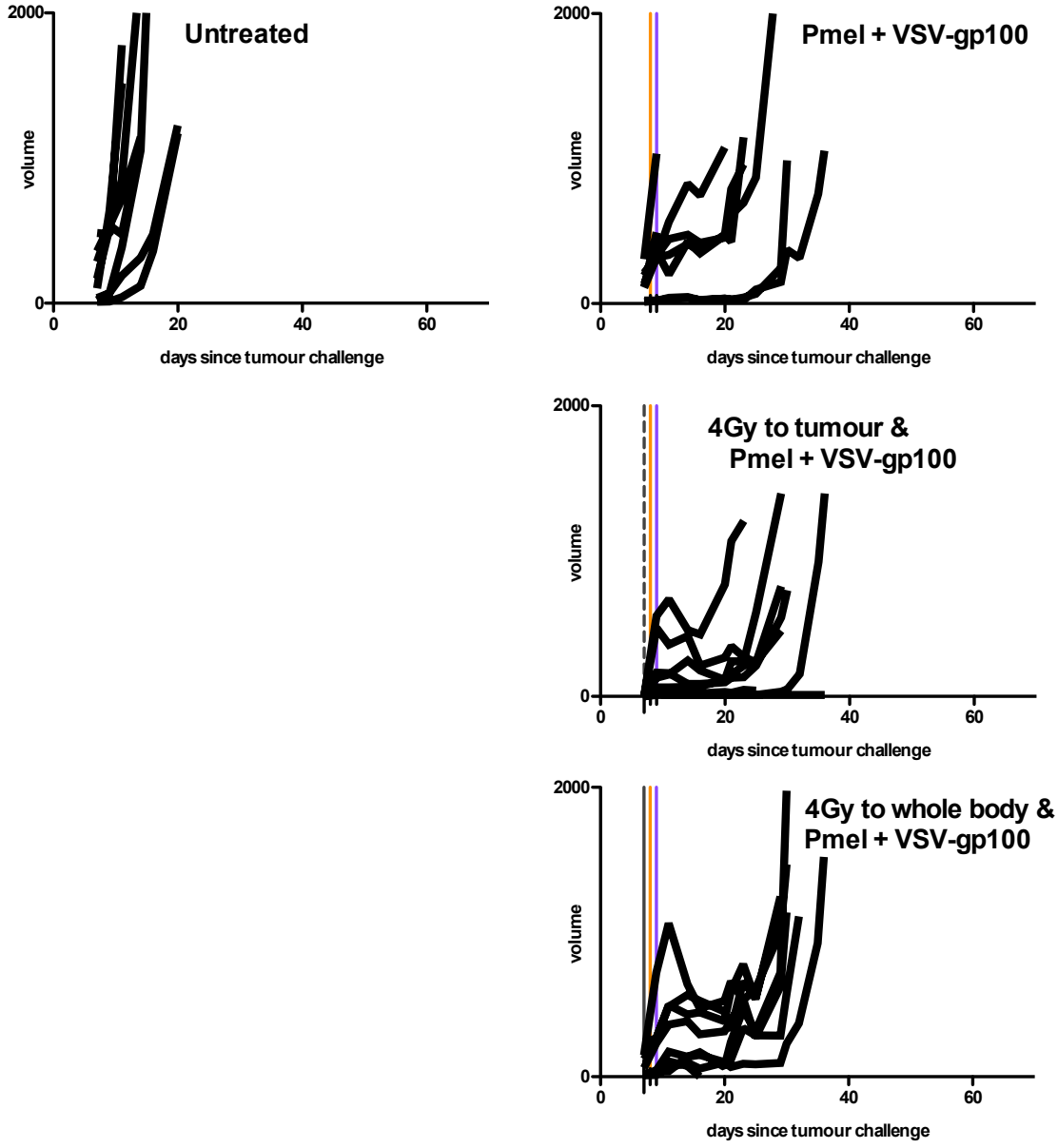

Figure 53 Local or whole body RT plus Pmel and VSV-gp100. 7 days after injection of B16-Ova mice were exposed to 4 Gy to the whole body using a ^{137}Cs source, or 4 Gy to the tumour, delivered by orthovoltage source. Naïve Pmel T-cells and intravenous VSV-gp100 were administered on days eight and nine respectively. Tumour growth was recorded in two perpendicular axes. Vertical bars indicate the treatment given to each group (n=8).

4 Gy local RT - dashed grey
4 Gy whole body RT - solid grey
Naïve Pmel – solid orange
iv VS-gp100 – solid mauve

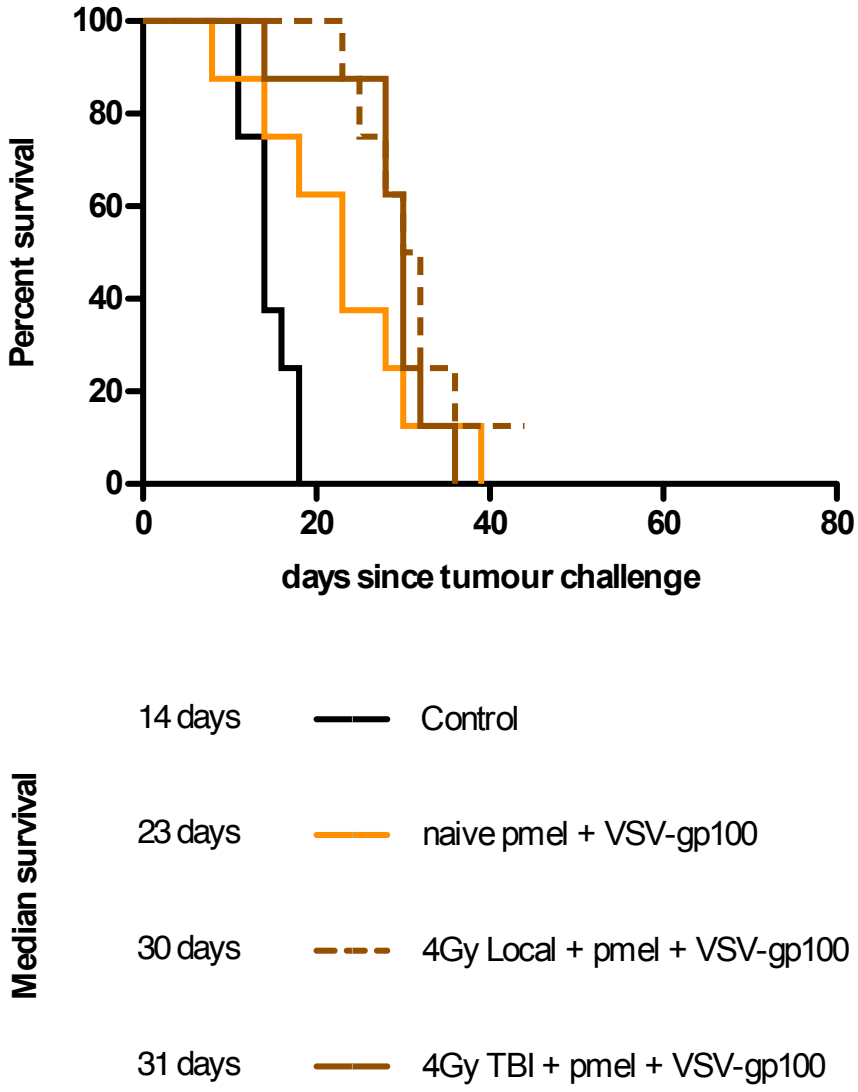

Figure 54 Survival following local or whole body RT plus Pmel and VSV-gp100. Mice from the experiment illustrated in Figure 53 were euthanized when tumours reached 1 cm in any direction. Survival and median survival for each group are indicated above

A

NAÏVE				
Radiotherapy	Pmel	VSV-gp100	Local	Whole body
		■	16	
	■		14	
	■	■	18	
■			18	14
■		■	21	14
■	■		18	14
■	■	■	28	14

B

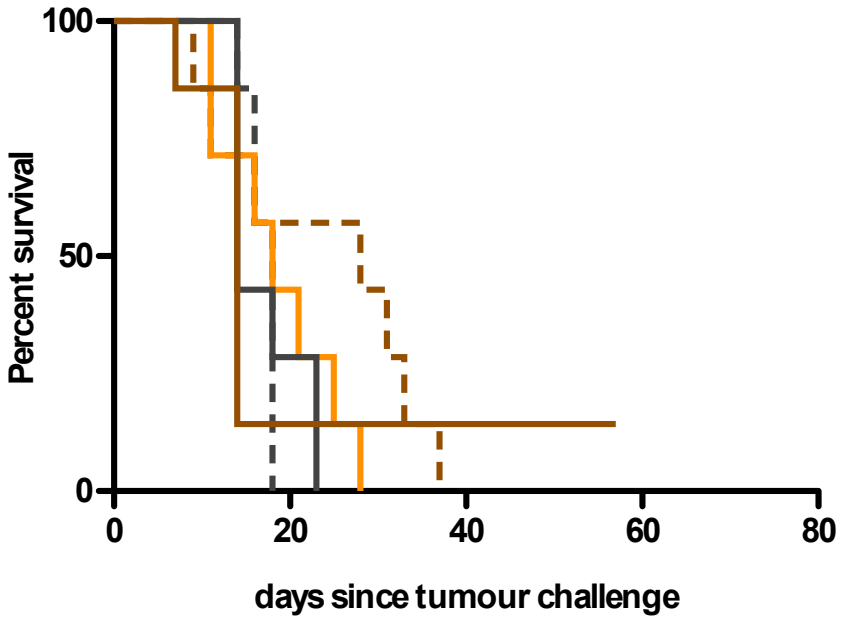

C

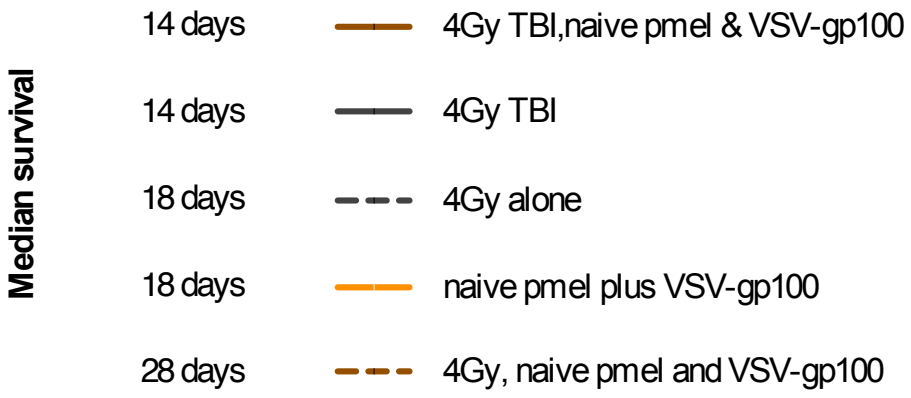

Figure 55. Local or whole body RT plus naïve Pmel and intravenous VSV-gp100. 7 days after injection of B16-Ova mice were exposed to 4 Gy to the whole body using a ^{137}Cs source, or 4 Gy to the tumour, delivered by orthovoltage source. Naïve Pmel T-cells and intravenous VSV-gp100 were administered on days eight and nine respectively. Mice were euthanized when tumours reached 1 cm in any direction. The median survival for each group is indicated in A (n=8 per group). The survival of relevant groups is also plotted in B & C; others were excluded for clarity. The groups shown were treated in the same experiment as those shown in Figure 56.

A

ACTIVATED				
Radiotherapy	Pmel	VSV-gp100	Local	Whole body
		■	16	
	■		18	
	■	■	21	
■			18	14
■		■	21	14
■	■		25	28
■	■	■	31	31

B

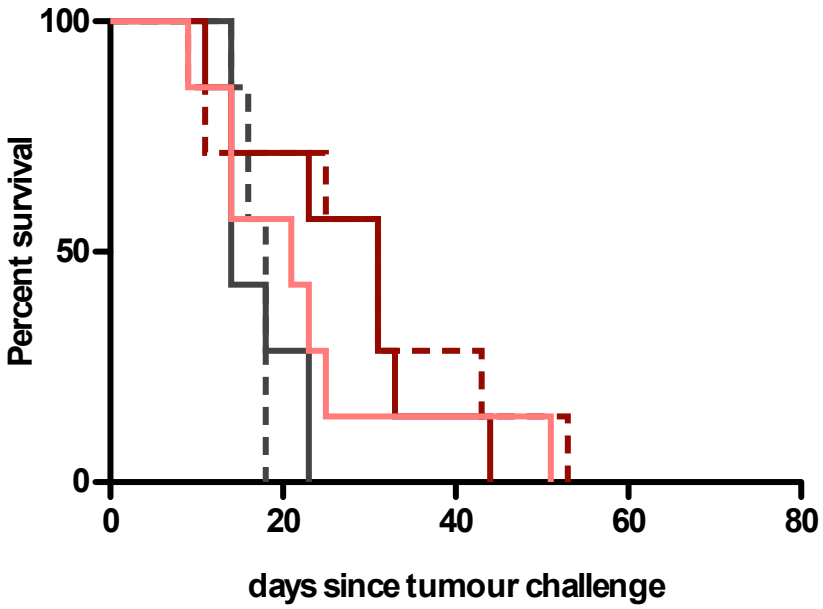

C

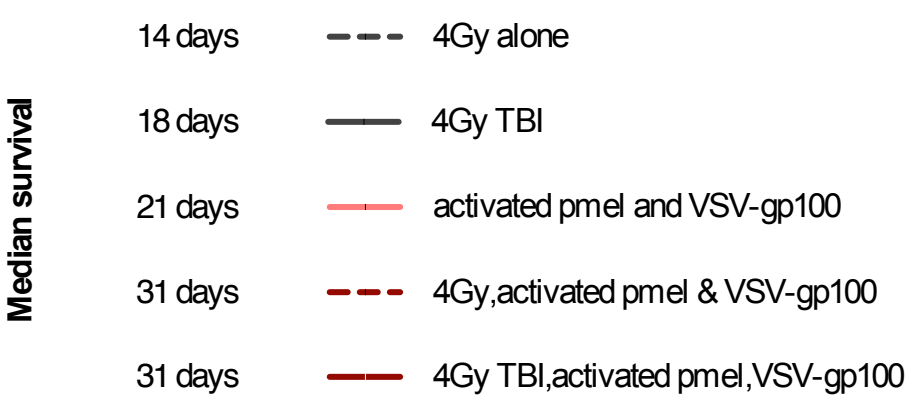

Figure 56. Local or whole body RT plus activated Pmel and intravenous VSV-gp100. 7 days after injection of B16-Ova mice were exposed to 4 Gy to the whole body using a ^{137}Cs source, or 4 Gy to the tumour, delivered by orthovoltage source. Activated Pmel T-cells and intravenous VSV-gp100 were administered on days eight and nine respectively. Mice were euthanized when tumours reached 1 cm in any direction. The median survival for each group is indicated in A (n=8 per group). The survival of relevant groups is also plotted in B & C; others were excluded for clarity. The groups shown were treated in the same experiment as those shown in Figure 55

5.2.6 Brachytherapy

The results illustrated earlier suggest that local radiotherapy or TBI have minimal effects on therapy with ACT and OV. It is possible that 4 Gy as an applied dose may have been inadequate to achieve the immunologically relevant changes that others have reported at higher doses. As described above, it was not possible to use higher doses delivered by an orthovoltage source without causing significant skin toxicity. Therefore brachytherapy was considered as an alternative method of irradiation that would allow higher doses to be delivered to the tumour.

Brachytherapy is the use of sealed radioactive sources placed, interstitially or into potential cavities, adjacent to tumour. In common use in the mid-to-late 20th century for a wide range of tumours, more recently advances in external beam technology have largely, though not completely, supplanted the use of brachytherapy in many tumour sites. Ongoing applications of the technique include:

- Intra-vaginal brachytherapy for cervical cancer
- Prostatic brachytherapy
- Retro-orbital plaques for ocular melanoma
- Intraoperative adjuvant brachytherapy for breast cancer
- Intravascular brachytherapy for non-malignant disease.

The necessity for operative procedures of varying complexity along with the evolution of conformal radiotherapy reduced the indications for brachytherapy, however some significant advantages remain. The source can be sited under direct vision or image guidance, in close proximity to tumours, allowing for confident localisation of dose. Furthermore brachytherapy sources essentially act as point sources thus dose varies as a function of the inverse square of the distance from the source. This allows, in many situations, excellent sparing of nearby tissues at risk whilst delivering very high dose to adjacent tumour.

Sealed sources of ^{125}I, recycled from prostatic brachytherapy, were mounted inside silastic discs (7 mm Ø, 3 mm thickness) (Figure 57A). These ‘plaques’ served to make the seeds easier and safer to handle, but also helped secure the source in place over tumours, reducing migration of the seeds within the subcutaneous space. Extensive work was done with the radiation safety group to

address concerns, both Federal and Institutional, about seed loss; seeds not mounted in plaques are 5 mm long with a diameter under 1 mm. In later experiments plaques were prepared with a half mm thick disc of lead mounted on one side to improve radiation safety. The tenth value layer of photons emerging from ^{125}I is around a tenth of a mm of lead, and estimates with a GM tube confirmed that the unilateral shielding considerably reduced the exposure rate.

In order to test the feasibility of the procedure, including the surgical placement of the plaques, two mice bearing day 7 B16-Ova tumours were anaesthetised with inhalational isofluorane (one C57BL6 and one OT1). Once adequate anaesthesia was achieved a 1 cm craniocaudal incision was made overlying the subcutaneous tumour and a small pocket established by blunt dissection. Plaques containing dummy-seeds were inserted and the incision closed with surgical staples. These mice were then used to obtain CT images for the purposes of dosimetry estimates (Figure 57B). After 4 days the plaques were removed under anaesthesia. In this and subsequent experiments it was noted that the mice tolerate the plaques; there was no evidence of excessive self-grooming, barbering, or gnawing at the plaque site, either by the mouse or its cage mates. The CT data acquired was used to prepare dosimetry estimates for subsequent experiments (Figure 57C).

In order to assess the effect of brachytherapy in this model active plaques were inserted in mice bearing established 7-day B16-Ova tumours. The dose delivered to tumour varies according to the activity of ^{125}I present within the sealed source, and the duration of the exposure. Plaques were therefore left in place for 2, 4, 7 or 9 days before removal. Tumour growth could not be recorded while plaques were in place, predominantly due to the unnecessary radiation exposure to personnel that would be entailed. Survival, however, was recorded and as shown in Figure 58 the doses delivered did not result in changes in survival between the treated groups, or mice bearing dummy plaques as controls. Although these doses clearly were inadequate to control tumours, it was hypothesised that given the nature of the inverse square rule there would be regions of the tumour exposed to ablative doses, capable of evincing tumour antigens and danger signals. Further from the source, the dose would be too low

to ablate tumour, but perhaps adequate to alter the tumour cells in immunologically relevant ways. Therefore a further experiment was performed in which mice bearing B16-Ova tumours were treated with active plaques for 48 hours followed, after plaque removal, by intravenous ACT and virotherapy. As illustrated in Figure 59, little difference in survival was seen in mice treated with the triple combination and those receiving ACT and virotherapy without brachytherapy.

Comparison of the effect of a dose from a single fraction of EBRT, delivered over 7 minutes, with that delivered over 48 hours by brachytherapy, is limited by the important effect of dose rate on the efficacy of a given dose; when dose is delivered at a low rate intracellular repair mechanisms abrogate the effects of irradiation, lowering the effective dose. However it is likely that the dose achieved in areas of the tumour directly adjacent to the plaque was high enough (in excess of 40 Gy, Figure 57C) to quell such concerns.

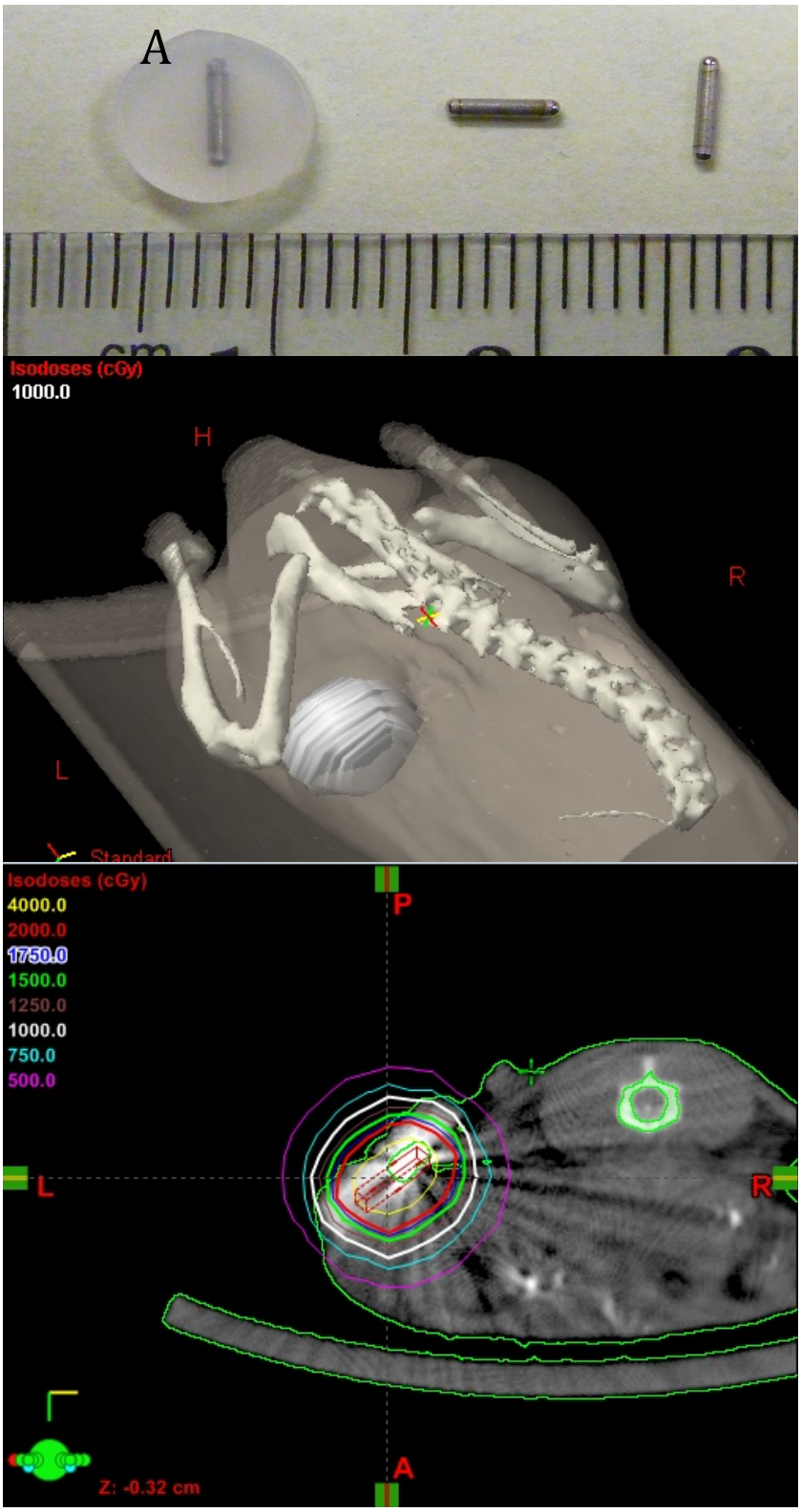

Figure 57. Development of brachytherapy. A. Iodine-125 seeds, used in prostatic brachytherapy are 0.8mm in diameter and 4mm long. They were secured in silastic discs to aid handling and subcutaneous placement. B. Silastic plaques bearing dummy pellets were implanted into a C57Bl/6 mouse bearing a 7-day established B16-Ova tumour. The following day the mouse was anaesthetised and scanned in a microCT. These data were then transmitted to the radiotherapy physics department and planning software used to estimate the dose distribution. B. The 10 Gy isodose is portrayed as a rendered sphere. C. Isodose curves are shown in a transverse slice. The key indicates doses delivered over 96 hours in cGy (1 Gy = 100 cGy)

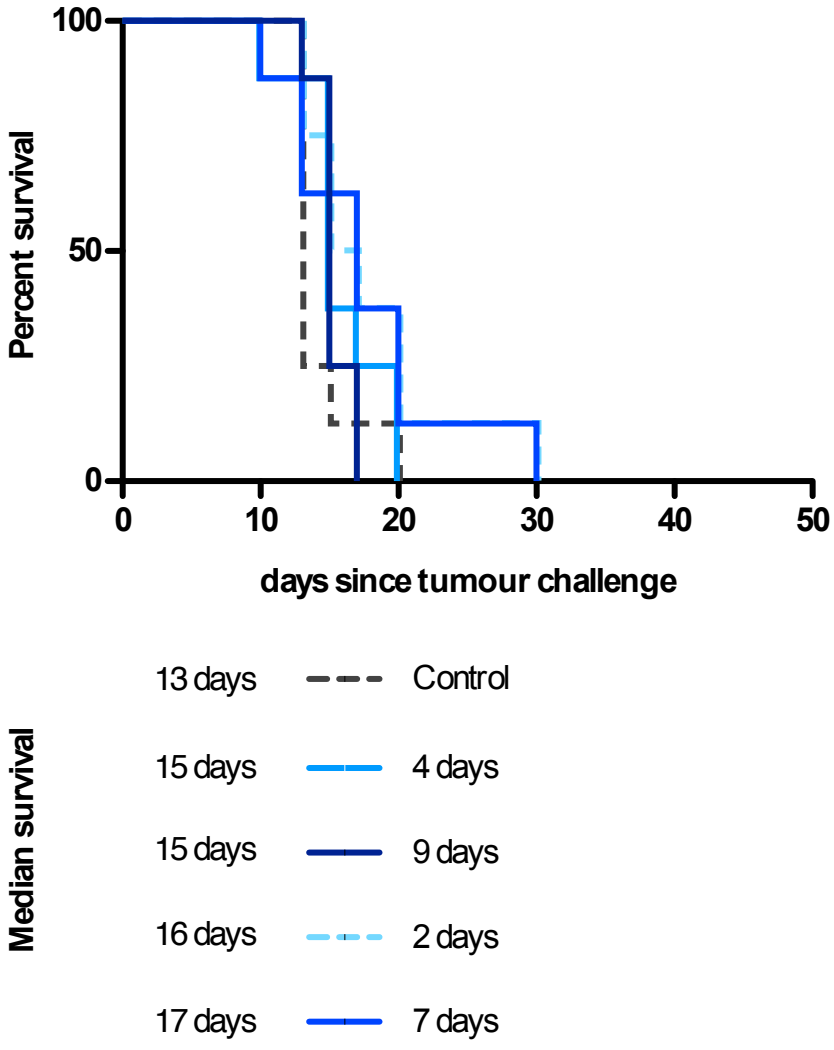

Figure 58. The effect of brachytherapy on B16-Ova tumours. C57Bl/6 mice bearing 7 day established B16-Ova were anaesthetised and either dummy or active ^{125}I plaques inserted over the tumour. After intervals of 2, 4, 7 or 9 days the plaques were removed. Mice were euthanized when tumours reached 1 cm in any direction. The survival of each group is plotted. The median survival for each group is indicated below (n=8)

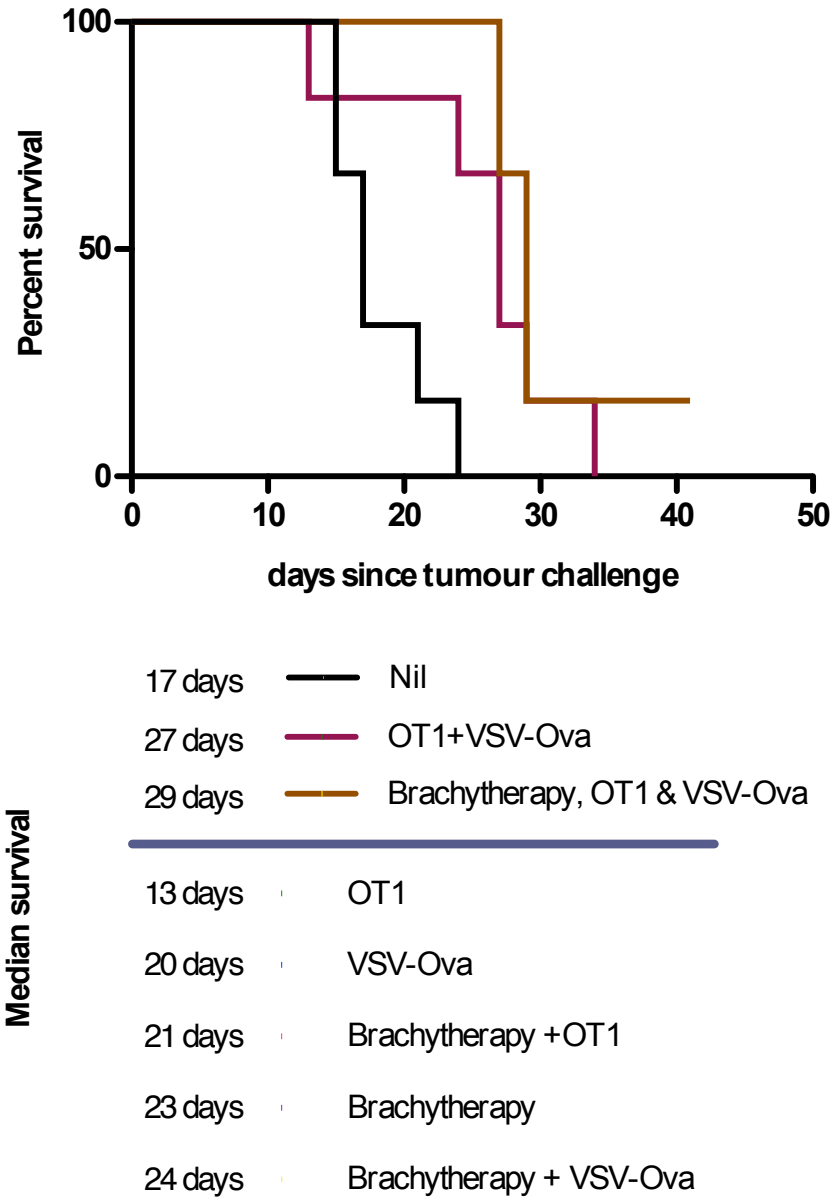

Figure 59 Brachytherapy in combination with virotherapy and adoptive cell therapy. C57Bl/6 mice bearing 6 day established B16-Ova were anaesthetised and either dummy or active ^{125}I plaques inserted over the tumour. After 48 hours the plaques were removed. Naïve OT1 T-cells and intravenous VSV-Ova were administered on days 9 and 10 respectively. Mice were euthanized when tumours reached 1 cm in any direction. The survival of key groups is plotted; others were excluded for clarity. The median survival for each group is indicated below (n=8).

5.3 Discussion

Radiotherapy is an effective treatment for many cancers, and has effects beyond simply inducing apoptosis or mitotic catastrophe in radiosensitive tumour cells and the immune effects of RT are being explored by several groups(Bernstein and Hodge, 2012). In the experiments presented above combinations of adoptive cell therapy and antigen-expressing virus were not significantly enhanced by palliative-dose external beam RT, or by brachytherapy. This is in contrast to the previous reports of successful synergies between RT & Flt-3 ligand (which causes expansion of DC numbers in vivo) and RT plus CTLA-4 blockade (which unshackles T-cell responses), albeit in different models and using a range of doses (Chakravarty et al., 1999, 2006; Demaria et al., 2004, 2005). Reits et al. demonstrated that tumours irradiated in vivo were more susceptible to killing by CTL and that the combination of CTL and RT (10 Gy as a single fraction) controlled tumours and cured mice(Reits et al., 2006). However, the CTL used in that publication were taken from a cell line maintained in vitro culture, and were activated in vitro prior to use. There are studies that have reported immunological effects of RT that would be deleterious to immunotherapy, rather than beneficial; Merrick et al. found that irradiating DC in vitro diminished their ability to prime T-cell responses, though others have reported contrasting results(Liao et al., 2004; Merrick et al., 2005; Huang et al., 2011b). Moreover the effects of local RT will be predominantly upon tumour cells and surrounding stroma. As most effector cells or APC would be expected to reside outside the field of palliative RT, so the direct effect of RT upon them is less relevant in the context of single fraction treatments; these effects will of course become important when conventionally fractionated treatments, which can last several weeks, are considered. Overall the published literature suggests that RT could be used to enhance immunotherapies, though of course the effect of any publication bias involved cannot be quantified.

The lack of synergy documented above contrasts with other reports that have identified beneficial effects of RT, generally with higher doses of RT. This suggests that strategies in melanoma, clinical or pre-clinical, to take advantage of the reported immune effects of RT may best explore higher dose and higher dose-rate forms of RT. For example it would be reasonably straightforward to

design a study in which patients due to receive palliative RT for a metastatic lesion, to a dose of 8Gy, also received a cancer vaccine or immunomodulatory treatment. However, based on the data above, it may be more prudent to investigate combinations with higher doses of RT, despite the challenges to recruitment and implementation that would be entailed.

Although the data presented above suggest no synergy between RT and immunotherapies targeting the synthetic ovalbumin antigen (OT1 + VSV-Ova), there was evidence (Figure 54 - Figure 56) of effective combination of RT and gp100-immunotherapy (Pmel + VSV-gp100). The two models are very different, and one role of RT in the latter may be to increase expression of gp100 on tumour cells, however this hypothesis could not be addressed in the time available. Further work is needed to confirm and explain the intriguing disparity between the two immunotherapy dyads.

The emergence of ipilimumab as the first effective therapy for melanoma coincides with growing use of stereotactic body radiotherapy (SBRT) for oligometastatic disease. The Mayo clinic's experience of SBRT for melanoma patients has been one of almost universal local control (Dr Sean Park, personal communication 2012). Hypothesising that the hypofractionated doses involved in SBRT would result in the release of TAA and danger signals, a protocol was developed (by the author, along with Dr Sean Park, Dr Kenneth Olivier and Dr Svetomir Markovic) in which patients undergoing SBRT for oligometastatic melanoma will have blood collected before, during and after treatment. The blood will be used for pentamer-based and functional assays, as well as ELISA of cytokine and chemokine levels, in order to monitor inflammatory and melanoma-antigen specific responses as a consequence of treatment with SBRT. The protocol was approved by the institutional review board and is currently open to accrual. Others are already testing the combination of SBRT and ipilimumab, on the logical hypothesis that SBRT may direct immune responses against melanoma that will be enhanced by the blockade of CTLA-4 (Clinical trials.gov and personal communication Dr Voichita Bar-Ad 2012).

Advances in radiotherapy have taken a relatively unusual path when compared to many other clinical treatments. Technological advancements (IMRT, IGRT, Stereotactic RT, ARC-therapy etc.) have been predominantly tested and

developed in the clinical and '*in silico*' settings, with relatively little animal testing undertaken(Bentzen, 2008; Verhaegen et al., 2011). In terms of modelling dose distribution within tumours or normal tissue, small animals are clearly of little value to radiation oncologists and medical physicists; the C57Bl/6 mice used within this chapter had an anterior-posterior thoracic dimension of under 1.5 cm, whereas the depth of maximum dose from a 6 MV photon beam is around 2 cm. If high dose and hypofractionated radiotherapy approaches are to be accurately modelled in mice, and in particular the immunological consequences thereof, then newer technology will be needed than the erstwhile clinical-grade equipment used in the bulk of this chapter. A small range of precision platforms is now commercially available which will allow strategies combining immunotherapies and modern RT, including the ability to deliver image-guided hypofractionated RT to mice, to be tested and refined pre-clinically, in parallel with ongoing clinical developments (Song et al., 2010; Verhaegen et al., 2011).

6 Developing a model of intracranial melanoma

6.1 Introduction

Melanoma metastasises to the brain more commonly than most cancers and augurs a grim prognosis when it does so. Autopsy studies suggest brain metastases may occur in up to 75% of patients with advanced disease, though they are diagnosed in far fewer (Fisher and Larkin, 2012). In those diagnosed pre-mortem there is often significant morbidity associated with intracranial disease, and with the subsequent treatments. Melanoma brain metastases are felt to be at high risk of haemorrhage, and catastrophic intracerebral bleeds may well be the terminal event in a significant proportion of patients.

The emergence of stereotactic radiotherapy techniques, and particularly stereotactic radiosurgery, have considerably changed the management of brain metastases, appearing to offer good local control for patients with oligometastatic disease (Linskey et al., 2010).

Commonly brain metastases, whether symptomatic or detected by trial-mandated screening, are an exclusion criterion in studies of systemic therapy. However there are reports suggesting Ipilimumab and adoptive cell therapies may have some efficacy within the brain (Hong et al., 2010; Margolin et al., 2012).

Any novel therapy for melanoma will ideally be effective against brain metastases, and moreover will need to be able to access the lesions. Furthermore many cell types of the CNS share a neural crest origin with melanocytes and melanomas, and may share antigens (Bridle et al., 2010). Successful immunotherapy for melanoma has been reported to result in vitiligo and dermatitis; therefore a model of melanoma in the brain will also allow for study of the risk of more significant neurological autoimmune toxicities.

6.1.1 The Blood-brain barrier (BBB)

The brain was first recognised to have some separation from the rest of the circulation following the work of Paul Ehrlich. When he injected a range of aniline dyes into the blood stream the brain alone remained unstained. Conversely dyes injected into the cerebrospinal fluid (CSF), by Ehrlich's student

Edwin Goldmann, stained the brain but didn't appear to have access to the other organs. In contrast to other vascular structures the capillaries of the brain are connected by particularly tight junctions, and reside on thick basement membranes, beyond which the Virchow-Robin space and foot processes of the glia limitans provide further impediments to cellular and humoral access (Wilson et al., 2010). Although disruption of the BBB is often asserted in the presence of tumours (and occasionally described as the blood-tumour barrier, BTB) there is evidence that it may remain intact and able to impede therapeutic access, particularly in the case of microscopic disease. The widespread use of trastuzumab for breast cancers that overexpress human epidermal growth factor receptor 2, has revealed the limited ability of trastuzumab to cross the BBB, as successful control of visceral disease has unmasked unfettered intracranial disease (Stemmler and Heinemann, 2008). Preclinical models suggest that monoclonal antibodies are unable to cross the intact BBB, although active immunotherapeutic approaches may be more effective (Sampson et al., 2000; Cranmer et al., 2005).

Bechmann et al argue eloquently in their review that in its strictest sense the BBB refers to the barrier to solute diffusion from capillaries within the brain, and should therefore not be used to refer to impediments of lymphocyte trafficking (Bechmann et al., 2007). They also highlight the importance of the perivascular or Virchow-Robin space (lying between the two basement membranes of the glia limitans and the vascular smooth muscle) (VRS) as a means of lymphatic drainage for the brain parenchyma and a repository of macrophages. Notably VRS do not occur about capillaries but are found instead at the pre and post capillary vessels, and are the site of leukocyte passage when it occurs. Rather than crossing the solute BBB, immune cells instead access the brain parenchyma by traversing venule walls to enter the VRS, and from there cross the barrier afforded by the glia limitans.

For the sake of simplicity for the remainder of this thesis BBB will be used to describe the collective impediments faced by the immune system in accessing targets, rather than delineating the specific solute barrier, in keeping with the approach adopted by other authors (Savarin et al., 2010).

The immune privilege of the brain, though mediated in large part by the physical barriers described above, has parallels with that of established tumours. Cells within the brain express low levels of MHC I and II, and antigen presenting cells are scarce. The foot processes of astrocytes bordering the VRS constitutively express the death ligand CD95L to deter cells that have reached the VRS from proceeding into the parenchyma (Wilson et al., 2010).

What is clear is that despite such immunosuppressive attributes the brain remains capable of recruiting immune responses when necessary. In mouse models of CNS infections CD8+ T-cells access the brain parenchyma under the direction of chemokines and cytokines produced by infected cells, and the resulting upregulation of adhesion molecules on CNS vascular epithelial cells (Wilson et al., 2010).

Preclinical models that are able to mimic the challenges to successful therapy of brain metastases have been developed in a number of cancers. This chapter describes the development and early application of a model melanoma that would allow investigation of a range of melanoma treatments otherwise being explored by the group (Diaz et al., 2007; Kottke et al., 2011a, 2011b; Rommelfanger et al., 2012).

6.1.2 Existing models of intracranial disease

The conventionally used melanoma cell lines do not spontaneously metastasise when injected subcutaneously but several methods exist to model intracranial disease, each with their own advantages and limitations (Cranmer et al., 2005).

- Intracardiac administration (ICD)

  Direct injection of tumour cells into the left ventricle bypasses the pulmonary circulation, with a reasonable proportion of the inoculum reaching the carotid circulation. It is a relatively easy technique, as most veterinary technicians can readily adapt their existing technique of cannulating the heart for terminal bleeds. However sufficient tumour cells will evade the carotid arteries that other, non-cranial, metastases will form, and cardiac deposits are common.

- Intracarotid artery administration (ICA)

By performing a unilateral neck dissection the internal carotid artery can be visualised and cannulated. The vessel must be ligated after the procedure, and subsequent brain perfusion relies on the patency of the circle of Willis. The procedure reduces, significantly but incompletely, the frequency of extra-cranial tumour growth but is an extremely challenging procedure; the mouse common carotid is generally less than half a millimetre in external diameter and fine microsurgical skills are required. Moreover the procedure is time consuming and only a limited number of mice can be prepared per day ((Lorger and Felding-Habermann, 2010) and personal communication Dr M. Lorger 2012).

- Intracranial injection (i.c.)

Direct inoculation of tumour cells into the brain is relatively straightforward. The mouse skull can readily be penetrated, freehand with conventional hypodermic needles but considerable variation in the position of inoculation can ensue ((Cranmer et al., 2005) and personal communication Mrs J. Thompson 2011). The use of a stereotactic frame improves inter-procedural consistency and others have described their experience with the method in detail (Carlson et al., 2011).

- Subcutaneous tumour metastasis

The immediate criticism of each of the methods outlined above is that they do not mimic metastatic evolution that occurs in nature. Accordingly others have passaged melanoma lines in mice by serial i.c. administration followed by brief in vitro culture to select neurotropic cells (Cranmer et al., 2005). These cells, apparently capable of developing brain metastases following subcutaneous injection, are not available from the conventional tissue culture repositories.

After consideration of each of the available options, and discussion with colleagues with some familiarity with the issues, it was decided that direct intracranial injection was the most appropriate method to develop, specifically adapting the method reported by Dr J. Sarkaria's group at the Mayo clinic (Carlson et al., 2011). In particular it was important to be able to use the cell lines on which previous data were obtained and for which the lab's existing reagents and methods would be most applicable.

In order to estimate the appropriate group size for planned experiments a power calculation was performed by the Mayo clinic biostatistical team. Previous reports indicate a median survival of untreated tumour-bearing mice of 14.6 days, with a standard deviation of 2.5 (Thomas et al., 2011). Therefore based on a two sample binomial test of proportions a group size of 6 is required to have a 90% chance of detecting that the proportion of mice alive at day 14 is at least 13% higher in the experimental arm than the control arm; i.e. this equates to a median survival of 21 days in the treated group, a hazard ratio of 1.5. However the above cited study reported heterogeneous group sizes suggesting the standard deviation of uncensored groups may exceed 2.5; accordingly, and concordant with the experience of existing therapeutic strategies, a group size of 8 is required to reliably detect clinically meaningful differences between therapy groups. This group size affirms the need to use, in initial experiments at least, the i.c. method of establishing tumours.

6.1.3 Adaptation of a previously described method

The procedure developed was adapted from the experience of colleagues who have considerable experience of i.c. administrations of human xenograft tissues in nude mice - relevant details are described below (Carlson et al., 2011). Mice were anaesthetised with intraperitoneal ketamine and xylazine in order to minimise movement caused by intercostal movements. Once the efficacy of analgesisa was confirmed an incision was made craniocaudally over the midline of the dorsal aspect of the skull. A burr hole was then made at the right bregma. The mouse was positioned on a stereotactic frame and a Hamilton syringe with mounted needle driven 2-3 mm into the brain parenchyma (Figure 60). Tumour

inoculum was administered 1 μL per minute to a maximum volume of 3 μL. After a further minute the needle was withdrawn and the incision sutured closed.

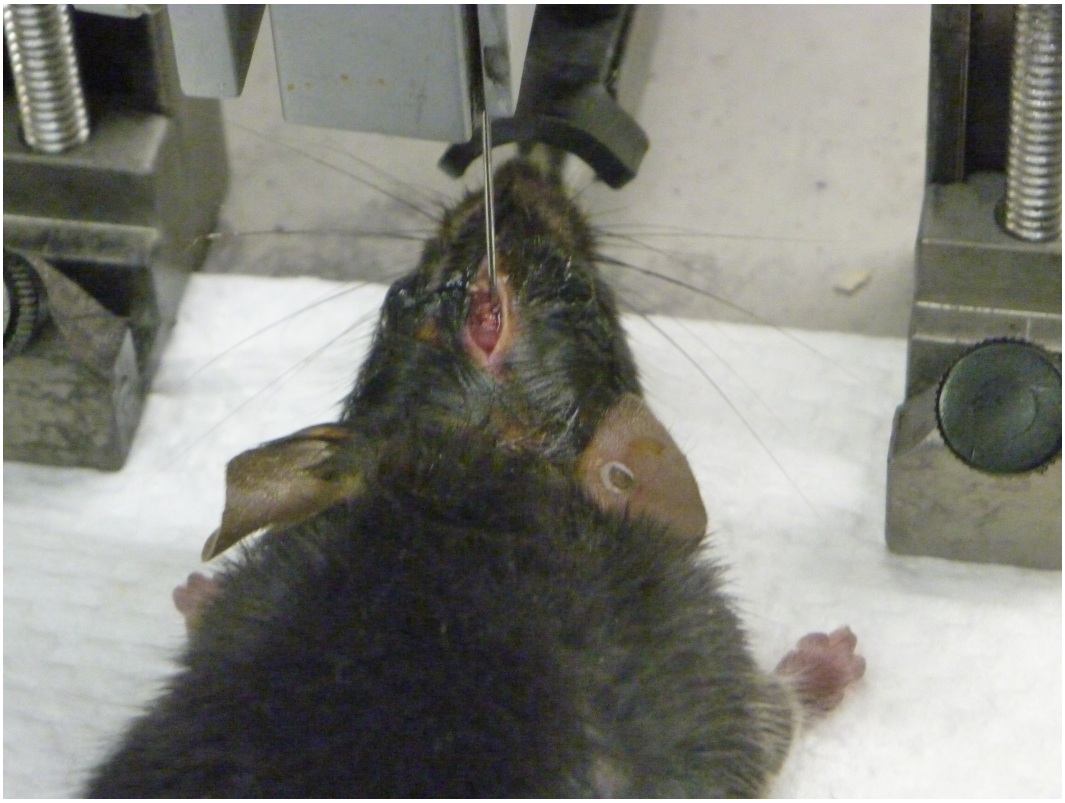

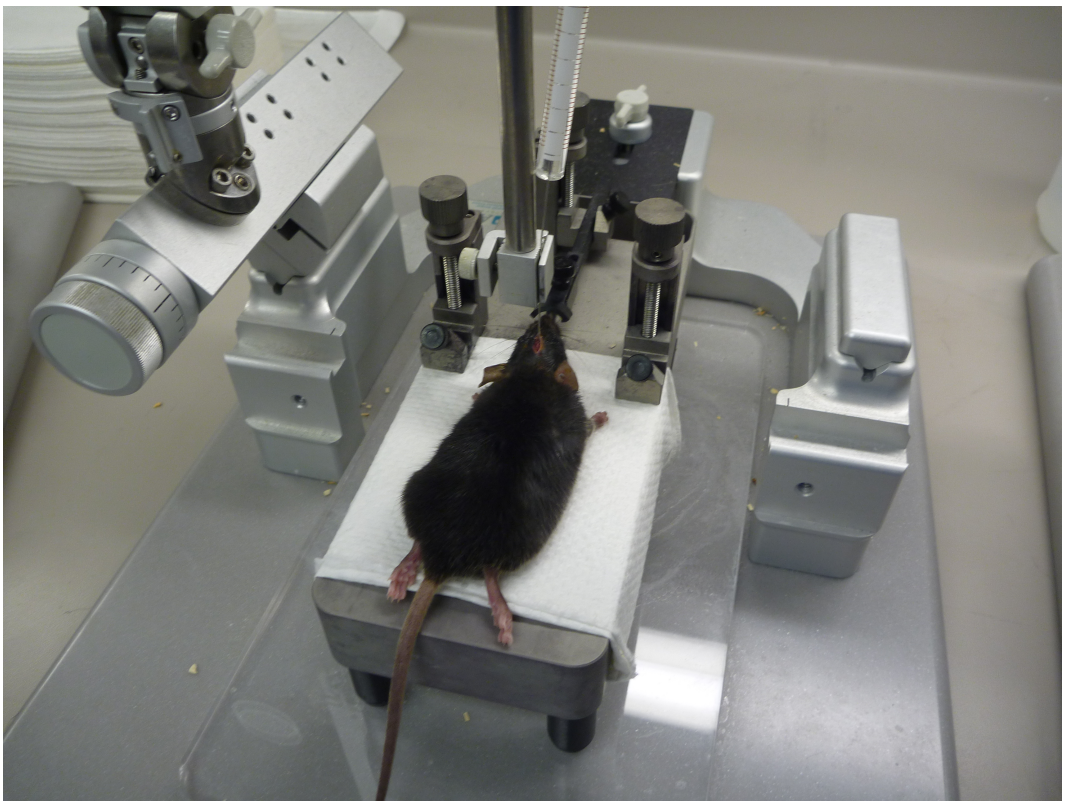

Figure 60. Stereotactic injection of tumour cells. Mice were anaesthetised with intraperitoneal ketamine and xylazine. The skull was exposed and a burr hole made over the lateral bregma. A stereotactic frame was used to inject tumour inoculum 2-3 mm below the dura into the right cerebral hemisphere. Injections were performed at 1uL per minute and the needle left in place for 2 minutes after the injection. The scalp incision was sutured closed and mice were observed in a warmed environment until fully recovered from the procedure and effects of the anaesthesia.

6.2 Results

6.2.1 Characteristics of the model

The method of intracranial administration described above has been used to implant human glioma primary cells into nude mice; Carlson et al. routinely administer 10^5 cells (Carlson et al., 2011). The doubling times of human primary cells derived from glioma, compared to the murine melanoma line B16, are very different; therefore in order to select a suitable dose for further experiments, an initial experiment was performed in order to titrate the appropriate number of tumour cells required for i.c. installation, such that tumours would develop in a reliable fashion.

Mice were injected with doses of B16-Ova between 5000 and 500,000 cells, and euthanized upon development of any concerning signs of neurological embarrassment. Figure 61A indicates survival following i.c. injection. Notably no mice died during the procedure or anaesthesia, nor in the 10 days thereafter. Amongst the groups given higher doses of tumour, extracranial growth of tumour was apparent in several mice, though survival was not significantly different between mice with or without extracranial growth, and neurological signs were still used as the indication to euthanize in all mice. At the lowest cell dose used, 3 mice did not develop neurological symptoms and were euthanized 40 days after i.c. injection. Following euthanasia the brains of those three mice were examined and no macroscopic tumour deposits could be identified. Accordingly 10^4 cells were administered in all subsequent experiments. In Figure 61B the untreated groups from subsequent experiments were compared, demonstrating the consistency of tumour growth between experiments. The median survival of untreated mice was 17 days after inoculation and all mice developed tumours.

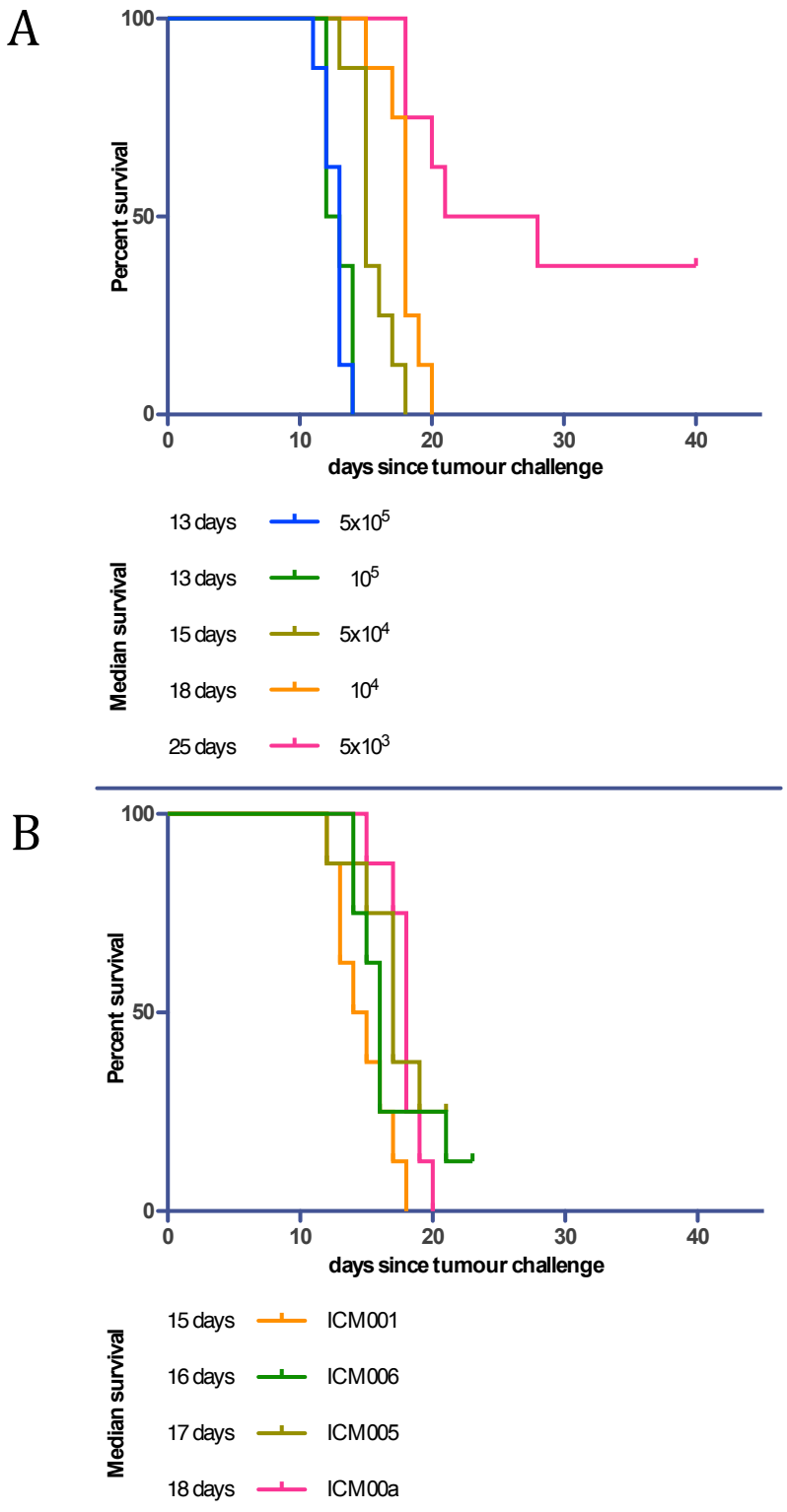

Figure 61. Characteristics of the intracranial melanoma model. A: Eight mice per group were injected with doses of B16-Ova from $5x10^3$ to $5x10^5$ and monitored for signs of neurological impairment. B: Having selected 10^4 as the optimal dose for subsequent experiments, untreated control groups from four separate experiments were compared, revealing broadly similar outcomes, and a pooled median survival of 17 days (total 32 mice).

6.2.2 Tolerability

Given the nature of the procedure, periprocedural deaths were anticipated, but thankfully little seen. Since implementation 519 mice have undergone i.c. injections and only 5 deaths have occurred within 7 days of the procedure. The cocktail of ketamine and xylazine causes prolonged anaesthesia, with recovery times of 1-2 hours; all 5 mice appeared to die as a result of the sedation, rather than the procedure. By the day after i.c. procedures mice behave normally, feeding and drinking without impediment and with no detectable behavioural changes.

6.2.3 Monitoring tumour burden

In conventional mouse models tumours are established subcutaneously, often in the flank. This makes the tumours easily palpable and easily measureable. Providing the cell line used grows consistently it is therefore possible to monitor tumour growth and euthanize the mice before the tumour is large enough to cause symptoms or suffering. Clearly this is not possible for intracranial disease. Given the thin skull of mice ultrasound may be able to penetrate sufficiently to allow crude tumour measurements, which would in turn allow for anticipatory rather than reactive euthanasia. Mice were therefore taken for high-frequency ultrasound, 8 days after i.c. inoculation of 10^4 B16-Ova into the right cerebellum. As illustrated in Figure 62 tumours were readily apparent adjacent to the falx cerebri. Although the procedure takes only a couple of minutes to obtain the images shown, the mice need to be anaesthetised in order to secure them for images of adequate quality, therefore the technique is not practical as a day-to-day method for monitoring tumour burden.

In the absence of a practical measure of tumour burden mice were instead monitored daily for evidence of neurological impairment or behavioural changes. Lateralising signs did not develop, even in mice with large tumours within the brain. Instead hunching, reduced mobility and signs of self-neglect were taken as indicators of tumour burden and used to indicate when to euthanize the mouse. Mice were inspected 7 days a week to ensure that tumours were not allowed to progress to the point that they caused distress to the animals.

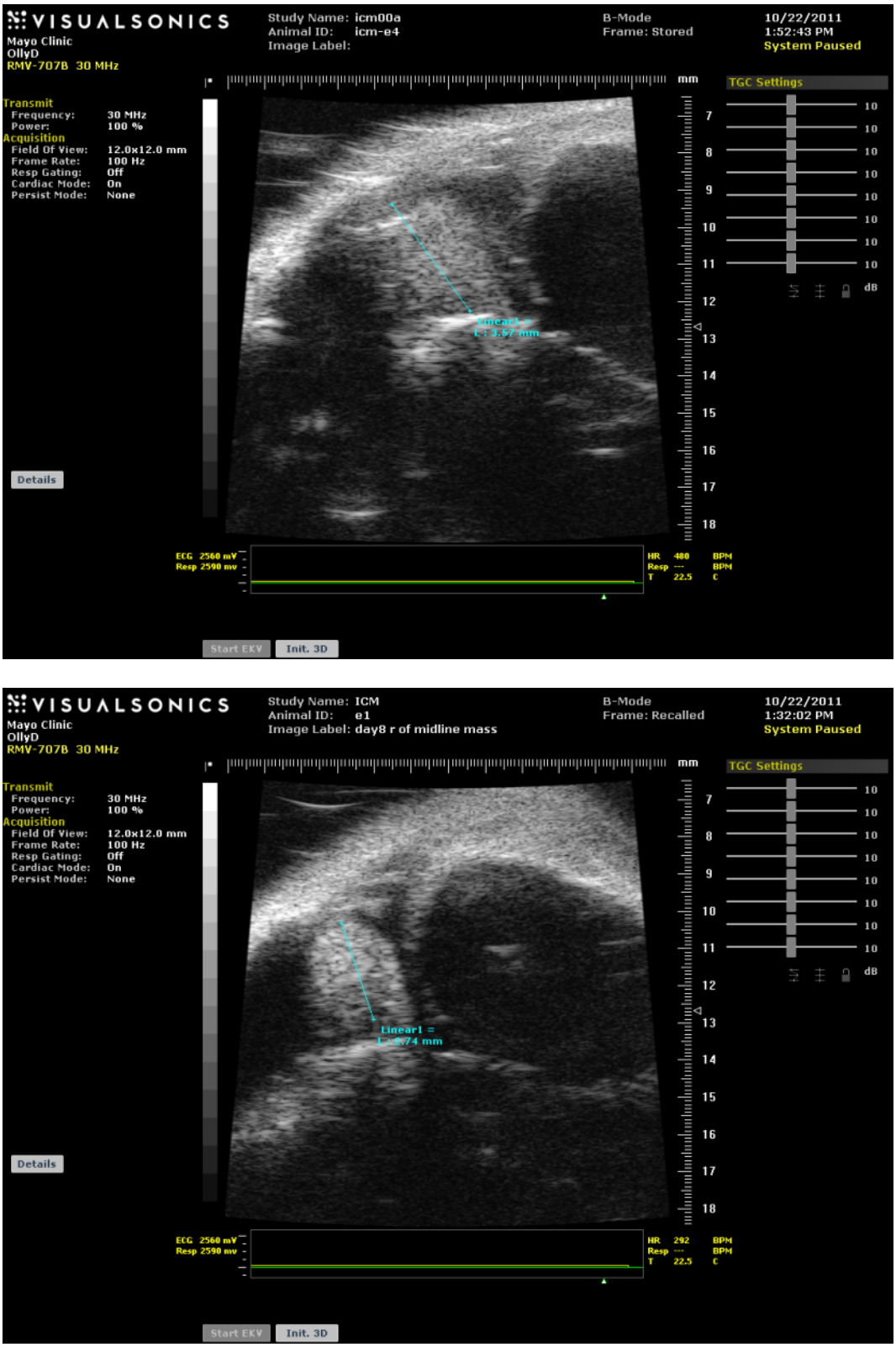

Figure 62. High frequency ultrasound of intracranially injected B16 melanoma. Ultrasound appearances of B16-Ova tumours established by intracranial injection. Mice were injected with 10^4 B16-Ova tumour cells (from experiment indicated in Figure 61) into the right cerebral hemisphere and after eight days imaged by high frequency ultrasound. Two mice were imaged as a preliminary test of the imaging modality and reprepesentative screen captures taken in the central axes of the tumours, from each mouse are presented. The blue bars indicate the size of the tumours, 3.57 mm and 2.74 mm respectively.

6.2.4 Immunohistochemistry

Further to characterise the tumours established by i.c. injection, brains were extracted from all mice at the time of euthanasia and immersed overnight in formalin to aid subsequent handling. In addition to macroscopic visual examination, tumours from two mice per group were selected at random and conveyed, intact and in formalin, to the Mayo research histology department in Scottsdale Arizona. These representative brains were prepared by the histopathology service and after H&E staining analysed by a clinical histopathologist (Dr Ronald Marler, DVM, PhD).

Tumours were visible macroscopically as black melanoma deposits within the substance of the brain parenchyma. Some tumours extended along the track of the inoculation needle and grew exophytically, occasionally extending through the burr hole and becoming subcutaneous masses. In subsequent inoculations, using an optimised tumour dose these phenomena abated, and instead tumours became established either as discreet lesions in the right cerebrum or adopted a more diffuse pattern, often developing along the surface of the cerebellum. The site of inoculation lies immediately above the right ventricle of the brain; therefore tumours are likely to have extended into, or have been directly inoculated in, the cerebrospinal fluid and then tracked bilaterally to areas around the brain. Initial histopathological assessment after H&E staining confirmed that the macroscopic deposits were melanoma lesions, generally behaving as space-occupying, rather than infiltrative lesions.

6.2.5 Magnetic resonance imaging

Magnetic resonance imaging (MRI) has been reported to be a useful imaging modality to assess intracranial tumours (Prabhu et al., 2000). In addition to providing high resolution anatomical data, the growing repertoire of MRI scan sequences can be used to obtain additional data about the effects of treatment on parameters such as the permeability of the blood brain barrier (Cao et al., 2005; Harry et al., 2010 and personal communication Dr A. Johnson 2011). Clinical trials have identified that, in contrast to many conventional cancer therapies, the efficacy of immunotherapies may not be best assessed by size criteria such as the widely used RECIST system. Accordingly the use of MRI was piloted alongside

the development of the intracranial model as an imaging method that might provide further useful data.

Mice were anaesthetised by inhalational isofluorane and mounted on a custom NMR (nuclear magnetic resonance) probe with a coil overlying the skull. After calibrating the NMR and coil, images were obtained using preprogramed T1 and T2 sequences. Scans were enhanced by injecting mice with intraperitoneal gadolinium contrast 15 minutes prior to T2-sequences were performed. Representative images are shown in Figure 63, illustrating both the extent of tumour burden that develops following intracranial injections, and the resolution and detail obtained using the protocol. The technique was relayed to other investigators within the lab and will be used for further assessments of tumour burden and response to therapy by size criteria in future.

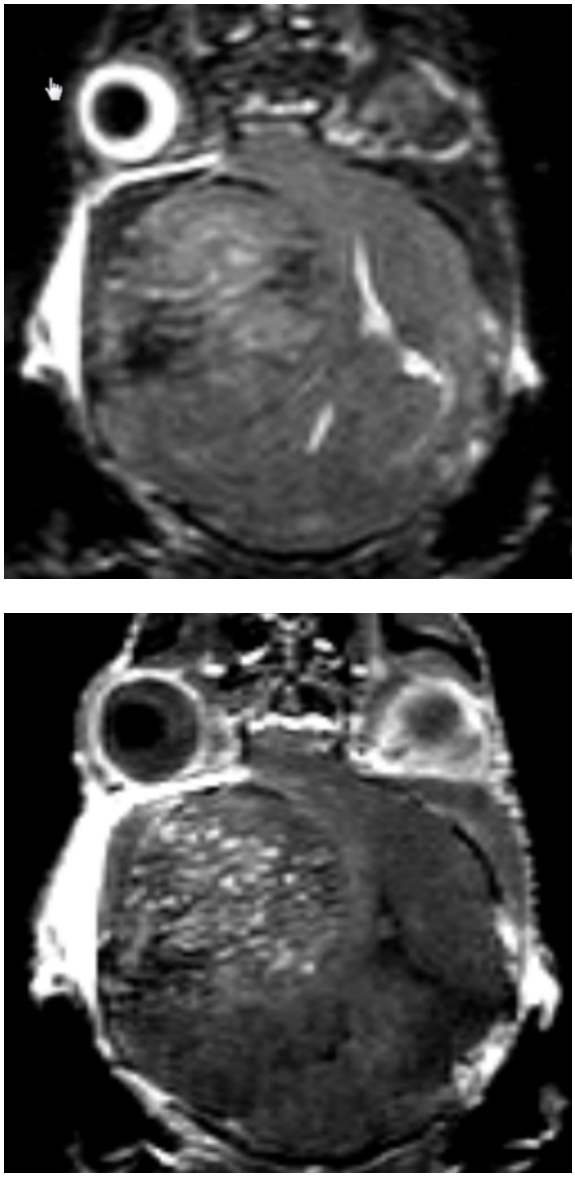

Figure 63. MRI images following intracranial injection of B16-Ova. Mice were anaesthetised prior to obtaining transverse T1 and gadolinium-enhanced T2 images by MRI. The images shown are from one mouse, to allow direct comparison between of T1 and T2 weighting, 15 days after administration of $5x10^4$ tumour cells (from experiment indicated in Figure 61). This mouse developed neurological impairment necessitating euthanasia for tumour burden, later on the day that these images were obtained.

6.2.6 Therapy studies

The purpose of establishing this intracranial model was to allow testing of immunotherapeutic strategies in the context of intracranial disease, and in particular to assess and address the impact of the blood-brain and blood-tumour barriers. Most immunotherapies tested in mice use subcutaneous disease models, though there are reports of immunotherapy in brain tumour models. Bridle et al. described an effective vaccination strategy using an adenovirus expressing a TAA, that protected against tumour challenge with B16-F10 melanoma (Bridle et al., 2010). Thomas et al. have reported therapy of established melanoma tumours implanted within the brain, using combinations of oncolytic virus (myxoma) and adoptively transferred transgenic T-cells, in mice lacking endogenous lymphocytes (Thomas et al., 2011). In that study OV was administered intratumourally, no trivial undertaking for brain tumours.
In the following studies fully systemic therapy was investigated, specifically therapy with combinations of systemically administered antigen-expressing oncolytic VSV (VSV-Ova) and adoptively transferred antigen specific transgenic T-cells (OT1), in the intracranial melanoma model against 7-day-old established tumours.
Initially mice were injected intracranially with 10^4 B16-Ova tumour cells, and 6 days later were treated with naïve OT1 T-cells (or PBS vehicle as a control) and the following day VSV-Ova (or PBS vehicle as a control), all intravenously. The resulting four groups were followed and their survival free from neurological symptoms is shown in Figure 64A. As shown there was no improvement in survival mediated by the addition of naïve OT1 T-cells, but virotherapy enhanced median survival from 14.5 days (control mice, or OT1 alone) by between 8 and 11 days. To further examine the effect of virotherapy a further experiment was established with three independent groups treated with VSV-Ova, including one group in which repeated VSV-Ova treatment was administered (Figure 64B). Notably within this experiment the use of a VSV expressing GFP, rather than tumour-associated antigen, did not generate any apparent therapeutic benefit. Furthermore three consecutive daily doses of VSV-Ova did not appear to be more or less efficacious than a single dose of the virus. Combining the data from these two independent experiments, and five separate groups treated with VSV-Ova

the virus appears to result in a significant improvement of survival from 15.5 days amongst PBS-treated animals to 26 days in mice receiving one or more doses of VSV-Ova (Figure 64C, Log-rank test p=0.0002). Although these are early data only, they do serve to demonstrate that the model is now well established; further work to explore the mechanism of therapy seen is underway along with other therapeutic strategies, but these were beyond the scope of this thesis.

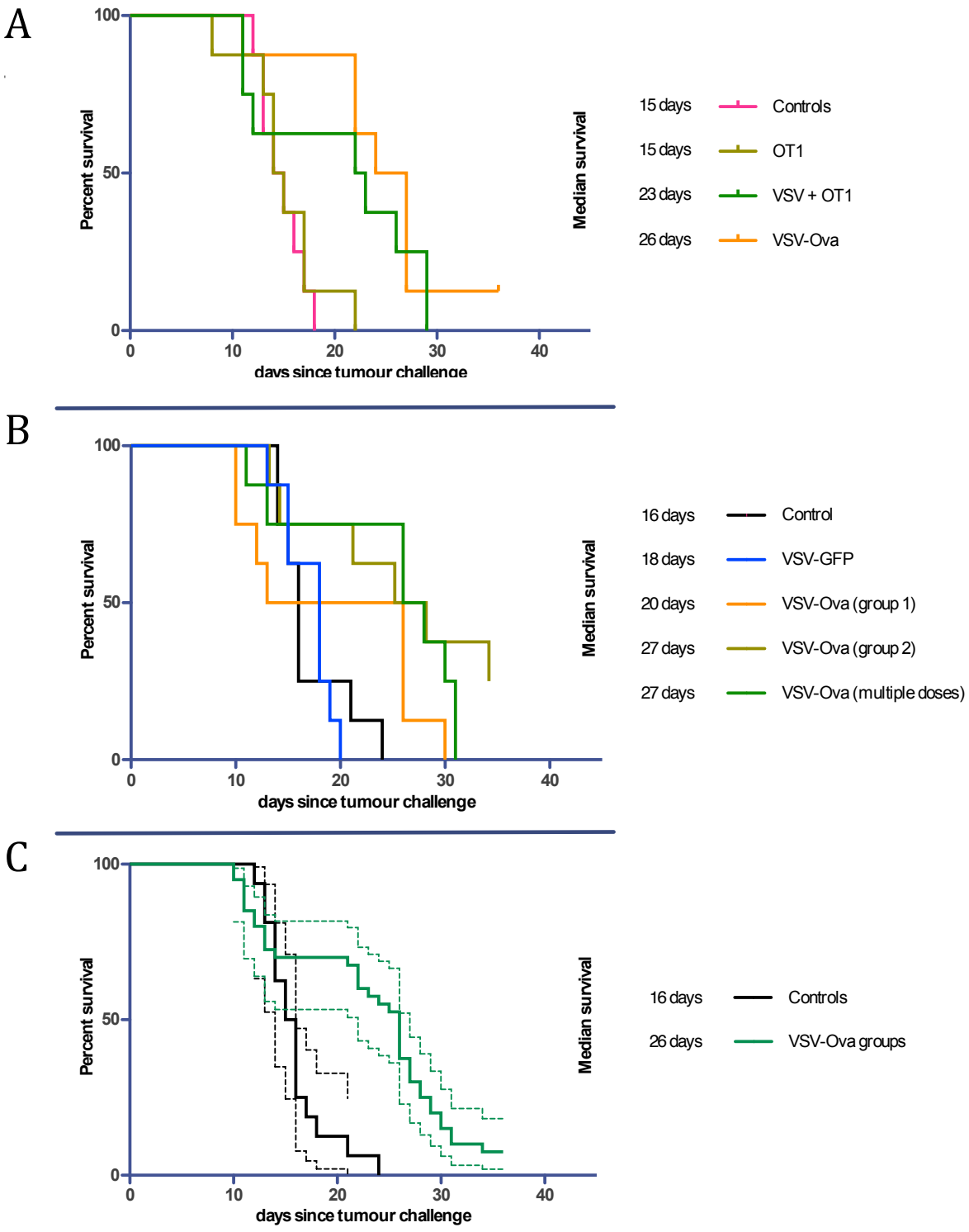

Figure 64 Pilot studies of therapeutic strategies in the intracranial model of metastatic melanoma. In all experiments mice were treated with 10^4 intracranial B16-Ova cells and started virotherapy 7 days later. A. Mice were treated intravenously with VSV-Ova, naive OT-1 T-cells, or both. B. Mice were treated with intravenous VSV. At the time of the experiment there was a transition from one batch of prepared virus to another, and so Groups 1 and 2 were compared within this one experiment to test the consistency of the therapeutic agent. Group 1 were treated with the batch of VSV-Ova used in A, group 2 received virus that was used in subsequent experiments. The effect of repeated dosing was explored by administering three daily doses of virus (group 2 batch) to one group of mice. VSV expressing GFP, but no tumour antigen, was used to explore the role of antigen, with the GFP insert serving to act as control for the effect of genetic modification on the virus. C. Data from A and B were combined to examine the to compare the efficacy of VSV-Ova with untreated groups. Dotted lines indicate the 95% confidence interval for each group. Median survival in control groups was 16 days, and 26 days amongst groups treated with VSV-Ova. Log-rank test of the two curves identified a statistically significant difference in survival (p=0.0002).

6.3 Discussion

A reliable and reproducible model of intracranial melanoma was established in the laboratory in order to test existing and novel immunotherapeutic strategies. In preliminary therapy studies intravenous therapy using an antigen-expressing oncolytic virus prolonged survival (Figure 64). This is in marked contrast to the subcutaneous models of melanoma used in the preceding chapter in which intravenous virotherapy alone confers little if any benefit. One facet of the intracranial model, which will be the subject of further study, is the smaller number of tumour cells used (10^4 c.f. 5 x 10^5); it is possible that this model will allow sensitive examination of the utility of virotherapies and immunotherapies in the context of small volume disease, which is a clinical scenario that many in the field believe would most benefit from such therapies.

An important criticism of the technique as described is that the assessment of survival is somewhat subjective. The degree of neurological impairment was considerable and it is appropriate to try to reduce or prevent any suffering in experimental animals by pre-emptive euthanasia. However it will be important in subsequent experiments that brains are harvested in order to provide objective evidence of the disease burden. Parallel experiments with predetermined timepoints for euthanasia should be performed to provide further objective demonstration of the effect of treatment. An appealing strategy would be to mimic many of the standard practices of clinical trials – namely randomisation and blinding, such that the practitioner assessing neurological burden is unaware of the treatment each animal has received.

Patients with metastatic melanoma commonly have disease, whether identified or sub-clinical, within the brain and therefore successful therapies, immunotherapies included, must have efficacy within the brain and be able to overcome the blood-brain barrier. Although there is some evidence of efficacy of ACT and CTLA-4 inhibition in the context of brain metastases, other therapies are impeded by the BBB. One of the ongoing aims associated with establishing this i.c. model is to investigate ancillary treatments that could augment existing strategies.

One function of the BBB is to preserve the immune privilege of the brain, serving to impede the access of leucocytes to the brain parenchyma by the range of

mechanisms discussed earlier, indeed disruption of the BBB is an important step in the development of autoimmune neurological diseases such as multiple sclerosis (Alvarez et al., 2011).

Radiotherapy has been shown to disrupt the BBB; Wilson et al. demonstrated that RT (delivered as a 20 Gy single fraction) leads to astrogliosis, increased permeability of the BBB and leukocyte adhesion in a TNFα dependent fashion (Wilson et al., 2009). Fractionated RT (40 Gy in 20 fractions) is also capable of enhancing BBB permeability but does so more slowly than high single fraction doses (Yuan et al., 2006). In patients undergoing radiotherapy (52-70 Gy in 1.8-3 Gy fractions, mostly 2 Gy per fraction) MRI based methods to estimate the permeability of the BBB suggested enhanced permeability during treatment, particularly in the blood-tumour barrier (Cao et al., 2005). These data suggest that immunotherapy approaches may be enhanced by the addition of radiotherapy, in order to enhance access to the tumour.

The hedgehog pathway, aberrant in a range of cancers and currently explored as a potential targeted therapy, is also involved in maintaining the integrity of the BBB (Robarge et al., 2009). Studies using cyclopamine, an inhibitor of SMO (Smoothened, a cell membrane protein upstream in the hedgehog pathway) and GDC-0449 (a clinical grade, orally available SMO inhibitor) found that the hedgehog pathway not only maintains the physical rectitude of the BBB but also mediates the levels of cytokine and chemokine expression (Alvarez et al., 2011). In a mouse model of MS, experimental autoimmune encephalomyelitis, inhibition of the hedgehog pathway by repeated dosing with GDC-0449 led to increased numbers of leukocytes, particularly of Th1 and Th17 phenotypes, accumulating within the CNS (Alvarez et al., 2011). Together the data suggest that the hedgehog pathway plays an important role in limiting immune access to the brain, and that its inhibition could enhance immunotherapy for brain tumours. Protocols testing the ability of GDC-0449, a hedgehog inhibitor being developed by Genentech (California USA), to augment adoptive cell therapies are underway using the intracerebral model. Dependent upon those results further studies may explore alternative methods of BBB disruption; mannitol, for example, is a widely available osmotic diuretic classically used to treat cerebral oedema and known to disrupt the function of the BBB (Brown et al., 2004). Accordingly it has

also been tested as a method of enhancing the penetration of chemotherapy into the brain (Doolittle et al., 2000).

In parallel with the pilot studies of B16 melanoma described above the technique has been used to establish an intracranial model of glioblastoma, using the murine glioma cell line (GL261). Glioblastoma remains a recalcitrant disease and further therapies are urgently required. Colleagues have injected GL261 transfected to express a luciferase reporter gene that allows monitoring of tumour development by live animal imaging (personal communication Dr R. Diaz 2012). A similar enhancement of B16-Ova would be a useful way to supplement the data obtained by MRI, not least as several mice can be imaged simultaneously using this technique.

As discussed earlier in this chapter several methods of modelling intracranial disease have been reported. Although direct intracranial injection, as used above, has advantages including the ease, reproducibility and scale of application, other models may better mimic some of the processes involved in metastasis in nature. Intracranial metastases established following ICA injection presumably have selected tumour cell clones that are capable of adherence and migration through vascular endothelium. Having identified successful therapeutic approaches in the intracranial model it may therefore be worthwhile testing the same therapies in smaller scale experiments using tumours established with an ICA approach for further validation. However, it must be recognised that both i.c. and ICA administrations have fundamental limitations in their ability to mimic the 'normal' metastatic process. Recent data has shown that one element of metastasis is the preparation of a premetastatic niche, mediated by bone marrow derived stromal cells, a process that presumably cannot be replicated by direct inoculation of a large number of tumour cells (Peinado et al., 2012).

Those caveats notwithstanding this model will allow refinement of existing and novel immunotherapeutic strategies, and where the BBB is found to impede efficacy allow testing of supportive treatments to overcome such impediments.

7 Summary and conclusions

Metastatic melanoma remains a considerable challenge, despite recently identified therapeutic successes. The enzyme inhibitor vemurafenib is only effective for the subset of patients whose tumours are found to express mutant forms of BRAF, and though the response rate is high, responses are not durable. Blockade of CTLA-4 with ipilimumab is profoundly toxic for a significant number of patients, and unfortunately only generates meaningful benefits for a minority of patients, however of that minority many seem to benefit from prolonged periods of disease control. Moreover the use of ipilimumab provides clear evidence that the immune system can be recruited to control metastatic disease. The aim of this thesis therefore, was to test additional therapies that may contribute to immune-based strategies.

Measles virus is an effective oncolytic agent against human melanoma in vitro, when tested against a panel of immortalised cell lines, against a three-dimensional model of melanoma and against low passage human melanoma cell primaries. MV-infected melanoma cells produced a range of cytokines, chemokines and danger signals that would be expected to generate an inflammatory milieu. Both MV and MV-infected melanoma cells matured antigen-presenting dendritic cells.MV also enhanced the innate anti-tumour functions of PBMC, principally through the activation of NK cells. MV-infected melanoma cells are processed by dendritic cells which can in turn stimulate an adaptive melanoma-specific cytotoxic CD8+ T-cell response.

Time constraints limited further exploration of MV, but future studies are planned. CD46 is upregulated in several tumours, presumably in an effort to evade the attentions of the complement system (Fishelson et al., 2003). Others have shown that CD46 is downregulated in response to infection with MV, though it was not explored in the confines of this thesis (Firsching et al., 1999). The in vitro work presented within the thesis has used sera that has been heat inactivated to neutralise complement proteins. The potential of complement as an anticancer effector is under-explored (Macor and Tedesco, 2007). An avenue of further exploration would therefore be to examine the ability of complement

proteins in targeting MV-treated melanoma cells, which would additionally exploration of the cross-talk that occurs between complement proteins and the innate or adaptive responses (Heeger and Kemper, 2012).

The most appealing way to continue the study of MV in melanoma, as discussed in chapter 3, would be by clinical trial. The clinical trial protocol outlined in that chapter predominantly focuses on assessing viral delivery based on evidence of expression of the sodium-iodine symporter gene, however such a clinical trial would also present opportunities to undertake correlative immune-based assays, looking for evidence that the anti-tumour immune priming effects seen in vitro may also occur in vivo. One challenge for such correlative studies is the absence of universal agreement of the best assay to detect immune responses. Indeed this is a problem for the entire field of immunotherapy. Conventional models of treatment development require study of pharmacodynamics and pharmacokinetics, along with toxicity assessments in order to define suitable treatment doses and schedules. Such parameters are difficult to measure for novel immune strategies such as adoptive cell therapies and oncolytic viruses. Though quite definitely outside the purview of research laboratories, efforts to standardise immune-based assays and implement quality control and assessment programs, and in so doing introduce the relevant techniques to routine diagnostic laboratories, may be of huge benefit for the field (Janetzki et al., 2008; Hoos et al., 2010).

Oncolytic viruses are gaining increasing attention as the epicentre of research is moving from preclinical study to clinical trials (Donnelly et al., 2012a). A recent high-profile study of reovirus administered intravenously found that although most virus is quickly neutralised by antibodies, some virus does reach tumour and appears to be delivered by various leukocytes and platelets (Adair et al., 2012; Donnelly et al., 2012c). The identification of this mechanism has significant implications for the field, and further research to characterise and enhance this mechanism is underway.

Despite a longstanding assumption that radiotherapy is distinctly immunosuppressive, a growing body of pre-clinical and clinical evidence suggests that RT can in fact cause immunologically relevant effects on tumour cells, and immune cells. In mouse models of melanoma, a single fraction of

external beam radiotherapy, mimicking commonly used palliative doses, did not enhance the effectiveness of an established preclinical immunotherapy strategy. The in vivo persistence of adoptively transferred T-cells, and their trafficking to tumour, or tumour-draining lymph nodes, did not appear to be enhanced by palliative dose external beam radiotherapy. Preliminary experiments using an alternative immunotherapy pairing showed some promise and merit further exploration. If RT is found to synergise with Pmel and VSV-gp100, having failed to do so with OT1 and VSV-Ova, then the mechanism behind that discrepancy would be particularly illuminating for directing future immune-based strategies. A model of brachytherapy treatment was developed – Brachytherapy did not enhance the effectiveness of an established preclinical immunotherapy strategy but the model may be useful for future studies of the effects of low versus high dose-rate RT.

The same challenges described above for clinical testing of the immune effects of OV, pose a problem in exploiting the immune effects of radiotherapy. Modern RT techniques, external or brachytherapy, are based on a view of radiobiology in which DNA damage is the sole mode of action. Accordingly timings and fractionation revolve around subverting DNA repair enzymes, rather than hitting windows of prime immunotherapeutic potential, if such windows exist. In order to design therapeutic combinations that take advantage of the immune effects of RT it will be necessary to have robust evidence of the 'radioimmunokinetics', and therefore such combinations will also benefit from improvements in immune assays. A similar concept allowed Markovic and colleagues to dramatically enhance response rates to chemotherapy for melanoma by ensuring that the treatment schedule conformed to immune dynamics, rather than traditional timings (Holtan et al., 2011; Leontovich et al., 2012).

Radiotherapy techniques have progressed considerably in the last two decades, including the ability to deliver hypofractionated and image-guided ablative radiotherapy to tumours with much smaller treatment margins than previously possible. Such stereotactic radiotherapy techniques can be applied to tumours in the brain and increasingly to areas throughout the body (SBRT). Interestingly the doses used in SBRT seem fortuitously to match many of the doses used in preclinical studies that have demonstrated the immune potential of RT.

Furthermore SBRT is generally given over only a handful of fractions with a short overall treatment time which arguably makes its combination with immune-based strategies much easier than conventional daily fractionations that may continue for up to 6 weeks. Although the RT equipment employed to deliver external beam RT (EBRT) in chapter 4 was able to deliver doses in the palliative range, it was not suitable for mimicking the precision or doses of SBRT. Small animal radiotherapy research platforms that can emulate frontline RT techniques are being developed and will greatly improve research in this field (Verhaegen et al., 2011). In future work we plan to exploit such platforms to combine SBRT and immunotherapies in mouse models of melanoma and glioblastoma. In the interim, we have opened an observational study of the immune responses of patients having SBRT for oligometastatic melanoma, based at the Mayo Clinic.

Brachytherapy is used for a fairly limited number of indications at present but retains the key advantage over EBRT that dose rapidly falls off with distance from the implanted source, often resulting in normal tissues being spared dose more so than can be achieved with EBRT. Although in a limited number of experiments presented in chapter 4 brachytherapy did not enhance immunotherapy, others have recently reported contrasting results. Hodge et al. injected mice with the Lewis lung cancer cell line, establishing both a flank tumour and metastases to the lung (Hodge et al., 2012). Combining brachytherapy to the flank tumour with a virus-based vaccine resulted in a significant reduction in the number of lung metastases. Given that the radioimmunokinetics may well vary considerably between cancer-types it is possible that SBRT and similar techniques could be used for some tumours, while lower dose rate therapies like brachytherapy are more effectively combined with immunotherapies in other tumours.

Melanoma commonly spreads to the brain and causes a terrible symptomatic burden when it does so. A model of intracranial tumour was implemented in order to allow testing of existing and novel therapeutic strategies, to ensure that the relative immunological sanctuary afforded by the blood-brain barrier does not hinder otherwise effective therapies. Though initially of interest purely for

melanoma-related research, this model is now also being used by the lab to study glioblastoma treatments.

Finally, it is important to note that countless groups worldwide are pursuing treatments that could generate and enhance anti-tumour immunity. Approaches being pursued to develop immunotherapy for melanoma and other tumours include (Donnelly et al., 2012b):

- IL-2 modified to improve its receptor affinity may reduce the toxicity associated with treatment (Levin et al., 2012).
- Monoclonal antibodies against a range of new immune targets, rather than tumour-associated targets are emerging; Daclizumab is an anti-CD25 agent that depletes regulatory T-cells and is being combined with other therapies (Rech and Vonderheide, 2009).
- Antibodies that target the 'other' immunological synapse (T-cell-to-tumour), specifically the interaction between programmed cell death receptor (PD-1) and its ligand PDL-1, may have fewer toxicities than ipilimumab and early trials have shown promise (Brahmer et al., 2010, 2012).
- Vemurafenib enhances antigen expression on the surface of melanoma tumours and therefore its combination with ipilimumab is to be tested clinically (Donnelly et al., 2012b).

Metastatic melanoma remains a cancer with one of the worst prognoses, despite recent therapeutic developments, however there is reason to be optimistic that further immunotherapeutic approaches may improve the outlook for patients with this disease.

8 References

Abbott, A. (2003). Cell culture: Biology's new dimension. Nature *424*, 870–872.

Adair, R.A., Roulstone, V., Scott, K.J., Morgan, R., Nuovo, G.J., Fuller, M., Beirne, D., West, E.J., Jennings, V.A., Rose, A., et al. (2012). Cell Carriage, Delivery, and Selective Replication of an Oncolytic Virus in Tumor in Patients. Sci Transl Med *4*, 138ra77–138ra77.

Allen, C., Paraskevakou, G., Iankov, I., Giannini, C., Schroeder, M., Sarkaria, J., Schroeder, M., Puri, R.K., Russell, S.J., and Galanis, E. (2008). Interleukin-13 displaying retargeted oncolytic measles virus strains have significant activity against gliomas with improved specificity. Mol. Ther *16*, 1556–1564.

Allen, C., Vongpunsawad, S., Nakamura, T., James, C.D., Schroeder, M., Cattaneo, R., Giannini, C., Krempski, J., Peng, K.-W., Goble, J.M., et al. (2006). Retargeted Oncolytic Measles Strains Entering via the EGFRvIII Receptor Maintain Significant Antitumor Activity against Gliomas with Increased Tumor Specificity. Cancer Res *66*, 11840–11850.

Alvarez, J.I., Dodelet-Devillers, A., Kebir, H., Ifergan, I., Fabre, P.J., Terouz, S., Sabbagh, M., Wosik, K., Bourbonnière, L., Bernard, M., et al. (2011). The Hedgehog Pathway Promotes Blood-Brain Barrier Integrity and CNS Immune Quiescence. Science *334*, 1727–1731.

Anderson, B.D., Nakamura, T., Russell, S.J., and Peng, K.-W. (2004). High CD46 Receptor Density Determines Preferential Killing of Tumor Cells by Oncolytic Measles Virus. Cancer Res *64*, 4919–4926.

Apetoh, L., Ghiringhelli, F., Tesniere, A., Criollo, A., Ortiz, C., Lidereau, R., Mariette, C., Chaput, N., Mira, J.-P., Delaloge, S., et al. (2007a). The interaction between HMGB1 and TLR4 dictates the outcome of anticancer chemotherapy and radiotherapy. Immunol. Rev *220*, 47–59.

Apetoh, L., Ghiringhelli, F., Tesniere, A., Obeid, M., Ortiz, C., Criollo, A., Mignot, G., Maiuri, M.C., Ullrich, E., Saulnier, P., et al. (2007b). Toll-like receptor 4–dependent contribution of the immune system to anticancer chemotherapy and radiotherapy. Nature Medicine *13*, 1050–1059.

Apostolidis, L., Schirrmacher, V., and Fournier, P. (2007). Host mediated anti-tumor effect of oncolytic Newcastle disease virus after locoregional application. Int. J. Oncol. *31*, 1009–1019.

Atkins, M.B., Lotze, M.T., Dutcher, J.P., Fisher, R.I., Weiss, G., Margolin, K., Abrams, J., Sznol, M., Parkinson, D., Hawkins, M., et al. (1999). High-Dose Recombinant Interleukin 2 Therapy for Patients With Metastatic Melanoma: Analysis of 270 Patients Treated Between 1985 and 1993. J Clin Oncol *17*, 2105.

Attia, P., Phan, G.Q., Maker, A.V., Robinson, M.R., Quezado, M.M., Yang, J.C., Sherry, R.M., Topalian, S.L., Kammula, U.S., Royal, R.E., et al. (2005). Autoimmunity correlates with tumor regression in patients with metastatic melanoma treated with anti-cytotoxic T-lymphocyte antigen-4. J. Clin. Oncol *23*, 6043–6053.

Balachandran, V.P., Cavnar, M.J., Zeng, S., Bamboat, Z.M., Ocuin, L.M., Obaid, H., Sorenson, E.C., Popow, R., Ariyan, C., Rossi, F., et al. (2011). Imatinib potentiates antitumor T cell responses in gastrointestinal stromal tumor through the inhibition of Ido. Nat Med *17*, 1094–1100.

Balch, C.M., Gershenwald, J.E., Soong, S., Thompson, J.F., Atkins, M.B., Byrd, D.R., Buzaid, A.C., Cochran, A.J., Coit, D.G., Ding, S., et al. (2009). Final Version of 2009 AJCC Melanoma Staging and Classification. J Clin Oncol *27*, 6199–6206.

Battaglia, A., Buzzonetti, A., Martinelli, E., Fanelli, M., Petrillo, M., Ferrandina, G., Scambia, G., and Fattorossi, A. (2010). Selective changes in the immune profile of tumor-draining lymph nodes after different neoadjuvant chemoradiation regimens for locally advanced cervical cancer. Int. J. Radiat. Oncol. Biol. Phys. *76*, 1546–1553.

Bechmann, I., Galea, I., and Perry, V.H. (2007). What is the blood–brain barrier (not)? Trends in Immunology *28*, 5–11.

Bell, J. (2010). Oncolytic Viruses: An Approved Product on the Horizon? Mol Ther *18*, 233–234.

Bentzen, S.M. (2008). Randomized controlled trials in health technology assessment: Overkill or overdue? Radiotherapy and Oncology *86*, 142–147.

Berghäll, H., Sirén, J., Sarkar, D., Julkunen, I., Fisher, P.B., Vainionpää, R., and Matikainen, S. (2006). The interferon-inducible RNA helicase, mda-5, is involved in measles virus-induced expression of antiviral cytokines. Microbes Infect. *8*, 2138–2144.

Bernstein, M.B., and Hodge, J.W. (2012). In the field: exploiting the untapped potential of immunogenic modulation by radiation in combination with immunotherapy for the treatment of cancer. Front. Oncol. *2*, 104.

Berthod, G., Lazor, R., Letovanec, I., Romano, E., Noirez, L., Stalder, J.M., Speiser, D.E., Peters, S., and Michielin, O. (2012). Pulmonary Sarcoid-Like Granulomatosis Induced by Ipilimumab. JCO *30*, e156–e159.

Betts, M.R., Brenchley, J.M., Price, D.A., De Rosa, S.C., Douek, D.C., Roederer, M., and Koup, R.A. (2003). Sensitive and viable identification of antigen-specific CD8+ T cells by a flow cytometric assay for degranulation. Journal of Immunological Methods *281*, 65–78.

Betts, M.R., and Koup, R.A. (2004). Detection of T-Cell Degranulation: CD107a and b. In Cytometry, 4th Edition: New Developments, (Academic Press), pp. 497–512.

Bianchi, M.E., and Manfredi, A.A. (2007). High-mobility group box 1 (HMGB1) protein at the crossroads between innate and adaptive immunity. Immunological Reviews *220*, 35–46.

Bladergroen, B.A., Meijer, C.J.L.M., Ten Berge, R.L., Hack, C.E., Muris, J.J.F., Dukers, D.F., Chott, A., Kazama, Y., Oudejans, J.J., Van Berkum, O., et al. (2002). Expression of the granzyme B inhibitor, protease inhibitor 9, by tumor cells in patients with non-Hodgkin and Hodgkin lymphoma: a novel protective mechanism for tumor cells to circumvent the immune system? Blood *99*, 232–237.

Blechacz, B., and Russell, S.J. (2008). Measles virus as an oncolytic vector platform. Curr Gene Ther *8*, 162–175.

Bluming, A.Z., and Ziegler, J.L. (1971). Regression of Burkitt's lymphoma in association with measles infection. Lancet *2*, 105–106.

Bonadies, D.C., and Bale, A.E. (2011). Hereditary melanoma. Curr Probl Cancer *35*, 162–172.

Boniol, M., Autier, P., Boyle, P., and Gandini, S. (2012). Cutaneous melanoma attributable to sunbed use: systematic review and meta-analysis. BMJ *345*, e4757.

Bonjardim, C.A. (2005). Interferons (IFNs) are key cytokines in both innate and adaptive antiviral immune responses--and viruses counteract IFN action. Microbes and Infection *7*, 569–578.

Brahmer, J.R., Drake, C.G., Wollner, I., Powderly, J.D., Picus, J., Sharfman, W.H., Stankevich, E., Pons, A., Salay, T.M., McMiller, T.L., et al. (2010). Phase I Study of Single-Agent Anti–Programmed Death-1 (MDX-1106) in Refractory Solid Tumors: Safety, Clinical Activity, Pharmacodynamics, and Immunologic Correlates. Journal of Clinical Oncology *28*, 3167 –3175.

Brahmer, J.R., Tykodi, S.S., Chow, L.Q.M., Hwu, W.-J., Topalian, S.L., Hwu, P., Drake, C.G., Camacho, L.H., Kauh, J., Odunsi, K., et al. (2012). Safety and Activity of Anti–PD-L1 Antibody in Patients with Advanced Cancer. New England Journal of Medicine *366*, 2455–2465.

Breitbach, C.J., Burke, J., Jonker, D., Stephenson, J., Haas, A.R., Chow, L.Q.M., Nieva, J., Hwang, T.-H., Moon, A., Patt, R., et al. (2011). Intravenous delivery of a multi-mechanistic cancer-targeted oncolytic poxvirus in humans. Nature *477*, 99–102.

Brenner, M.K., and Heslop, H.E. (2010). Adoptive T cell therapy of cancer. Current Opinion in Immunology *22*, 251–257.

Bridle, B.W., Li, J., Jiang, S., Chang, R., Lichty, B.D., Bramson, J.L., and Wan, Y. (2010). Immunotherapy Can Reject Intracranial Tumor Cells without Damaging the Brain despite Sharing the Target Antigen. J Immunol *184*, 4269–4275.

Brown, R.C., Egleton, R.D., and Davis, T.P. (2004). Mannitol opening of the blood-brain barrier: regional variation in the permeability of sucrose, but not 86Rb+ or albumin. Brain Res. *1014*, 221–227.

Bucheit, A.D., Kumar, S., Grote, D.M., Lin, Y., Von Messling, V., Cattaneo, R.B., and Fielding, A.K. (2003). An oncolytic measles virus engineered to enter cells through the CD20 antigen. Mol. Ther *7*, 62–72.

Buonaguro, L., Petrizzo, A., Tornesello, M.L., and Buonaguro, F.M. (2011). Translating Tumor Antigens into Cancer Vaccines. Clin Vaccine Immunol *18*, 23–34.

Burmeister, B.H., Henderson, M.A., Ainslie, J., Fisher, R., Di Iulio, J., Smithers, B.M., Hong, A., Shannon, K., Scolyer, R.A., Carruthers, S., et al. (2012). Adjuvant radiotherapy versus observation alone for patients at risk of lymph-node field relapse after therapeutic lymphadenectomy for melanoma: a randomised trial. The Lancet Oncology *13*, 589–597.

Campoli, M., and Ferrone, S. (2008). HLA antigen changes in malignant cells: epigenetic mechanisms and biologic significance. Oncogene *27*, 5869–5885.

Cao, Y., Tsien, C.I., Shen, Z., Tatro, D.S., Haken, R.T., Kessler, M.L., Chenevert, T.L., and Lawrence, T.S. (2005). Use of Magnetic Resonance Imaging to Assess Blood-Brain/Blood-Glioma Barrier Opening During Conformal Radiotherapy. JCO *23*, 4127–4136.

Carlson, B.L., Pokorny, J.L., Schroeder, M.A., and Sarkaria, J.N. (2011). Establishment, Maintenance and in vitro and in vivo Applications of Primary Human Glioblastoma Multiforme (GBM) Xenograft Models for Translational Biology Studies and Drug Discovery. Curr Protoc Pharmacol *52*, 1–14.

Casares, N., Pequignot, M.O., Tesniere, A., Ghiringhelli, F., Roux, S., Chaput, N., Schmitt, E., Hamai, A., Hervas-Stubbs, S., Obeid, M., et al. (2005). Caspase-dependent immunogenicity of doxorubicin-induced tumor cell death. J Exp Med *202*, 1691–1701.

Castermans, K., and Griffioen, A.W. (2007). Tumor blood vessels, a difficult hurdle for infiltrating leukocytes. Biochimica Et Biophysica Acta (BBA) - Reviews on Cancer *1776*, 160–174.

Chakraborty, M., Abrams, S.I., Coleman, C.N., Camphausen, K., Schlom, J., and Hodge, J.W. (2004). External beam radiation of tumors alters phenotype of tumor cells to render them susceptible to vaccine-mediated T-cell killing. Cancer Res. *64*, 4328–4337.

Chakravarty, P.K., Alfieri, A., Thomas, E.K., Beri, V., Tanaka, K.E., Vikram, B., and Guha, C. (1999). Flt3-Ligand Administration after Radiation Therapy Prolongs Survival in a Murine Model of Metastatic Lung Cancer. Cancer Research *59*, 6028–6032.

Chakravarty, P.K., Guha, C., Alfieri, A., Beri, V., Niazova, Z., Deb, N.J., Fan, Z., Thomas, E.K., and Vikram, B. (2006). Flt3L therapy following localized tumor irradiation generates long-term protective immune response in metastatic lung cancer: its implication in designing a vaccination strategy. Oncology *70*, 245–254.

Chapman, P.B., Hauschild, A., Robert, C., Haanen, J.B., Ascierto, P., Larkin, J., Dummer, R., Garbe, C., Testori, A., Maio, M., et al. (2011). Improved Survival with Vemurafenib in Melanoma with BRAF V600E Mutation. New England Journal of Medicine *364*, 2507–2516.

Cho, H.-I., Reyes-Vargas, E., Delgado, J.C., and Celis, E. (2012). A potent vaccination strategy that circumvents lymphodepletion for effective antitumor adoptive T-cell therapy. Cancer Res. *72*, 1986–1995.

Ciampricotti, M., Hau, C.-S., Doornebal, C.W., Jonkers, J., and Visser, K.E. de (2012). Chemotherapy response of spontaneous mammary tumors is independent of the adaptive immune system. Nature Medicine *18*, 344–346.

Clemente, C.G., Mihm Jr, M.C., Bufalino, R., Zurrida, S., Collini, P., and Cascinelli, N. (1996). Prognostic value of tumor infiltrating lymphocytes in the vertical growth phase of primary cutaneous melanoma. Cancer *77*, 1303–1310.

Correa, R.J.M., Komar, M., Tong, J.G.K., Sivapragasam, M., Rahman, M.M., McFadden, G., Dimattia, G.E., and Shepherd, T.G. (2012). Myxoma virus-mediated oncolysis of ascites-derived human ovarian cancer cells and spheroids is impacted by differential AKT activity. Gynecol. Oncol. *125*, 441–450.

Coulie, P.G., Brichard, V., Van Pel, A., Wölfel, T., Schneider, J., Traversari, C., Mattei, S., De Plaen, E., Lurquin, C., Szikora, J.P., et al. (1994). A new gene coding for a differentiation antigen recognized by autologous cytolytic T lymphocytes on HLA-A2 melanomas. J. Exp. Med. *180*, 35–42.

Cranmer, L.D., Trevor, K.T., Bandlamuri, S., and Hersh, E.M. (2005). Rodent models of brain metastasis in melanoma. Melanoma Research *15*, 325.

Critchley-Thorne, R.J., Simons, D.L., Yan, N., Miyahira, A.K., Dirbas, F.M., Johnson, D.L., Swetter, S.M., Carlson, R.W., Fisher, G.A., Koong, A., et al. (2009). Impaired interferon signaling is a common immune defect in human cancer. Proceedings of the National Academy of Sciences *106*, 9010 –9015.

Culig, Z., and Puhr, M. (2012). Interleukin-6: a multifunctional targetable cytokine in human prostate cancer. Mol. Cell. Endocrinol. *360*, 52–58.

Curiel, T.J., Coukos, G., Zou, L., Alvarez, X., Cheng, P., Mottram, P., Evdemon-Hogan, M., Conejo-Garcia, J.R., Zhang, L., Burow, M., et al. (2004). Specific recruitment of regulatory T cells in ovarian carcinoma fosters immune privilege and predicts reduced survival. Nature Medicine *10*, 942–949.

Curti, A., Trabanelli, S., Salvestrini, V., Baccarani, M., and Lemoli, R.M. (2009). The role of indoleamine 2,3-dioxygenase in the induction of immune tolerance: focus on hematology. Blood *113*, 2394–2401.

Demaria, S., Kawashima, N., Yang, A.M., Devitt, M.L., Babb, J.S., Allison, J.P., and Formenti, S.C. (2005). Immune-Mediated Inhibition of Metastases after Treatment with Local Radiation and CTLA-4 Blockade in a Mouse Model of Breast Cancer. Clinical Cancer Research *11*, 728 –734.

Demaria, S., Ng, B., Devitt, M.L., Babb, J.S., Kawashima, N., Liebes, L., and Formenti, S.C. (2004). Ionizing radiation inhibition of distant untreated tumors (abscopal effect) is immune mediated. International Journal of Radiation Oncology*Biology*Physics *58*, 862–870.

Dewan, M.Z., Galloway, A.E., Kawashima, N., Dewyngaert, J.K., Babb, J.S., Formenti, S.C., and Demaria, S. (2009). Fractionated but not single-dose radiotherapy induces an immune-mediated abscopal effect when combined with anti-CTLA-4 antibody. Clin. Cancer Res *15*, 5379–5388.

Dhiman, N., Jacobson, R.M., and Poland, G.A. (2004). Measles virus receptors: SLAM and CD46. Rev Med Virol *14*, 217–229.

Diaz, R.M., Galivo, F., Kottke, T., Wongthida, P., Qiao, J., Thompson, J., Valdes, M., Barber, G., and Vile, R.G. (2007). Oncolytic Immunovirotherapy for Melanoma Using Vesicular Stomatitis Virus. Cancer Research *67*, 2840–2848.

Dingli, D., Offord, C., Myers, R., Peng, K.-W., Carr, T.W., Josic, K., Russell, S.J., and Bajzer, Z. (2009). Dynamics of multiple myeloma tumor therapy with a recombinant measles virus. Cancer Gene Ther *16*, 873–882.

Dingli, D., Peng, K.-W., Harvey, M.E., Greipp, P.R., O'Connor, M.K., Cattaneo, R., Morris, J.C., and Russell, S.J. (2004). Image-guided radiovirotherapy for multiple myeloma using a recombinant measles virus expressing the thyroidal sodium iodide symporter. Blood *103*, 1641–1646.

Donnelly, O.G., Errington-Mais, F., Prestwich, R., Harrington, K., Pandha, H., Vile, R., and Melcher, A.A. (2012a). Recent clinical experience with oncolytic viruses. Curr Pharm Biotechnol *13*, 1834–1841.

Donnelly, O.G., Errington-Mais, F., Steele, L., Hadac, E., Jennings, V., Scott, K., Peach, H., Phillips, R.M., Bond, J., Pandha, H., et al. (2013). Measles virus causes immunogenic cell death in human melanoma. Gene Ther. *20*, 7–15.

Donnelly, O.G., Melcher, A.A., Vile, R.G., and Pulido, J. (2012b). What new immunotherapeutic techniques are currently being investigated for the treatment of melanoma? Immunotherapy *4*, 749–751.

Donnelly, O.G., Vile, R., Pandha, H., Harrington, K., and Melcher, A. (2012c). The Hitchhiker's Guide to Virotherapy. Oncotarget *3*, 735–736.

Doolittle, N.D., Miner, M.E., Hall, W.A., Siegal, T., Jerome, E., Osztie, E., McAllister, L.D., Bubalo, J.S., Kraemer, D.F., Fortin, D., et al. (2000). Safety and efficacy of a multicenter study using intraarterial chemotherapy in conjunction with osmotic opening of the blood-brain barrier for the treatment of patients with malignant brain tumors. Cancer *88*, 637–647.

Dörig, R.E., Marcil, A., Chopra, A., and Richardson, C.D. (1993). The human CD46 molecule is a receptor for measles virus (Edmonston strain). Cell *75*, 295–305.

Dranoff, G. (2005). The Therapeutic Implications of Intratumoral Regulatory T Cells. Clin Cancer Res *11*, 8226–8229.

Dudley, M.E., and Rosenberg, S.A. (2003). Adoptive-cell-transfer therapy for the treatment of patients with cancer. Nature Reviews Cancer *3*, 666–675.

Dudley, M.E., Wunderlich, J.R., Robbins, P.F., Yang, J.C., Hwu, P., Schwartzentruber, D.J., Topalian, S.L., Sherry, R., Restifo, N.P., Hubicki, A.M., et al. (2002). Cancer Regression and Autoimmunity in Patients After Clonal Repopulation with Antitumor Lymphocytes. Science *298*, 850–854.

Dudley, M.E., Wunderlich, J.R., Shelton, T.E., Even, J., and Rosenberg, S.A. (2003). Generation of tumor-infiltrating lymphocyte cultures for use in adoptive transfer therapy for melanoma patients. J. Immunother. *26*, 332–342.

Dunn, G.P., Bruce, A.T., Ikeda, H., Old, L.J., and Schreiber, R.D. (2002). Cancer immunoediting: from immunosurveillance to tumor escape. Nat Immunol *3*, 991–998.

Duprex, W.P., McQuaid, S., Hangartner, L., Billeter, M.A., and Rima, B.K. (1999). Observation of Measles Virus Cell-to-Cell Spread in Astrocytoma Cells by Using a Green Fluorescent Protein-Expressing Recombinant Virus. J. Virol. *73*, 9568–9575.

Duprex, W.P., and Rima, B.K. (2002). Using Green Fluorescent Protein to Monitor Measles Virus Cell-to-Cell Spread by Time-Lapse Confocal Microscopy. In Green Fluorescent Protein, pp. 297–307.

Eggermont, A.M.M., and Kirkwood, J.M. (2004). Re-evaluating the role of dacarbazine in metastatic melanoma: what have we learned in 30 years? European Journal of Cancer *40*, 1825–1836.

Elliott, F., Suppa, M., Chan, M., Leake, S., Karpavicius, B., Haynes, S., Barrett, J.H., Bishop, D.T., and Newton-Bishop, J.A. (2012). Relationship between sunbed use and melanoma risk in a large case-control study in the United Kingdom. Int. J. Cancer *130*, 3011–3013.

Erlenhofer, C., Duprex, W.P., Rima, B.K., Ter Meulen, V., and Schneider-Schaulies, J. (2002). Analysis of receptor (CD46, CD150) usage by measles virus. J Gen Virol *83*, 1431–1436.

Errington, F., Steele, L., Prestwich, R., Harrington, K.J., Pandha, H.S., Vidal, L., De Bono, J., Selby, P., Coffey, M., Vile, R., et al. (2008a). Reovirus activates human dendritic cells to promote innate antitumor immunity. J Immunol *180*, 6018–6026.

Errington, F., White, C.L., Twigger, K.R., Rose, A., Scott, K., Steele, L., Ilett, L.J., Prestwich, R., Pandha, H.S., Coffey, M., et al. (2008b). Inflammatory tumour cell

killing by oncolytic reovirus for the treatment of melanoma. Gene Ther *15*, 1257–1270.

Evans, C.J., Phillips, R.M., Jones, P.F., Loadman, P.M., Sleeman, B.D., Twelves, C.J., and Smye, S.W. (2009). A mathematical model of doxorubicin penetration through multicellular layers. Journal of Theoretical Biology *257*, 598–608.

Fielding, A.K. (2005). Measles as a potential oncolytic virus. Reviews in Medical Virology *15*, 135–142.

Fields, B.N., Knipe, D.M., Howley, P.M., and Griffin, D.E. (2007). Fields' virology (Lippincott Williams & Wilkins).

Finn, O.J. (2012). Immuno-oncology: understanding the function and dysfunction of the immune system in cancer. Annals of Oncology *23*, viii6–viii9.

Firsching, R., Buchholz, C.J., Schneider, U., Cattaneo, R., Ter Meulen, V., and Schneider-Schaulies, J. (1999). Measles virus spread by cell-cell contacts: uncoupling of contact-mediated receptor (CD46) downregulation from virus uptake. J Virol *73*, 5265–5273.

Fishelson, Z., Donin, N., Zell, S., Schultz, S., and Kirschfink, M. (2003). Obstacles to cancer immunotherapy: expression of membrane complement regulatory proteins (mCRPs) in tumors. Mol. Immunol *40*, 109–123.

Fisher, R., and Larkin, J. (2012). Treatment of brain metastases in patients with melanoma. The Lancet Oncology *13*, 434–435.

Formenti, S.C., and Demaria, S. (2009). Systemic effects of local radiotherapy. The Lancet Oncology *10*, 718–726.

Forsyth, P., Roldan, G., George, D., Wallace, C., Palmer, C.A., Morris, D., Cairncross, G., Matthews, M.V., Markert, J., Gillespie, Y., et al. (2008). A Phase I Trial of Intratumoral Administration of Reovirus in Patients With Histologically Confirmed Recurrent Malignant Gliomas. Mol Ther *16*, 627–632.

Gabrilovich, D.I., and Nagaraj, S. (2009). Myeloid-derived suppressor cells as regulators of the immune system. Nature Reviews Immunology *9*, 162–174.

Garbe, C., Peris, K., Hauschild, A., Saiag, P., Middleton, M., Spatz, A., Grob, J.-J., Malvehy, J., Newton-Bishop, J., Stratigos, A., et al. (2012). Diagnosis and treatment of melanoma. European consensus-based interdisciplinary guideline--Update 2012. Eur. J. Cancer *48*, 2375–2390.

Gauvrit, A., Brandler, S., Sapede-Peroz, C., Boisgerault, N., Tangy, F., and Grégoire, M. (2008). Measles Virus Induces Oncolysis of Mesothelioma Cells and Allows Dendritic Cells to Cross-Prime Tumor-Specific CD8 Response. Cancer Res *68*, 4882–4892.

Gerlier, D., Varior-Krishnan, G., and Devaux, P. (1995). CD46-mediated measles virus entry: a first key to host-range specificity. Trends Microbiol *3*, 338–345.

Ghosh, S., Spagnoli, G.C., Martin, I., Ploegert, S., Demougin, P., Heberer, M., and Reschner, A. (2005). Three-dimensional culture of melanoma cells profoundly affects gene expression profile: A high density oligonucleotide array study. Journal of Cellular Physiology *204*, 522–531.

Golden, E.B., Demaria, S., Barcellos-Hoff, M.H., and Formenti, S.C. (2012). The convergence of radiation and immunogenic cell death signaling pathways. Front. Oncol *2*, 88.

Gommerman, J.L., and Summers deLuca, L. (2011). LTβR and CD40: working together in dendritic cells to optimize immune responses. Immunological Reviews *244*, 85–98.

González-Martín, A., Mira, E., and Mañes, S. (2012). CCR5 in cancer immunotherapy. Oncoimmunology *1*, 106–108.

Griffin, D.E., and Oldstone, M.B. (2009). Measles. History and basic biology. Introduction. Current Topics in Microbiology and Immunology *329*, 1.

Groh, V., Wu, J., Yee, C., and Spies, T. (2002). Tumour-derived soluble MIC ligands impair expression of NKG2D and T-cell activation. Nature *419*, 734–738.

Gros, A., Turcotte, S., Wunderlich, J.R., Ahmadzadeh, M., Dudley, M.E., and Rosenberg, S.A. (2012). Myeloid cells obtained from the blood but not from the tumor can suppress T-cell proliferation in patients with melanoma. Clin. Cancer Res. *18*, 5212–5223.

Grosjean, I., Caux, C., Bella, C., Berger, I., Wild, F., Banchereau, J., and Kaiserlian, D. (1997). Measles Virus Infects Human Dendritic Cells and Blocks Their Allostimulatory Properties for CD4+ T Cells. J. Exp. Med. *186*, 801–812.

Grote, D., Cattaneo, R., and Fielding, A.K. (2003). Neutrophils contribute to the measles virus-induced antitumor effect: enhancement by granulocyte macrophage colony-stimulating factor expression. Cancer Res *63*, 6463–6468.

Grote, D., Russell, S.J., Cornu, T.I., Cattaneo, R., Vile, R., Poland, G.A., and Fielding, A.K. (2001). Live attenuated measles virus induces regression of human lymphoma xenografts in immunodeficient mice. Blood *97*, 3746–3754.

Gulley, J.L., Arlen, P.M., Bastian, A., Morin, S., Marte, J., Beetham, P., Tsang, K.-Y., Yokokawa, J., Hodge, J.W., Ménard, C., et al. (2005). Combining a Recombinant Cancer Vaccine with Standard Definitive Radiotherapy in Patients with Localized Prostate Cancer. Clinical Cancer Research *11*, 3353 –3362.

Hall, E.J., and Giaccia, A. (2011). Radiobiology for the Radiologist (Lippincott Williams & Wilkins).

Hallak, L.K., Merchan, J.R., Storgard, C.M., Loftus, J.C., and Russell, S.J. (2005). Targeted Measles Virus Vector Displaying Echistatin Infects Endothelial Cells via {alpha}v{beta}3 and Leads to Tumor Regression. Cancer Res *65*, 5292–5300.

Hammond, A.L., Plemper, R.K., Zhang, J., Schneider, U., Russell, S.J., and Cattaneo, R. (2001). Single-Chain Antibody Displayed on a Recombinant Measles Virus Confers Entry through the Tumor-Associated Carcinoembryonic Antigen. J. Virol. *75*, 2087–2096.

Hanahan, D., and Weinberg, R.A. (2011). Hallmarks of cancer: the next generation. Cell *144*, 646–674.

Haralambieva, I., Iankov, I., Hasegawa, K., Harvey, M., Russell, S.J., and Peng, K.-W. (2007). Engineering oncolytic measles virus to circumvent the intracellular innate immune response. Mol Ther *15*, 588–597.

Harry, V.N., Semple, S.I., Parkin, D.E., and Gilbert, F.J. (2010). Use of new imaging techniques to predict tumour response to therapy. The Lancet Oncology *11*, 92–102.

Hasegawa, K., Pham, L., O'Connor, M.K., Federspiel, M.J., Russell, S.J., and Peng, K.-W. (2006). Dual therapy of ovarian cancer using measles viruses expressing carcinoembryonic antigen and sodium iodide symporter. Clin. Cancer Res *12*, 1868–1875.

Hasumi, K., Aoki, Y., Watanabe, R., Hankey, K.G., and Mann, D.L. (2011). Therapeutic Response in Patients with Advanced Malignancies Treated with Combined Dendritic Cell–Activated T Cell Based Immunotherapy and Intensity–Modulated Radiotherapy. Cancers *3*, 2223–2242.

Heeger, P.S., and Kemper, C. (2012). Novel roles of complement in T effector cell regulation. Immunobiology *217*, 216–224.

Heinzerling, L., Kunzi, V., Oberholzer, P.A., Kundig, T., Naim, H., and Dummer, R. (2005). Oncolytic measles virus in cutaneous T-cell lymphomas mounts antitumor immune responses in vivo and targets interferon-resistant tumor cells. Blood *106*, 2287–2294.

Herschke, F., Plumet, S., Duhen, T., Azocar, O., Druelle, J., Laine, D., Wild, T.F., Rabourdin-Combe, C., Gerlier, D., and Valentin, H. (2007). Cell-Cell Fusion Induced by Measles Virus Amplifies the Type I Interferon Response. J. Virol. *81*, 12859–12871.

Hodge, J.W., Sharp, H.J., and Gameiro, S.R. (2012). Abscopal regression of antigen disparate tumors by antigen cascade after systemic tumor vaccination in combination with local tumor radiation. Cancer Biother. Radiopharm. *27*, 12–22.

Hodi, F.S., O'Day, S.J., McDermott, D.F., Weber, R.W., Sosman, J.A., Haanen, J.B., Gonzalez, R., Robert, C., Schadendorf, D., Hassel, J.C., et al. (2010). Improved Survival with Ipilimumab in Patients with Metastatic Melanoma. N Engl J Med *363*, 711–723.

Hoejberg, L., Bastholt, L., and Schmidt, H. (2012). Interleukin-6 and melanoma. Melanoma Research.

Holm, C.K., Jensen, S.B., Jakobsen, M.R., Cheshenko, N., Horan, K.A., Moeller, H.B., Gonzalez-Dosal, R., Rasmussen, S.B., Christensen, M.H., Yarovinsky, T.O., et al. (2012). Virus-cell fusion as a trigger of innate immunity dependent on the adaptor STING. Nature Immunology *13*, 737–743.

Holtan, S.G., Dronca, R.S., Nevala, W.K., Porrata, L.F., Mansfield, A.S., Block, M.S., Leontovich, A.A., Grotz, T.E., Turner, J.D., Frisch, H.P., et al. (2011). The dynamic human immune response to cancer: it might just be rocket science. Immunotherapy *3*, 1021–1024.

Hong, J.J., Rosenberg, S.A., Dudley, M.E., Yang, J.C., White, D.E., Butman, J.A., and Sherry, R.M. (2010). Successful treatment of melanoma brain metastases with adoptive cell therapy. Clin. Cancer Res. *16*, 4892–4898.

Hoos, A., Eggermont, A.M.M., Janetzki, S., Hodi, F.S., Ibrahim, R., Anderson, A., Humphrey, R., Blumenstein, B., Old, L., and Wolchok, J. (2010). Improved endpoints for cancer immunotherapy trials. J. Natl. Cancer Inst. *102*, 1388–1397.

Houghton, A.N., Gold, J.S., and Blachere, N.E. (2001). Immunity against cancer: lessons learned from melanoma. Current Opinion in Immunology *13*, 134–140.

Huang, B., Sikorski, R., Kirn, D.H., and Thorne, S.H. (2011a). Synergistic anti-tumor effects between oncolytic vaccinia virus and paclitaxel are mediated by the IFN response and HMGB1. Gene Ther *18*, 164–172.

Huang, J., Wang, Q.J., Yang, S., Li, Y.F., El-Gamil, M., Rosenberg, S.A., and Robbins, P.F. (2011b). Irradiation Enhances Human T-cell Function by Upregulating CD70 Expression on Antigen-presenting Cells In Vitro. Journal of Immunotherapy *34*, 327–335.

Hughes, M.S., Yu, Y.Y.L., Dudley, M.E., Zheng, Z., Robbins, P.F., Li, Y., Wunderlich, J., Hawley, R.G., Moayeri, M., Rosenberg, S.A., et al. (2005). Transfer of a TCR gene derived from a patient with a marked antitumor response conveys highly active T-cell effector functions. Hum. Gene Ther. *16*, 457–472.

Iankov, I.D., Allen, C., Federspiel, M.J., Myers, R.M., Peng, K.W., Ingle, J.N., Russell, S.J., and Galanis, E. (2012). Expression of immunomodulatory neutrophil-activating protein of Helicobacter pylori enhances the antitumor activity of oncolytic measles virus. Mol. Ther. *20*, 1139–1147.

Iankov, I.D., Blechacz, B., Liu, C., Schmeckpeper, J.D., Tarara, J.E., Federspiel, M.J., Caplice, N., and Russell, S.J. (2007). Infected Cell Carriers: A New Strategy for Systemic Delivery of Oncolytic Measles Viruses in Cancer Virotherapy. Mol Ther *15*, 114–122.

Iankov, I.D., Msaouel, P., Allen, C., Federspiel, M.J., Bulur, P.A., Dietz, A.B., Gastineau, D., Ikeda, Y., Ingle, J.N., Russell, S.J., et al. (2010). Demonstration of anti-tumor activity of oncolytic measles virus strains in a malignant pleural effusion breast cancer model. Breast Cancer Res. Treat *122*, 745–754.

Ilett, E.J., Bárcena, M., Errington-Mais, F., Griffin, S., Harrington, K.J., Pandha, H.S., Coffey, M., Selby, P.J., Limpens, R.W.A.L., Mommaas, M., et al. (2011). Internalization of oncolytic reovirus by human dendritic cell carriers protects the virus from neutralization. Clin. Cancer Res. *17*, 2767–2776.

Ilett, E.J., Prestwich, R.J., Kottke, T., Errington, F., Thompson, J.M., Harrington, K.J., Pandha, H.S., Coffey, M., Selby, P.J., Vile, R.G., et al. (2009). Dendritic cells and T cells deliver oncolytic reovirus for tumour killing despite pre-existing anti-viral immunity. Gene Ther. *16*, 689–699.

Jahanshahi, P., Nasr, N., Unger, K., Batouli, A., and Gagnon, G.J. (2012). Malignant melanoma and radiotherapy: past myths, excellent local control in 146 studied lesions at Georgetown University, and improving future management. Front Oncol *2*, 167.

Janetzki, S., Panageas, K.S., Ben-Porat, L., Boyer, J., Britten, C.M., Clay, T.M., Kalos, M., Maecker, H.T., Romero, P., Yuan, J., et al. (2008). Results and harmonization guidelines from two large-scale international Elispot proficiency panels conducted by the Cancer Vaccine Consortium (CVC/SVI). Cancer Immunol Immunother *57*, 303–315.

Jing, Y., Tong, C., Zhang, J., Nakamura, T., Iankov, I., Russell, S.J., and Merchan, J.R. (2009). Tumor and vascular targeting of a novel oncolytic measles virus retargeted against the urokinase receptor. Cancer Res *69*, 1459–1468.

Joffre, O., Nolte, M.A., Spörri, R., and Reis e Sousa, C. (2009). Inflammatory signals in dendritic cell activation and the induction of adaptive immunity. Immunol. Rev. *227*, 234–247.

Johns, T.G., Mackay, I.R., Callister, K.A., Hertzog, P.J., Devenish, R.J., and Linnance, A.W. (1992). Antiproliferative Potencies of Interferons on Melanoma Cell Lines and Xenografts: Higher Efficacy of Interferon beta. J. Natl. Cancer Inst. *84*, 1185–1190.

Johnson, L.A., Morgan, R.A., Dudley, M.E., Cassard, L., Yang, J.C., Hughes, M.S., Kammula, U.S., Royal, R.E., Sherry, R.M., Wunderlich, J.R., et al. (2009). Gene therapy with human and mouse T-cell receptors mediates cancer regression and targets normal tissues expressing cognate antigen. Blood *114*, 535–546.

Joiner, M., and Van der Kogel, A. (2009). Basic clinical radiobiology (Hodder Arnold).

Kalos, M., Levine, B.L., Porter, D.L., Katz, S., Grupp, S.A., Bagg, A., and June, C.H. (2011). T Cells with Chimeric Antigen Receptors Have Potent Antitumor Effects and Can Establish Memory in Patients with Advanced Leukemia. Sci Transl Med *3*, 95ra73–95ra73.

Katz, S.L. (2009). John F. Enders and measles virus vaccine--a reminiscence. Curr. Top. Microbiol. Immunol *329*, 3–11.

Kaufman, H.L., Kim, D.W., DeRaffele, G., Mitcham, J., Coffin, R.S., and Kim-Schulze, S. (2010). Local and distant immunity induced by intralesional vaccination with an oncolytic herpes virus encoding GM-CSF in patients with stage IIIc and IV melanoma. Ann. Surg. Oncol *17*, 718–730.

Kawakami, Y., Eliyahu, S., Delgado, C.H., Robbins, P.F., Rivoltini, L., Topalian, S.L., Miki, T., and Rosenberg, S.A. (1994). Cloning of the gene coding for a shared human melanoma antigen recognized by autologous T cells infiltrating into tumor. Proc Natl Acad Sci U S A *91*, 3515–3519.

Kawamura, K., Bahar, R., Natsume, W., Sakiyama, S., and Tagawa, M. (2002). Secretion of interleukin-10 from murine colon carcinoma cells suppresses systemic antitumor immunity and impairs protective immunity induced against the tumors. Cancer Gene Ther. *9*, 109–115.

Kelly, E., and Russell, S.J. (2007). History of Oncolytic Viruses: Genesis to Genetic Engineering. Mol Ther *15*, 651–659.

Kemper, C., and Atkinson, J.P. (2009). Measles Virus and CD46. In Measles, pp. 31–57.

Kilkenny, C., and Altman, D.G. (2010). Improving bioscience research reporting: ARRIVE-ing at a solution. Lab Anim *44*, 377–378.

Kim, R., Emi, M., and Tanabe, K. (2007). Cancer immunoediting from immune surveillance to immune escape. Immunology *121*, 1–14.

Kirn, D., Martuza, R.L., and Zwiebel, J. (2001). Replication-selective virotherapy for cancer: Biological principles, risk management and future directions. Nat. Med *7*, 781–787.

Klune, J.R., Dhupar, R., Cardinal, J., Billiar, T.R., and Tsung, A. (2008). HMGB1: Endogenous Danger Signaling. Mol Med *14*, 476–484.

Kottke, T., Chester, J., Ilett, E., Thompson, J., Diaz, R., Coffey, M., Selby, P., Nuovo, G., Pulido, J., Mukhopadhyay, D., et al. (2011a). Precise Scheduling of Chemotherapy Primes VEGF-producing Tumors for Successful Systemic Oncolytic Virotherapy. Mol Ther *19*, 1802–1812.

Kottke, T., Errington, F., Pulido, J., Galivo, F., Thompson, J., Wongthida, P., Diaz, R.M., Chong, H., Ilett, E., Chester, J., et al. (2011b). Broad antigenic coverage induced by vaccination with virus-based cDNA libraries cures established tumors. Nat Med *17*, 854–859.

Kozin, S.V., Kamoun, W.S., Huang, Y., Dawson, M.R., Jain, R.K., and Duda, D.G. (2010). Recruitment of Myeloid but not Endothelial Precursor Cells Facilitates Tumor Regrowth after Local Irradiation. Cancer Research *70*, 5679 –5685.

Kubo, H., Ashida, A., Matsumoto, K., Kageshita, T., Yamamoto, A., and Saida, T. (2008). Interferon-β therapy for malignant melanoma: the dose is crucial for

inhibition of proliferation and induction of apoptosis of melanoma cells. Arch Dermatol Res *300*, 297–301.

Kunzi, V., Oberholzer, P.A., Heinzerling, L., Dummer, R., and Naim, H.Y. (2006). Recombinant Measles Virus Induces Cytolysis of Cutaneous T-Cell Lymphoma In Vitro and In Vivo. J Invest Dermatol *126*, 2525–2532.

Lam, J.T., Hemminki, A., Kanerva, A., Lee, K.B., Blackwell, J.L., Desmond, R., Siegal, G.P., and Curiel, D.T. (2007). A three-dimensional assay for measurement of viral-induced oncolysis. Cancer Gene Ther. *14*, 421–430.

Lapteva, N., and Huang, X.F. (2010). CCL5 as an adjuvant for cancer immunotherapy. Expert Opin Biol Ther *10*, 725–733.

Lasfar, A., Lewis-Antes, A., Smirnov, S.V., Anantha, S., Abushahba, W., Tian, B., Reuhl, K., Dickensheets, H., Sheikh, F., Donnelly, R.P., et al. (2006). Characterization of the Mouse IFN-λ Ligand-Receptor System: IFN-λs Exhibit Antitumor Activity against B16 Melanoma. Cancer Res *66*, 4468–4477.

Lechner, M.G., Liebertz, D.J., and Epstein, A.L. (2010). Characterization of Cytokine-Induced Myeloid-Derived Suppressor Cells from Normal Human Peripheral Blood Mononuclear Cells. J Immunol *185*, 2273–2284.

Lee, G.Y., Kenny, P.A., Lee, E.H., and Bissell, M.J. (2007). Three-dimensional culture models of normal and malignant breast epithelial cells. Nat Meth *4*, 359–365.

Lee, K.C., and Weinstock, M.A. (2009). Melanoma is up: are we up to this challenge? J. Invest. Dermatol. *129*, 1604–1606.

Lee, Y., Auh, S.L., Wang, Y., Burnette, B., Wang, Y., Meng, Y., Beckett, M., Sharma, R., Chin, R., Tu, T., et al. (2009). Therapeutic effects of ablative radiation on local tumor require CD8+ T cells: changing strategies for cancer treatment. Blood *114*, 589 –595.

Leontovich, A.A., Dronca, R.S., Suman, V.J., L Ashdown, M., Nevala, W.K., Thompson, M.A., Robinson, A., Kottschade, L.A., Kaur, J.S., McWilliams, R.R., et al. (2012). Fluctuation of systemic immunity in melanoma and implications for timing of therapy. Front Biosci (Elite Ed) *4*, 958–975.

Levin, A.M., Bates, D.L., Ring, A.M., Krieg, C., Lin, J.T., Su, L., Moraga, I., Raeber, M.E., Bowman, G.R., Novick, P., et al. (2012). Exploiting a natural conformational switch to engineer an interleukin-2 “superkine”. Nature *484*, 529–533.

Li, H., Peng, K.-W., Dingli, D., Kratzke, R.A., and Russell, S.J. (2010). Oncolytic measles viruses encoding interferon beta and the thyroidal sodium iodide symporter gene for mesothelioma virotherapy. Cancer Gene Ther *17*, 550–558.

Liao, Y.-P., Wang, C.-C., Butterfield, L.H., Economou, J.S., Ribas, A., Meng, W.S., Iwamoto, K.S., and McBride, W.H. (2004). Ionizing radiation affects human

MART-1 melanoma antigen processing and presentation by dendritic cells. J. Immunol *173*, 2462–2469.

Linos, E., Swetter, S.M., Cockburn, M.G., Colditz, G.A., and Clarke, C.A. (2009). Increasing Burden of Melanoma in the United States. J Invest Dermatol *129*, 1666–1674.

Linskey, M.E., Andrews, D.W., Asher, A.L., Burri, S.H., Kondziolka, D., Robinson, P.D., Ammirati, M., Cobbs, C.S., Gaspar, L.E., Loeffler, J.S., et al. (2010). The role of stereotactic radiosurgery in the management of patients with newly diagnosed brain metastases: a systematic review and evidence-based clinical practice guideline. J Neurooncol *96*, 45–68.

Liu, C., Hasegawa, K., Russell, S.J., Sadelain, M., and Peng, K.-W. (2009). Prostate-specific membrane antigen retargeted measles virotherapy for the treatment of prostate cancer. Prostate *69*, 1128–1141.

Liu, W., and Dalgleish, A. (2009). MTT assays can underestimate cell numbers. Cancer Chemotherapy and Pharmacology *64*, 861–862.

Lorger, M., and Felding-Habermann, B. (2010). Capturing Changes in the Brain Microenvironment during Initial Steps of Breast Cancer Brain Metastasis. The American Journal of Pathology *176*, 2958–2971.

Lotze, M.T., and Tracey, K.J. (2005). High-mobility group box 1 protein (HMGB1): nuclear weapon in the immune arsenal. Nat Rev Immunol *5*, 331–342.

Ma, Y., Kepp, O., Ghiringhelli, F., Apetoh, L., Aymeric, L., Locher, C., Tesniere, A., Martins, I., Ly, A., Haynes, N.M., et al. (2010). Chemotherapy and radiotherapy: cryptic anticancer vaccines. Semin. Immunol *22*, 113–124.

Macor, P., and Tedesco, F. (2007). Complement as effector system in cancer immunotherapy. Immunol. Lett *111*, 6–13.

Mader, E., Maeyama, Y., Lin, Y., Butler, G., Russell, H., Galanis, E., Russell, S., Dietz, A., and Peng, K. (2009). Mesenchymal stem cell carriers protect oncolytic measles viruses from antibody neutralization in an orthotopic ovarian cancer therapy model. Clinical Cancer Research *15*, 7246–7255.

Maio, M. (2012). Melanoma as a model tumour for immuno-oncology. Ann. Oncol. *23 Suppl 8*, viii10–viii14.

Mapara, M.Y., and Sykes, M. (2004). Tolerance and Cancer: Mechanisms of Tumor Evasion and Strategies for Breaking Tolerance. JCO *22*, 1136–1151.

Margolin, K., Ernstoff, M.S., Hamid, O., Lawrence, D., McDermott, D., Puzanov, I., Wolchok, J.D., Clark, J.I., Sznol, M., Logan, T.F., et al. (2012). Ipilimumab in patients with melanoma and brain metastases: an open-label, phase 2 trial. The Lancet Oncology *13*, 459–465.

Martires KJ, B.-S.J. (2012). A call for consistent reporting of regression in melanoma. Arch Dermatol *148*, 1081–1083.

Matzinger, P. (1994). Tolerance, danger, and the extended family. Annu. Rev. Immunol *12*, 991–1045.

Matzinger, P. (2002). The Danger Model: A Renewed Sense of Self. Science *296*, 301–305.

McCarter, M.D., Baumgartner, J., Escobar, G.A., Richter, D., Lewis, K., Robinson, W., Wilson, C., Palmer, B.E., and Gonzalez, R. (2007). Immunosuppressive dendritic and regulatory T cells are upregulated in melanoma patients. Annals of Surgical Oncology *14*, 2854–2860.

Meissner, M., Reichert, T.E., Kunkel, M., Gooding, W., Whiteside, T.L., Ferrone, S., and Seliger, B. (2005). Defects in the Human Leukocyte Antigen Class I Antigen Processing Machinery in Head and Neck Squamous Cell Carcinoma: Association with Clinical Outcome. Clin Cancer Res *11*, 2552–2560.

Meng, X., Nakamura, T., Okazaki, T., Inoue, H., Takahashi, A., Miyamoto, S., Sakaguchi, G., Eto, M., Naito, S., Takeda, M., et al. (2010). Enhanced Antitumor Effects of an Engineered Measles Virus Edmonston Strain Expressing the Wild-type N, P, L Genes on Human Renal Cell Carcinoma. Mol Ther *18*, 544–551.

Menzies, S.W. (2008). Is sun exposure a major cause of melanoma? Yes. BMJ *337*, a763.

Menzies, S.W., and McCarthy, W.H. (1997). Complete regression of primary cutaneous malignant melanoma. Arch Surg *132*, 553–556.

Merrick, A., Errington, F., Milward, K., O'Donnell, D., Harrington, K., Bateman, A., Pandha, H., Vile, R., Morrison, E., Selby, P., et al. (2005). Immunosuppressive effects of radiation on human dendritic cells: reduced IL-12 production on activation and impairment of naive T-cell priming. Br J Cancer *92*, 1450–1458.

Merrick, A.E., Ilett, E.J., and Melcher, A.A. (2009). JX-594, a targeted oncolytic poxvirus for the treatment of cancer. Curr Opin Investig Drugs *10*, 1372–1382.

Mihm Jr, M.C., Clemente, C.G., Cascinelli, N., and others (1996). Tumor infiltrating lymphocytes in lymph node melanoma metastases: a histopathologic prognostic indicator and an expression of local immune response. Laboratory Investigation; a Journal of Technical Methods and Pathology *74*, 43.

Mocellin, S., Pasquali, S., Rossi, C.R., and Nitti, D. (2010). Interferon Alpha Adjuvant Therapy in Patients With High-Risk Melanoma: A Systematic Review and Meta-analysis. Journal of the National Cancer Institute *102*, 493 –501.

Mole, R.H. (1953). Whole Body Irradiation—Radiobiology or Medicine? Br J Radiol *26*, 234–241.

Morgan, R.A., Dudley, M.E., Wunderlich, J.R., Hughes, M.S., Yang, J.C., Sherry, R.M., Royal, R.E., Topalian, S.L., Kammula, U.S., Restifo, N.P., et al. (2006). Cancer Regression in Patients After Transfer of Genetically Engineered Lymphocytes. Science *314*, 126–129.

Msaouel, P., Dispenzieri, A., and Galanis, E. (2009). Clinical testing of engineered oncolytic measles virus strains in the treatment of cancer: an overview. Curr. Opin. Mol. Ther *11*, 43–53.

Mühlebach, M.D., Mateo, M., Sinn, P.L., Prüfer, S., Uhlig, K.M., Leonard, V.H.J., Navaratnarajah, C.K., Frenzke, M., Wong, X.X., Sawatsky, B., et al. (2011). Adherens junction protein nectin-4 is the epithelial receptor for measles virus. Nature *480*, 530–533.

Mumm, J.B., Emmerich, J., Zhang, X., Chan, I., Wu, L., Mauze, S., Blaisdell, S., Basham, B., Dai, J., Grein, J., et al. (2011). IL-10 elicits IFNγ-dependent tumor immune surveillance. Cancer Cell *20*, 781–796.

Myers, R., Harvey, M., Kaufmann, T.J., Greiner, S.M., Krempski, J.W., Raffel, C., Shelton, S.E., Soeffker, D., Zollman, P., Federspiel, M.J., et al. (2008). Toxicology study of repeat intracerebral administration of a measles virus derivative producing carcinoembryonic antigen in rhesus macaques in support of a phase I/II clinical trial for patients with recurrent gliomas. Hum. Gene Ther *19*, 690–698.

Myers, R.M., Greiner, S.M., Harvey, M.E., Griesmann, G., Kuffel, M.J., Buhrow, S.A., Reid, J.M., Federspiel, M., Ames, M.M., Dingli, D., et al. (2007). Preclinical pharmacology and toxicology of intravenous MV-NIS, an oncolytic measles virus administered with or without cyclophosphamide. Clin. Pharmacol. Ther *82*, 700–710.

Navaratnarajah, C.K., Leonard, V.H.J., and Cattaneo, R. (2009). Measles Virus Glycoprotein Complex Assembly, Receptor Attachment, and Cell Entry. In Measles, pp. 59–76.

Navaratnarajah, C.K., Vongpunsawad, S., Oezguen, N., Stehle, T., Braun, W., Hashiguchi, T., Maenaka, K., Yanagi, Y., and Cattaneo, R. (2008). Dynamic Interaction of the Measles Virus Hemagglutinin with Its Receptor Signaling Lymphocytic Activation Molecule (SLAM, CD150). Journal of Biological Chemistry *283*, 11763–11771.

Noyce, R.S., Bondre, D.G., Ha, M.N., Lin, L.-T., Sisson, G., Tsao, M.-S., and Richardson, C.D. (2011). Tumor Cell Marker PVRL4 (Nectin 4) Is an Epithelial Cell Receptor for Measles Virus. PLoS Pathog *7*, e1002240.

O'Day, S., Hodi, F.S., McDermott, D.F., Weber, R.W., Sosman, J.A., Haanen, J.B., Zhu, X., Yellin, M.J., Hoos, A., and Urba, W.J. (2010). A phase III, randomized, double-blind, multicenter study comparing monotherapy with ipilimumab or gp100 peptide vaccine and the combination in patients with previously treated, unresectable stage III or IV melanoma. J Clin Oncol (Meeting Abstracts) *28*, 4.

Obeid, M., Panaretakis, T., Joza, N., Tufi, R., Tesniere, A., Van Endert, P., Zitvogel, L., and Kroemer, G. (2007a). Calreticulin exposure is required for the immunogenicity of [gamma]-irradiation and UVC light-induced apoptosis. Cell Death Differ *14*, 1848–1850.

Obeid, M., Tesniere, A., Ghiringhelli, F., Fimia, G.M., Apetoh, L., Perfettini, J.-L., Castedo, M., Mignot, G., Panaretakis, T., Casares, N., et al. (2007b). Calreticulin exposure dictates the immunogenicity of cancer cell death. Nat. Med *13*, 54–61.

Offringa, R. (2009). Antigen choice in adoptive T-cell therapy of cancer. Current Opinion in Immunology *21*, 190–199.

Ohshima, Y., Tsukimoto, M., Takenouchi, T., Harada, H., Suzuki, A., Sato, M., Kitani, H., and Kojima, S. (2010). gamma-Irradiation induces P2X(7) receptor-dependent ATP release from B16 melanoma cells. Biochim. Biophys. Acta *1800*, 40–46.

Olsen, C.M., Carroll, H.J., and Whiteman, D.C. (2010). Familial melanoma: a meta-analysis and estimates of attributable fraction. Cancer Epidemiol. Biomarkers Prev. *19*, 65–73.

Ong, H.T., Hasegawa, K., Dietz, A.B., Russell, S.J., and Peng, K.-W. (2006a). Evaluation of T cells as carriers for systemic measles virotherapy in the presence of antiviral antibodies. Gene Ther *14*, 324–333.

Ong, H.T., Timm, M.M., Greipp, P.R., Witzig, T.E., Dispenzieri, A., Russell, S.J., and Peng, K.-W. (2006b). Oncolytic measles virus targets high CD46 expression on multiple myeloma cells. Exp. Hematol *34*, 713–720.

Ong, H.T., Trejo, T.R., Pham, L.D., Oberg, A.L., Russell, S.J., and Peng, K.-W. (2009). Intravascularly administered RGD-displaying measles viruses bind to and infect neovessel endothelial cells in vivo. Mol. Ther *17*, 1012–1021.

Overwijk, W.W. (2005). Breaking tolerance in cancer immunotherapy: time to ACT. Current Opinion in Immunology *17*, 187–194.

Ovsyannikova, I.G., Reid, K.C., Jacobson, R.M., Oberg, A.L., Klee, G.G., and Poland, G.A. (2003). Cytokine production patterns and antibody response to measles vaccine. Vaccine *21*, 3946–3953.

Paik, S.-Y., Oh, J.-T., Choi, Y.-J., Kwon, K.-W., and Yang, W.-I. (2002). Measles-related appendicitis. Arch. Pathol. Lab. Med *126*, 82–84.

Panaretakis, T., Kepp, O., Brockmeier, U., Tesniere, A., Bjorklund, A.-C., Chapman, D.C., Durchschlag, M., Joza, N., Pierron, G., Van Endert, P., et al. (2009). Mechanisms of pre-apoptotic calreticulin exposure in immunogenic cell death. EMBO J *28*, 578–590.

Peinado, H., Alečković, M., Lavotshkin, S., Matei, I., Costa-Silva, B., Moreno-Bueno, G., Hergueta-Redondo, M., Williams, C., García-Santos, G., Ghajar, C.M., et al.

(2012). Melanoma exosomes educate bone marrow progenitor cells toward a pro-metastatic phenotype through MET. Nature Medicine *18*, 883–891.

Peng, K.-W., Dogan, A., Vrana, J., Liu, C., Ong, H.T., Kumar, S., Dispenzieri, A., Dietz, A.B., and Russell, S.J. (2009). Tumor-associated macrophages infiltrate plasmacytomas and can serve as cell carriers for oncolytic measles virotherapy of disseminated myeloma. Am. J. Hematol *84*, 401–407.

Peng, K.-W., Donovan, K.A., Schneider, U., Cattaneo, R., Lust, J.A., and Russell, S.J. (2003a). Oncolytic measles viruses displaying a single-chain antibody against CD38, a myeloma cell marker. Blood *101*, 2557–2562.

Peng, K.-W., Facteau, S., Wegman, T., O'Kane, D., and Russell, S.J. (2002). Non-invasive in vivo monitoring of trackable viruses expressing soluble marker peptides. Nat. Med. *8*, 527–531.

Peng, K.-W., Frenzke, M., Myers, R., Soeffker, D., Harvey, M., Greiner, S., Galanis, E., Cattaneo, R., Federspiel, M.J., and Russell, S.J. (2003b). Biodistribution of oncolytic measles virus after intraperitoneal administration into Ifnar-CD46Ge transgenic mice. Hum. Gene Ther *14*, 1565–1577.

Perez, C.A., Fu, A., Onishko, H., Hallahan, D.E., and Geng, L. (2009). Radiation induces an antitumour immune response to mouse melanoma. Int. J. Radiat. Biol *85*, 1126–1136.

Permar, S.R., Griffin, D.E., and Letvin, N.L. (2006). Immune Containment and Consequences of Measles Virus Infection in Healthy and Immunocompromised Individuals. Clin. Vaccine Immunol. *13*, 437–443.

Porter, D.L., Levine, B.L., Kalos, M., Bagg, A., and June, C.H. (2011). Chimeric Antigen Receptor–Modified T Cells in Chronic Lymphoid Leukemia. New England Journal of Medicine *365*, 725–733.

Postow, M.A., Callahan, M.K., Barker, C.A., Yamada, Y., Yuan, J., Kitano, S., Mu, Z., Rasalan, T., Adamow, M., Ritter, E., et al. (2012). Immunologic correlates of the abscopal effect in a patient with melanoma. N. Engl. J. Med. *366*, 925–931.

Prabhu, S.S., Broaddus, W.C., Oveissi, C., Berr, S.S., and Gillies, G.T. (2000). Determination of intracranial tumor volumes in a rodent brain using magnetic resonance imaging, Evans blue, and histology: a comparative study. IEEE Trans Biomed Eng *47*, 259–265.

Prestwich, R., Errington, F., Hatfield, P., Merrick, A., Ilett, E., Selby, P., and Melcher, A. (2008a). The Immune System — is it Relevant to Cancer Development, Progression and Treatment? Clinical Oncology *20*, 101–112.

Prestwich, R.J., Errington, F., Diaz, R.M., Pandha, H.S., Harrington, K.J., Melcher, A.A., and Vile, R.G. (2009a). The Case of Oncolytic Viruses Versus the Immune System: Waiting on the Judgment of Solomon. Hum Gene Ther *20*, 1119–1132.

Prestwich, R.J., Errington, F., Ilett, E.J., Morgan, R.S.M., Scott, K.J., Kottke, T., Thompson, J., Morrison, E.E., Harrington, K.J., Pandha, H.S., et al. (2008b). Tumor Infection by Oncolytic Reovirus Primes Adaptive Antitumor Immunity. Clinical Cancer Research *14*, 7358–7366.

Prestwich, R.J., Harrington, K.J., Pandha, H.S., Vile, R.G., Melcher, A.A., and Errington, F. (2008c). Oncolytic viruses: a novel form of immunotherapy. Expert Rev Anticancer Ther *8*, 1581–1588.

Prestwich, R.J., Ilett, E.J., Errington, F., Diaz, R.M., Steele, L.P., Kottke, T., Thompson, J., Galivo, F., Harrington, K.J., Pandha, H.S., et al. (2009b). Immune-Mediated Antitumor Activity of Reovirus Is Required for Therapy and Is Independent of Direct Viral Oncolysis and Replication. Clinical Cancer Research *15*, 4374 –4381.

Pringle, C.R. (2001). Vesicular Stomatitis Virus. In eLS, (John Wiley & Sons, Ltd),.

Radecke, F., Spielhofer, P., Schneider, H., Kaelin, K., Huber, M., Dötsch, C., Christiansen, G., and Billeter, M.A. (1995). Rescue of measles viruses from cloned DNA. EMBO J *14*, 5773–5784.

Real, L.M., Jimenez, P., Kirkin, A., Serrano, A., García, A., Cantón, J., Zeuthen, J., Garrido, F., and Ruiz-Cabello, F. (2001). Multiple mechanisms of immune evasion can coexist in melanoma tumor cell lines derived from the same patient. Cancer Immunology, Immunotherapy *49*, 621–628.

Rech, A.J., and Vonderheide, R.H. (2009). Clinical use of anti-CD25 antibody daclizumab to enhance immune responses to tumor antigen vaccination by targeting regulatory T cells. Ann. N. Y. Acad. Sci. *1174*, 99–106.

Reed, L.J., and Muench, H. (1938). A simple method of estimating fifty per cent endpoints. American Journal of Epidemiology *27*, 493.

Reits, E.A., Hodge, J.W., Herberts, C.A., Groothuis, T.A., Chakraborty, M., K.Wansley, E., Camphausen, K., Luiten, R.M., De Ru, A.H., Neijssen, J., et al. (2006). Radiation modulates the peptide repertoire, enhances MHC class I expression, and induces successful antitumor immunotherapy. The Journal of Experimental Medicine *203*, 1259 –1271.

Restifo, N.P., Dudley, M.E., and Rosenberg, S.A. (2012). Adoptive immunotherapy for cancer: harnessing the T cell response. Nature Reviews Immunology *12*, 269–281.

Ribas, A. (2012). Tumor Immunotherapy Directed at PD-1. New England Journal of Medicine *366*, 2517–2519.

Robarge, K.D., Brunton, S.A., Castanedo, G.M., Cui, Y., Dina, M.S., Goldsmith, R., Gould, S.E., Guichert, O., Gunzner, J.L., Halladay, J., et al. (2009). GDC-0449—A potent inhibitor of the hedgehog pathway. Bioorganic & Medicinal Chemistry Letters *19*, 5576–5581.

Rommelfanger, D., Wongthida, P., Diaz, R.M., Kaluza, K.M., Thompson, J., Kottke, T., and Vile, R.G. (2012). Systemic Combination Virotherapy For Melanoma With Tumor Antigen-Expressing Vesicular Stomatitis Virus And Adoptive T Cell Transfer. Cancer Research.

Rosenberg, S.A. (2012). Raising the Bar: The Curative Potential of Human Cancer Immunotherapy. Sci Transl Med *4*, 127ps8–127ps8.

Rosenberg, S.A., and Dudley, M.E. (2009). Adoptive cell therapy for the treatment of patients with metastatic melanoma. Current Opinion in Immunology *21*, 233–240.

Rosenberg, S.A., Yang, J.C., Sherry, R.M., Kammula, U.S., Hughes, M.S., Phan, G.Q., Citrin, D.E., Restifo, N.P., Robbins, P.F., Wunderlich, J.R., et al. (2011). Durable Complete Responses in Heavily Pretreated Patients with Metastatic Melanoma Using T-Cell Transfer Immunotherapy. Clinical Cancer Research *17*, 4550 –4557.

Russell, S.J., Peng, K.-W., and Bell, J.C. (2012). Oncolytic virotherapy. Nature Biotechnology *30*, 658–670.

Sakaguchi, S., Wing, K., Onishi, Y., Prieto-Martin, P., and Yamaguchi, T. (2009). Regulatory T cells: how do they suppress immune responses? Int. Immunol. *21*, 1105–1111.

Sambrook, J. (1989). Fritsch, EF, and Maniatis, T.(1989) Molecular cloning: a laboratory manual. Cold Spring Harbor Laboratory, Cold Spring Harbor, NY *267*, 9289–9293.

Sampson, J.H., Crotty, L.E., Lee, S., Archer, G.E., Ashley, D.M., Wikstrand, C.J., Hale, L.P., Small, C., Dranoff, G., Friedman, A.H., et al. (2000). Unarmed, tumor-specific monoclonal antibody effectively treats brain tumors. Proc. Natl. Acad. Sci. U.S.A. *97*, 7503–7508.

Sanchez-Perez, L., Gough, M., Qiao, J., Thanarajasingam, U., Kottke, T., Ahmed, A., Thompson, J.M., Maria Diaz, R., and Vile, R.G. (2007). Synergy of adoptive T-cell therapy and intratumoral suicide gene therapy is mediated by host NK cells. Gene Ther. *14*, 998–1009.

Sattentau, Q. (2008). Avoiding the void: cell-to-cell spread of human viruses. Nature Reviews Microbiology *6*, 815–826.

Savarin, C., Stohlman, S.A., Atkinson, R., Ransohoff, R.M., and Bergmann, C.C. (2010). Monocytes Regulate T Cell Migration through the Glia Limitans during Acute Viral Encephalitis. J. Virol. *84*, 4878–4888.

Scaffidi, P., Misteli, T., and Bianchi, M.E. (2002). Release of chromatin protein HMGB1 by necrotic cells triggers inflammation. Nature *418*, 191–195.

Schaue, D., Comin-Anduix, B., Ribas, A., Zhang, L., Goodglick, L., Sayre, J.W., Debucquoy, A., Haustermans, K., and McBride, W.H. (2008). T-Cell Responses to

Survivin in Cancer Patients Undergoing Radiation Therapy. Clin Cancer Res *14*, 4883–4890.

Schmidt, J., Mocevicius, P., Werner, J., and Ryschich, E. (2012). The role of the tumor endothelium in leukocyte recruitment in pancreatic cancer. Surgery *152*, S89–S94.

Schneider-Schaulies, S., and Schneider-Schaulies, J. (2009). Measles virus-induced immunosuppression. Curr. Top. Microbiol. Immunol *330*, 243–269.

Senzer, N.N., Kaufman, H.L., Amatruda, T., Nemunaitis, M., Reid, T., Daniels, G., Gonzalez, R., Glaspy, J., Whitman, E., Harrington, K., et al. (2009). Phase II clinical trial of a granulocyte-macrophage colony-stimulating factor-encoding, second-generation oncolytic herpesvirus in patients with unresectable metastatic melanoma. J. Clin. Oncol *27*, 5763–5771.

Shankaran, V., Ikeda, H., Bruce, A.T., White, J.M., Swanson, P.E., Old, L.J., and Schreiber, R.D. (2001). IFNγ and lymphocytes prevent primary tumour development and shape tumour immunogenicity. Nature *410*, 1107–1111.

Shields, J.D., Kourtis, I.C., Tomei, A.A., Roberts, J.M., and Swartz, M.A. (2010). Induction of Lymphoidlike Stroma and Immune Escape by Tumors That Express the Chemokine CCL21. Science *328*, 749–752.

Shuster, S. (2008). Is sun exposure a major cause of melanoma? No. BMJ *337*, a764.

Skelly, C. (2012). Measles Versus Melanoma. Science Translational Medicine *4*, 116ec7.

Somosy, Z., Horváth, G., Telbisz, Á., Réz, G., and Pálfia, Z. (2002). Morphological aspects of ionizing radiation response of small intestine. Micron *33*, 167–178.

Song, K.H., Pidikiti, R., Stojadinovic, S., Speiser, M., Seliounine, S., Saha, D., and Solberg, T.D. (2010). An x-ray image guidance system for small animal stereotactic irradiation. Physics in Medicine and Biology *55*, 7345–7362.

Stemmler, H.-J., and Heinemann, V. (2008). Central Nervous System Metastases in HER-2–Overexpressing Metastatic Breast Cancer: A Treatment Challenge. The Oncologist *13*, 739–750.

Stevens, G., and McKay, M.J. (2006). Dispelling the myths surrounding radiotherapy for treatment of cutaneous melanoma. Lancet Oncol. *7*, 575–583.

Stojdl, D.F., Lichty, B., Knowles, S., Marius, R., Atkins, H., Sonenberg, N., and Bell, J.C. (2000). Exploiting tumor-specific defects in the interferon pathway with a previously unknown oncolytic virus. Nat Med *6*, 821–825.

Tabi, Z., Spary, L.K., Coleman, S., Clayton, A., Mason, M.D., and Staffurth, J. (2010). Resistance of CD45RA- T cells to apoptosis and functional impairment, and

activation of tumor-antigen specific T cells during radiation therapy of prostate cancer. J. Immunol. *185*, 1330–1339.

Tang, D., Loze, M.T., Zeh, H.J., and Kang, R. (2010). The redox protein HMGB1 regulates cell death and survival in cancer treatment. Autophagy *6*, 1181–1183.

Tatsuo, H., Ono, N., Tanaka, K., and Yanagi, Y. (2000). SLAM (CDw150) is a cellular receptor for measles virus. Nature *406*, 893–897.

Teng, M.W.L., Darcy, P.K., and Smyth, M.J. (2011). Stable IL-10: A New Therapeutic that Promotes Tumor Immunity. Cancer Cell *20*, 691–693.

Thomas, D.L., Doty, R., Tosic, V., Liu, J., Kranz, D.M., McFadden, G., MacNeill, A.L., and Roy, E.J. (2011). Myxoma virus combined with rapamycin treatment enhances adoptive T cell therapy for murine melanoma brain tumors. Cancer Immunol Immunother.

Tissari, J., Sirén, J., Meri, S., Julkunen, I., and Matikainen, S. (2005). IFN-alpha enhances TLR3-mediated antiviral cytokine expression in human endothelial and epithelial cells by up-regulating TLR3 expression. J. Immunol. *174*, 4289–4294.

Toda, M., Rabkin, S.D., Kojima, H., and Martuza, R.L. (1999). Herpes simplex virus as an in situ cancer vaccine for the induction of specific anti-tumor immunity. Hum. Gene Ther. *10*, 385–393.

Travis, E.L., Parkins, C.S., Holmes, S.J., and Down, J.D. (1982). Effect of misonidazole on radiation injury to mouse spinal cord. Br J Cancer *45*, 469–473.

Tsao, H., Atkins, M.B., and Sober, A.J. (2004). Management of Cutaneous Melanoma. N Engl J Med *351*, 998–1012.

Ungerechts, G., Springfeld, C., Frenzke, M.E., Lampe, J., Johnston, P.B., Parker, W.B., Sorscher, E.J., and Cattaneo, R. (2007a). Lymphoma chemovirotherapy: CD20-targeted and convertase-armed measles virus can synergize with fludarabine. Cancer Res *67*, 10939–10947.

Ungerechts, G., Springfeld, C., Frenzke, M.E., Lampe, J., Parker, W.B., Sorscher, E.J., and Cattaneo, R. (2007b). An immunocompetent murine model for oncolysis with an armed and targeted measles virus. Mol. Ther *15*, 1991–1997.

Uyttenhove, C., Pilotte, L., Théate, I., Stroobant, V., Colau, D., Parmentier, N., Boon, T., and Eynde, B.J.V. den (2003). Evidence for a tumoral immune resistance mechanism based on tryptophan degradation by indoleamine 2,3-dioxygenase. Nature Medicine *9*, 1269–1274.

Uzé, G., and Monneron, D. (2007). IL-28 and IL-29: newcomers to the interferon family. Biochimie *89*, 729–734.

Verhaegen, F., Granton, P., and Tryggestad, E. (2011). Small animal radiotherapy research platforms. Physics in Medicine and Biology *56*, R55–R83.

Vries, I.J.M. de, Castelli, C., Huygens, C., Jacobs, J.F.M., Stockis, J., Schuler-Thurner, B., Adema, G.J., Punt, C.J.A., Rivoltini, L., Schuler, G., et al. (2011). Frequency of Circulating Tregs with Demethylated FOXP3 Intron 1 in Melanoma Patients Receiving Tumor Vaccines and Potentially Treg-Depleting Agents. Clin Cancer Res *17*, 841–848.

Waugh, D.J.J., and Wilson, C. (2008). The interleukin-8 pathway in cancer. Clin. Cancer Res *14*, 6735–6741.

White, C.L., Twigger, K.R., Vidal, L., De Bono, J.S., Coffey, M., Heinemann, L., Morgan, R., Merrick, A., Errington, F., Vile, R.G., et al. (2008). Characterization of the adaptive and innate immune response to intravenous oncolytic reovirus (Dearing type 3) during a phase I clinical trial. Gene Ther *15*, 911–920.

Whiteside, T.L. (2002). Tumor-induced death of immune cells: its mechanisms and consequences. Seminars in Cancer Biology *12*, 43–50.

Wilson, C.M., Gaber, M.W., Sabek, O.M., Zawaski, J.A., and Merchant, T.E. (2009). Radiation-Induced Astrogliosis and Blood-Brain Barrier Damage Can Be Abrogated Using Anti-TNF Treatment. International Journal of Radiation Oncology*Biology*Physics *74*, 934–941.

Wilson, E.H., Weninger, W., and Hunter, C.A. (2010). Trafficking of immune cells in the central nervous system. J. Clin. Invest. *120*, 1368–1379.

De Witte, L., Abt, M., Schneider-Schaulies, S., Van Kooyk, Y., and Geijtenbeek, T.B.H. (2006). Measles Virus Targets DC-SIGN To Enhance Dendritic Cell Infection. J. Virol. *80*, 3477–3486.

Wongthida, P., Diaz, R.M., Galivo, F., Kottke, T., Thompson, J., Pulido, J., Pavelko, K., Pease, L., Melcher, A., and Vile, R. (2010). Type III IFN Interleukin-28 Mediates the Antitumor Efficacy of Oncolytic Virus VSV in Immune-Competent Mouse Models of Cancer. Cancer Research *70*, 4539–4549.

Worschech, A., Haddad, D., Stroncek, D., Wang, E., Marincola, F., and Szalay, A. (2009). The immunologic aspects of poxvirus oncolytic therapy. Cancer Immunology, Immunotherapy *58*, 1355–1362.

Wu, T.-C. (2007). The Role of Vascular Cell Adhesion Molecule-1 in Tumor Immune Evasion. Cancer Res *67*, 6003–6006.

Xia, Z.-J., Chang, J.-H., Zhang, L., Jiang, W.-Q., Guan, Z.-Z., Liu, J.-W., Zhang, Y., Hu, X.-H., Wu, G.-H., Wang, H.-Q., et al. (2004). [Phase III randomized clinical trial of intratumoral injection of E1B gene-deleted adenovirus (H101) combined with cisplatin-based chemotherapy in treating squamous cell cancer of head and neck or esophagus.]. Ai Zheng *23*, 1666–1670.

Yuan, H., Gaber, M.W., Boyd, K., Wilson, C.M., Kiani, M.F., and Merchant, T.E. (2006). Effects of fractionated radiation on the brain vasculature in a murine model: Blood–brain barrier permeability, astrocyte proliferation, and

ultrastructural changes. International Journal of Radiation Oncology*Biology*Physics *66*, 860–866.

Zhang, Y., Patel, B., Dey, A., Ghorani, E., Rai, L., Elham, M., Castleton, A.Z., and Fielding, A.K. (2012). Attenuated, oncolytic, but not wild-type measles virus infection has pleiotropic effects on human neutrophil function. J. Immunol. *188*, 1002–1010.

Zimmermann, M., Armeanu, S., Smirnow, I., Kupka, S., Wagner, S., Wehrmann, M., Rots, M.G., Groothuis, G.M.M., Weiss, T.S., Königsrainer, A., et al. (2009). Human precision-cut liver tumor slices as a tumor patient-individual predictive test system for oncolytic measles vaccine viruses. Int. J. Oncol *34*, 1247–1256.

Zitvogel, L., Apetoh, L., Ghiringhelli, F., André, F., Tesniere, A., and Kroemer, G. (2008). The anticancer immune response: indispensable for therapeutic success? J Clin Invest *118*, 1991–2001.

Zitvogel, L., and Kroemer, G. (2012). Reply to: Chemotherapy response of spontaneous mammary tumors is independent of the adaptive immune system. Nature Medicine *18*, 346–346.

Zitvogel, L., Tesniere, A., and Kroemer, G. (2006). Cancer despite immunosurveillance: immunoselection and immunosubversion. Nature Reviews Immunology *6*, 715–727.

9 Appendices

9.1 Max Perutz submissions

The following are essays submitted to the annual MRC science writing competition and selected by the shortlisting panel. The 2011 essay was highly commended by the judges.

2010

An enemy's enemy

Viruses get a pretty bad press. From coughs and colds, right through to serious viruses like man-flu, most people would say viruses are just no good. Our research is trying to offer them a shot at penance, as a treatment for cancer.

When a virus infects a cell it takes control of the cell's machinery and coerces it into producing more virus, instead of the normal proteins that keep the cell happy and functioning. Eventually the cell dies, bursting as it does so and releasing the newly copied viruses to go and infect other cells nearby. Can this be turned against cancer?

Viruses often have a favourite type of cell to infect, one that they're particularly comfortable in and find easy to control. Herpes is most at home in nerve cells and can stay put for decades, coming back every winter to give you a cold sore. Norovirus has a penchant for the gut and each year millions suffer diarrhoea as a result. Some viruses seem to be especially fond of cancer cells and are far better at infecting and killing cancer cells than they are normal cells. It's these oncolytic viruses (onco- tumour, lysis – destruction) that we study as potential treatments for cancer patients.

Given the advances in virology and molecular biology over the last 20 years we're now able to study the way viruses infect and kill cells. We're able to choose viruses that prefer cancer, or modify them so that they'll only infect the cells we're targeting. We can grow human cancer cells in Petri dishes and watch them be destroyed by adding tiny amounts of an oncolytic virus. We can measure how well a virus can multiply in different types of cancer cells and look for ways to improve its effectiveness.

A further mechanism for these viruses lies in the way they interact with the

body's natural defences. The immune system is cold and unsympathetic. When a normal cell becomes infected with a virus it releases distress signals to warn its neighbours and call in help from the immune system to stave off the infection. When the immune system discovers the infected cell it will politely invite the hapless victim to kill itself, lest it produces even more virus and infects its as yet unharmed neighbours. If the virally laden cell doesn't obey (as cancer cells are wont to do) the patrolling immune cell will summon colleagues and ruthlessly attack and destroy it in an effort to contain the virus.

This is at the heart of our research efforts. It is hard to persuade the immune system to recognise cancer, mainly because cancer is very good at hiding itself. Our theory is that virally-infected cancer cells call for help in much the same way as normal cells do when under similar attack. In fact it's quite possible that cancer cells produce even more distress signals than normal cells because they've lost even the basic self-defence systems that most other cells possess. By doing this the cancer becomes vulnerable, revealing itself and triggering an attack by the immune system. Most exciting for researchers though is that there is evidence that the immune system, once alerted to infected cancer cells in this way, becomes alerted to uninfected cancer cells as well, attacking the cancer in other parts of the body too; parts that the virus may not have reached.

There are still challenges. How do we get the virus to the tumours? Administering a virus directly into the bloodstream risks triggering a well-meant, but unhelpful immune response against it. This can destroy the virus before it's had a chance to get to the cancer and do any good. An alternative is to inject virus directly into tumours, but this can be awkward and painful, and reduces the amount of virus getting to cancer that has spread elsewhere in the body. By either route, injecting a large dose of virus into someone makes them feel pretty horrible for a few days too, though no worse than many of the commonly used chemotherapy treatments.

Viruses do have potential as another treatment for cancer, but it's very early days. Several viruses are being studied in labs. Some are already being tested in clinical trials in patients with promising results. So far the studies suggest that giving the right viruses in the right way and in the right doses is safe; it's just too early to say whether the theory turns into real benefits for patients. Will viruses

keep people with cancer alive longer? Answering that is going to take more trials, more lab work and I'm afraid, more time yet.

By the way, please don't cosy up to that flu-ridden person on the train, or search out someone with chickenpox and have a cuddle; it won't work like that, and you might just get yourself arrested.

2011
Hunting out the enemy

Sarah died at two in the morning, about three hours after I sent her parents home for the night- she was 19.

A couple of weeks before Christmas, completely out of the blue, she'd had a seizure. A CT scan of her head and a battery of other tests revealed widespread metastatic cancer. Metastatic melanoma is one of the most aggressive cancers and normally starts in the skin. In Sarah's case it had spread throughout her body, including her brain, before she'd ever known it was there.

The cancer in her brain made her have more and more fits. The fits weren't well controlled with medications and so Sarah had to come in and out of hospital to try and get on top of them. On one of those admissions I was working as a junior doctor in my second year. We gave the teenager more drugs to try and control the most recent fit and admitted her to the cancer ward for observation overnight.

I thought I was helping her parents by reassuring them that we'd look after their daughter and that nothing more was going to happen overnight. Sarah died on the ward, without her family, in that hinterland between Christmas and New Year's Day, less than a month after her first seizure.

Sarah had always been well, she had no other medical problems and like most other people who develop cancer, her immune system was perfectly normal. The cells of the immune system police the body, having evolved over a thousand millennia to tackle infection and parasites, but also possessing the potential to act against cancers. Our research looks for ways to trigger an immune response against cancer cells to help patients fight the disease.

If the immune system is the body's police force then melanoma is a very sophisticated and aggressive criminal. Melanomas, and other cancers, conceal their identity by reducing the number of molecules on their surface that normally provide information to immune cells- essentially a system of fake IDs and disguises. When an immune cell does recognise a cancer cell then it is prevented from triggering the alarm by a range of chemicals released by the cancer; akin to jamming the police radios. On the rare occasion that a cancer cell is successfully recognised and accosted it is resistant to the actions of the

immune cell, as if the master criminal has already planned its jail break.

These barriers can be overcome. One approach we're trying is to use radiotherapy, a treatment to which melanoma in particular is considered relatively resistant. By giving radiotherapy to an area of metastatic melanoma we hope to generate inflammation not just in the tumour cells but also in the nearby normal cells. This way even if the tumour refuses to release inflammatory signals then the adjacent healthy tissue will, which in turn will trigger an immune response. It's essentially calling the fire brigade when you need the police, but either way help is coming, and the cancer's ability to 'jam the radios' has been circumvented.

Another part of our work has been to use viruses chosen for their ability to infect and kill cancer cells. We've shown with a number of different viruses that the immune system is better able to recognise a virally-infected tumour cell. In fact having recognised a tumour cell riddled with virus the immune system is primed to better recognise other tumour cells too, overcoming the cancer's system of disguises.

With both of these treatments the therapy is confined to the area treated; you can't give radiotherapy to the entire body if the disease is widespread without doing more harm than good. Our aim is to find a treatment, or combination of treatments, that act on one area of disease but trigger an immune response to attack the cancer throughout the body.

Many have doubted that the immune system could ever play an important role in the fight against cancer but recent studies have debunked that. For the first time a drug has been tested in clinical trials that seems to have real benefits for patients with metastatic melanoma, and amazingly it has no direct action on the cancer itself. Ipilimumab acts on cells of the patient's immune system, not the tumour, and effectively takes the brakes off the immune system, unleashing it to attack the cancer. Like most cancer treatments there are side effects, but it is a huge leap forward for patients with melanoma and may have impacts for other cancers too. It is proof that the immune system can be harnessed- that it can be persuaded to join a fight it was previously blinkered to.

It feels a long time ago that Sarah died, but I still remember telling her parents to go and get some sleep, and still I think it's the worst mistake I've ever made.

Since then progress is finally being made in the search for effective treatments for melanoma and hopefully there's more to come.

9.2 SET for Britain poster 2012

The following is a poster presented at the Science Engineering and Technology meeting, hosted by the Parliamentary Science Committee at the Houses of Parliament. It was designed with Harry Donnelly, and was intended for a mixed audience of scientists and MPs.

Olly Donnelly

MRC clinical research training fellow and SpR clinical oncology
Leeds Institute Molecular Medicine, University of Leeds and St James University Hospital
Supervisors: Prof Alan Melcher, Prof P J Selby, Dr F Errington-Mais
o.donnelly@leeds.ac.uk

Measles as an oncolytic virus for the treatment of melanoma

Introduction

Oncolytic Viruses (OV); viruses which preferentially infect and lyse cancer cells, are being studied for their potential as cancer treatments. Several, including measles, have been tested in early phase clinical trials and the first phase III clinical trials are underway. Oncolytic strains of measles (MV) are derived from the original vaccine, attenuated in the 1960s by Enders and Peebls. Thus the virus we describe has been administered to hundreds of millions over the last half century with an excellent safety record. This safety profile has been confirmed by phase I trials, including intracranial administration for patients with GBM.

Virotherapy for melanoma

Melanoma is not the commonest of cancers but certainly one of the most aggressive. Few effective treatments exist for the disease once metastatic, though immune therapies have demonstrated promise. In addition to directly killing cancer cells, OV are known to stimulate significant immune responses; our group has previously demonstrated innate and adaptive responses both preclinically and clinically, with several viruses. MV has not previously been studied in melanoma, therefore we chose to study the potential of MV both as an oncolytic agent in melanoma, and as an immunostimulatory therapy.

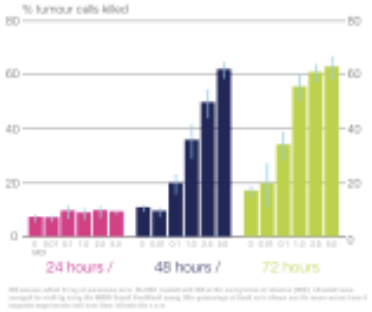

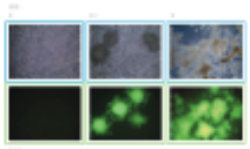

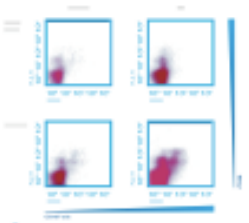

Measles successfully infects and replicates in human melanoma cells, causing an immunogenic death and the release of danger signals

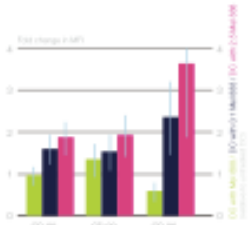

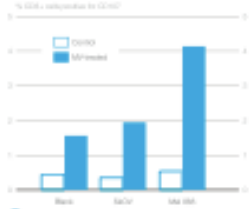

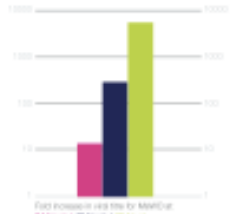

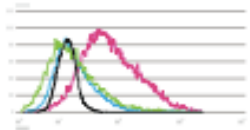

MV-induced melanoma death matures DC and licenses innate and adaptive anti-melanoma immune responses

Measles is a promising treatment for patients with melanoma; clinical trials are being developed

Professors Alan Melcher and Peter Selby, and Dr Fiona Errington-Mais supervised and supported this work, as did Dr Lynette Steele. Dr Steve Russell and Dr Kah-Whye Peng kindly provided the measles virus and advice.

MRC Medical Research Council

UNIVERSITY OF LEEDS

9.3 Publications

The following publications were published during the period of study:

Donnelly, O.G., Errington-Mais, F., Prestwich, R., Harrington, K., Pandha, H., Vile, R., and Melcher, A.A. (2012a). Recent clinical experience with oncolytic viruses. Curr Pharm Biotechnol *13*, 1834–1841.

Donnelly, O.G., Errington-Mais, F., Steele, L., Hadac, E., Jennings, V., Scott, K., Peach, H., Phillips, R.M., Bond, J., Pandha, H., et al. (2011). Measles virus causes immunogenic cell death in human melanoma. Gene Ther.

Donnelly, O.G., Melcher, A.A., Vile, R.G., and Pulido, J. (2012b). What new immunotherapeutic techniques are currently being investigated for the treatment of melanoma? Immunotherapy *4*, 749–751.

Donnelly, O.G., Vile, R., Pandha, H., Harrington, K., and Melcher, A. (2012c). The Hitchhiker's Guide to Virotherapy. Oncotarget *3*, 735–736.